

DISCLAIMER

This report was prepared as an account of work sponsored by an agency of the United States Government. Neither the United States Government nor any agency thereof, nor any of their employees, makes any warranty, expressed or implied, or assumes any legal liability or responsibility for the accuracy, completeness, or usefulness of any information, apparatus, product, or process disclosed, or represents that its use would not infringe privately owned rights. Reference herein to any specific commercial product, process, or service by trade name, trademark, manufacturer, or otherwise does not necessarily constitute or imply its endorsement, recommendation, or favoring by the United States Government or any agency thereof. The views and opinions of authors expressed herein do not necessarily state or reflect those of the United States Government.

This report has been reproduced directly from the best available copy.

Available to DOE and DOE contractors from the Office of Scientific and Technical Information, P.O. Box 62, Oak Ridge, TN 37831; prices available from (615) 576-8401.

Available to the public from the National Technical Information Service, U.S. Department of Commerce, 5285 Port Royal Rd., Springfield, VA 22161

DOE/PC/91008-15
Distribution Category UC-122

In Situ Permeability Modification Using Gelled Polymer Systems

By
D.W. Green
G.P. Willhite
C.S. McCool
J.A. Heppert
S. Vossoughi
M.J. Michnick

October 1998

Work Performed Under Subcontract G4S60331 and Prime Contract DE-AC22-94PC91008

Prepared for
U.S. Department of Energy
Assistant Secretary for Fossil Energy

Jerry F. Casteel, Project Manager
National Petroleum Technology Office
P.O. Box 3628
Tulsa, OK 74101

Prepared by:
Center for Research, Inc.
The University of Kansas
4006 Learned Hall
Lawrence, KS 66045-2223

Table of Contents

	<u>Page No.</u>
List of Figures	v
List of Tables	xi
Abstract	xiii
Executive Summary	xv
Chapter 1 Introduction.....	1-1
Chapter 2 Resorcinol-Formaldehyde Based Gel Systems	2-1
Chapter 3 Measurement of Aggregated Size During Gelation.....	3-1
Chapter 4 Chemical Interactions Between Brine Solutions and Dolomite and Chromium Precipitation from Chromium (III) Acetate Solutions	4-1
Chapter 5 Permeability and Dehydration of Polymer Gels after Placement	5-1
Chapter 6 An Experimental Study of the Flow of a HiVis 300 Polymer Solution Through a Sandpack	6-1
Chapter 7 A Study of Gelation and Injection Characteristics of a Polyacrylamide- Chromium Acetate System in the Presence of Added Acetate Ions	7-1
Chapter 8 Gel Behavior in Fractured Media	8-1
Chapter 9 Gel Treatments in Production Wells.....	9-1
Chapter 10 Gel Systems for Carbon Dioxide Flooding.....	10-1
Chapter 11 References.....	11-1

List of Figures

<u>Figure No.</u>		<u>Page No.</u>
2.1	Sulfomethylation of resorcinol.....	2-2
2.2	Hydrolysis of hexamethylenetetramine.....	2-2
3.1	Schematic of flow field-flow fractionation channel.....	3-2
3.2	Schematic of pumps and flow paths for FFFF channel.....	3-4
3.3	Response of detector as a function of time for FFFF run	3-5
3.4	Size distribution of a sample containing particles with a diameter of 102nm	3-6
3.5	Size distribution of a sample containing particles with a diameter of 300nm	3-6
3.6	Size distribution of a sample containing particles with diameters of 102 and 300nm..	3-7
4.1	Effluent pH and magnesium concentrations as a function of the pH of the injected brine.....	4-3
4.2	Solubility of chromium(III) as a function of pH.....	4-3
4.3	Schematic of the apparatus for pH-stat experiments.....	4-5
4.4	Chromium concentration and turbidity as a function of time during pH-stat experiment.....	4-6
4.5	Effect of pH on chromium concentration as a function of time.....	4-8
4.6	Effect of salt concentration on chromium precipitation during pH stat titration	4-8
4.7	Effect of the temperature on chromium precipitation	4-10
4.8	Effect of the acetate concentration on chromium precipitation	4-10
4.9	Effect of chromium salt on the precipitation of chromium.....	4-11
4.10	Effect of divalent and monovalent ions (same ionic strength) on chromium precipitation.....	4-11
4.11	Chromium concentrations as a function of time and pH.....	4-14

<u>Figure No.</u>	<u>Page No.</u>
4.12	Determination of β from rate constants of experiments conducted at different pH values..... 4-14
4.13	Determination of γ from rate constants of experiments conducted at different OAc concentrations..... 4-15
4.14	Comparison between the experimental data and predicted results of the rate equation 4-15
5.1	Schematic diagram of the apparatus used for measuring the gel permeability 5-4
5.2	Inherent gel permeability for sulfomethylated resorcinol-formaldehyde (SMRF) gel system at 25°C and different applied pressures 5-4
5.3	Gel permeability for KUSP1-boric acid gel with 0.5 mole boric acid per kilogram of gel at 25°C and 2 psi 5-6
5.4	Gel permeability for KUSP1-boric acid gel with 0.2 mole boric acid per kilogram of gel at 25°C and 2 psi 5-6
5.5	Schematic sketch of setup to study dehydration of PHPA/Cr (III) gel system..... 5-7
5.6	Gel behavior at pressures less than 150 psi when brine (1% KCl) is used to displace the gel in 10 mm columns 5-8
5.7	Gel behavior at pressures greater than 150 psi when brine is used to displace the gel in 10-mm columns..... 5-8
5.8	Gel behavior when brine is used to displace the gel in 35-mm columns at pressures greater than 4 psi 5-9
5.9	Gel behavior when brine is used to displace gel in 35-mm columns at pressures of approximately 4 psi 5-10
5.10	Permeability of gel and filter combination versus time at 100 psi when brine is used to dehydrate the gel. Gel composition – 5000 ppm polymer, 200 ppm chromium and 1% KCl..... 5-10
5.11	Permeability of gel and filter combination versus time at 250 psi when brine is used to dehydrate the gel. Gel composition – 5000 ppm polymer, 200 ppm chromium and 1% KCl..... 5-12

<u>Figure No.</u>	<u>Page No.</u>
5.12 Permeability of gel and filter combination versus time at 400 psi when brine is used to dehydrate the gel. Gel composition – 5000 ppm polymer, 200 ppm chromium and 1% KCl.....	5-12
5.13 Permeability of gel and filter combination at the end of the experiment versus pressure.....	5-13
5.14 Dehydration of gel during brine flow in 35 mm columns as a function of initial pressure gradient	5-13
5.15 Comparison of gel dehydration in 10 mm and 35 mm columns as a function of initial pressure gradient	5-14
5.16 Gel behavior when oil is used to displace the gel	5-14
5.17 Dehydration as a fraction of the original gel volume vs. time when oil is used to displace the gel in glass column with inside diameter 10 mm at 50 and 10 and 5 psi. Gel composition – 7500 ppm polymer, 300 ppm chromium and 1% KCl.....	5-16
5.18 Dehydration as a fraction of the original gel volume vs. time when oil is used to displace gel in a glass column with inside diameter of 35-mm. Gel composition – 7500 ppm polymer, 300 ppm chromium and 1% KCl	5-17
5.19 Comparison of dehydration of gels by oil in 10 mm and 35 mm columns. Gel composition – 7500 ppm polymer, 300 ppm chromium and 1% KCl	5-18
6.1 Polymer displacement apparatus.....	6-2
6.2 Normalized polymer concentration and viscosity, and apparent viscosity as a function of pore volumes injected during SP3.A Series.....	6-5
6.3 Normalized polymer concentration and viscosity, and apparent viscosity as a function of pore volumes injected during SP3.B Series	6-8
6.4 Normalized polymer concentration and apparent viscosity as a function of pore volumes injected during SP3.C Series	6-9
6.5 Normalized polymer concentration and viscosity, and apparent viscosity as a function of pore volumes injected during SP1.A Series.....	6-12
6.6 Normalized polymer concentration and viscosity, and apparent viscosity as a function of pore volumes injected during SP1.B Series.....	6-13

<u>Figure No.</u>	<u>Page No.</u>
6.7	6-15
7.1	7-2
7.2	7-3
7.3	7-6
7.4	7-7
7.5	7-7
8.1	8-3
8.2	8-4
8.3	8-5
8.4	8-7
8.5	8-7
8.6	8-8
8.7	8-10
8.8	8-10
8.9	8-11
8.10	8-12

<u>Figure No.</u>	<u>Page No.</u>
8.11	Evolution of apparent viscosity at the sections of the unfractured core during displacement of zero hour old gelant (upper), and three-hour-old gelant (lower) 8-14
8.12	Cumulative flow of gelant as function of square root of time 8-15
8.13	A comparison of experimental and simulated flow at the fracture outlet for displacement of glycerol 8-15
8.14	A comparison of experimental and simulated pressure drop across the matrix sections in the fracture model during glycerol displacement..... 8-16
8.15	A comparison of leakoff rate at constant pressure at the fracture, with the same at constant differential pressure along the fracture 8-17
8.16	A comparison of experimental and regressed permeability averaged over the gelant slug 8-18
8.17	Simulated profile for apparent viscosity in the unfractured core during displacement of zero and three hour old gelant..... 8-19
9.1	Schematic of microwave apparatus..... 9-2
9.2	Apparatus for flow experiments 9-3
9.3	Water saturation profiles during gelant injection; Injection from right side (Direction #2) 9-5
9.4	Water saturation profiles during injection of oil overflush; Injection from right side (Direction #2) 9-5
9.5	Water saturation profiles during different fractional flows before gel treatment; Drainage path and steady state 9-6
9.6	Water saturation profiles during different fractional flows after gel treatment; Drainage path and steady state 9-6
9.7	Relative permeability curves of Section 4 before and after gel treatment 9-7
9.8	The effect of flow rate on effective permeability to water and oil after gel treatment; Water fractional flow of 25% 9-10
10.1	Schematic diagram for the apparatus used for flow experiments 10-3
10.2	KUSP1-boric acid syneresis at 41°C..... 10-5

<u>Figure No.</u>	<u>Page No.</u>
10.3 Effect of syneresis of KUSP1-boric acid in a sandpack on permeability and available volume for flow	10-6
10.4 Brine injection into the core gelled with KUSP1-boric acid gel.....	10-7
10.5 AlcoFlood 254S gelant injection into the core.....	10-10
10.6 Pressure response in different sections of the core gelled with AlcoFlood 254S. Brine injection at 0.007 mL/min	10-10
10.7 Overall pressure response in the core gelled with Alcoflood 254S. Brine injection at 0.007 mL/min	10-11
10.8 Brine injection into the core gelled with AlcoFlood 254S at constant pressure of 300 psi	10-13
10.9 Pressure response for brine injection into the core gelled with AlcoFlood 254S at constant pressure of 300 psi after two months	10-13
10.10 Pressure response between the core exit and back-pressure regulator (AlcoFlood 254S experiment)	10-14

List of Tables

<u>Table No.</u>		<u>Page No.</u>
2.1	Gelation times for the R-HMTA gel system	2-3
3.1	Size distributions measured with equilibrium-dialysis technique.....	3-2
4.1	Representative experimental list.....	4-7
4.2	Calculation of rate dependence on pH and acetate concentration	4-13
5.1	Inherent permeability to water for several gels [Seright and Martin, 1991].....	5-2
5.2	Dehydration of chromium acetate-polyacrylamide gel in Sandpack SP12.....	5-19
5.3	Dehydration of chromium acetate-polyacrylamide gel in Sandpack SP19.....	5-20
5.4	Dehydration of chromium acetate-polyacrylamide gel in Sandpack SP20.....	5-20
6.1	Initial permeability of sections for sandpack SP3	6-2
6.2	Conditions for the displacement experiments	6-3
6.3	Polymer retention during SP3.A series	6-6
6.4	Polymer retention during SP3.B series	6-10
6.5	Polymer retention during SP3.C series	6-10
6.6	Flow conditions for displacement experiments SP1.A and SP1.B	6-11
6.7	Polymer retention during SP1.A series	6-14
6.8	Polymer retention during SP1.B series	6-14
7.1	Summary of displacement experiments	7-4
9.1	Residual resistance factors for water.....	9-9
9.2	Residual resistance factors for oil	9-9
9.3	Permeability of Section 4 as a function of Darcy velocity.....	9-11

<u>Table No.</u>	<u>Page No.</u>
10.1 Core permeability before and after gelation with KUSP1-ester gel (atmospheric pressure)	10-4
10.2 Brine permeability in the core gelled with KUSP1-ester gel (1200 psi pressure)	10-5
10.3 Permeability and residual resistance factors of the gelled core to carbon dioxide and brine for different cycles. 1200 psi and 41°C.....	10-8
10.4 Permeability modification for SMRF gel system (atmospheric pressure and 41°C) ..	10-8
10.5 Permeability of different sections of the SMRF gelled core to carbon dioxide at 1200 psi and 41°C	10-9
10.6 Initial brine permeability in core.....	10-9
10.7 Viscosity of 5% polymer solution as measured by Brookfield viscometer at 25°C.....	10-9
10.8 Effluent and flow rate data for brine injection at constant pressure of 100 psi.....	10-11
10.9 Effluent and flow rate and data for brine injection at constant pressure of 150 psi..	10-12

Abstract

The research program is directed at improving the understanding of gelled polymer systems and how these systems can be used to increase oil recovery from petroleum reservoirs. The research is focused on five areas: (1) Gel treatment in fractured systems; (2) Gel treatment in carbonate rocks; (3) In-depth placement of gels; (4) Gel systems for application in carbon dioxide flooding; (5) Gel treatment in production wells. Results were obtained from displacement of a Cr(III)-acetate-partially hydrolyzed polyacrylamide (PHPA) gelant in a physical model of a fracture and a study of the behavior of the gel after treatment. Substantial gel leakoff occurred during treatment. The mature gel was extruded from the fracture on application of a small pressure gradient. Data were obtained on the leakoff of gelant of different ages in Berea sandstone cores. A model describing leakoff during gel placement in a linear system with deep filtration of gel aggregates was developed. Hexamethylenetetramine (HMTA) was studied as a potential substitute for formaldehyde in resorcinol-formaldehyde and sulfomethylated resorcinol-formaldehyde (SMRF) gel systems. Gels were formed using HMTA over a restricted range of conditions. Propagation of chromium in carbonate rock is a limitation of gel systems based on chromium acetate and partially hydrolyzed polyacrylamide. Precipitation of chromium occurs if the pH of the injected fluid increases due to fluid rock interactions. Effluent compositions and pH were determined by injecting KCl brine at selected values of pH into a six-inch long Baker dolomite core. Effluent pH and concentrations stabilized when the residence time in the dolomite core was increased to values of just a few hours. The most significant observation was the strong buffering effect of the rock observed when the injected pH varied between 4 and 10. The effluent pH remained at pH 10 due to buffering caused by dissolution of dolomite. Effluent pH and concentrations were in good agreement with values simulated using the computer program PHREEQE, a geochemical model based on equilibrium relationships. The study of fluid-rock interactions showed that dramatic increases in pH occur by carbonate dissolution when brine solutions that do not have strong buffering capacities are injected through carbonate rocks. The precipitation of chromium from chromium acetate solutions was studied and rates of precipitation were determined for a range of pH values from 7 to 11 and temperatures between 25°C and 45°C. The rate of precipitation increased with pH, temperature and salinity. Procedures to determine aggregate size distributions of gelling solutions using equilibrium dialysis were developed and tested. A flow field-flow fractionation unit (FFFF) was acquired to separate gel aggregates by size. Runs were conducted on polystyrene standard spheres to test the performance of the FFFF unit. A study was completed in which the gelation time of chromium acetate-polyacrylamide gel systems was increased by adding acetate ion to reduce the rate of crosslinking between chromium and polyacrylamide. Displacement experiments in unconsolidated sandpacks verified results expected from bulk gelation tests. In-depth placement was possible by increasing the acetate to chromium ratio above a critical value. Experimental work was initiated to determine the flow behavior of HiVis 350, a partially hydrolyzed polyacrylamide, in a sandpack. A 300-ppm solution of HiVis 350 exhibited shear-thickening behavior over a range of frontal advance rates between 2.3 and 58 ft/d. Polymer retention was a function of flow rate and hydrodynamic retention was observed. Polymer degradation occurred at low flow rates. A series of experiments was completed to determine the permeability and the amount of dehydration that occurs after placement when a gel is under a pressure gradient of either oil or water. Gels studied had permeabilities to water ranging from 5 to 30 microdarcies. Applying a pressure gradient across the gel with either brine or oil dehydrated Cr(III)-acetate-

PHPA gels. Oil dehydrated these gels at pressure gradients as low as 30 psi/ft. Experiments were conducted in sandpacks gelled with chromium acetate-polyacrylamide gelant to demonstrate that dehydration observed in bulk experiments occurred in porous media. Dehydration with oil creates a new pore structure for fluid flow as the gelled polymer is squeezed into a smaller volume and water is displaced from the gel. Flow of fluids occurs primarily in the pore structure created by the dehydration of the gel. The immobile gel reduces the effective porosity. When oil and water phases are present, the "waterflood residual oil saturation" is significantly higher than the water saturation in the new pore space. Differential permeability reduction was observed when dehydration occurred. Experiments were completed to simulate the effect of a gel treatment in a production well to reduce water production. The experiments were done in a Berea sandstone slab (60 cm long by 10 cm wide) which was divided into four equal length segments. The end segment was treated with a chromium(VI)-thiourea-polyacrylamide gel. Relative permeabilities to water and oil were decreased significantly by the gel treatment in the treated section. The range of mobile oil and water saturation decreased significantly after gel treatment. Permeabilities to both phases were functions of flow rates in the treated section. The effective permeability of each phase increased with increasing flow rate of that phase. The permeability data were correlated with flow rate with a power-law function.

Executive Summary

Results from a research program on the application of gelled polymer technology for in situ permeability modification are presented in this report. The objective of this technology when used with displacement processes such as waterflooding is to reduce the permeability in fractures and/or high permeability matrix zones to improve volumetric sweep efficiency of the displacement process. In production wells, the objective is to reduce water influx.

The research program focused on five areas:

- Gel treatment in fractured systems
- Gel treatment in carbonate rocks
- In-depth placement of gels
- Gel systems for application in carbon dioxide flooding
- Gel treatment in production wells

The research program is primarily an experimental program directed toward improving the understanding of gelled polymer systems and how these systems can be used to increase oil recovery from petroleum reservoirs. Results obtained from research conducted in the 28-month program are described in the following sections. In programs where research is ongoing, progress to the end of the contract date is given.

Summary of Results

Gel treatment in fractured systems. Results were obtained from displacement of a partially hydrolyzed polyacrylamide (PHPA)-Cr (III) gelant in a physical model of a fracture and a study of the behavior of the gel after treatment. During displacement of the gelant (mixed in-line) through the fracture, the gelant behaved like a viscous fluid. There was little change in pH or chromium concentration of the gelant flowing in the fracture. A substantial volume of gelant leaked from the fracture into the matrix. Chromium retention was high in the matrix and the gelant that leaked off was not capable of forming a gel.

The mature gel was extruded from the fracture on application of a small pressure gradient. Brine permeabilities of the matrix after contact with the gelant were reduced. Residual resistance factors varied from 70-200 near the fracture to 7.4-11, a distance of about 0.5 ft from the fracture. Values of residual resistance factors from the injection of polymer alone were estimated to be 2.0. Leakoff was simulated by treating the gelant as a viscous fluid flowing through the matrix under a constant pressure drop.

Experiments were conducted to determine the amount of leakoff from gelants of various ages into Berea sandstone cores (1 ft in length) when a constant pressure drop was maintained across the core during placement. Leakoff was significant but decreased as the age of the injected gelant increased from 0 to 6 hours of delay. During gel placement, the pH of the gelant rose from 4.8 at the inlet to 8.0 at the effluent. Chromium retention was high and the effluent did not form a gel. The apparent viscosity increased rapidly with time near the inlet of each core and quickly exceeded the viscosity of the base polymer solution at the same flow rate. Filtration of gel aggregates is believed to be responsible for the high flow resistance developed in the front of the cores. Aging of the gelant prior to displacement causes a faster buildup of flow resistance

near the inlet face of the core. A model describing leakoff during gel placement in a linear system with deep filtration of gel aggregates was developed.

Results from the study of gelation in fractures will enable the development of design procedures to predict the distance that a gelant can penetrate into a fracture when there is leakoff to the surrounding formations. This will assist in the sizing of gel treatments. Our research shows that these gels are easily displaced in fractures, which may explain why it is possible to inject water into wells that have been treated with a gelant.

Gel treatment in carbonate rocks. In previous research, we discovered that sulfomethylation of resorcinol led to increased salinity and pH tolerance of a gel system based on the reaction of sulfomethylated resorcinol (SMR) with formaldehyde. This system provided superior permeability reduction in carbonate rocks compared to current systems.

The focus of our research was to eliminate formaldehyde from the system because of environmental and safety concerns. It was determined that formaldehyde was not present in the SMR even though it was a reactant to produce SMR. Hexamethylenetetramine (HMTA) was studied as a potential substitute for formaldehyde in the resorcinol-formaldehyde and SMRF gel systems. The studies show that the R-HMTA formed gels at 40, 70 and 100°C. The gel system has significantly longer gel times than those observed in the RF or SMRF gel systems due to the hydrolysis of HTMA to form formaldehyde. SMR-HTMA formed hydrogels but higher concentrations were required than in previous research on the SMRF system. The SMR-HMTA gels were thermally sensitive, decomposing at temperatures higher than 40°C, possibly due to the reaction of excess sulfite ion with the polymer. Hydroxymethanesulfonate was investigated as a substitute for formaldehyde in the preparation of SMR, but this did not perform well.

Propagation of chromium in carbonate rock is a limitation of gel systems based on chromium acetate and partially hydrolyzed polyacrylamide. Precipitation of chromium occurs if the pH of the injected fluid increases due to fluid-rock interactions. The first phase of the research program involved a study of fluid-rock interactions between a brine solution and Baker dolomite. Effluent compositions and pH were determined by injecting KCl brine at selected values of pH into a six-inch long Baker dolomite core. Effluent pH and concentrations stabilized when the residence time in the dolomite core was increased to values of just a few hours. This indicated that an equilibrium model would simulate dolomite dissolution when the contact times were a few hours or more.

The effluent pH exhibited a three-stage behavior when the pH of the injected solution increased from 1 to 13. The most significant observation was the strong buffering effect of the rock observed when the injected pH varied between 4 and 10. The effluent pH remained at pH 10 due to buffering caused by dissolution of dolomite. Effluent pH and concentrations were in good agreement with values simulated using the computer program PHREEQE, a geochemical model based on equilibrium relationships. The study of fluid-rock interactions showed that dramatic increases in pH occur by carbonate dissolution when brine solutions that do not have strong buffering capacities are injected through carbonate rocks.

Increased pH triggers chromium precipitation in chromium-acetate solutions. A study of the precipitation of Cr(III) from aqueous solutions was completed. This study includes the effects of pH, temperature and salinity on chromium precipitation and covers a range of pH values from 7 to 11 and temperatures between 25°C and 45°C. Our data show that chromium precipitates faster as pH increases. At low temperatures, there is an induction period before the precipitation begins. The induction time and precipitation rate are functions of pH, temperature and salinity of the solution. The precipitation rate is first order with respect to aqueous chromium concentration after onset of precipitation. The precipitation rate increases with increasing temperature and salinity. Precipitated chromium does not cause the polymer to gel. An empirical kinetic model was developed to correlate the data obtained at 25°C for the precipitation of chromium from chromium acetate solutions.

Results from this research extend the capability of gelled polymer systems for in depth treatment of the matrix in carbonate rocks. A new gelant (SMRF) was developed to reduce the permeability of carbonate reservoir rock at moderate temperatures (~45°C) without using chromium as the crosslinker. This gelant has superior pH tolerance to chromium carboxylate-polyacrylamide gels. Precipitation of chromium occurs from chromium acetate solutions as the pH increases to values anticipated in carbonate rocks. Both pH and mineral composition of the fluid can be estimated using an existing chemical equilibrium simulator. A mathematical model was developed to correlate the rate of precipitation of chromium from chromium acetate solutions at 25°C. Incorporation of this model into a gel simulation program will improve the capability of the program to predict the distance that a chromium acetate solution can be propagated in a carbonate matrix rock.

In-depth placement of gels. Gel systems used to treat a porous matrix are composed of a polymer and a crosslinker. As these components react, pre-gel aggregates are formed and grow in size. The depth of treatment is limited by the filtration of aggregates from solution as they flow through the reservoir rock. Three studies are in progress related to in-depth placement of gels. The first study concerns the rate that gel aggregates grow to form a three-dimensional gel structure. The remaining studies involved two gel systems that were investigated to study in-depth treatment of matrix rock to reduce permeability. These systems were the chromium acetate-polyacrylamide system and an aluminum citrate-polyacrylamide system.

An experimental program was initiated to determine the size distribution of gel aggregates as they grow from polymer molecules to form a gel. A critical part of the study is the development of methods to determine the size distribution of pre-gel aggregates. Two methods were investigated to determine size distribution. The first method was equilibrium dialysis. Aggregates were separated by diffusion through a set of membranes that have selected pore sizes. The concentration of polymer in the dialysate was determined by size-exclusion chromatography (SEC) with an UV detector. Aggregate growth with reaction time was observed for a polyacrylamide-chromium acetate gelant. Procedures to determine aggregate size distributions using equilibrium dialysis were developed and tested.

The second method to determine the size of polymer aggregates is based on Flow Field-Flow Fractionation (FFF). Flow field-flow fractionation is a technique for separating particles by size in order to characterize the particles. The separation occurs in a ribbon-like channel that is

open and contains no packing material. Equipment was acquired and runs were conducted on polystyrene standard spheres to test the performance of the FFFF unit. Preliminary runs on spherical particles indicate that the FFFF is a viable method to determine the size distribution of pre-gel aggregates.

Development of the chromium acetate-polyacrylamide system for in-depth permeability modification requires control of the rate of aggregate growth to slow down the rate of permeability reduction due to filtration of gel aggregates. A study was completed in which the gelation time of chromium-polyacrylamide systems was increased by adding acetate ions to reduce the rate of crosslinking between chromium and polyacrylamide. Bulk gelation data were obtained for a range of acetate/chromium ratios. Displacement experiments were conducted in unconsolidated sandpacks of various lengths to determine the effect of acetate/chromium ratio on in-depth placement. Adding acetate ions as sodium acetate or acetic acid increased gel times of PHPA-chromium acetate systems. Gel times in the range of a few hours to several days at 25°C were attained by varying the acetate/chromium ratio from 3 to 91 in solutions containing 5000 ppm Alcoflood 935 and 109 ppm chromium. Acetate/chromium ratios greater than 260 inhibited gelation for more than a year. Gelation delays were significant beyond a threshold acetate/chromium concentration of about 80 mole/mole for this gel composition. Gel solutions prepared from aged chromium stock had significantly shorter gel times than fresh stock samples. High concentrations of acetate ions in solution were found to offset the effect of chromium stock age.

Sandpacks were conditioned to pH 5 prior to treatment using an acetic acid/sodium acetate buffer. Increasing acetate/chromium ratios delayed the development of flow resistance (and thus aggregate filtration) during gel injection into sandpacks. High acetate concentrations (acetate/chromium = 600) completely inhibited in situ gelation. The time available for gel injection using reasonable injection pressures was significantly shorter than the gel times measured in beakers. This was probably due to filtration of pre-gel aggregates.

Experimental work was initiated to determine the flow behavior of HiVis 350, a partially hydrolyzed polyacrylamide, in a sandpack. This work was done prior to studying the in situ behavior of a gelant consisting of a solution of aluminum citrate and HiVis 350. Experiments were conducted to determine the effect of flow rate and retention on the apparent viscosity of HiVis 350 in unconsolidated sandpacks. All work was done using a 300 ppm concentration of polymer at 25°C. Displacement experiments were conducted in one-foot long unconsolidated sandpacks equipped with pressure ports to determine the pressure drop at specific locations along the sandpack.

The 300-ppm solution of HiVis 350 exhibited shear thickening behavior over the range of frontal advance rates between 2.3 and 58 ft/d. Polymer retention was a function of flow rate. Increased amounts of polymer were retained with each increase in flow rate. Some polymer was expelled when the flow rate was reduced, indicating hydrodynamic retention. Polymer degradation was observed during displacement experiments at low flow rates. The retention of polymer played a significant role in the development of flow resistance of HiVis 350 solutions in a sandpack. Retention of polymer occurred over many pore volumes of injection and was affected by flow that had occurred previously.

Results from this research program show that in depth permeability reduction can be attained in a porous matrix by increasing the ratio of acetate to chromium in chromium acetate-polyacrylamide gelant. This method is effective in low temperature reservoirs (~45°C) and will extend the application of this technology from the near wellbore region as currently applied to in depth treatment of the porous matrix.

Gel systems for application in carbon dioxide flooding. Due to the unfavorable mobility ratio between carbon dioxide and oil, carbon dioxide tends to finger through high permeability zones. In this program, three systems were investigated as possible gelants for in-depth permeability reduction and control of carbon dioxide flow. These were: 1) KUSP1, biopolymer that is soluble in alkaline solution and forms a gel when the pH is reduced or a borate crosslinker is used, 2) a gel (SMRF) formed by the reaction of sulfomethylated resorcinol with formaldehyde and 3) a chromium acetate-polyacrylamide gel capable of total shutoff of brine and carbon dioxide. Most experiments were conducted at a temperature of 41°C in Berea sandstone cores. KUSP1 gelants reduced the permeabilities of brine and supercritical carbon dioxide by 95% to 97% of the original brine permeability. However, KUSP1-boric acid gels exhibited syneresis and were less effective in sustaining the permeability reduction. The SMRF system effectively shut off the flow of both brine and supercritical carbon dioxide. A gelant made from chromium acetate and AlcoFlood 254S (50,000 ppm polymer, 4,167 ppm Cr(III)) shut off flow of brine and supercritical carbon dioxide in the gelled Berea core at pressure drops as high as 300 psi/ft.

Selected gelants can reduce the permeability of porous rocks to the flow of supercritical carbon dioxide at low temperatures (~45°C) and thus reduce channeling due to the high mobility of carbon dioxide. These gelants could be used to control the flow of carbon dioxide in the porous matrix in a carbon dioxide flood.

Gel treatment in production wells. Gels placed in a production well to reduce water production are subjected to pressure gradients of oil and/or water for long periods of time after placement. A series of exploratory experiments was completed on bulk gels to determine the permeability and the amount of dehydration that can occur after placement when a gel is under a pressure gradient of either oil or water. Dehydration experiments were conducted on gels confined in columns that were 10 mm and 35 mm in diameter. Gel systems studied include KUSP1-ester, KUSP1-boric acid, SMRF and Cr (III) acetate-PHPA. All gels were permeable to water with permeabilities ranging from 5 –130 microdarcies. Both KUSP1 gel systems dehydrated extensively under pressure gradients from 35 psi/ft to 76 psi/ft. The SMRF gel did not dehydrate under pressure gradients ranging from 76 psi/ft to 305 psi/ft. Applying a pressure gradient across the gel with either brine or oil can dehydrate Cr (III)-acetate-PHPA gels. Oil dehydrated Cr (III)/PHPA gels at pressure gradients as low as 30.5 psi/ft. In Cr (III)-PHPA gels at low-pressure gradients, the brine flows through the gel and dehydration is low. Dehydration causes a decrease in the permeability of the gel.

Exploratory experiments were conducted in sandpacks gelled with chromium acetate-polyacrylamide gelant to demonstrate that dehydration observed in bulk experiments occurred in porous media. Dehydration was investigated when oil was injected into sandpacks. Dehydration with oil creates a new pore structure for fluid flow as the gelled polymer is squeezed into a

smaller volume and water is displaced from the gel. Flow of fluids occurs primarily in the pore structure created by the dehydration of the gel. The immobile gel reduces the effective porosity. When oil and water phases are present, the "waterflood residual oil saturation" is significantly higher than the water saturation in the new pore space. Differential permeability reduction was observed when dehydration occurred.

Experiments were completed to simulate the effect of a gel treatment in a production well to reduce water production. The experiments were conducted in a Berea sandstone slab (60 cm in length by 10 cm wide) which was divided into four equal lengths. Relative permeabilities to oil and water were determined prior to treatment. Water saturations were measured using a microwave apparatus. A quarter of the length of the slab was treated with a polyacrylamide-chromium (VI)-thiourea gelant and relative permeability measurements were repeated after gelation. Microwave saturation measurements could not distinguish between gel and water after treatment.

Relative permeabilities to water and oil were decreased significantly by the gel treatment in the treated section. Residual resistance factors for oil and water were about the same. Thus, there was no disproportionate permeability modification for this gelant. The range of mobile oil and water saturation in the treated section decreased significantly after gel treatment. Permeabilities to both phases were functions of flow rates. The effective permeability of each phase increased with increasing flow rate of that phase. The relationship between effective permeability and flow rate of each phase was correlated with a power law function. There was no effect of the gel treatment on permeabilities in the untreated sections.

Gel treatments in production wells are not understood. Operators do not know how to select a production well or gelant that will reduce water production with minimal effect on oil production. Results obtained in this contract provide new insight into the mechanisms that control the effectiveness of a gelant to alter water and oil flow in porous rock. Dehydration of a commonly used gel occurs after placement when subjected to a pressure gradient such as occurs when the well is put on production. The gel structure loses water when subjected to a pressure gradient either in oil phase or water phase. Dehydration with oil creates a new pore structure, which exhibits disproportionate permeability to oil. This may explain why some zones penetrated by the gelant during placement can become productive when placed on production. Relative permeability data were obtained for one gelant. These data demonstrate some fundamental changes in flow properties of a porous rock after it is gelled with a chromium acetate-polyacrylamide gelant. Permeabilities to oil and water were reduced by approximately the same factor. However, the relative permeability curves were found to be a function of flow rate. Current "post gelation" reservoir models assume that relative permeability curves are independent of flowrate. This is not correct for the system studied. Further research is needed to translate these results into design procedures.

Chapter 1

Introduction

Research was conducted on the application of gelled polymer technology for in situ permeability modification. The objective of this technology when used in injection wells is to reduce the permeability of fractures or high permeability zones in order to improve the volumetric sweep efficiency of oil recovery processes. In production wells, the objective is to reduce water influx. These technologies are low cost and have the potential to prolong the life of existing reservoirs through reduction of operating costs and increased oil recovery from regions containing by-passed mobile oil.

Alternative gel systems were investigated as a potential substitutes for chromium-polyacrylamide systems. The chemistry of resorcinol-formaldehyde and sulfomethylated resorcinol-formaldehyde gels was studied to determine the possibility of substituting hexamethylenetetramine (HMTA) for formaldehyde in the formulation of gels. Results of this study are presented in Chapter 2.

In-depth permeability modification in a porous matrix is limited by the rate that gel aggregates are formed and removed from the gelant as it flows through the pore space. Chapter 3 describes a study to determine the size distribution of pre-gel aggregates as they form in the gelation of a Cr (III)-partially hydrolyzed polyacrylamide (PHPA) solution. One method is based on equilibrium dialysis of pre-gel aggregates. The second method under study is the use of flow field flow fractionation (FFFF).

Gel placement in the porous matrix of carbonate rocks is influenced by fluid-rock interactions where the calcium and magnesium are dissolved with a corresponding increase in pH of the gelant. Chapter 4 summarizes results from two phases of a three-phase program. The first phase focused on fluid rock-interactions between brine and dolomite core material including experimental and mathematical simulation. The second phase investigated the precipitation of chromium hydroxide from Cr (III)-acetate solutions as a function of pH, temperature salinity and ionic strength.

Gels placed in fractures or a porous matrix can be dehydrated after placement, losing a portion of the water within the gel structure when subjected to pressure gradients. Results from a series of experiments to determine the amount of dehydration that can occur after gelation when a gel is under a pressure gradient of either oil or water are reported in Chapter 5. Estimates of the permeability of gels were obtained. Dehydration of gels in sandpacks was investigated through exploratory experiments.

HiVis 350 is a partially hydrolyzed polyacrylamide, which is used with aluminum citrate to obtain in-depth permeability modification. This gel system is claimed to be a "colloidal dispersion" gelant with aluminum crosslinking with the polyacrylamide to form gel aggregates that reduce the permeability of porous rock. This polymer has unusual properties, particularly when displaced through porous media. Results from a study of the effects of flow rate on flow

resistance and polymer retention on the polymer without the aluminum crosslinker are reported in Chapter 6.

A method to extend the application of the Cr(III)-acetate-PHPA gel system to in-depth treatment of porous rocks by adding acetate ions was demonstrated through results of beaker and displacement experiments. Results are summarized in Chapter 7.

Cr (III)-acetate-PHPA gelants are widely used to treat fractured formations. During placement of these gelants, an unknown amount of the gelant leaks off from the fracture into the adjacent formation. A study to determine leakoff of gelant is described in Chapter 8. This study includes both experimental measurements of leakoff in a physical model of a fracture and development of models to correlate leakoff during gel placement in a linear system with deep filtration of gel aggregates.

Experiments were completed to simulate the effect of a gel treatment in a production well to reduce water production. Changes in relative permeability relationships that occurred after the treatment of a Berea sandstone slab with a chromium(VI)-thiourea-polyacrylamide gelant are presented in Chapter 9.

In the carbon dioxide miscible flooding process, carbon dioxide tends to finger through high permeability zones of a reservoir, bypassing oil in lower permeability zones. Chapter 10 presents results from a study of several gel systems that can be used to reduce the permeability of a porous rock to the flow of supercritical carbon dioxide.

Chapter 2

Resorcinol-Formaldehyde Based Gel Systems

Principle Investigators: J. Heppert, C.S. McCool, and G.P. Willhite

Graduate Research Assistant: Jeff Botts

Summary

Resorcinol - formaldehyde (RF) and sulfomethylated resorcinol - formaldehyde (SMRF) based hydrogels are being developed as an alternative to the chromium-polyacrylamide gel system. Hexamethylenetetramine (HMTA) was studied as a potential substitute for formaldehyde in the RF gel system. These studies showed that the R-HMTA gel system has significantly longer gel times than those seen in the RF and SMRF gel systems due to the time necessary for hydrolysis of HMTA to occur. Hydroxymethanesulfonate (HMS) was studied as a potential substitute for formaldehyde in the sulfomethylation reaction, but this compound would not work under conditions utilized in this reaction. Also, it was determined that formaldehyde was not present after the sulfomethylation reaction was completed. SMR and HMTA also formed hydrogels; the gelation times were the longest observed in the phenolic hydrogel systems studied. The SMR-HMTA gels were thermally sensitive, decomposing at temperatures higher than 40°C. This decomposition results from the reaction of the sulfite ion with the polymer. Effective removal of sulfite ion from the monomer stream is necessary to ensure reproducible gelation of the SMR-HMTA systems.

Background

Resorcinol polymerizes readily with formaldehyde to produce polymers. In the neat reaction, these polymers tend to be hard, highly crosslinked resins [Ravve, 1967]. However, in dilute solutions, resorcinol forms hydrogels with formaldehyde under both acidic and basic conditions. This property allows the gel to substitute for the widely used chromium-polyacrylamide gel system in the oil recovery process.

Under acidic conditions, the RF polymer produced is initially a gel precipitate. However, under basic conditions, firm gels are produced. The gels could form even when the monomer concentration was as low as 1%. Previous researchers also found that the RF gel system possessed a high degree of brine sensitivity [Green et al., 1996]. This property, along with the use of formaldehyde, prompted more research in the area.

To combat the brine sensitivity, the SMRF gel system was developed. In the SMRF gel system, the resorcinol was pre-treated with formaldehyde and sodium sulfite. This mixture was made in the mole ratio of 2 resorcinol : 1.5 formaldehyde : 1 sodium sulfite as shown in Figure 2.1.

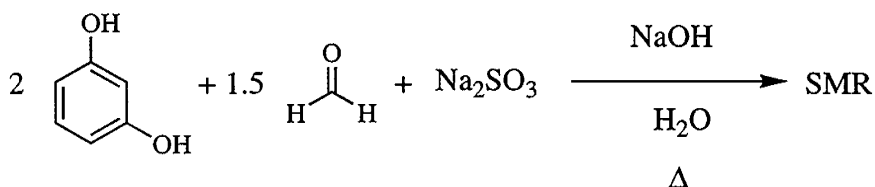


Figure 2.1 - Sulfomethylation of resorcinol

The gel system obtained with this SMR monomer displayed significantly reduced brine sensitivity and longer gelation times. Interestingly, it also displayed apparent reverse kinetic behavior since the gelation process was longer at higher temperatures [Green et al., 1996]. The SMRF system still used formaldehyde in both the SMR preparation step and the gelation step. Elimination of the formaldehyde reactant is desirable based on environmental considerations.

Hexamethylenetetramine (HMTA) is known to be a source of formaldehyde. One mole of HMTA theoretically can supply six moles of formaldehyde as shown in Figure 2.2 [Blazevic and Kolbah, 1979].

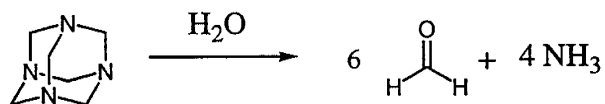


Figure 2.2 - Hydrolysis of hexamethylenetetramine

Therefore, substitution of HMTA for formaldehyde in the gelation process is a potential route to eliminate formaldehyde from the gel system. Also, hydroxymethanesulfonate (formaldehyde-sodium bisulfite addition compound) is reported to be the intermediate in the sulfomethylation reaction [Alaburda et al., 1987; Bordwell et al., 1945]. Therefore, this material is considered to be a potential substitute for the formaldehyde and sodium sulfite in the SMR preparation step.

Results and Discussion

R-HMTA gels. The results of the bottle tests are shown in Table 2.1. At 10% resorcinol and a 0.33:1 HMTA to resorcinol ratio, gel times ranged from 30 minutes at 100°C to 12 days at 40°C. Increasing the concentration of HMTA to a 0.67:1 ratio increased the rate of gelation. These gels formed overnight at 40°C. Decreasing the amount of resorcinol significantly increased the time for gelation to occur. At 3% resorcinol, gelation required about one week even at 100°C. The removal of oxygen affected the appearance of the gels that formed (e.g. the color of the gels). After 30 minutes at 40°C, the control (the one that was not purged with nitrogen) was a rusty orange color, while the sample purged of oxygen was colorless. By the next day, the non-purged gelant was a dark blue solution, while the purged gelant was still colorless. Both gelled by the third day; the non-purged sample was a dark blue gel while the purged sample was a pink gel. No adverse effects of oxygen were seen on the gel times or gel characteristics in the R-HMTA gel system.

Table 2.1 - Gelation times for the R-HMTA gel system.

Resorcinol (wt%)	HMTA (wt%)	Molar Ratio	pH	Temp. (°C)	Gelation Time
10	4.2	0.33:1	8.00	40	12 days
			8.00	70	2 hours
			8.00	100	30 minutes
	6.4	0.5:1	?	40	3 days
			?	70	2 hours
			?	100	30 minutes
	8.5	0.67:1	?	40	Overnight
			?	70	2 hours
			?	100	30 minutes
5.0	2.1	0.33:1	8.17	40	12 days
			8.17	70	1 day
			8.17	100	6 hours
3.0	1.3	0.33:1	8.58	40	5 days
			8.58	70	6 days
			8.58	100	4 days
	1.9	0.5:1	8	40	4 days
			8	70	5 days
			8	100	5 days
	2.6	0.67:1	8.47	40	4 days
			8.47	70	5 days
			8.47	100	5 days
2.0	0.8	0.33:1	8.86	40	no gel formed
			8.86	70	6 days
			8.86	100	6 days
	1.7	0.67:1	8.31	40	6 days
			8.31	70	48 hours
			8.31	100	48 hours
1.0	0.4	0.33:1	9.19	40	no gel formed
			9.19	70	24 hours
			9.19	100	24 hours

Note: some of the pH data is missing due to solubility problems

Sulfomethylation Reaction. Experiments to sulfomethylate resorcinol using HMS yielded no SMR product based on the NMR spectra of the isolated product. Under basic conditions, the solution remained a rusty brown color, even after a week of refluxing the mixture. This was indicative of the oxidation of resorcinol to a quinone, but not of the production of SMR. The peaks (in the NMR spectrum) for the product were at δ 6.88 (t), δ 6.05 (d), and δ 5.87(s). This pattern was significantly different from those obtained in the known sulfomethylation reaction

[Green et al., 1996]. The pattern was indicative of unreacted resorcinol. Acidic conditions also yielded no SMR (peaks were at δ 7.05 (t), δ 6.35 (d), and δ 6.30(s)). Chemical tests verified that all the formaldehyde reacted with resorcinol in the sulfomethylation reaction.

Reactions of RF polymers with sulfite, hydroxide, or ammonia indicated that sulfite and ammonia had negative effects on the polymer. After four hours of refluxing the polymer in the presence of sodium sulfite at a pH of about 9.0, the solid in the flask dissolved. During the dissolution of the polymer, the total sulfite ion concentration (sulfite ion and bisulfite ion) by ion chromatography decreased by over 60 percent. Size exclusion chromatography showed a corresponding increase in the quantity of lower molecular weight organic fragments in solution. It seems likely that the sulfite ion reacts with the polymer to produce smaller, more water-soluble molecules. The pH of this solution after refluxing showed a dramatic increase in the concentration of hydroxide. The final pH of the solution was around 11.0. This indicated that a large amount of hydroxide was being produced from the reaction. The same result was seen when sulfite was added to a bottle containing the RF gel. The question of whether it was actually the sulfite ion or the hydroxide ion that was causing the breakdown of the polymer was answered by refluxing the polymer at a pH of 9.0 and 11.0 without sulfite present. In both cases, the polymer formed a purple gelatinous material within one hour. This material did not breakdown, even after refluxing for a week. In the bottle test, all that occurred was swelling of the gel. Since HMTA produces ammonia (the pH of the R-HMTA and SMR-HMTA gels increased during the gelation period indicating the production of ammonia), the question of whether ammonia affected the gels was answered by the following tests. Refluxing an RF polymer at a pH of around 9 to 10 in the presence of ammonia resulted in a much finer suspension of the polymer. The bottle tests, however, showed the same behavior as that seen in the hydroxide test. This indicated that ammonia had a negative effect on the polymer, but not of the magnitude of the effect of sulfite ion.

SMR-HMTA gels. SMR does not readily gel with HMTA at concentrations of SMR lower than 5% resorcinol. At both 10% and 5% SMR, gels formed at 40°C (within 1 day at 10% SMR and 3 days at 5% SMR.) These gels form at low concentrations of HMTA (0.33:1 to 0.67:1 HMTA to SMR ratios.) However, only at 10% SMR will gels form at elevated temperatures at these HMTA concentrations. Also, a 5% SMR gel that formed at 40°C will decompose if heated to 70°C. This solution will not “re-gel” if maintained at 40°C. The cause for this behavior was attributed to residual sulfite that may be remaining in the solution after the SMR preparation step. The formula may be modified to force SMR to gel with HMTA at SMR concentrations as low as 3% resorcinol. This requires the increase in HMTA content to around 19%, however. No gels have ever formed at SMR concentrations lower than 3% resorcinol content.

The results of the model studies showed that removal of the most reactive site on resorcinol significantly increased the time required for gelation. 2-methylresorcinol was originally thought to be a good model for SMR. The question of SMR having longer gelation time could be explained simply by assuming that the sulfomethyl group is “blocking” the most reactive site on resorcinol (the 2-position.) 2-methylresorcinol, however, is highly insoluble. Only at 3% monomer concentration and a pH of about 11 will this compound dissolve in water. Once dissolved, though, the time for gelation is increased greatly. In fact, after nearly two weeks at

70°C, the only product obtained was a gel precipitate. Pyrogallol was chosen as another model for SMR since this compound has comparable solubility as resorcinol. At 10% pyrogallol (at a pH of 8.42 and temperature of 65°C), gelation took about an hour. At 3% pyrogallol and under similar conditions, gelation takes about a week. To contrast the removal of the most reactive site to the addition of two more sites, phloroglucinol was used. At 10% phloroglucinol (at a pH of 8.48) gelation took 1 minute 57 seconds at 20°C. This shows that the longer gelation times seen with SMR are due at least partly to the removal of the most reactive site on the resorcinol monomer.

Conclusions

1. Resorcinol forms hydrogels with HMTA at resorcinol concentrations as low as 1% resorcinol. These gels form at 40°C, 70°C, and 100°C.
2. R-HMTA gels have longer (approximately 100 times longer) gel times than those observed in the RF and SMRF systems. This is due to the time necessary for hydrolysis of the HMTA to occur and the production of unreactive side products [Blazevic and Kolbah, 1979; Nielsen et al., 1979].
3. Oxygen does not adversely effect the R-HMTA gel times and the R-HMTA gel's physical characteristics.
4. "SMR" is a complex mixture of sulfomethylated products, oligomers, and unreacted resorcinol. The composition of the products is quite sensitive to reaction conditions.
5. Formaldehyde is not present after sulfomethylation of resorcinol in completed based on chemical tests.
6. HMS, which had been proposed as an intermediate in the reaction, will not work as a substitute for formaldehyde in the preparation of SMR under the conditions used.
7. Sulfomethylated resorcinol will gel with HMTA at concentrations of SMR as low as 3%.
8. SMR-HMTA gels are more thermally sensitive than R-HMTA gels since gels form at 40°C, but not at 70°C. This behavior is due to a reaction between SMR based gels and residual sulfite on the polymer at higher temperatures. Formulations must be modified to develop SMR-HMTA gels that do not exhibit this thermal sensitivity.
9. Model studies show that SMR gelation kinetics can also be attributed to the removal of the most reactive site on the resorcinol monomer.

Chapter 3

Measurement of Aggregate Size During Gelation

Principal Investigators: G. P. Willhite, D. W. Green, and C.S. McCool

Graduate Research Assistant: Pau Ying Chong

Introduction

Gel treatments are used to control fluid movement in oil reservoirs by reducing the permeability of selected zones. Gels are formed in situ by the crosslinking of polymer molecules. Pre-gel aggregates form and grow in size to form gel [McCool et al., 1991]. Aggregates are filtered from the injected solution during flow through reservoir rock. The filtered aggregates create flow resistance and affect the placement of the gelant.

Knowledge of the size of gel aggregates as they grow from polymer molecules to form a gel allows for the improvement of the application of gelled polymer treatments. The objective of this work is to develop methods to determine the size distribution of pre gel aggregates.

Two methods to measure the size distributions of pre-gel aggregates were investigated. One method was based on equilibrium dialysis (EqD). The results of the EqD method were reported in an annual report [Green et al., 1998] and are summarized below. A second method to measure size distributions utilized flow field flow fractionation (FFFF). This method separates particle/aggregates by size during flow through a channel [Benincasa and Giddings, 1992, 1997]. Progress on applying FFFF to the measurement of aggregate size distributions is reported.

Summary of Results Using the Equilibrium Dialysis Method. Size distributions of polymer/aggregates were determined in a gelant that had reacted for selected time periods. The gelant contained 5000 ppm Alcoflood 935, 100 ppm chromium (as chromium acetate) and 1% potassium chloride. The gelant had a gel time of 12 hours. After a gelant sample had reacted for a specified time period, the crosslinking reactions were quenched. Aggregates were separated in a set of dialysis cells using membranes that had selected pore sizes. Polymer concentrations in the dialysis products were determined by size-exclusion chromatography. Size distributions were calculated knowing the amount of polymer on each side of the membrane. [Green et al., 1998] gives experimental details.

Size distributions were determined for the polymer solution (without crosslinker) and for gelants that were allowed to react for ten minutes and for nine hours. The gel time for this gelant was 12 hours. The size distributions are given in Table 3.1. The results show that there was little difference in aggregate size between the polymer solution and the 10-minute old gel. Aggregate growth was observed in the 9-hour old gel sample.

Flow Field Flow Fractionation. Flow field-flow fractionation is a technique for separating particles by size in order to characterize the particles [Giddings, 1984; Meyers, 1997]. Unlike other chromatographic methods, the separation occurs in a ribbon-like channel that is open and contains no packing material. A schematic of a FFFF fractionator is shown in Figure 3.1. Carrier

Table 3.1 – Size distributions measured with equilibrium-dialysis technique.

Size range (μm)	Size Distribution (wt.%)		
	Polymer solution	Gel 10-minutes old	Gel 9-hours old
0.0--0.1	15	15	17
0.1--0.2	24	27	24
0.2--0.4	36	34	28
0.4--0.6	18	15	17
0.6--0.8	2	6	3
>0.8	5	3	11

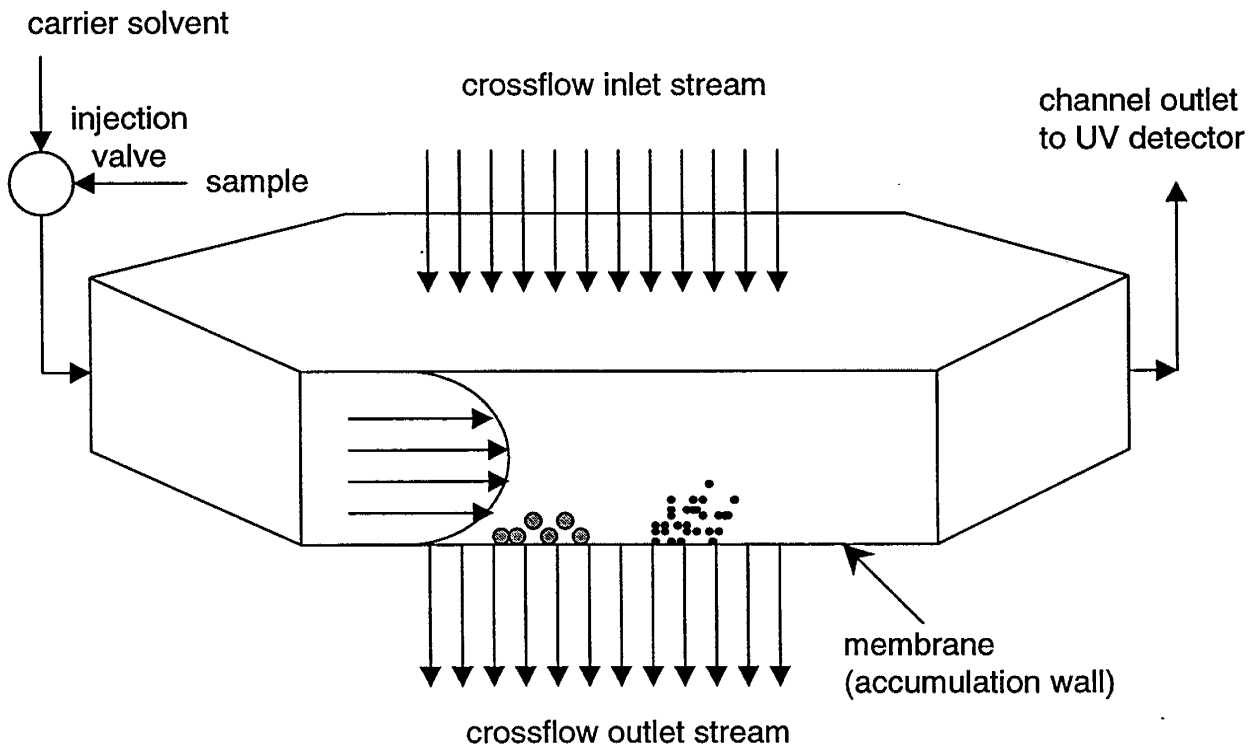


Figure 3.1. - Schematic of flow field-flow fractionation channel.

fluid flows through the channel (channel flow) with a parabolic velocity profile. The top and bottom of the channel are fabricated from porous material, which allows for the flow of a second carrier fluid (crossflow) across and perpendicular to the channel. A sample is introduced into the channel flow using an injection valve. As the sample travels through the channel, the crossflow forces the particles in the sample to the crossflow outlet or accumulation wall. A semi-permeable membrane located at the accumulation wall allows for solvent passage but not particles in the sample. As the particles flow through the channel, the viscous drag of the cross flow on the

particles is offset by diffusion. Diffusion rates of particles are related to their size. Large particles diffuse slower and accumulate closer to the accumulation wall. Smaller particles diffuse faster and accumulate farther from the wall. Being farther from the wall, the smaller particles elute from the channel faster due to the parabolic velocity profile in the channel. An inline UV detector determines the mass of the particles as a function of elution time from the fractionator.

The relationship between elution time and particle size is derived from theoretical models of the transport processes (laminar flow along the channel length, viscous drag and diffusion in the direction of the crossflow) and the Stokes-Einstein equation that relates particle size to the diffusion coefficient [Giddings et al., 1976]. Equation 3.1 provides the relationship between particle diameter, d , and elution time, t

$$t = \frac{t^o}{\frac{2kTV^o}{\pi\eta dw^2V_c} - 12\left(\frac{kTV^o}{3\pi\eta dw^2V_c}\right)^2} \quad \text{Eq. 3.1}$$

where,

- d = diameter of particle
- k = Boltzmann's constant
- t = elution time
- t^o = time for non-retained particle to elute from channel (channel void volume/flow rate in channel)
- V^o = channel void volume
- V_c = volumetric rate of crossflow
- w = channel thickness
- T = temperature
- η = viscosity of carrier liquid

FFFF is a versatile separation technique in that the forces responsible for separation are easily adjusted. Modifications to the fractionator, such as the frit-inlet and frit-outlet, have improved the versatility and fractionating power of the method [Giddings, 1990]. The frit inlet speeds the initial process of positioning the sample at the accumulation wall in the fractionator. The frit outlet improves the detection capabilities by concentrating the sample going through the detector.

Experimental Details

Experiments were conducted with a Model F-1000 FIFO Universal Fractionator (FFFractionation, LLC; Salt Lake City, UT). The channel dimensions were 2.0 cm wide, 28 cm long and 0.0141 cm thick. The channel was equipped with a frit inlet and a frit outlet. Three pumps were required for operation as shown in Figure 3.2. The channel flow pump provided flow through the sample valve, channel and detector. A second pump was configured in a loop to control flow into the frit inlet and out of the frit-outlet. A third pump was configured in a loop to control the crossflow. Samples were introduced with an injection valve equipped with a 10 μ L sample loop. Material eluted from the channel was measured using a Waters 490 UV detector. Data were collected during a run by computer using the Flow-160 program (FFFractionation,

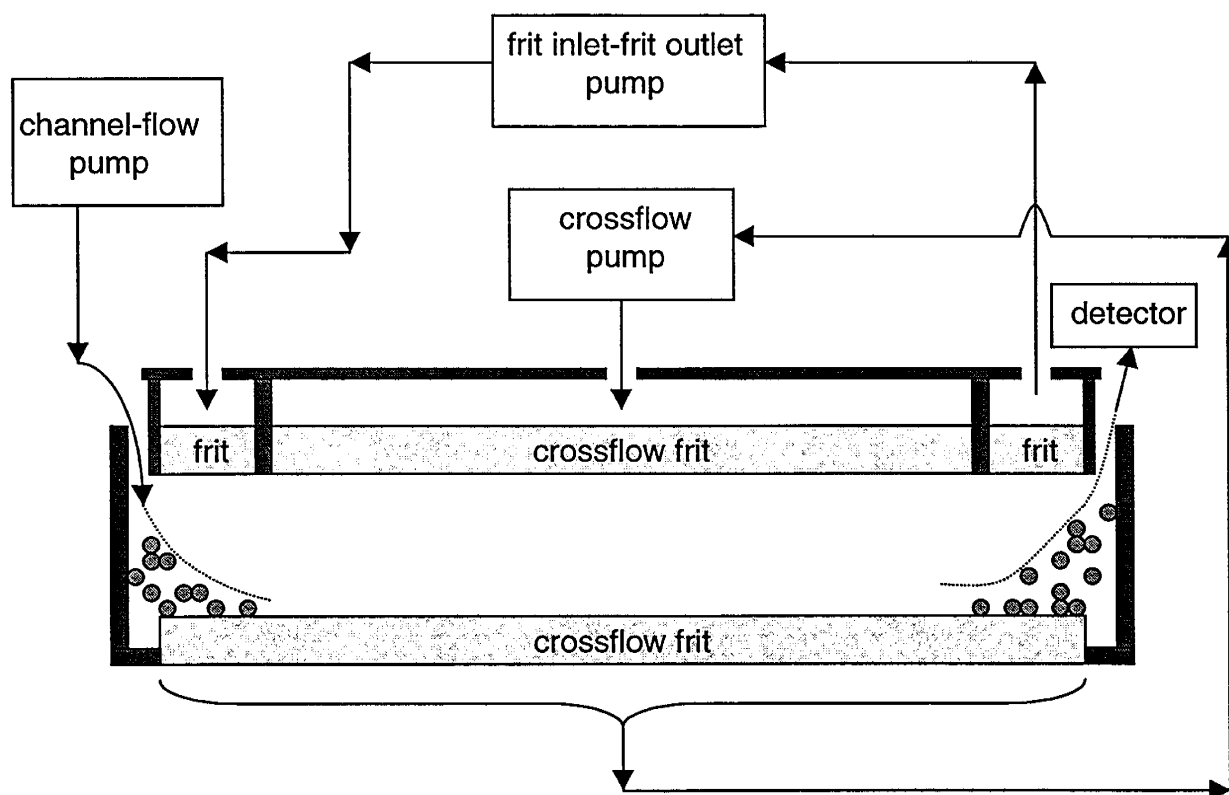


Figure 3.2. – Schematic of pumps and flow paths for FFFF channel.

LLC; Salt Lake City, UT). Data were analyzed on a computer using the FFF Analysis program (FFFractionation, LLC).

Polystyrene latex spheres with diameters of 102 ± 3 nm and 300 ± 5 nm were obtained from Duke Scientific. The carrier solvent (for all flow streams) was distilled, deionized water containing 0.02 wt% sodium azide (bactericide), 20 mM sodium phosphate (buffer agent) and 0.02 wt% Triton X-100 (surfactant). The solvent was degassed and filtered through a $0.22 \mu\text{m}$ membrane prior to use.

Results and Discussion

Runs were conducted to test and improve the performance of the FFFF system to fractionate samples. These runs were conducted on samples prepared with polystyrene standard spheres that have narrow size distributions. The size of the particles was chosen to correspond to the aggregate sizes determined by the method using equilibrium dialysis.

The response of the UV detector as a function of the time for a series of runs on samples containing polystyrene standards (diameter = 102 ± 3 nm) is shown in Figure 3.3. The peaks of the response curves occurred at essentially the same time for the range of concentration studied.

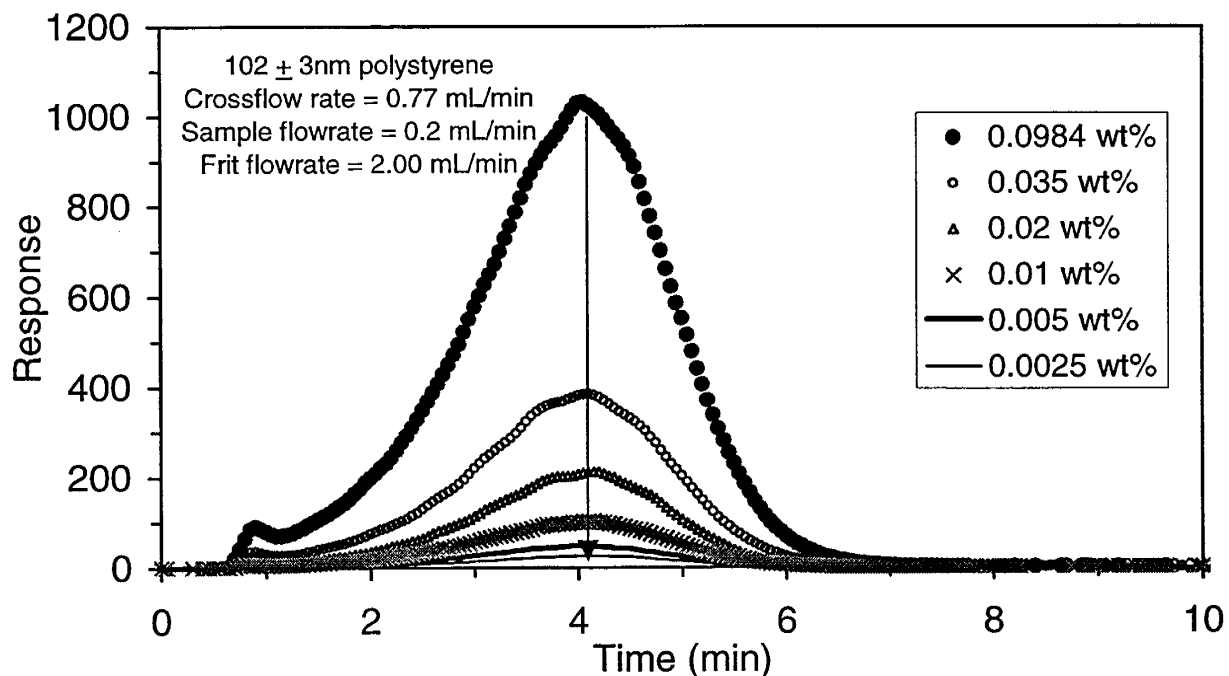


Figure 3.3. – Response of detector as a function of time for FFFF run.

These data were converted to size distributions that are shown in Figure 3.4. The distribution has a peak at 105 nm, close to the diameter specified by the manufacture of the spheres.

The size distributions for a series of runs on samples containing spheres with diameters of 300 ± 5 nm are shown in Figure 3.5. The distributions exhibit peaks at 285 nm, reasonably close the specified diameter. Larger-diameter tails were observed in the distributions as the concentration of the sample decreased.

Size distributions for samples containing spheres with diameters of 102 and 300 nm are shown in Figure 3.6. Peaks in the distribution were observed at the appropriate diameters showing the capability of the FFFF system to fractionate particles.

The size distributions of samples containing one or two sizes of sphere showed the proper diameter at the peak response. However, the peaks were broad and showed considerable percentages of mass at diameters greater than and less than the narrow distribution reported by the manufacturer. Additional testing is required to improve the resolution of the FFFF method. Work is in progress to improve the resolution by optimizing the channel thickness and the flow rates of the three flow streams. Size distributions of aggregates in gelant samples will then be measured using the FFFF equipment. The preliminary runs on spherical particles indicate that the FFFF is a viable method to determine the size distributions of pre-gel aggregates.

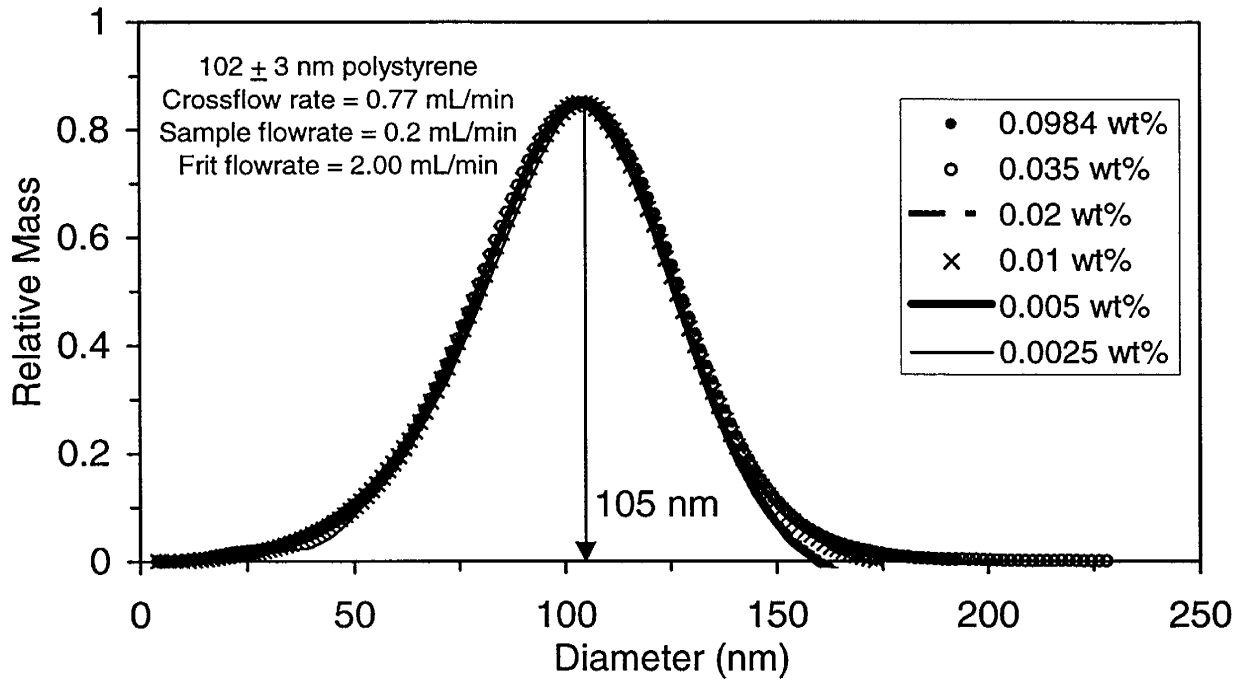


Figure 3.4. – Size distribution of a sample containing particles with a diameter of 102 nm.

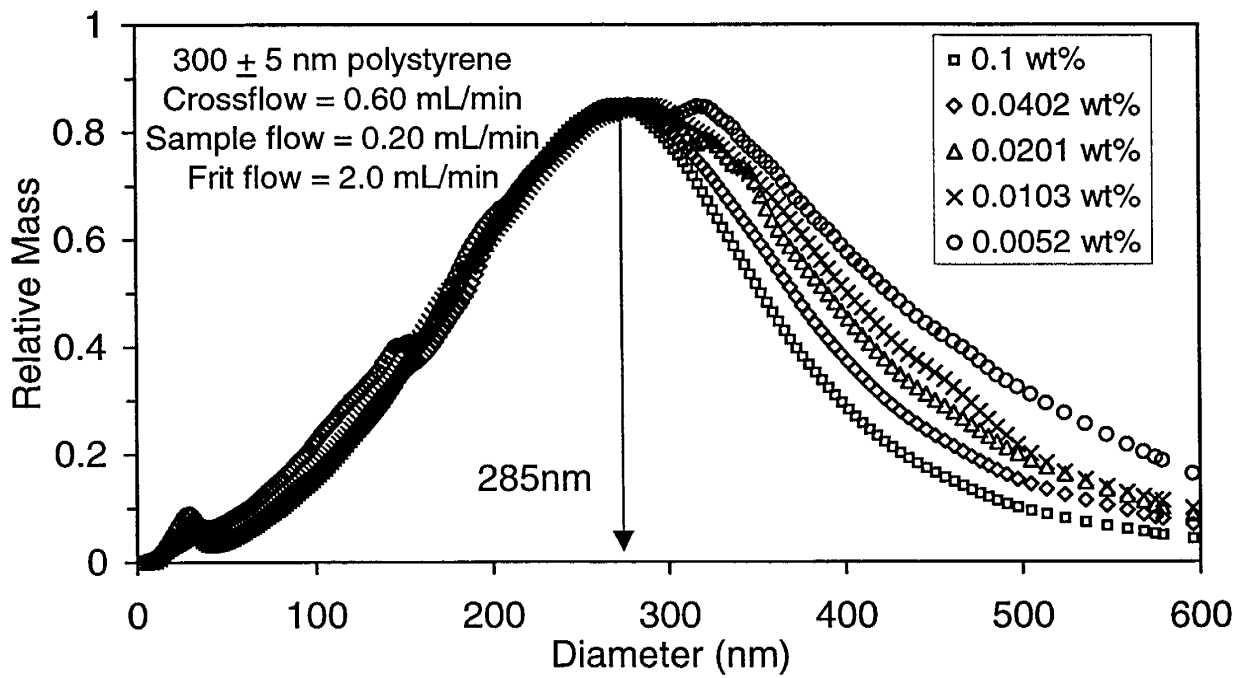


Figure 3.5 – Size distribution of a sample containing particles with a diameter of 300 nm.

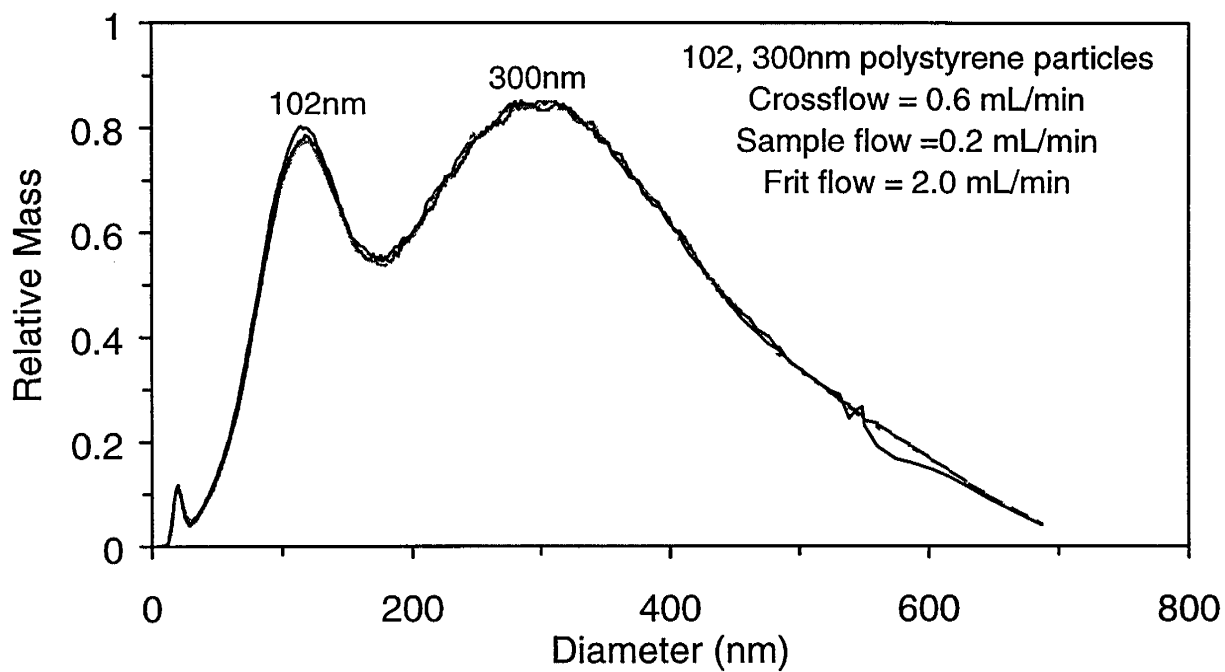


Figure 3.6 - Size distribution of a sample containing particles with diameters of 102 and 300 nm.

Conclusions

1. Procedures to determine aggregate size distributions using equilibrium dialysis were developed and tested.
2. Aggregate growth with reaction time was observed for a polyacrylamide-chromium acetate gelant.
3. Size distributions of spherical particles were determined using FFFF (flow field-flow fractionation).

Chapter 4

Chemical Interactions Between Brine Solutions and Dolomite and Chromium Precipitation from Chromium (III) Acetate Solutions

Principal Investigators: G.P. Willhite, D.W. Green, C.S. McCool
Graduate Research Assistant: Bin Zou

Introduction

Injecting gelant to change the flow characteristics of a reservoir is a viable improved oil recovery technique. Systems utilizing chromium(III) as a polymer crosslinker are one of the most popular gel systems. Successful treatments using chromium-crosslinked gels in carbonate reservoirs requires the understanding of fluid-rock interaction and the transport of chromium in reservoir materials. This chapter reports research conducted to improve the understanding of the propagation of chromium-crosslinked gels in carbonate reservoirs. The work was divided into three phases. Fluid-rock interaction between a brine solution and Baker dolomite was studied in the first phase. Experimental results and mathematical simulations of the fluid-rock interactions were reported earlier [Green et al., 1997; Zou et. al., 1998] and are summarized below.

The precipitation of chromium hydroxide from chromium acetate solution was investigated in the second phase. Green et al. [1998] reported initial experimental results. The completed experimental results and a kinetic analysis of the data are reported here.

The third phase of the work includes chromium transport and in situ gelation experiments, and the numerical modeling of these experiments, all in carbonate materials. Results from the third phase will be reported later. This three-phase project will contribute to a better understanding of the gelation of chromium-crosslinked systems in carbonate reservoirs as well as to carbonate embedded sandstone reservoirs, especially for in-depth profile control.

Background

Several research groups [Sorbie; 1991; McCool et al, 1995; Seright, 1992; Stavland, 1993] have studied the application of chromium-crosslinked gel systems to carbonate (or carbonate containing) reservoirs. Results show that the polymer propagates through carbonate (or carbonate containing) rock but poor propagation was observed for Cr(III). It was concluded that the retention of chromium was caused by precipitation brought on by the elevated pH environment that was caused by the dissolution of carbonates.

McCool et al. [1995] studied the interaction between a dolomite core and a xanthan-Cr(III) gel system. Solutions containing chromium chloride or chromium acetate were injected through a 10-cm long dolomite cores. Only 0.5 ppm (which corresponded to 1% of the chromium concentration in the injected solution) was detected in the effluent after four pore volumes of solution were injected as a chromium chloride solution. Significant amounts of Cr(III) precipitated when chromium was injected as a chromium acetate solution. McCool et al. concluded that the chromium was retained due to precipitation at elevated in-situ pH levels.

Seright [1992] studied the propagation of chromium acetate or chromium chloride through 14-cm long Indiana limestone cores. Cr(III) concentration in the effluent never reached the injected concentration after injecting about 10 pore volumes of chromium solution. Chromium propagated more rapidly when the counterion was acetate as opposed to chloride. No chromium was detected in the effluent after injecting 10 pore volumes of chromium chloride solution through a limestone core, indicating that chromium was removed from solution by precipitation.

Stavland et al. [1993] studied the retention of chromium in Brent and Berea sandstone cores (with about 2% carbonate content). They found precipitation was the most important reason for chromium retention in cores. Precipitation was caused by the dissolution of carbonate minerals that increased the pH of the injected solution. Their experiments also revealed that the retention rate of Cr(III) was lower with less carbonate present in the cores.

Chromium precipitation was the result of the elevated pH environment caused by carbonate dissolution. Carbonate dissolution and the effect on pH behavior was the focus of the first phase of this research and reported in detail by Green et al. [1997]. Chemical interactions between injected brine and a dolomite core were studied by injecting KCl brine at selected pH values through a six-inch long Baker dolomite rock. The effects of injected pH and residence time (or flow velocity) on the pH and concentrations of calcium and magnesium in the effluent were determined. These effluent values stabilized when the residence time in the dolomite core was increased to values of just a few hours. These results suggested that an equilibrium model would simulate dolomite dissolution for the flow of brines in dolomite in which the contact times are a few hours or more.

The measured pH and magnesium concentration in the effluent (for contact times of a few hours) as a function of the pH of the injected KCl brine are shown by the symbols in Figure 4.1. Also shown by the lines in Figure 4.1 is a simulation of appropriate geochemical reactions using the computer program PHREEQE [Parkhurst et al., 1980]. The effluent pH exhibited a three-stage behavior when the pH of the injected solution increased from 1 to 13. The effluent pH was much higher and increased as the injected pH was increased up to a value of 4. When the injected pH was between 4 to 10, the effluent pH was around 10 due to a strong buffering effect. The effluent pH closely matched the injected pH for injected pH values above 10. At the lowest pH stage, effluent concentration of magnesium (and calcium) decreased sharply as the pH of the injected brine increased. In the middle stage, the divalent ion concentrations were constant and not a strong function of pH. In another set of experiments where magnesium and/or calcium were present in the injected brine, dissolution of dolomite was depressed and effluent pH was lowered as compared to the cases when the divalent ions were not in the injected solution.

The study of fluid-rock interactions showed the dramatic increases in pH that can occur by carbonate dissolution when brine solutions that do not have strong buffering capacities are injected through carbonate rocks. The increased pH environment triggers chromium precipitation. Chromium precipitation is a kinetic process [McCool et al., 1995] and the rate and solubility are dependent upon many parameters. The solubility of Cr(OH)₃ as a function of pH is shown in Figure 4.2. These curves were calculated using constants from Rai et al. [1987].

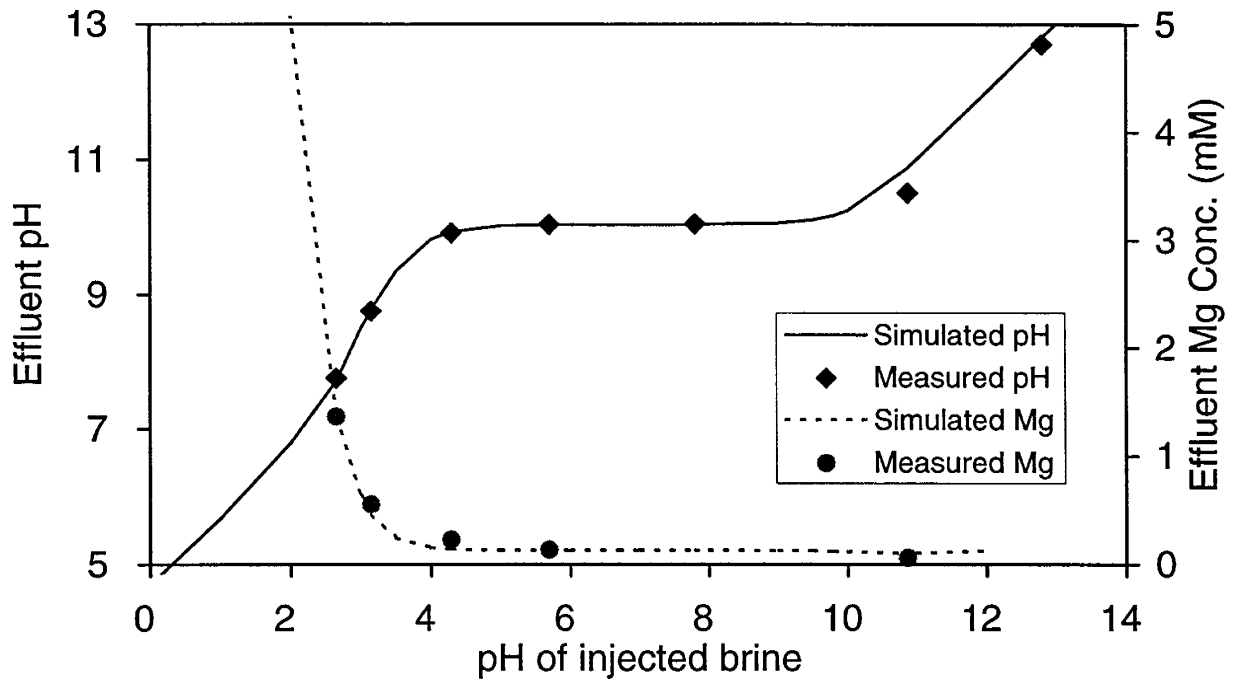


Figure 4.1 - Effluent pH and magnesium concentrations as a function of the pH of the injected brine.

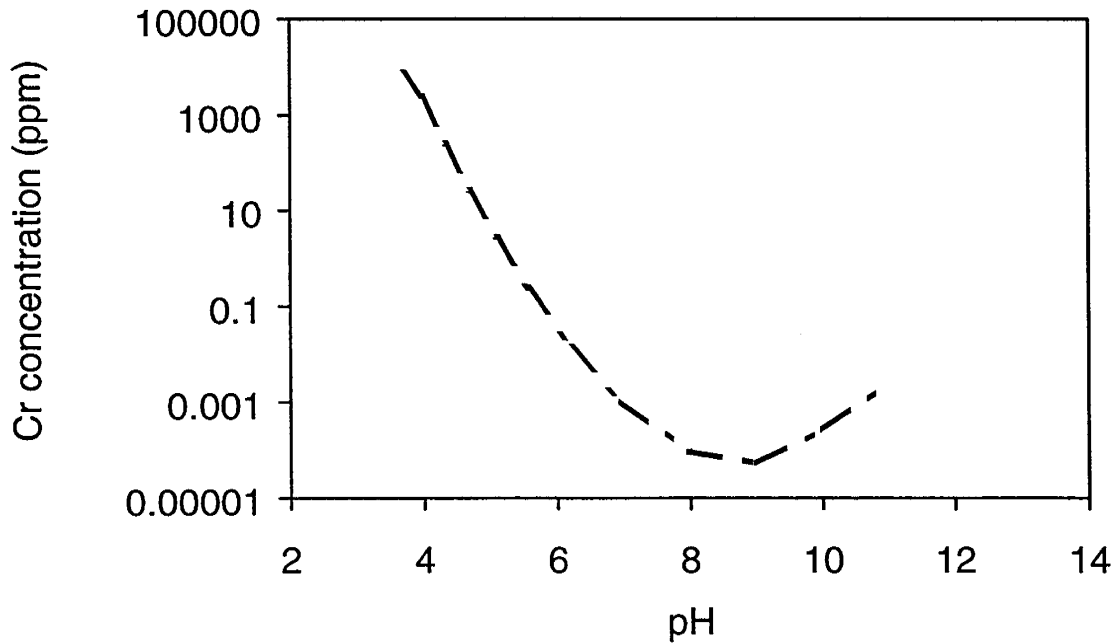


Figure 4.2 - Solubility of chromium(III) as a function of pH.

A characterization study of aqueous chromium acetate [Tackett, 1989] showed that dissolving solid chromic triacetate in water produced a complex mixture in which bridge-structured trimers were the dominant species, including both cyclic and linear trimers. The base hydrolysis of the trimers led to the substitution of hydroxyl groups for the bridging acetate groups, and a break of the polynucleic bond. Tackett did not determine if the chromium precipitated from solution directly in a polymeric form or by forming monomeric $\text{Cr}(\text{OH})_3$. Bryant [1996] indicates that the precipitation of chromium is a slow irreversible formation of insoluble $\text{Cr}(\text{III})$ colloids $[\text{Cr}(\text{OH})_3(\text{H}_2\text{O})_3]$.

There are many factors affecting the precipitation rate of chromium. In this work, the effects of pH, temperature, salinity, acetate ligand concentration and salt type on chromium precipitation were studied using pH-stat titrations. The pH range studied was between 7 and 11, the temperature range between 25 to 45°C, the salinity range between 0 and 5% KCl, and the ratio of acetate to chromium from 3 to 9. The effect of the type of salts on precipitation was also studied for monovalent and divalent chlorides.

Experimental

Materials. The chromium triacetate used in the pH-stat spontaneous precipitation experiments was obtained from Alfa Products. The empirical formula of the material is $\text{Cr}(\text{OAc})_3 \cdot \text{H}_2\text{O}$. The chromic chloride, $\text{CrCl}_3 \cdot 6\text{H}_2\text{O}$, was obtained from Fisher Scientific. The titrant was 0.1 M NaOH (Fisher Scientific) unless described otherwise. Reagent grade potassium chloride was used to adjust the ionic strength in the solution. Distilled, de-ionized and de-aerated water was used to prepare all solutions. Except for those specified otherwise, all chromic acetate solutions were prepared by dissolving solid $\text{Cr}(\text{OAc})_3 \cdot \text{H}_2\text{O}$ in 1% KCl brine. The pH of 200 ppm $\text{Cr}(\text{OAc})_3$ solution was around 4.5, which remained unadjusted during the aging period prior to titration. Generally, the aging period for chromium solution was at least 7 days. Acetic acid (1.0 M) prepared from reagent-grade glacial acetic acid was used to adjust the ratio of acetate to chromium.

Apparatus and Procedure. A Fisher Titrimeter II Titration System, consisting of electrometer, titrate demand, and burette/dispenser modules, was used for the pH-stat titration. A motor driven adjustable stirrer was used to provide a constant stirring speed. A 250 mL double-walled glass reaction beaker was used to contain the chromium triacetate solution. Water was circulated through the jacket to provide a constant temperature. A nitrogen blanket was used to minimize the invasion of CO_2 from the atmosphere. The pH was monitored by a Fisher pH electrode, and recorded by either a chart recorder or a computer. A schematic of the apparatus for the titration system is shown in Figure 4.3.

The turbidity of the solution during titration was measured using a Perkin Elmer UV/VIS spectrometer Lambda 20. The chromium concentration in solution was measured using a Perkin Elmer 460 atomic absorbency spectrophotometer.

For each run, 223 grams of a 200 ppm chromium acetate solution were charged to the reaction beaker and allowed to attain the desired temperature. Addition of 0.1 M NaOH into the reaction beaker initiated the experiment. The addition rate of the NaOH solution was dependent on the

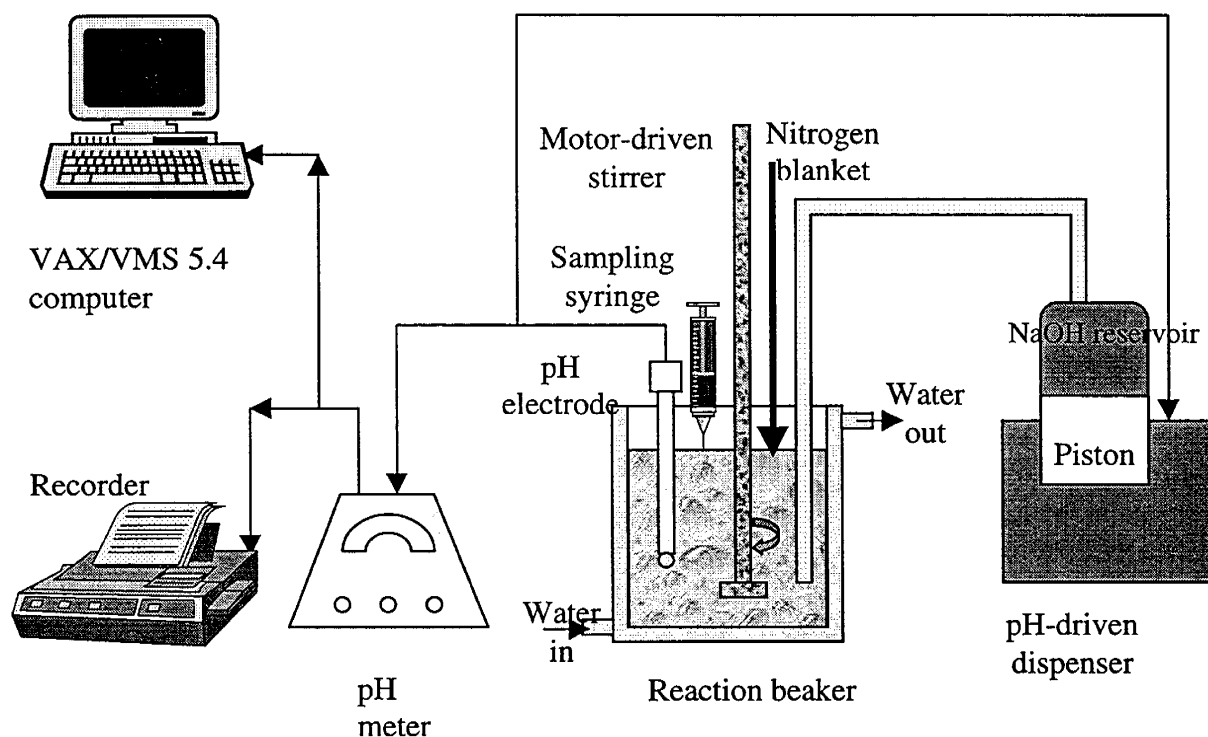


Figure 4.3 - Schematic of the apparatus for pH-stat experiments.

difference between the solution pH and the set value. The desired pH value was targeted in about 1-5 minutes. Thereafter, the Titrimeter system added NaOH solution to keep the pH at the desired value.

Samples were taken periodically from the reaction beaker for turbidimetric and chromium concentration analysis. Turbidity was measured at 900 nm wavelength. Samples taken for measuring turbidity were measured within 30 seconds to prevent flocculation and settlement. Samples taken for determining aqueous chromium concentration were processed immediately to separate precipitated solids from liquid phase. The separation methods used were either filtering the solution through 220 nm filter or centrifuging at 14000 rpm for 3 minutes. Samples were then acidified to around pH 2 by addition of 1.0 M hydrochloric acid to stop precipitation.

Results and Discussion

Precipitation was determined by measuring the remaining chromium dissolved in the solution. Studies [Grundl, 1993] have identified the separation of colloidal particles from the solution as the primary obstacle to obtaining accurate measurement of concentration in solution. The two separation methods used in this study, micro-filtration by filtering the solution through a 220 nm filter and centrifuging the solution at 14000 rpm for 3 minutes, were equally effective at separating precipitated solids from the solution.

Typical results from a chromium precipitation experiment are shown in Figure 4.4. The temperature was 25°C and the pH was 10. Two stages were observed during the runs, an induction period and a precipitation period that slowly approached an equilibrium chromium concentration. Very little precipitation was observed during the induction period. Thereafter, the chromium concentration decreased markedly for a period of time. The onset of increased turbidity occurred almost simultaneously with the loss of chromium in solution, which showed the turbidity measurement correlated with precipitation. Quantitative correlation of turbidity with the amount of precipitated chromium was difficult because the size, shape and refractive index of the particle affect the light scattering properties of the suspension.

Runs were conducted to study the effects of different parameters on the precipitation of chromium. Experimental conditions for each run are given in Table 4.1.

Effect of pH. The effect of pH on chromium precipitation at 25°C is shown in Figure 4.5. The pH was controlled at values between 7 and 10. The induction period decreased from 1200 minutes to less than 200 minutes as pH increased from 7 to 10. Precipitation rates were higher at higher pH values.

Effect of salinity. The effect of salinity on chromium precipitation was studied by adjusting the potassium chloride concentration from 0 to 5wt% in the chromium solutions. The experiments were performed at 25°C and the pH was controlled at 9. The induction period decreased and the precipitation rate increased with increased KCl concentration as shown in Figure 4.6.

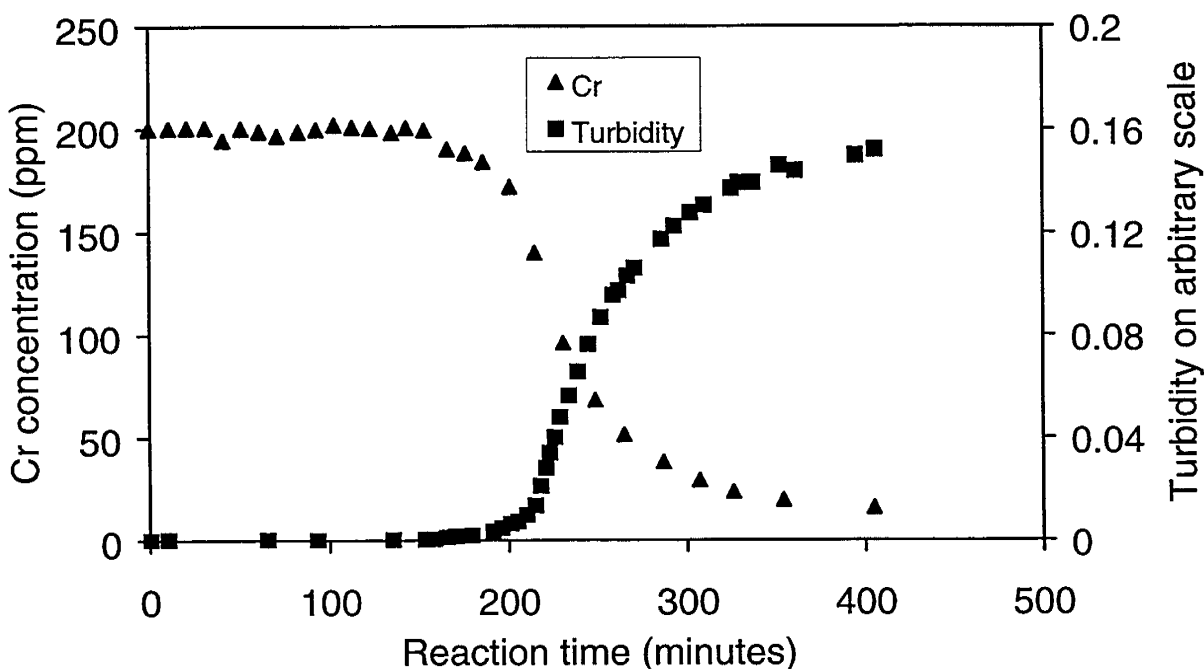


Figure 4.4 - Chromium concentration and turbidity as a function of time during pH-stat experiment.

Table 4.1 - Representative experimental list.

Series I :Effect of pH						
Run #	Initial solution	Salinity	Temp. (°C)	OAc/Cr	pH controlled	Ionic strength* (M)
20	200 ppm Cr(III) in chromium acetate	1% KCl	25	3	7	0.16
10		1% KCl	25	3	8	0.16
17		1% KCl	25	3	9	0.16
14		1% KCl	25	3	10	0.16
Series II: Effect of Salinity						
34	200 ppm Cr(III) in chromium acetate	0	25	3	9	0.03
35		0.4% KCl	25	3	9	0.08
17		1% KCl	25	3	9	0.16
36		5% KCl	25	3	9	0.64
Series III: Effect of Temperature						
17	200 ppm Cr(III) in chromium acetate	1% KCl	25	3	9	0.16
22		1% KCl	35	3	9	0.16
23		1% KCl	45	3	9	0.16
Series IV: Effect of OAc/Cr Ratio						
17	200 ppm Cr(III) in chromium acetate	1% KCl	25	3	9	0.16
32		1% KCl	25	6	9	0.16
33		1% KCl	25	9	9	0.17
Series V: Effect of Chromium Salt Type						
10	200 ppm Cr as in acetate	1% KCl	25	3	8	0.16
11	200 ppm Cr as in chloride	1% KCl	25	0	8	0.16
Series VI: Effect of Salt Type						
17	200 ppm Cr(III) in chromium acetate	1% KCl	25	3	9	0.16
40		0.5% CaCl ₂	25	3	9	0.16

* Average value during run.

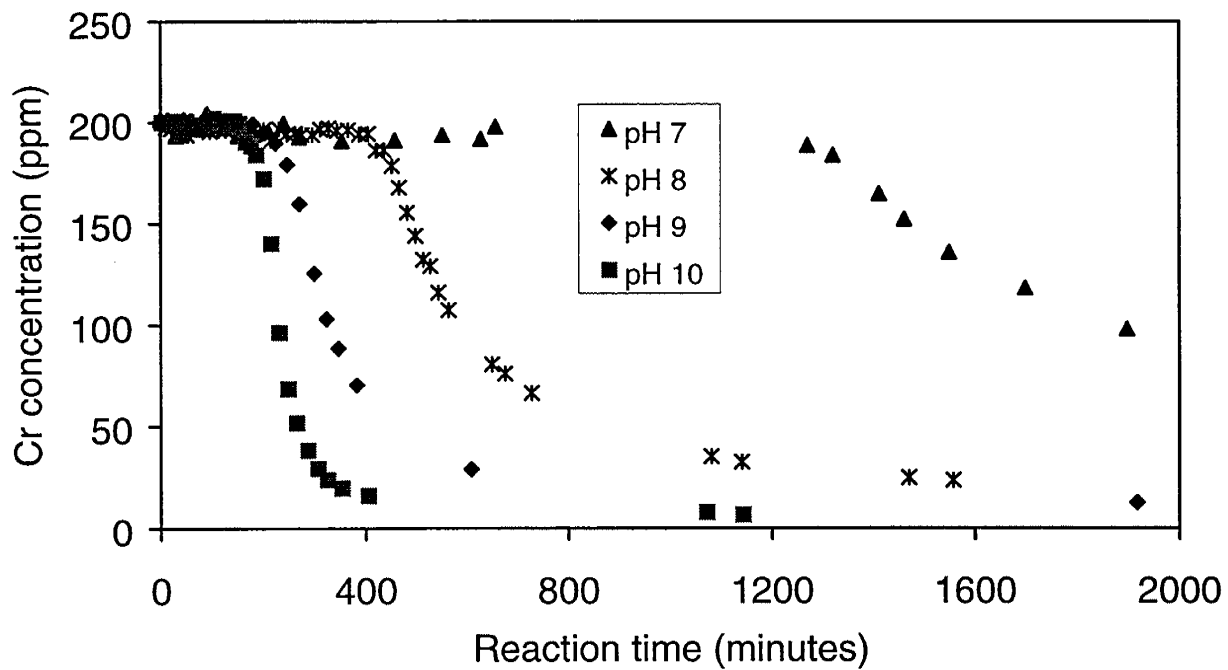


Figure 4.5 - Effect of pH on chromium concentration as a function of time.

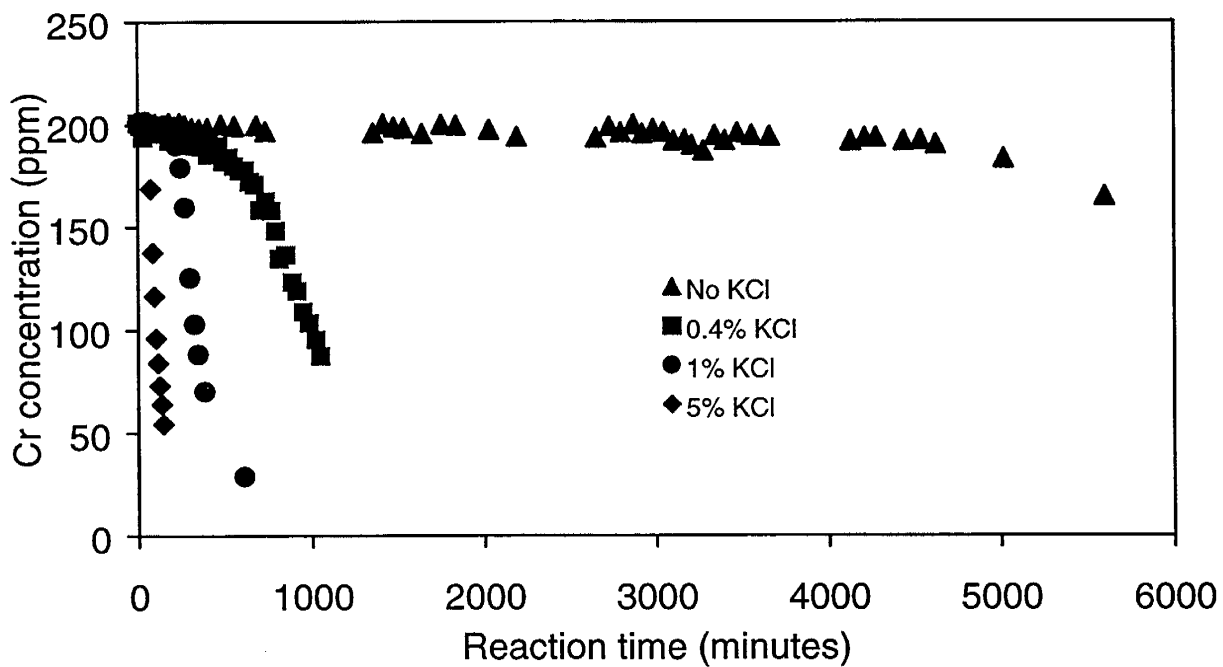


Figure 4.6 - Effect of salt concentration on chromium precipitation during pH stat titration.

Precipitation in the solution containing 5% KCl occurred immediately while very little precipitation was observed for three days in the solution containing no KCl.

Effect of temperature. The effect of temperature on chromium precipitation is shown in Figure 4.7. The runs were conducted at 25, 35 and 45°C and the pH was controlled at 9. The induction period decreased sharply with increasing temperature. The chromium profile was steeper at higher temperature, indicating the precipitation rate was more rapid. An analysis using the Arrhenius equation gave an activation energy of 111 kJ/mol. The magnitude of the activation energy suggested that the precipitation process was controlled by either the hydrolysis reaction or nucleation [Konishi et al., 1997].

Effect of acetate-to-chromium ratio. The effect of acetate ligand concentration on chromium precipitation was studied by varying the acetate to chromium ratio from three to nine. A ratio of three represents a solution prepared with the chromium acetate salt without added sodium acetate. The average ionic strength for each varied from 0.155 to 0.173 M, which should not significantly affect the chromium precipitation. The results of this series of runs are shown in Figure 4.8. No significant change in the length of the induction period or the precipitation rate was observed for the acetate-to-chromium ratios between 3 and 9.

Effect of chromium salt type. In the studies of McCool et al. [1995] and Seright [1992], the retention of chromium in the rock samples was much greater when the solution was prepared with chromic chloride than when it was prepared with chromic acetate. Experiments were conducted at 25°C and a pH of 8 to compare the precipitation rates of solutions prepared with chromium chloride and chromium acetate. The results are shown in Figure 4.9. Precipitation in the chromium chloride solution occurred immediately as the pH of the solution was being adjusted to a value of 8. More than 99% of the chromium precipitated within 10 minutes. The concentration of chromium in the chromium acetate solution showed no significant change during a 400 minute induction period.

Effect of salt type. Two experiments were conducted at 25°C, pH of 9 and at the same ionic strength to compare the effect of salt type. One solution contained 0.5% CaCl₂ and the other solution contained 1% KCl. Chromium concentrations in solution as a function of time are shown in Figure 4.10. Precipitation occurred immediately with no induction period for the chromium solution containing CaCl₂. The precipitation rate in solution with CaCl₂ was about two orders of magnitude faster than that in solution with 1% KCl.

Auxiliary experiments. Experiments were performed to understand the characteristics of the precipitated chromium, presumably chromic hydroxide. The precipitated chromium hydroxide from a titration experiment was collected on a 0.45 µm membrane during filtration. The filtrate was rinsed with water three times. The precipitate was then divided in three portions. One portion was mixed in a solution containing 5000 ppm polyacrylamide. Chromium concentration in the mixture (if fully dissolved) was approximately 200 ppm and the pH of the mixture was 6.2. The mixture did not gel within 6 months and the added precipitate was still present as a solid. The second and third portions of the precipitate were emerged into pH 2 and pH 13.3 solutions. The precipitate dissolved at both high and low pH values by measuring the chromium concentration in the solutions, confirming that chromium hydroxide is amphoteric.

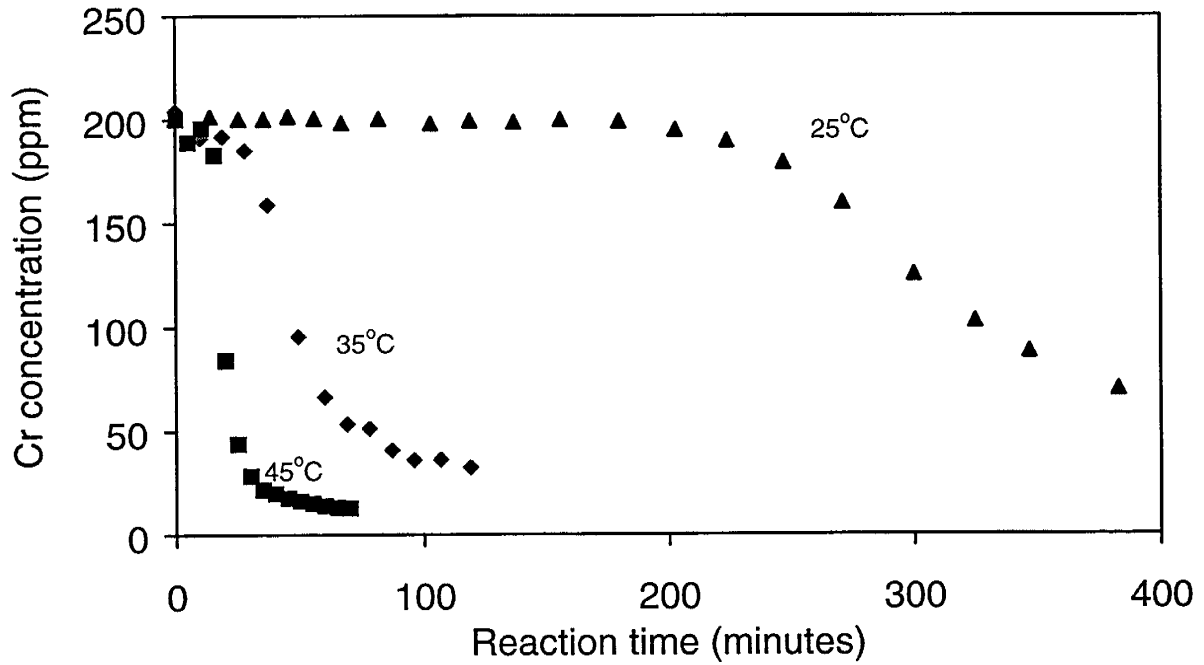


Figure 4.7 - Effect of the temperature on chromium precipitation.

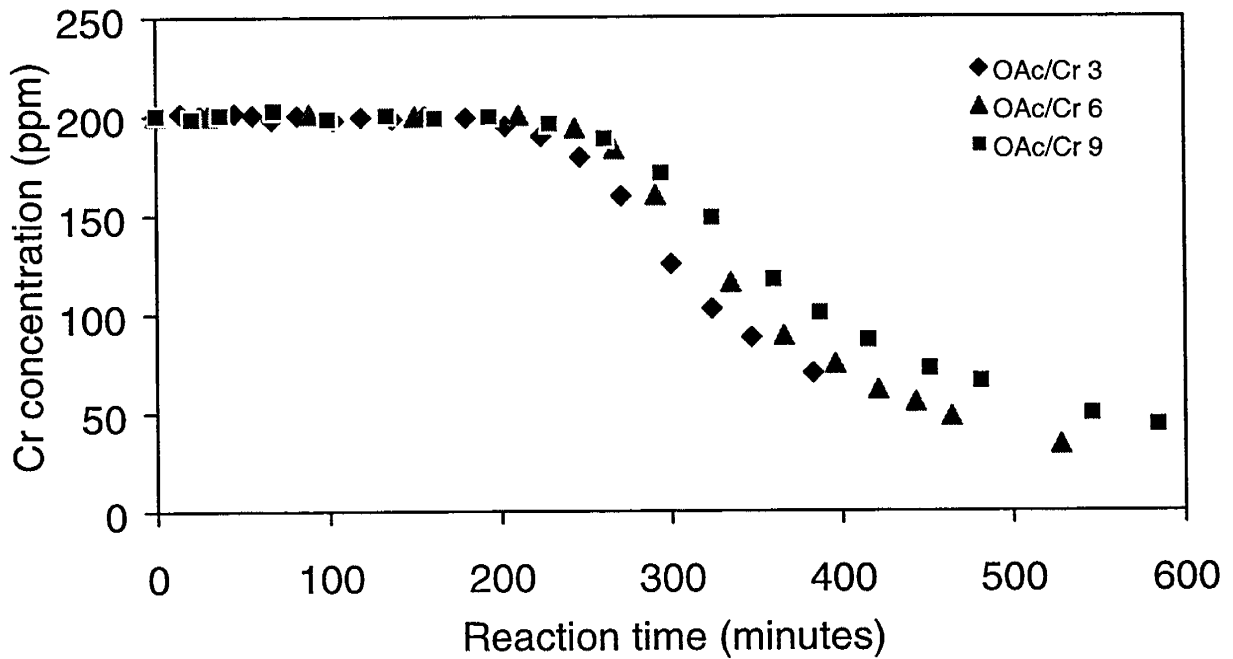


Figure 4.8 - Effect of the acetate concentration on chromium precipitation.

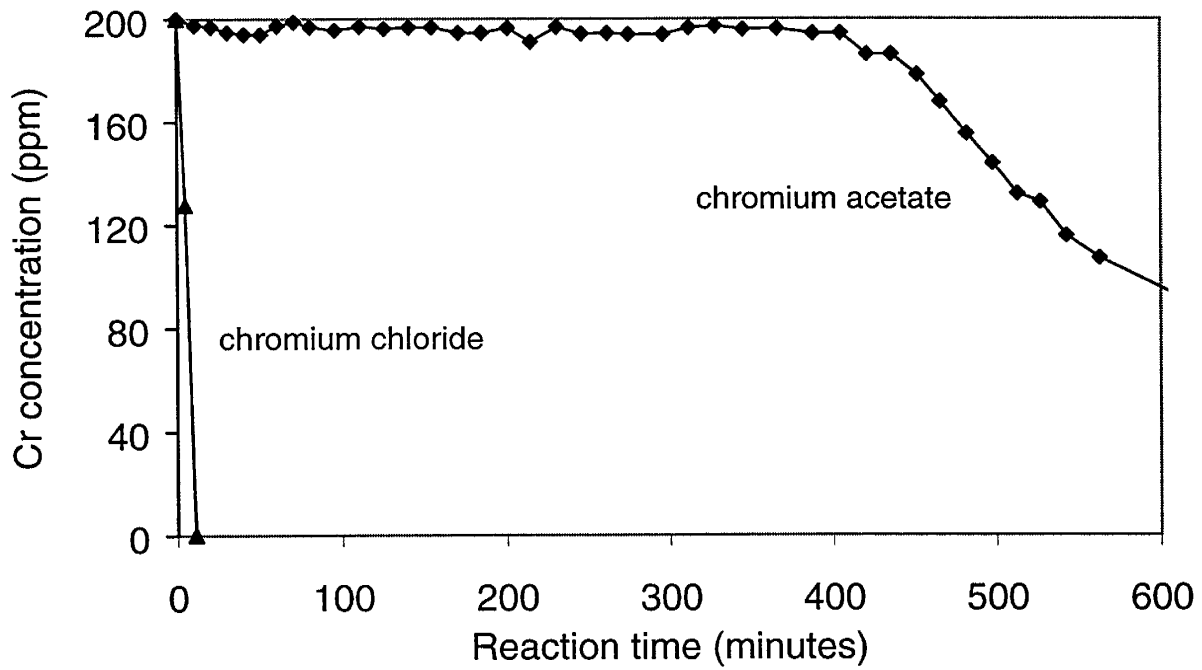


Figure 4.9 - Effect of chromium salt on the precipitation of chromium.

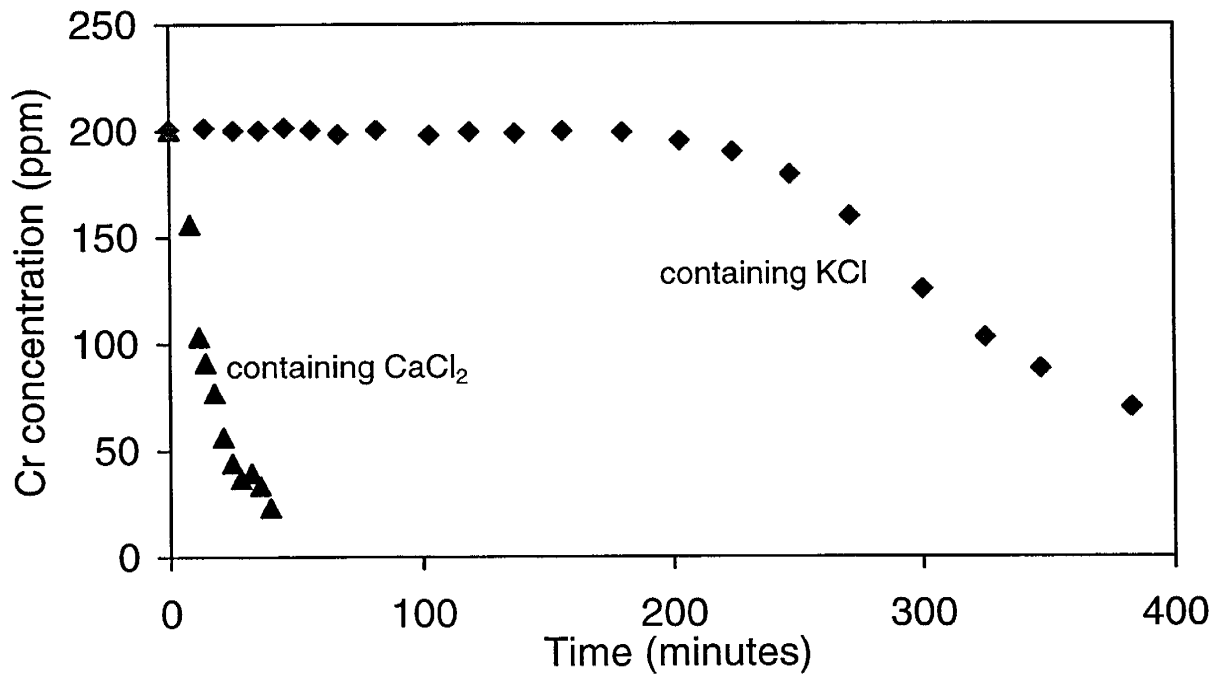


Figure 4.10 - Effect of divalent and monovalent ions (same ionic strength) on chromium precipitation.

Kinetic Model

A kinetic model was developed to represent the data on the precipitation of chromium from chromium acetate solutions. The model describes the precipitation after the initial induction period. Work is in progress on correlating the length of the induction period to the parameters investigated, particularly for the situation when pH varies during precipitation.

The precipitation of chromium was described by following the chromium concentration in solution, a quantity that is more useful for modeling gel polymer treatments. The empirical rate equation used to describes the chromium concentration in solution was

$$\frac{dC_t^*}{dt'} = -k_0 C_t^* [OH^-]^\beta [OAc]^\gamma, \quad \text{Eq. 4.1}$$

where

$$C_t^* = \frac{C_t - C_{eq}}{C_0 - C_{eq}}$$

C_t = chromium concentration at time t'
 C_{eq} = chromium concentration at equilibrium
 C_0 = chromium concentration at time $t' = 0$
 t' = time from onset of precipitation (after induction period)
 k = kinetic constant
 $[OH^-]$ = hydroxide ion concentration
 $[OAc]$ = total acetate concentration
 β, γ = fitting parameters.

Integrating Eq. 4.1, with the initial condition

$$C_t^* = 1 \text{ at } t' = 0, \quad \text{Eq. 4.2}$$

gives

$$\ln \frac{C_t - C_{eq}}{C_0 - C_{eq}} = \ln C_t^* = -k_0 [OH^-]^\beta [OAc]^\gamma t'. \quad \text{Eq. 4.3}$$

Eq. 4.3 can be written as

$$\ln C_t^* = k' t' \quad \text{Eq. 4.4}$$

where

$$k' = -k_0 [OH^-]^\beta [OAc]^\gamma \quad \text{Eq. 4.5}$$

The precipitation experiments were conducted at constant hydroxide and constant total-acetate concentrations. Values of k' were determined for each run by a linear least-squares regression of the data in the form of $\ln C_t^*$ and t' according to Eq. 4.4. Examples of the regressions for several runs are shown in Figure 4.11.

The values of k_0 , β and γ were regressed according to Eq. 4.5 that was written as

$$\log (-k') = \log k_0 + \beta \log [OH^-] + \gamma \log [OAc] \quad \text{Eq. 4.6}$$

Values of the $\log(-k')$ were plotted as a function of the $\log[OH^-]$ for runs conducted at the same acetate concentration. The value of k_0 , β are given in Table 4.2 and were derived from the intercept and slope of the regressed line through the data as shown in Figure 4.12. The same procedure was used to determine k_0 and γ from runs that were conducted at the same pH and different total acetate concentrations as shown in Figure 4.13. The values k_0 and γ are given in Table 4.2. The values of k_0 from the two sets of data were similar and the average was 2.6×10^{-3} /second.

From the above analysis, the kinetics of chromium precipitation kinetics (at 25°C, 1% KCl) can be described by

$$\ln C_t^* = -k_0 [OH^-]^{0.37} [OAc]^{-1.2} t' \quad \text{Eq. 4.7}$$

where, $k_0 = 2.6 \times 10^{-3}$ /s.

A comparison between the experimental data and Eq. 4.7 is shown in Figure 4.14.

Table 4.2 - Calculation of rate dependence on pH and acetate concentration.

For β (Oac/Cr = 3)	Log (- K')				β	k_0 (1/s)
	pH 7	pH 8	pH 9	pH 10		
	-2.85	-2.28	-2.04	-1.71		
For γ (pH = 9)	Log(- K')			γ	k_0 (1/s)	
	Oac/Cr 3	OAc/Cr 6	OAc/Cr 9			
	-2.15	-2.47	-2.70			-1.2

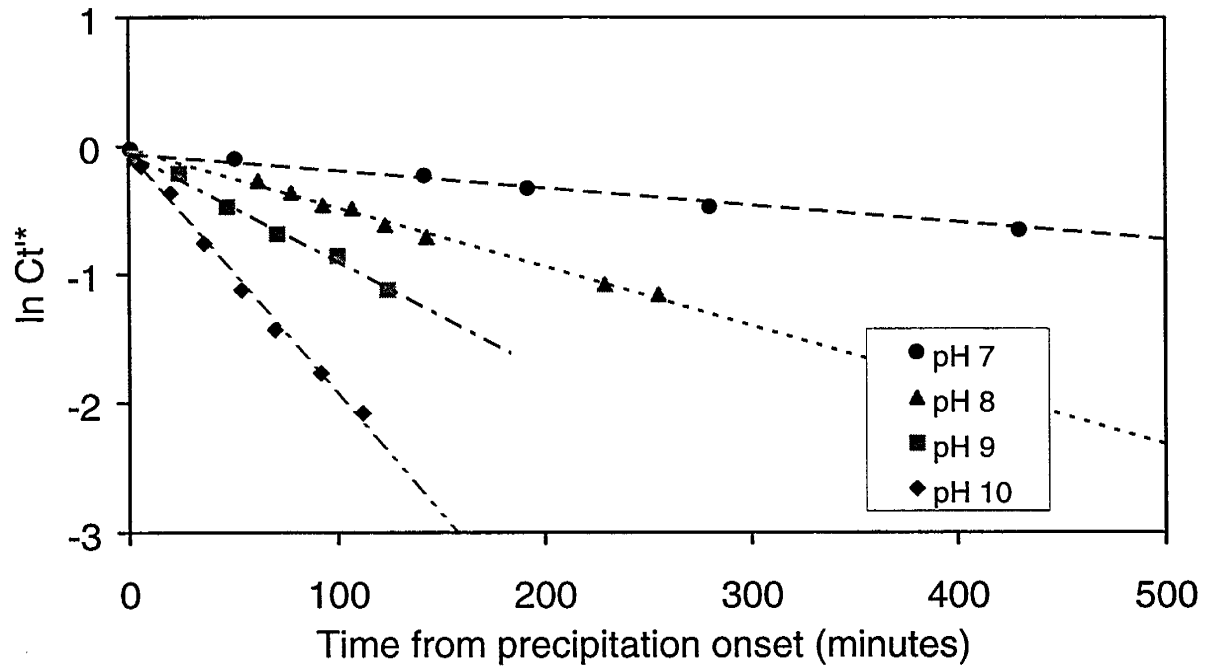


Figure 4.11 - Chromium concentrations as a function of time and pH.

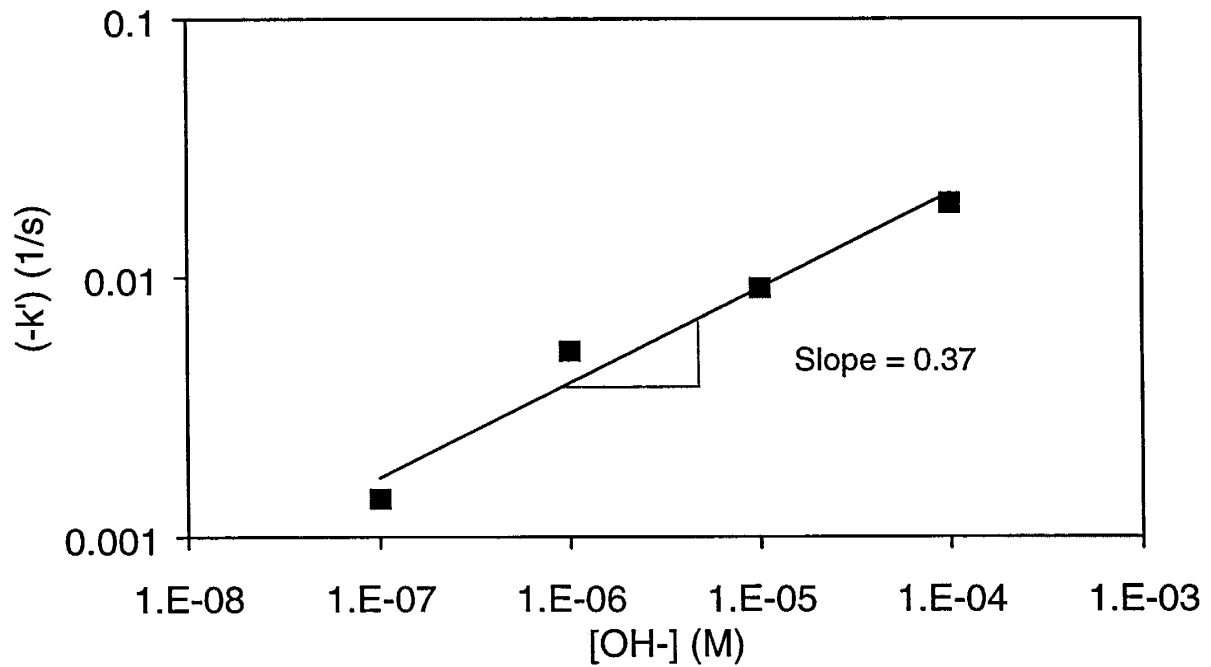


Figure 4.12 - Determination of β from rate constants of experiments conducted at different pH values

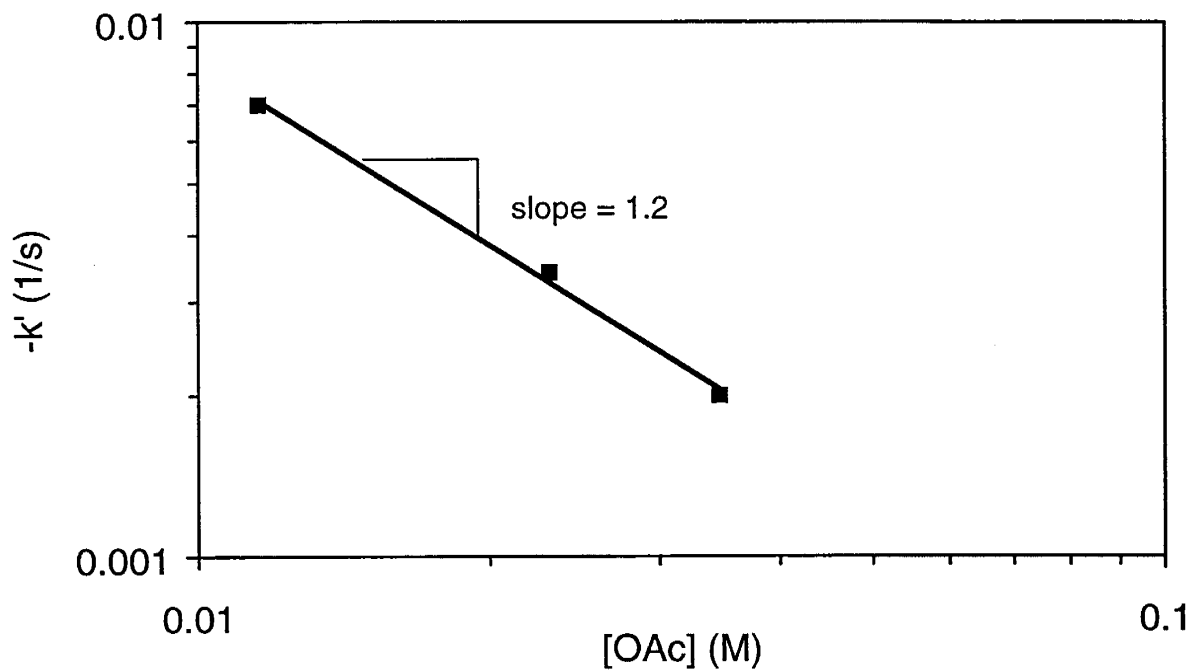


Figure 4.13 - Determination of γ from rate constants of experiments conducted at different Oac concentrations.

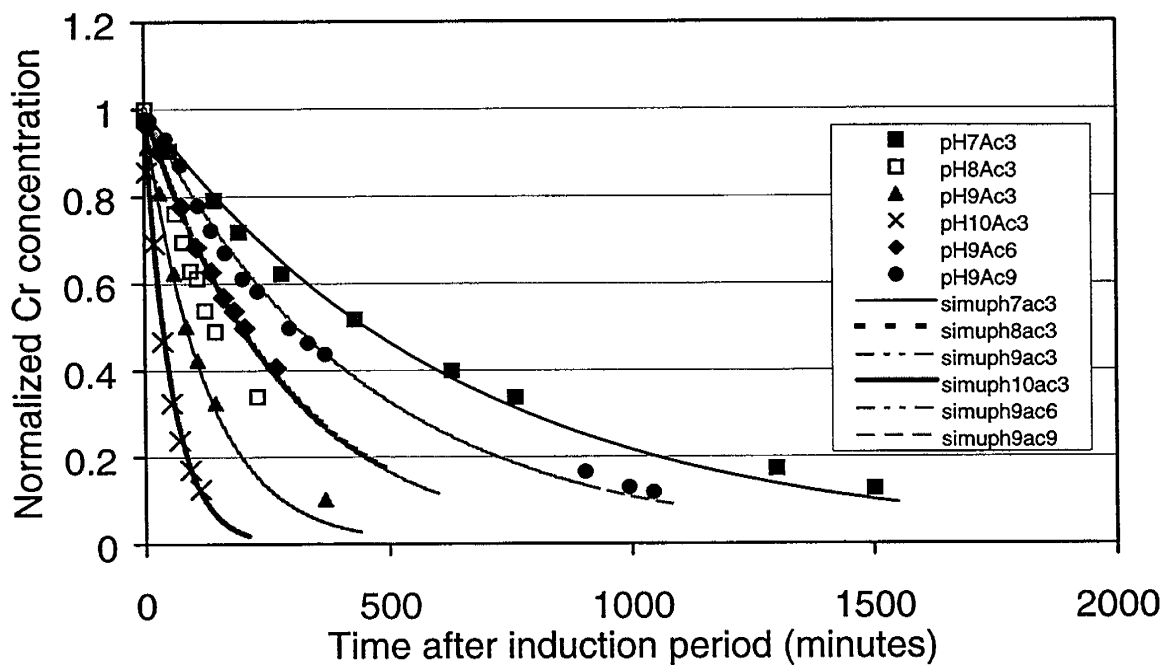


Figure 4.14 - Comparison between the experimental data and predicted results of the rate equation.

Conclusions

1. The stability of chromium acetate in caustic solution was studied by spontaneous precipitation of chromium hydroxide under pH-stat titration. The induction time and precipitation rate are highly dependent on temperature, pH, ionic strength, the chemical nature of salt, and acetate concentration.
2. The induction time decreases and precipitation rate increases with increasing pH.
3. An increase on temperature results in faster precipitation. An apparent activation energy of 111 kJ/mol was obtained between 25°C to 45°C.
4. An increase in salinity from none to 5% KCl was found to accelerate the precipitation.
5. The chemical nature of salt exerts a significant effect on precipitation. At the same ionic strength, precipitation was much faster in solution containing CaCl₂ than in solution containing KCl.
6. Precipitation was retarded by addition of acetate between an acetate-to-chromium ratio of 3 to 9.
7. Precipitated solids [Cr(OH)₃] were not directly available for crosslinking.
8. At 25°C, 1% KCl, the precipitation rate measured from onset of precipitation is adequately described as:

$$\ln C_t^* = -k_0 [OH^-]^{0.37} [OAc]^{-1.2} t'$$

where, $k_0 = 2.6 \times 10^{-3} /s$.

Chapter 5

Permeability and Dehydration of Polymer Gels after Placement

Principal Investigators: G. P. Willhite, D.W. Green, C.S. McCool, M.J. Michnick,
and S. Vossoughi

Graduate Research Assistants: Koorosh Asghari, Praveen Krishnan, Dilip Natarajan

Introduction

In injection wells, aqueous gelants are injected into high permeability regions and/or in fractured formations to reduce the permeability of water with the expectation that water injected after the treatment will flow through less permeable portions of the reservoir and displace oil. In production wells, gelants are placed to reduce water production without affecting oil production. In both situations, the gelled polymer is subjected to a pressure gradient of oil and/or water for a long period of time after placement.

In a recent paper by [Dawe and Zhang, 1994], the flow of oil and water through a chromium xanthan gel was investigated using micromodels. One observation in this paper was that oil could be displaced relatively easy through their gel, creating its own flow path. This could occur only if the oil displaced water from the gel structure (dehydrating the gel) as the flow path was created. In contrast, brine flowed through the gel indicating that the gel was permeable to brine. The behavior of gels subjected to pressure gradients is not understood.

The research presented in this chapter was carried out in three separate sets of experiments. The first set consisted of exploratory experiments designed to investigate, for different gels, gel permeability and dehydration under a pressure gradient. Results from these experiments indicated that several gels could be dehydrated under pressure gradients of the magnitude expected in field applications. The second set of experiments was a systematic study of the dehydration and gel permeability of a chromium acetate-polyacrylamide gel. The third set of experiments was conducted to determine if dehydration could be measured in sandpacks that were treated with chromium acetate-polyacrylamide gels to reduce the permeability. This part of the experimental program was exploratory.

Background

When an aqueous gelant is placed in most porous rocks or fractures, the gelant displaces the aqueous phase and fills the volume that is accessible to the aqueous phase. There is no observable change in volume of the gelant upon gelation. If the gel does not swell or shrink (synerese), the permeability to brine after treatment is determined primarily by the permeability of brine in the gel and its ability to resist deterioration when a pressure gradient is applied across the gel. Because most gels used in oil recovery applications contain from 90% to 99.5% (by weight) water, the reduction in brine permeability is attributed to the immobilization of water by the three dimensional, crosslinked polymer network that forms when gelation occurs. When a stable gel forms, the permeability to brine is often quite low.

In laboratory experiments in porous rocks, a high-pressure gradient is usually required to initiate brine flow after placement of a gel. When the injection rate is constant, the pressure gradient

declines with time as flow channels are developed in the gel, usually reaching a stable value at a specified injection rate. Flow channels are created by deterioration of the gel under the imposed pressure gradient. Aqueous gels have no permeability to oil when they remain intact. However, permeability can be developed as the oil phase creates its own flow channels through the gel [Dawe and Zhang, 1994].

Gel Permeability. The permeability of a gel to the flow of brine determines the initial flow resistance of a region filled with a gel. The permeability of aqueous gels (hydrogels) has been studied by a few investigators [Green et al., 1997; Seright and Martin, 1991] determined the permeability of selected gels to brine after placement in micromodels that were 10.83 cm in length, 2000 microns wide by 200 microns thick. Gel permeabilities were on the order of 6-60 microdarcies when pressure drops between 5 psi and 25 psi were applied. Their data are presented in Table 5.1.

Table 5.1 - Inherent permeability to water for several gels [Seright and Martin, 1991].

Gel System	Permeability, μ d
Resorcinol-formaldehyde 3% resorcinol, 3% formaldehyde, 0.5% KCl, pH=9	6.2
Cr(III)-xanthan 4000 ppm Flocon 4800, 154 ppm Cr ⁺³ (as CrCl ₃) 0.5% KCl, pH=4	50
Chromium(redox)-polyacrylamide 2.8% Cynamid Cyanagel 100, 500 ppm Na ₂ CrO ₄ , 1500 Na ₂ S ₂ O ₄ , 0.5% KCl, pH=5	30
Cr ⁺³ (acetate)-polyacrylamide 1.39% polyacrylamide, 360 ppm Cr+3(as acetate) 1%NaCl, pH=5.0	42
Colloidal silica 10 % DuPont Ludox SM, [®] 0.7% NaCl, pH=8.2	60
Polyvinyl alcohol-glutaraldehyde 2.5% PVA, 3% HOAc, 0.25% GTA, 0.5% KCl, pH=5	Syneresed-no stable gel

These permeabilities suggest that gelants placed in porous rocks and fractures will reduce the permeability to microdarcy levels if the pore space or fracture volume is filled with gel and the gel remains intact when subjected to pressure gradients.

Gel Dehydration. The deterioration of a gel after placement has not been studied extensively. Some aqueous gels undergo syneresis with time, spontaneously expelling solvent and shrinking in volume [Gales et al., 1988]. Syneresis creates liquid filled volume that may be accessible to the flow of fluids, thereby increasing the brine permeability. Experimental data [Eggert et al., 1992] show that gels provide significant permeability reduction in porous rocks even after syneresis. However, gels that do not exhibit syneresis can also be deformed under a pressure gradient to create flow channels.

Dehydration of a gel occurs when the solvent (brine/water) is removed from the gel under a pressure gradient or when the gel structure is destroyed. Dawe and Zhang [1994] used a glass micro model to study the reason(s) for disproportionate permeability reduction in flow through gelled porous media. Their findings showed that while water flows through the gel, oil creates channels and pathways in the gel. As a result of the formation of channels in the gel during the flow of oil, the gel dehydrates and loses some of its structural water. This observation stimulated the study of gel dehydration and its effect on gel performance in the porous medium reported in this chapter. The only other research on gel dehydration was done by Seright [1996] who observed gel dehydration while injecting gel into capillary tubes and fractures.

I: Exploratory Permeability and Dehydration Experiments

Experimental Procedure. The initial experiments to determine gel permeability and investigate dehydration were done using KUSP1-boric acid [McCool et al., 1998], KUSP1-ester [McCool, 1998], and sulfomethylated resorcinol formaldehyde [Zhuang et al., 1997] gel systems which were studied earlier in this program. Experiments were conducted using the apparatus as shown in Figure 5.1 [Green et al., 1998].

In these experiments, a gelant was placed in a gel cell (10-mm I.D. glass chromatographic tube) and allowed to gel. The gel was confined to the tube by a 10-micron Teflon filter that was placed at the end of the gel. After gelation, the remaining volume of the gel cell was filled with brine and connected to the capillary tube. Since flowrates through gels are small, the flow rate was determined by positioning the air-brine interface in the capillary tube and measuring the location of the air-brine interface at different times. A constant air pressure was set. All experiments were done at a constant temperature of 25°C.

The experimental procedure for measuring gel permeability and gel dehydration is described in the 1998 Annual Report [Green et al., 1998]

Results and Discussion – Exploratory Experiments. Results from exploratory experiments on three different gel systems follow. These systems are described elsewhere [McCool et al., 1998; Zhuang et al., 1997].

Sulfomethylated resorcinol formaldehyde (SMRF). Figure 5.2 presents permeabilities determined for the SMRF system as a function of pressure drop. The permeability of the SMRF gel system is 26 microdarcies at an applied pressure of 5 psi (pressure gradient is 76.2 psi/ft) and decreases with increasing pressure gradient. The decrease in the measured permeability with increasing applied pressure is attributed to the compression of the gel structure. Dehydration of SMRF was not measurable under the pressure gradients studied (76.2 psi/ft to 305 psi/ft).

KUSP1-ester gel system. KUSP1 is a biopolymer that is soluble in alkaline solutions and forms a gel when the pH is decreased to 10.8 [McCool, 1998]. In this system, the pH is dropped by hydrolysis of the ester monoethylphthalate. Water at 5 psi was applied at the gel-water interface. The volume of the gel decreased slowly with time as water was “squeezed” from the gel and flowed out of the gel cell. Dehydration was nearly complete as a thin gel film remained on the 10-micron filter at the end of the experiment. Since this gel exhibited nearly total dehydration

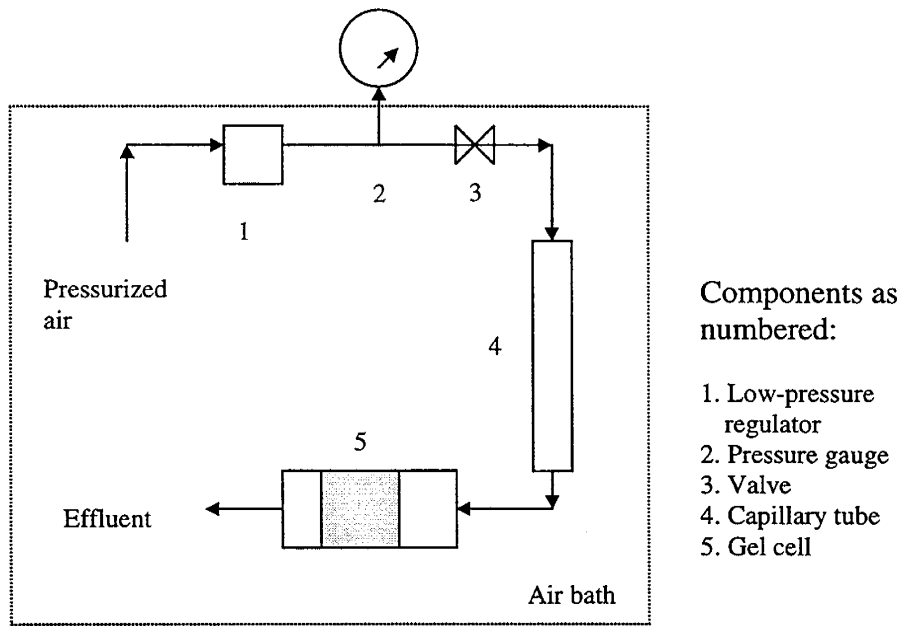


Figure 5.1 - Schematic diagram of the apparatus used for measuring the gel permeability.

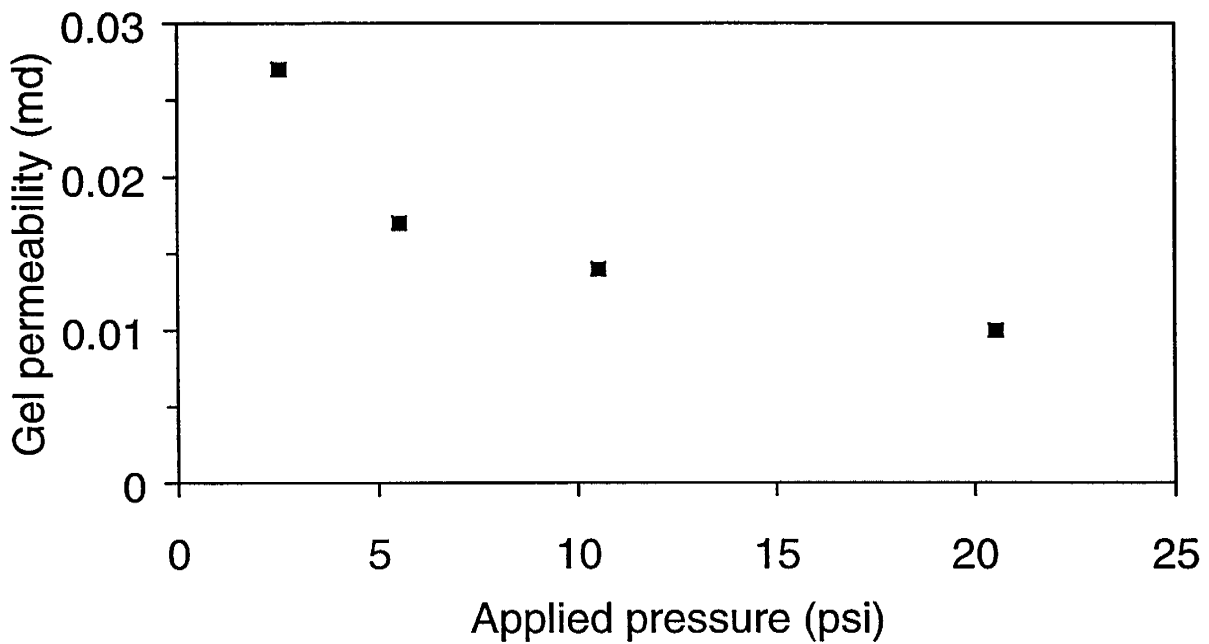


Figure 5.2 - Inherent gel permeability for sulfomethylated resorcinol-formaldehyde (SMRF) gel system at 25°C and different applied pressures.

under a pressure of 5 psi, the permeability of another KUSP1-ester gel was measured by using a constant head of water as the pressure source (0.253-psi) and collecting the effluent under oil. The gel sample was 2.3 cm long and the pressure gradient was 3.35 psi/ft. The permeability of KUSP1-ester gel was 0.13 md.

KUSP1-boric acid gel system. KUSP1 can also be gelled with borate [McCool et al., 1998]. Two compositions were used to investigate dehydration of the gel. In the first three experiments, the gelant composition was 1 wt% KUSP1 and 0.5 moles boric acid/kg gelant in 1% sodium chloride brine. The gel lost most of its volume and dehydrated to a thin filter cake that was retained on the filter at the end of the tube.

In the second experiment, water was used to dehydrate the gel. Strong syneresis was observed and the experiment was terminated. The third experiment was done to determine brine permeability. Figure 5.3 shows the change in permeability with time for this gel at constant pressure of 2 psi. The permeability of the gel decreases with time and finally levels off. This behavior shows the effect of constant pressure on compressing the gel because of the dehydration of the gel. These measurements were conducted in a very short time because of the severe syneresis behavior of KUSP1-boric acid at 0.5 mole boric acid/kg gelant.

A fourth KUSP1-boric acid gel was studied that would not synerese when contacted with brine. The gelant contained 1 wt% KUSP1 and 0.2 mole boric acid/kg gelant in 1 wt% sodium chloride brine. The dehydration experiment was done by injecting water at 2 psi. This gel lost 47% of its volume as the pressure gradient increased from 35.2 psi/ft to 67 psi/ft. Permeabilities are shown in Figure 5.4 as a function of time.

These exploratory experiments demonstrated that some gels are dehydrated under pressure gradients that might be expected in field applications. All gels had some brine permeability. Permeability to brine was low which is consistent with previous work of Seright and Martin [1991] discussed earlier in this chapter. Data on the dehydration of gels under a pressure gradient have not been reported in the petroleum literature. These results led to the study of gel dehydration and permeability of chromium acetate-polyacrylamide gels described in the next section.

II: Dehydration and Permeability of Chromium Acetate-Polyacrylamide Gels

The dehydration of chromium acetate-polyacrylamide gels was studied in a series of experiments in which both brine and oil were used to apply pressure to the gel. The experimental apparatus depicted in Figure 5.5 is essentially the same as in Figure 5.1 except the air pressure is applied to a transfer cylinder that contains either water or oil. Use of a transfer cylinder to maintain constant pressure in the brine or oil allowed the running of several gel dehydration experiments simultaneously. Experimental details are presented in the 1998 Annual Report [Green et al., 1998]. The polymer used was Alcoflood 935 (Lot 3243A) and the chromium acetate was obtained from McGean-Rohco Inc. Gels were made, adjusted to pH 5 and placed in glass chromatographic columns. Columns with an inside diameter of 10 and 35 mm were used in these experiments. Most of the experiments were done in 10 mm columns.

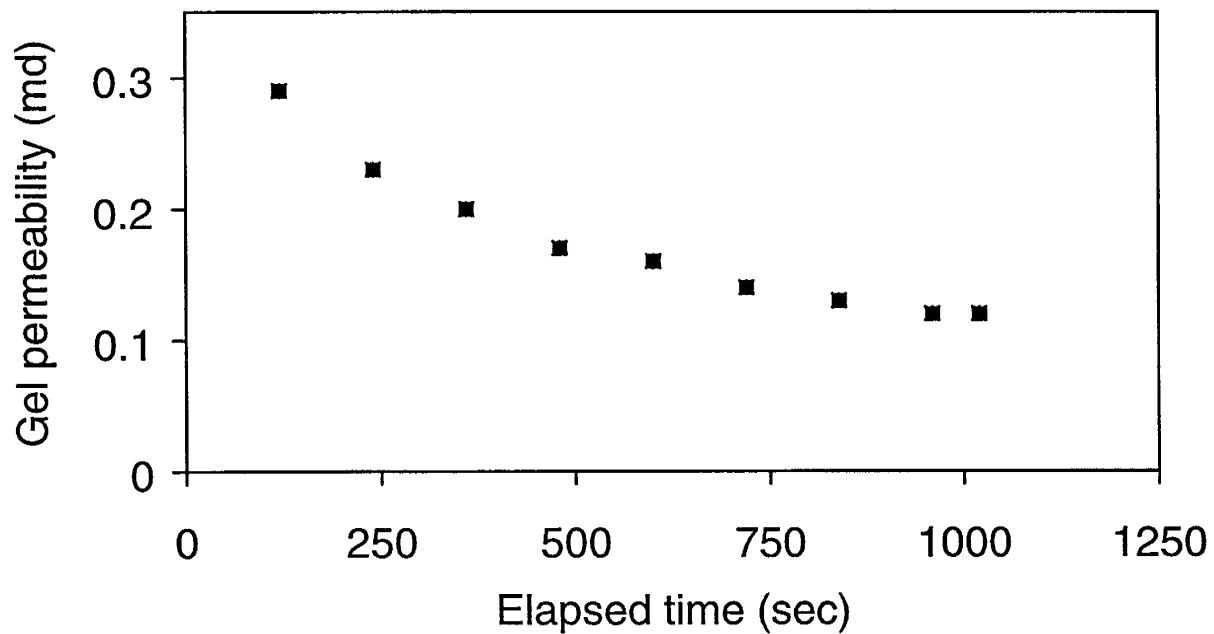


Figure 5.3 - Gel permeability for KUSP1-boric acid gel with 0.5 mole boric acid per kilogram of gel at 25°C and 2 psi.

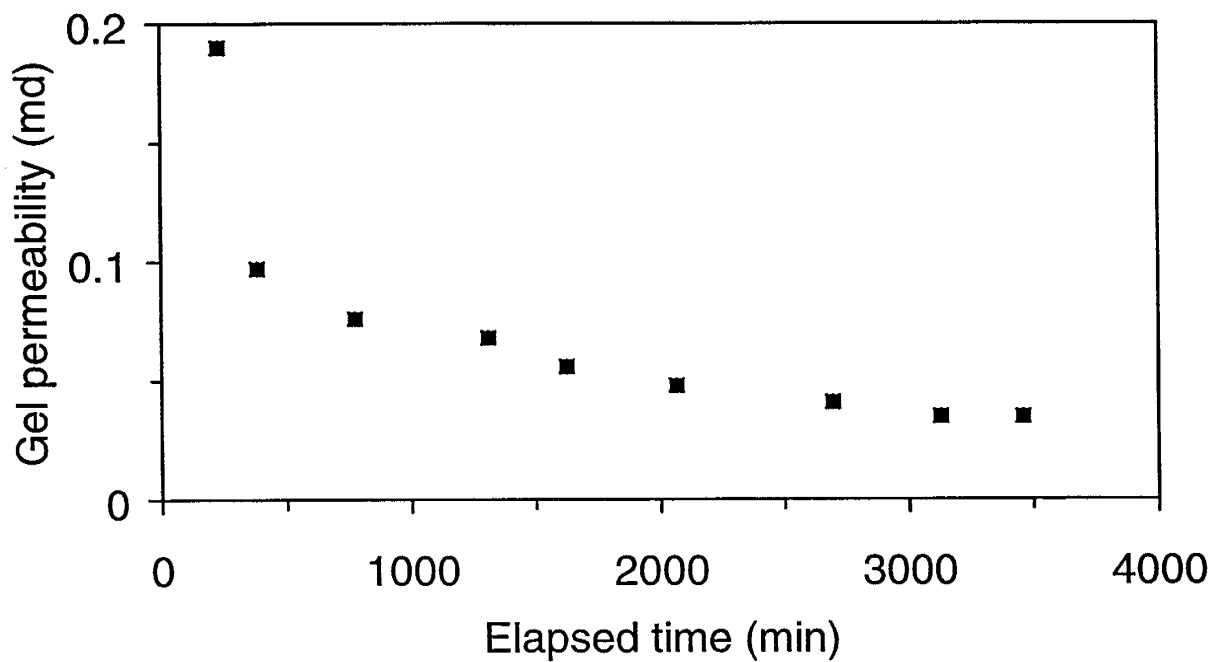


Figure 5.4 - Gel permeability for KUSP1-boric acid gel with 0.2 mole boric acid per kilogram of gel at 25°C and 2 psi.

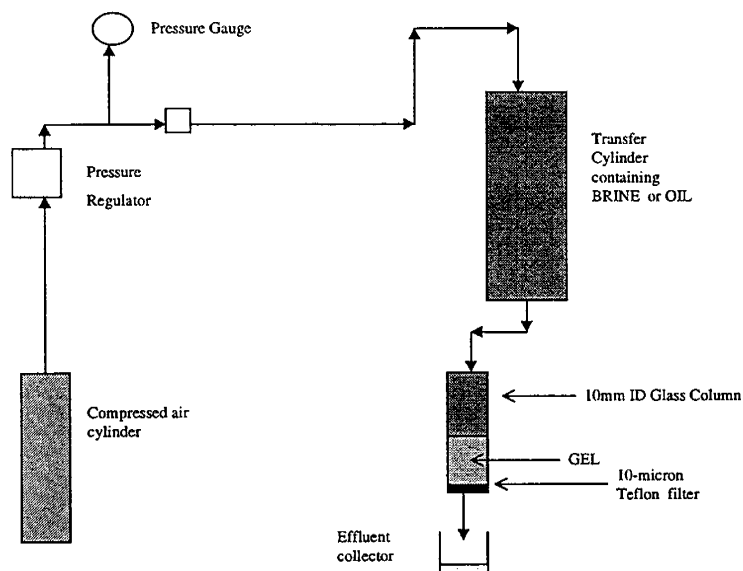


Figure 5.5 - Schematic sketch of setup to study dehydration of PHPA/Cr (III) gel system.

Results and Discussion - Brine Dehydration and Permeability Experiments. Brine experiments were initially conducted at constant pressure with pressures ranging from 50 to 450 psi in 10 mm columns. Pressures ranging from 1.5 psi to 100 psi were studied in 10 and 35 mm columns after the initial experiments in 10 mm columns were completed. When the pressure in the brine is increased at the front of the gel, brine flows through the gel. The color of the gel gradually changes from bluish-green to colorless indicating that the excess chromium is displaced by brine flowing through the gel. In one experiment, a water-soluble dye was added to the injected brine. A visible displacement front was observed to propagate through the gel, demonstrating that the entire gel was permeable to water.

The behavior of the gel in 10 mm columns when the brine pressure is constant at the front of the gel can be described in terms of the appearance of the gel depicted in Figure 5.6. A narrow "brine-finger" forms along the central axis of the tube as pressures increase. The "brine finger" was irregular in shape and was difficult to see because the refractive index of the gel is nearly the same as the refractive index of water. Towards the end of the research program, the volume of the brine finger was estimated by dropping chloroform into the finger using a micro syringe or by calculating the dehydrated volume from a material balance on the filter cake.

At pressures greater than 150 psi in 10 mm columns, the brine finger propagates through the gel until it reaches the filter cake that forms above the 10-micron filter at the end of the tube. The progressive dehydration of gel when brine pressure exceeds 150 psi is shown in Figure 5.7.

In 35 mm columns, the brine-gel interface is deformed initially when brine pressure is applied as shown in Figure 5.8. At gradients greater than about 2.5 psi/inch, a large brine finger formed that

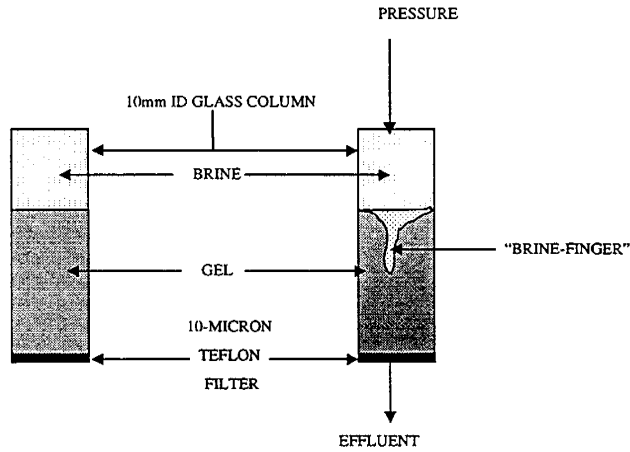


Figure 5.6 - Gel behavior at pressures less than 150 psi when brine (1% KCl) is used to displace the gel in 10 mm columns.

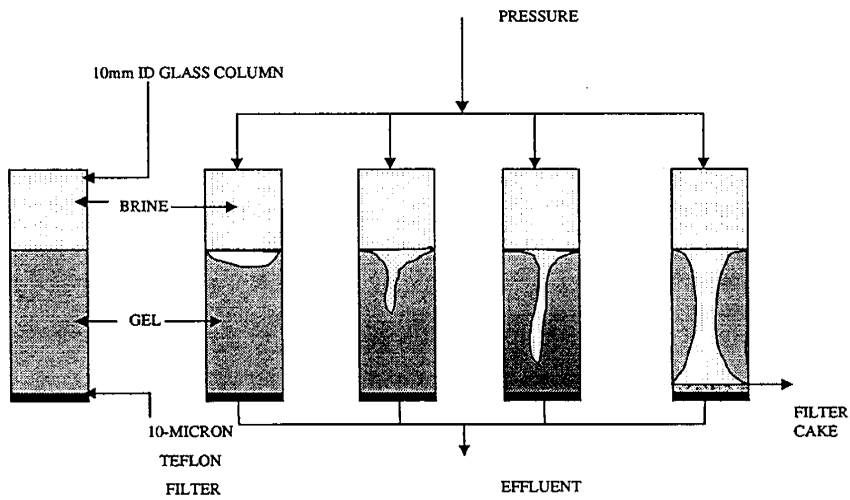


Figure 5.7 - Gel behavior at pressures greater than 150 psi when brine is used to displace the gel in 10-mm columns.

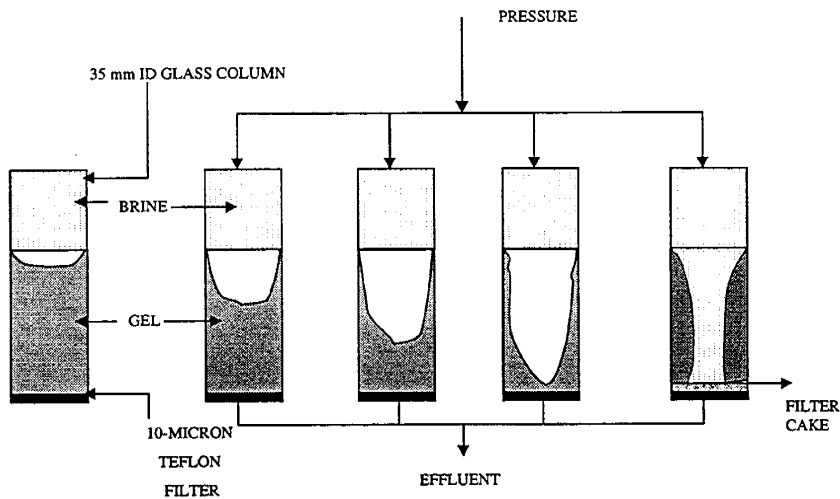


Figure 5.8 - Gel behavior when brine is used to displace the gel in 35-mm columns at pressures greater than 4 psi.

moved slowly toward the end of the column as the gel dehydrated. The brine finger propagates slowly through the gel reaching the bottom of the column where a filter cake forms. Brine also flowed through the gel as dehydration occurred. Dehydration of the gel and compaction of the filter cake continues until the flow rate through the column becomes steady. At low pressures (less than 2.5 psi) the brine finger stabilizes as shown in Figure 5.9 and brine flows through the gel at a steady rate.

The volume of gel dehydrated in 35 mm columns was determined by two methods. The "brine finger" was large enough that the brine could be removed from the cell and measured without destroying the gel structure. The filter cake was also weighed before and after drying. The increase in mass was attributed to dehydrated polymer. Material balances were used to estimate the volume of the dehydrated gel. The agreement between measured volume and material balances was within 4% in most cases.

10-mm Columns--Behavior of PHPA/Cr (III) Gel System at Pressures Equal To or Less Than 150 psi When Brine Is Used to Dehydrate the Gel When brine is used to dehydrate the gel at pressures less than 150 psi, the finger reaches a constant length. The brine flow rate becomes steady meaning that there is no further dehydration of the gel. Values of the combined gel/filter permeability are plotted against time for runs conducted at 100 psi in Figure 5.10. The combined gel and filter permeability decreases with time but attains a steady state value. This permeability was on the order of a few microdarcies. Since the permeability of the 10-micron Teflon filters was found to be on the order of a few millidarcies, the permeability obtained from the data is primarily the permeability of the dehydrated gel. Although a filter cake does not form on the 10

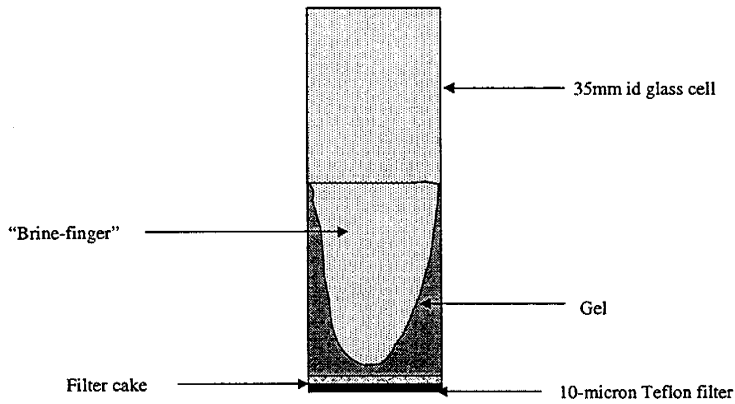


Figure 5.9 - Gel behavior when brine is used to displace gel in 35-mm columns when the initial pressure gradient was less than 2.5 psi/inch.

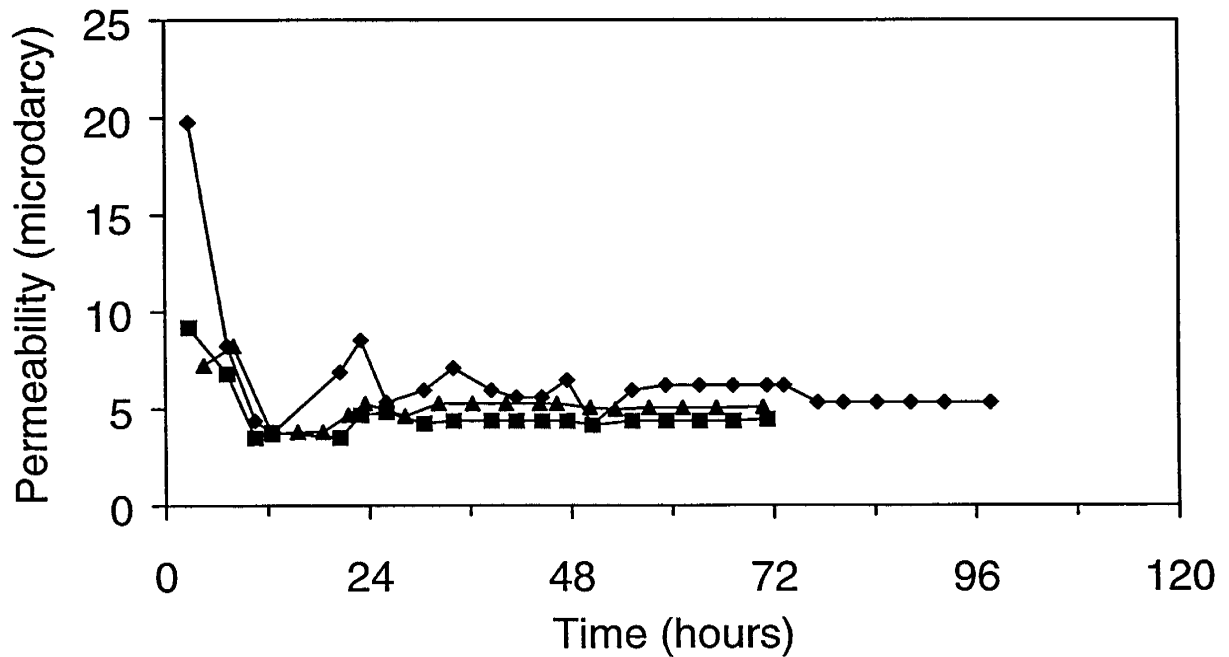


Figure 5.10 - Permeability of gel and filter combination versus time at 100 psi when brine is used to dehydrate the gel. Gel composition – 5000 ppm polymer, 200 ppm chromium and 1% KCl.

micron Teflon filter, much of the dehydration probably occurs in the region above the filter where a structured gel layer forms. The polymer concentration increases in this region. Thus, the composition of the dehydrated gel is probably not uniform. Permeability of the structured gel was investigated [Green et al., 1998] and found to be on the order of 1 μ d.

10 mm Columns--Behavior of PHPA/Cr (III) Gel System at Pressures Greater Than 150 psi When Brine is Used to Dehydrate the Gel. When the experiment was conducted at pressures greater than 150 psi the brine finger reached the filter and formed a channel that widened with time as shown in Figure 5.7. The volume of this channel is the volume of gel that has been dehydrated. A filter cake formed on the filter, which indicated that polymer was being retained on the filter. The permeability of the gel and filter combination was found to be much lower than values obtained in experiments conducted at low pressures. It was observed that as the pressure increased the permeability decreased.

The resistance to flow of brine through the gel at the brine-gel interface increases at high pressure thereby favoring the propagation of the "brine-finger" through the gel which results in dehydration of the gel. The permeability of the Teflon filter was measured at the end of the experiment and found to be two to three orders of magnitude higher than the permeability of the gel and filter combination. The changes in permeability with time for the gel and filter combination at 250 and 400 psi are shown in Figures 5.11 and 5.12.

The permeability of the gel and filter combination at the end of the experiment was measured for pressures from 50 to 450 psi and is shown in Figure 5.13. The decrease in permeability with increase in pressure may be due to the more compact nature of the filter cake at higher pressures.

35 mm-Columns--Behavior of PHPA/Cr (III) Gel System When Brine is Used to Dehydrate the Gel. Brine pressures ranging from 1.5 psi to 100 psi were applied to gels of various lengths in 35 mm columns. Figure 5.14 shows dehydration data for 35 mm columns as a function of initial pressure gradient. Pressure gradients increased as gels dehydrated. Dehydration occurred even at pressure gradients as low as 2.2 psi/inch. Figure 5.15 compares dehydration in 10 mm and 35 mm columns as a function of initial pressure gradient. Dehydration occurred at lower pressure gradients in the 35 mm column because gel adhesion effects at the column walls did not extend as far into the interior of the gel as in 10 mm columns.

Dehydration by brine was extensive in the 35 mm columns. These results suggest that in injection wells, fractures that are filled with similar gels will experience dehydration of the gels after placement when brine injection resumes and pressure gradients similar to those studied in this work are encountered.

Oil dehydration experiments. Experiments were conducted with oil as the displacing fluid. As noted earlier, the gel is not permeable to oil. Oil fingered through the gel as shown in Figure 5.16 until the oil reached the filter cake that formed on the 10-micron Teflon filter. Once the oil reaches the filter cake it cannot pass through it so it moves laterally and widens into a hourglass shape as shown in Figure 5.16d. Brine can flow through those portions of the filter cake not covered with oil. Flow of brine ceased and the oil finger was stable. The volume of the

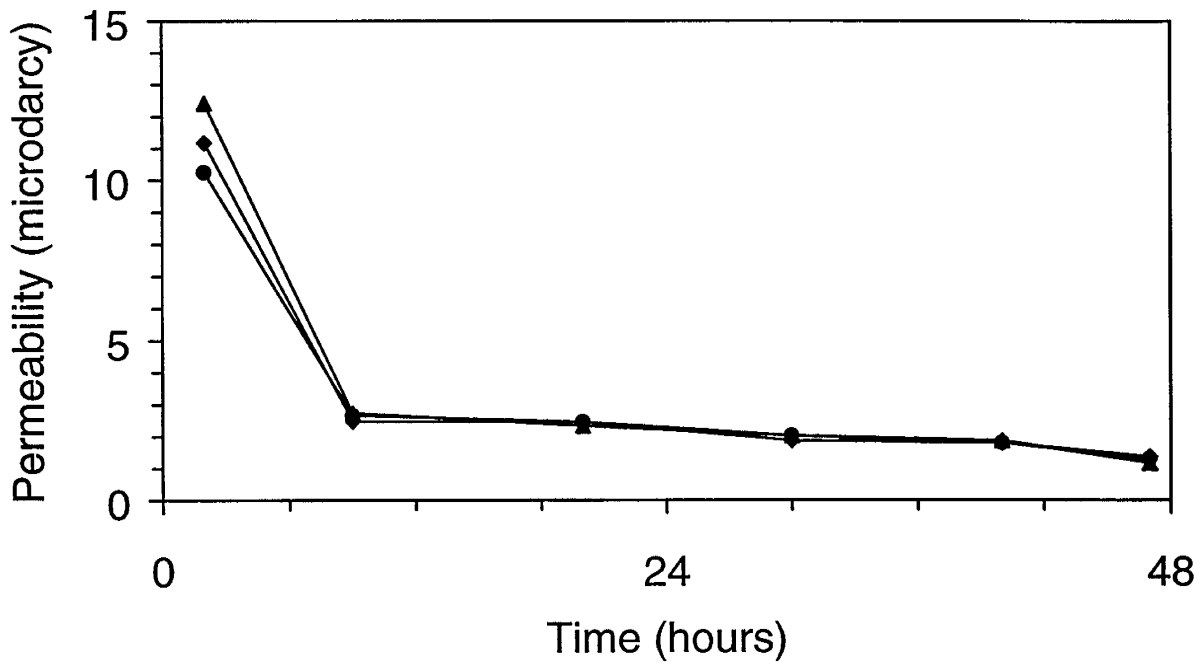


Figure 5.11 - Permeability of gel and filter combination versus time at 250 psi when brine is used to dehydrate the gel. Gel composition – 5000 ppm polymer, 200 ppm chromium and 1% KCl.

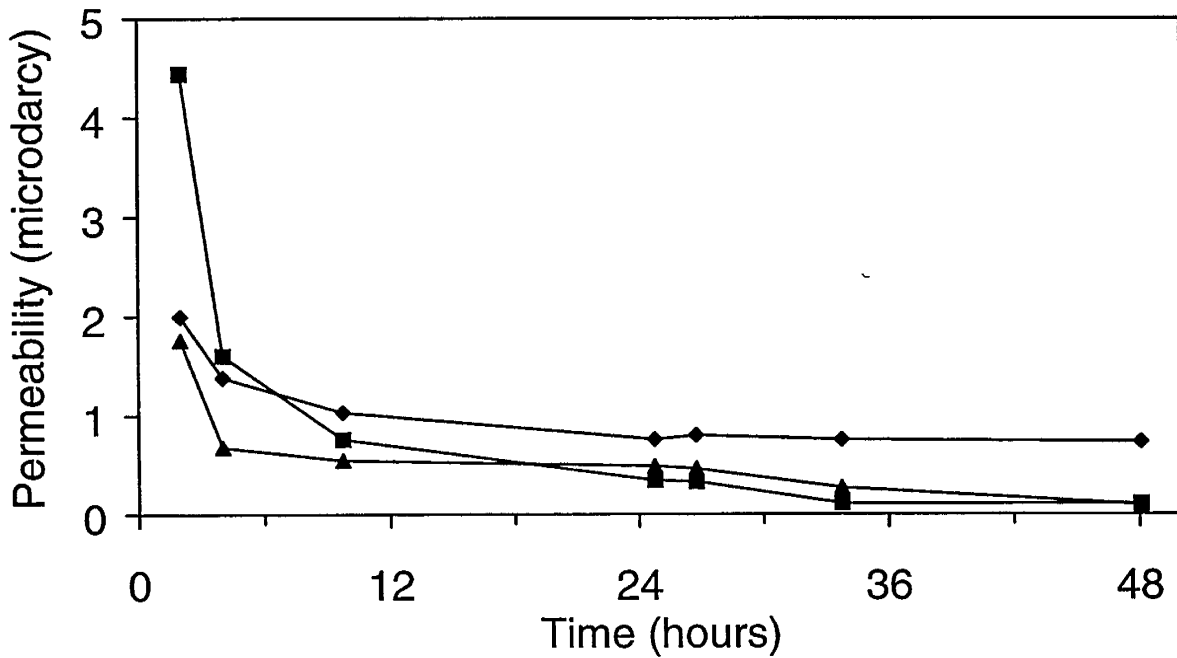


Figure 5.12 - Permeability of gel and filter combination versus time at 400 psi when brine is used to dehydrate the gel. Gel composition – 5000 ppm polymer, 200 ppm chromium and 1% KCl.

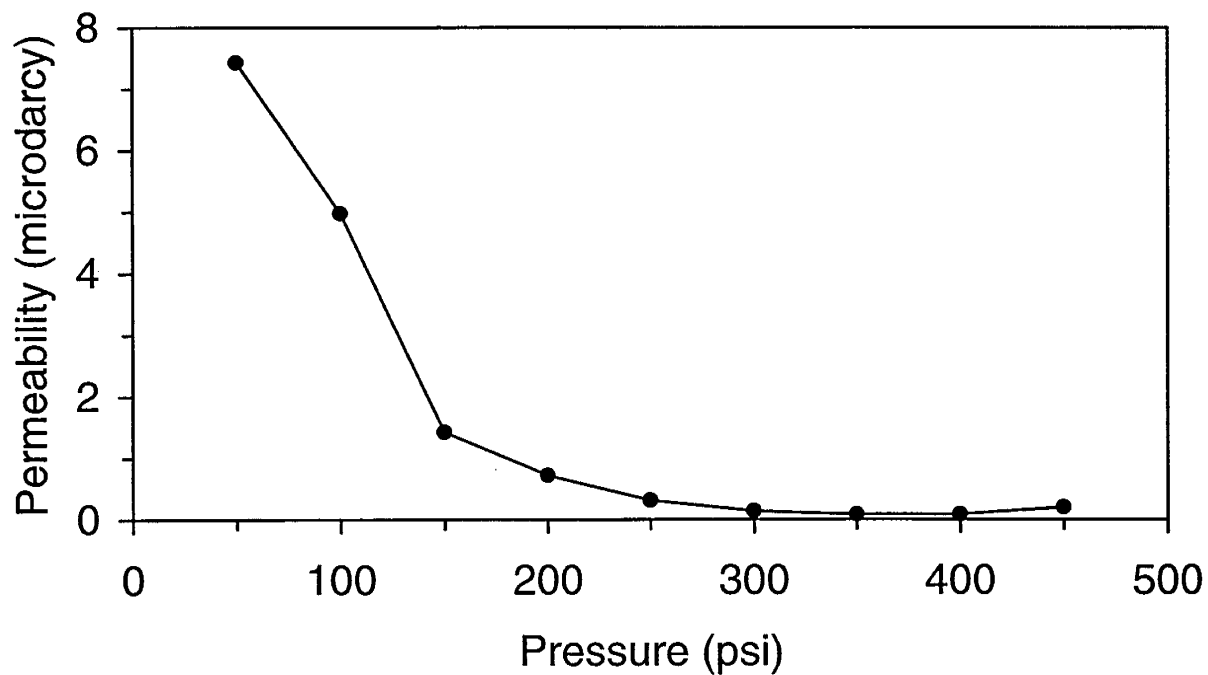


Figure 5.13 - Permeability of gel and filter combination at the end of the experiment versus pressure.

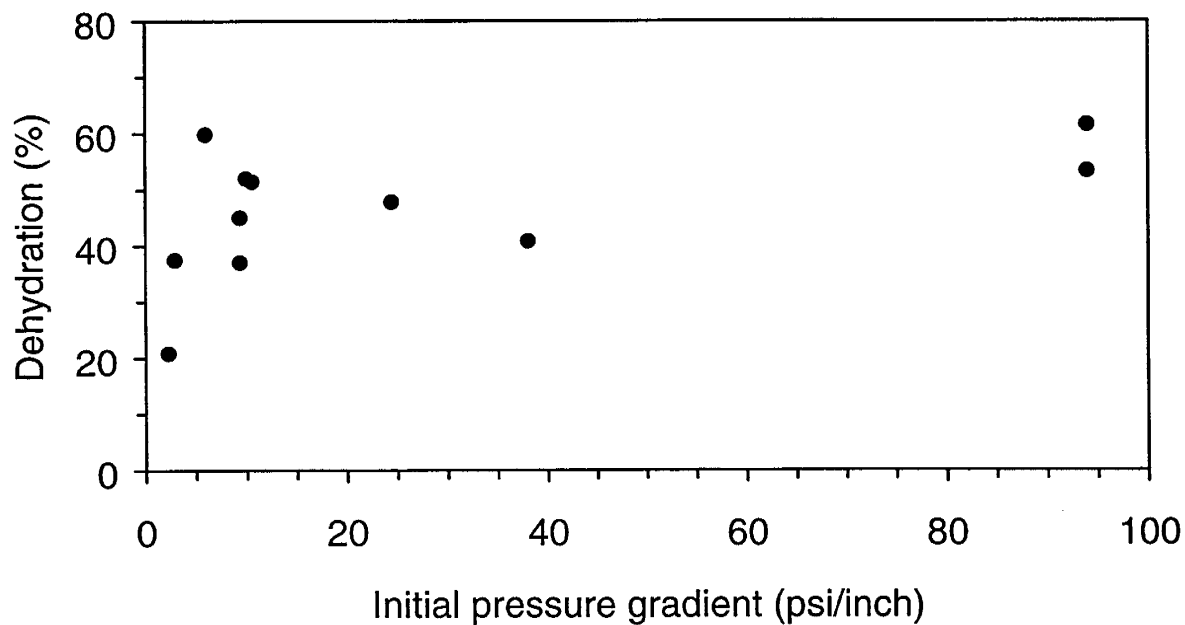


Figure 5.14 - Dehydration of gel during brine flow in 35 mm columns as a function of initial pressure gradient.

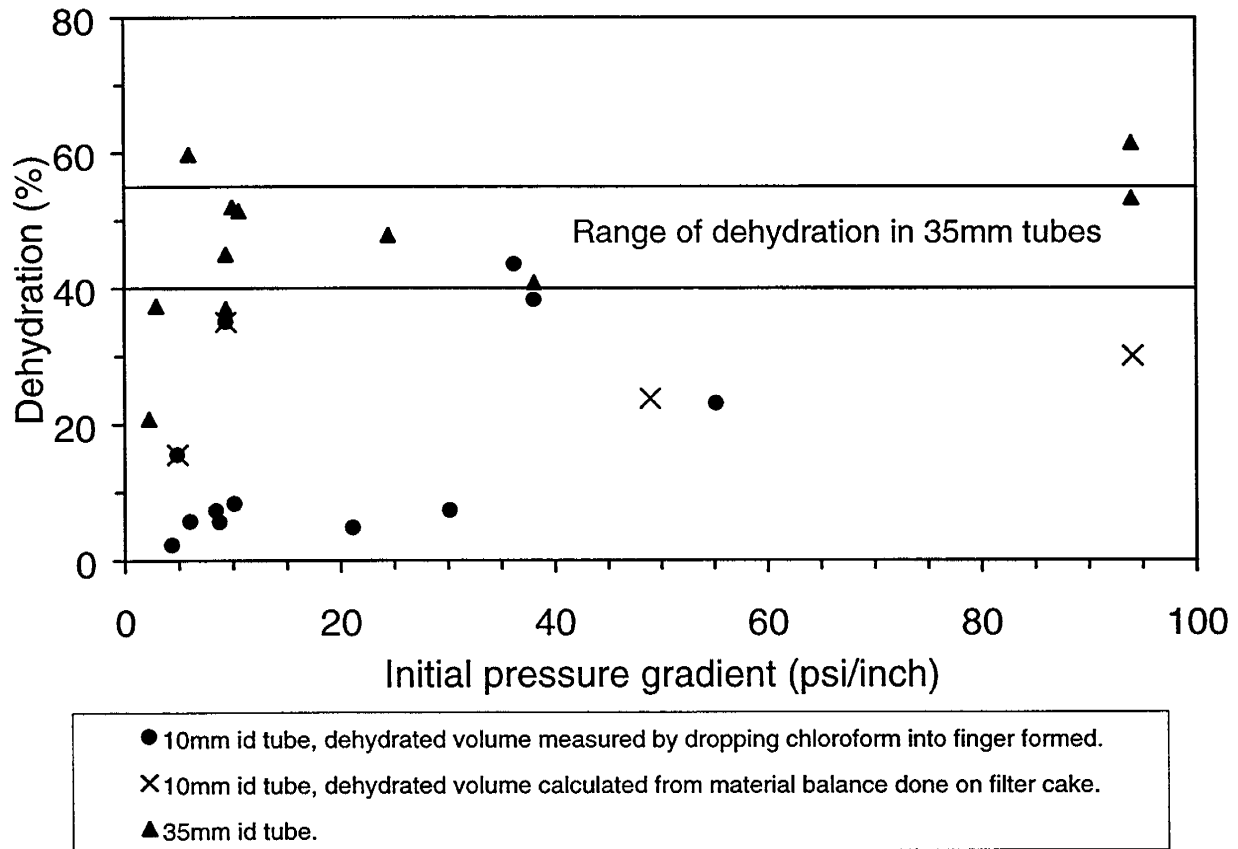


Figure 5.15 - Comparison of gel dehydration in 10 mm and 35 mm columns as a function of initial pressure gradient.

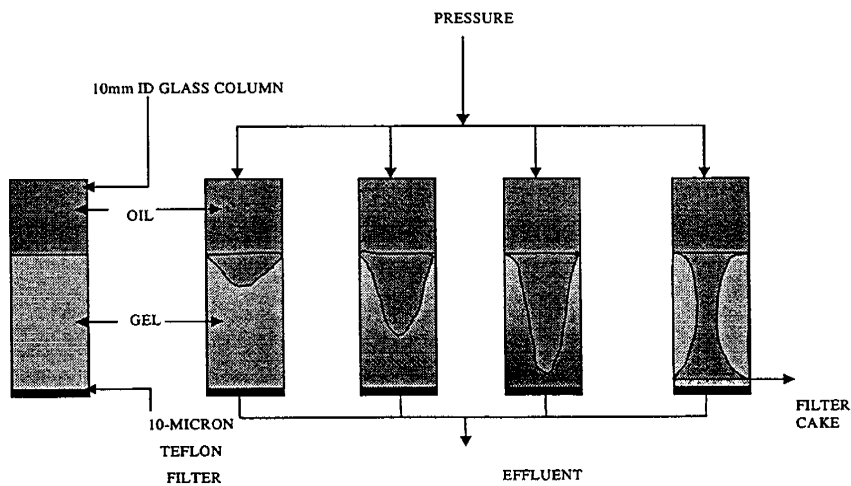


Figure 5.16 - Gel behavior when oil is used to displace the gel.

dehydrated gel is equal to the volume of the oil in the finger. The volume of the dehydrated gel was checked by material balances.

Dehydration occurred at pressures as low as 5 psi applied across a gel that was 2 cm in length. This is equivalent to a pressure gradient of about 76 psi/ft. This pressure gradient is well within gradients observed in the reservoir, particularly around the production well. The chromium acetate-polyacrylamide gel is much more susceptible to dehydration by the oil phase than by the brine phase.

The volumes of gel dehydrated as a fraction of the original gel volume at three pressures (5, 10 and 50 psi) in 10-mm columns are shown in Figure 5.17. Several runs were conducted at each pressure. The dehydration rate and the amount of dehydration depend on the pressure and these two parameters increase as the pressure increases. The experiments were also conducted in glass columns with an inside diameter of 35 mm. Figure 5.18 shows the dehydration of gels as a function of time at two pressure gradients in 35 mm columns. Figure 5.19 compares the volume of gel dehydrated in 10 mm and 35 mm columns. The volume dehydrated was close to 70% in 35 mm columns compared to 50-60% in the case of the 10 mm columns. This difference is attributed to the effect of adhesion of the gel to the walls of the column is reduced as the diameter of the glass column increases.

III: Dehydration of Chromium Acetate Gels after Placement in Sandpacks.

A series of experiments was designed to determine if the phenomena of gel dehydration observed in bulk tests also occurred in porous media. Four sandpacks were prepared, treated with gel and dehydrated by injection of oil at a constant pressure. The experimental procedures for preparation of sandpacks and placement of the gelant are summarized in Chapter 7 [Green et al., 1988]. Material balances on the effluent were used to determine the pore volume occupied by the mobile fluid phases. In one experiment, the gelant was injected into the sandpack in the presence of a waterflood residual oil saturation.

Run SP12. The initial experiments were conducted in the sandpack SP12. In this test, a 1-foot sandpack (1.5 " ID) [Green et al., 1998] was saturated with brine and displaced with a chrome-acetate gelant consisting of 5000 ppm Alcoflood 935, 109 ppm Cr⁺³, with an Ac/Cr ratio of 91. The pH of the gelant was adjusted to 5.0 by adding acetic acid. Nominal gelation time was 17-18 days. Following gelation, the permeability of the gelled sandpack to brine was estimated to be about 30-40 μ d.

The dehydration experiments began by connecting the inlet of the sandpack to a transfer cylinder containing oil where the pressure was maintained at 80 psi by air injection. The pressure gradient across the sandpack was 80 psi/ft. The oil was dyed red so that the progression of the oil zone could be observed through the transparent walls of the sandpack holder. The oil fingered slowly into the gelled sandpack, dehydrating the gel. Brine was collected continuously at the effluent and measured to enable material balance calculations. At the beginning of the experiment, the amount of "free" water in the sandpack was considered negligible.

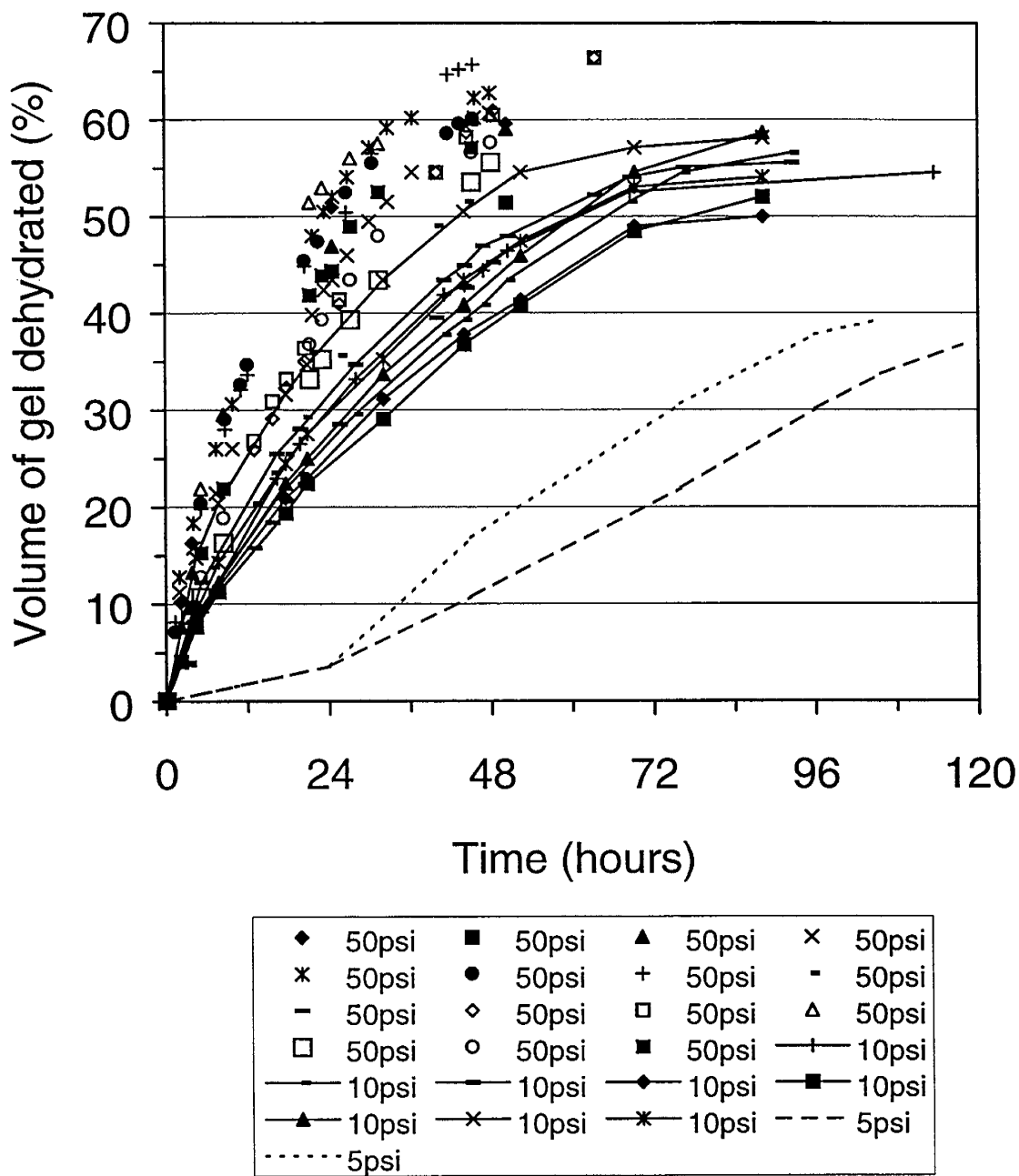


Figure 5.17 - Dehydration as a fraction of the original gel volume vs. time when oil is used to displace the gel in glass column with inside diameter 10 mm at 50 and 10 and 5 psi. Gel composition – 7500 ppm polymer, 300 ppm chromium and 1% KCl.

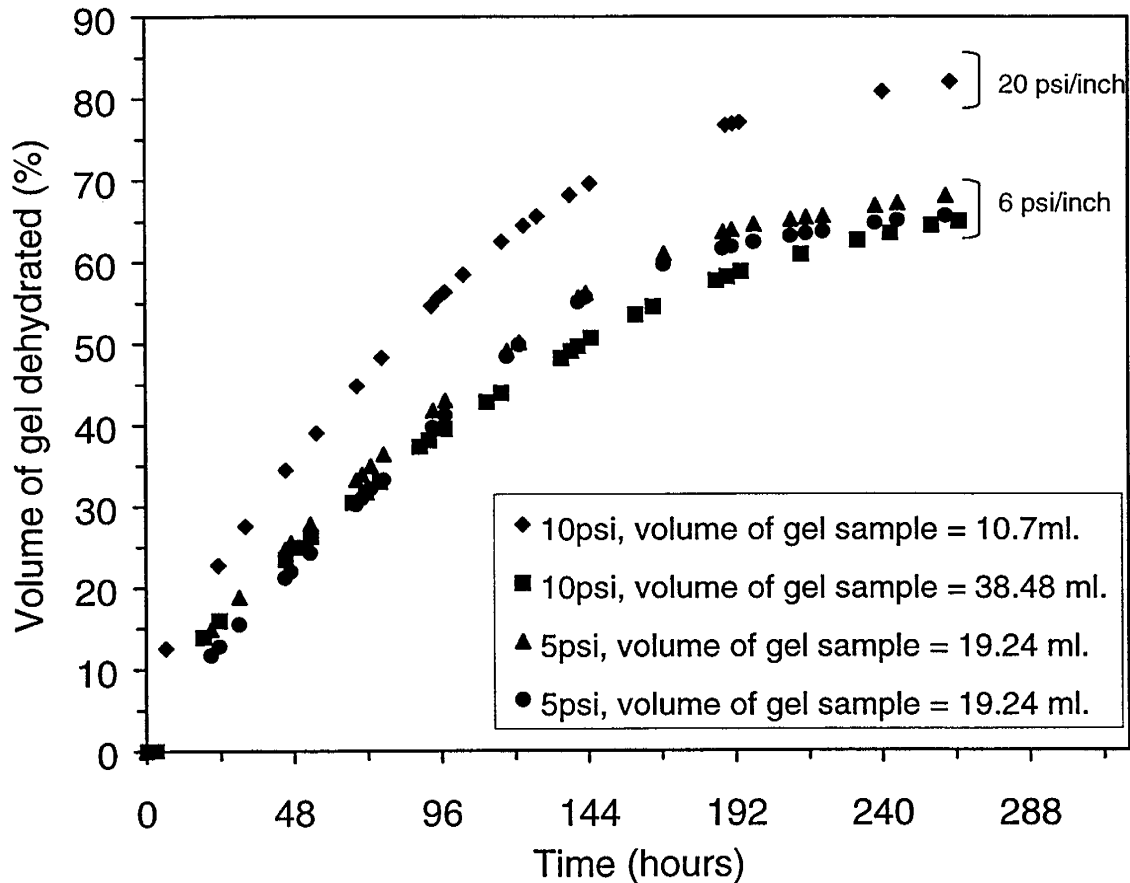


Figure 5.18 - Dehydration as a fraction of the original gel volume vs. time when oil is used to displace gel in a glass column with inside diameter of 35 mm. Gel composition – 7500 ppm polymer, 300 ppm chromium and 1% KCl.

Dehydration of the gel occurred at a slow rate. Oil broke through after about 70 hours of injection and a mixture of oil and brine was produced. After 200 hours of oil injection, the brine volume decreased with time to levels where one drop of brine (0.05 mL) as produced over 24 hours. Volume of brine produced was 41.8 mL, which is 37% of the initial pore volume of the sandpack (112 mL). The brine in the effluent was not slippery to the touch, indicating that the amount of polymer "squeezed" out of the gel was small. Thus, the remainder of the pore space (63%) was considered filled with gel that had been dehydrated. Polymer concentration of the "dehydrated gel" was estimated to be 8100 ppm. If the pore space filled by the gel is disregarded, the effective porosity of the sandpack was reduced from 32% to 12%. Permeability of the core to oil was 8.2 md at 80 psi and 6.88 md at 40 psi. Oil permeabilities were measured with the flow not quite at steady state.

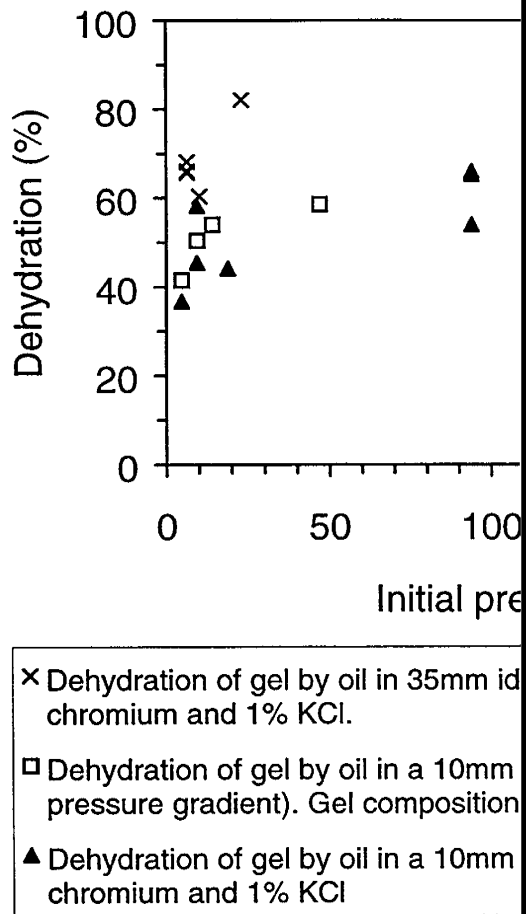


Figure 5.19 Comparison of dehydration of composition – 7500 ppm polymer, 300 pp

The second stage of this experiment was to produce oil and determine permeability saturation in the "new" pore space after brine. The waterflood displaced 11.4 mL of oil, which is equivalent to a residual oil saturation of 0.27 neglecting the gel phase. Permeability to brine at residual oil saturation the brine phase flows in thin films and channels a large fraction of the pore space in the "new"

An oil flood was made at 80 psi to determine the new pore space as well as the interstitial brine saturation. 7.8 mL. The interstitial brine saturation was determined in this series of displacement experiments and

Table 5.2 Dehydration of chromium acetate-polyacrylamide gel in Sandpack SP12

Run	Displacement	V _p (mL)	V _{pgel} (mL)	V _{peff} (mL)	ϕ _{eff}	S _w	S _o	k _o (md)	k _w (md)
1	Brine injection before gel treatment	112			0.32	1.00	0		4000
2	Gel treatment	112	112		0.32	S _{gel} =1.00	0		0.03-0.04
3	Dehydration with oil @80 psi/ft	112	70.2	41.8	0.12	0	1.00	8.2	0
4	Brine flood at 80 psi/ft	112	70.2	41.8	0.12	0.27	0.73	0	0.0064
5	Oil flood at 80 psi/ft	112	70.2	41.8	0.12	0.09	0.91	9.05	0

SP11. The second dehydration experiment was done in SP11, a four-ft sandpack that had been studied previously in this research [Green et al., 1998]. The sandpack was saturated with brine and displaced with a chrome-acetate gelant consisting of 5000 ppm Alcoflood 935, 109 ppm Cr⁺³, with an Ac/Cr ratio of 91. The pH of the gelant was adjusted to 5.0 by adding acetic acid. Nominal gelation time was 17-18 days. Following gelation, the permeability of the gelled sandpack to brine was estimated to be about 20-30 μd. This sandpack had been kept in a constant temperature bath for 6 months following completion of gelation experiments described in Chapter 7.

Oil was injected into the sandpack at a constant pressure of 80 psi, which is equivalent to a pressure gradient of 20 psi/ft for about 65 days. Oil breakthrough occurred after 18 days of injection. Water production became insignificant after 65 days of oil injection. The volume of water dehydrated from the sandpack was 133 mL, which is about 29% of the pore volume of 460 mL. Thus, the effective porosity of the sandpack was reduced from ~33% to 9.5%. Permeability of the dehydrated sandpack to oil was 3.7 md. Brine was not injected into this sandpack.

SP19 and SP20. Two experiments (SP19 and SP20) were conducted in six-inch sandpacks to compare dehydration of a gelled sandpack that contained waterflood residual oil saturation with a sandpack without residual oil saturation. SP20 was saturated with brine, oilflooded and then waterflooded to residual oil saturation. Properties of the sandpacks are summarized in Tables 5.3 and 5.4. The pH of the sandpacks was adjusted to 5.0 using an acetic acid/sodium acetate buffer. A gel solution containing 5000 ppm Alcoflood 935, 109 ppm chromium (as chromium acetate) in 1% NaCl was injected into both sandpacks. There was no added acetate. The gel was bulk mixed and about 3 PV were injected into each sandpack at a rate of about 5 mL/min. Sandpacks were shut-in for 2.5 days to permit gelation before beginning oil injection at a pressure of 80 psi.

Dehydration occurred faster than anticipated in these runs. In SP20, the injected oil displaced 13 mL of brine. However, during the dehydration of SP20, oil broke through rapidly and the entire volume of oil in the transfer cylinder (700-mL) was displaced through the sandpack along with some air. Interpretation of the permeability measurements is flawed by the fact that some air

Table 5.3 - Dehydration of chromium acetate-polyacrylamide gel in Sandpack SP19.

Run	Displacement	V_p (mL)	V_{pgel} (mL)	V_{peff} (mL)	ϕ_{eff}	S_w	S_o	k_o (md)	k_w (md)
1	Brine injection before gel treatment	55			0.32	1.00	0		4670
2	Gel treatment	55	55		0.32	$S_{gel}=1.00$	0		
3	Dehydration with oil @160 psi/ft	55	41	14	0.08	0	1.00	50	0

Table 5.4 - Dehydration of chromium acetate-polyacrylamide gel in Sandpack SP20.

Run	Displacement	V_p (mL)	V_{pgel} (mL)	V_{peff} (mL)	ϕ_{eff}	S_w	S_o	k_o (md)	k_w (md)
1	Brine injection before gel treatment	58			0.33	1.00	0		4324
2	Oil flood	58			0.33	0.21	0.79		
3	Waterflood	58			0.33	0.62	0.38		1485
4	Gel treatment	58	36	22	0.13	$S_{gel}=0.62$	0.38		
5	Dehydration with oil @160 psi/ft	58	22	36	0.21	0	1.00	280	0
6	Brine flood @160 psi/ft	58	22	36	0.21	-	-	0	10

entered the sandpack. SP20 was flushed with oil to displace air from the system prior to oil and water permeability measurements. The permeability of oil was 280 md while the permeability to brine at "residual oil saturation" was 10 md. In SP19, 100 mL of oil was displaced through the sandpack in 14 hours, displacing 14 mL of brine. Permeability to oil was 50 md. Permeability to brine after dehydration was not determined. We believe the high oil permeability in SP20 occurred because the injected oil became hydraulically connected with the residual oil from the previous waterflood. However, additional research is needed to verify this hypothesis.

Discussion

These experiments demonstrate that dehydration observed in bulk experiments described in this chapter and in previous annual reports [Green et al., 1997; Green et al., 1998] occurs in unconsolidated sandpacks. Dehydration with oil creates a new pore structure for fluid flow as the gelled polymer is squeezed into a smaller volume. The effective polymer concentration increases in the remaining gel, further strengthening its resistance to deformation. Since the permeability of gelled polymer is quite low, flow of fluids occurs primarily in the pore structure created by the dehydration of the gel. The immobile gel reduces the effective porosity. When oil and water phases are present, the "waterflood residual oil saturation" is significantly higher

than the water saturation in the new pore space. Interstitial water saturations at 100% oil flow are small.

Differential permeability reduction was observed when dehydration occurred. Permeability to water at residual oil saturation (when oil permeability is zero) is reduced by factors on the order of 400-100,000 depending on the initial saturation and applied pressure gradient. Permeability to oil at the water saturation where water permeability is zero is reduced by a factor of 5.30. Differential permeability reduction does not occur for this system without reducing the oil permeability.

These experiments show that some oil permeability may be regained in unconsolidated reservoirs that have been treated with a gelled polymer system if the treated interval is subjected to pressure gradient by injecting oil or by production of oil from that interval under a controlled drawdown. With sufficient pressure gradient, the oil is able to dehydrate the gelled region, creating preferential permeability to oil. Excessive pressure gradients will probably destroy the dehydration process, promoting channeling through the gelled region as well as the differential permeability modification.

Results from our research were obtained for a single porous media (unconsolidated sand) and one gelant system. Further research is needed to define conditions under which dehydration of gelled polymer systems occurs in porous rocks.

Conclusions

The conclusions are based on the gel systems studied in this chapter at temperatures of about 25°C.

1. The KUSP1-ester and KUSP1-boric acid gels dehydrate extensively under pressure gradients imposed in this work, from 35.2 psi/ft to 76.2 psi/ft.
2. The SMRF gel did not dehydrate under pressure gradients from 76.2 psi/ft to 305 psi/ft.
3. Cr (III)-acetate/PHPA gels can be dehydrated by applying a pressure gradient across the gel with either brine or oil. Oil dehydrates Cr (III)/PHPA gels at pressure gradients as low as 60 psi/ft. With brine flow at relatively low-pressure gradients, the brine flow through the Cr (III)/PHPA gels dominates and dehydration is small.
4. The amount of dehydration is greater with oil than with brine as the displacing fluids.
5. The rate of dehydration and degree of dehydration increase as the pressure gradient increases.
6. All gels studied were permeable to water with permeabilities ranging from 5 μ d to 130 μ d.
7. Dehydration results in a decrease in the permeability of the gel.
8. Dehydration was observed in unconsolidated sandpacks with and without residual oil saturation.
9. The effective porosity is reduced by dehydration.
10. Differential permeability reduction was observed in the pore structure created by dehydration of the gelled polymer.
11. Dehydration by oil after in-situ gelation reconnected some of the residual oil saturation from the previous waterflood.

Chapter 6

An Experimental Study of the Flow of a HiVis 350 Polymer Solution Through a Sandpack

Principal Investigators: G.P. Willhite, C.S. McCool, and D.W. Green
Graduate Research Assistant: Abdulwahed Al-Assi

Introduction

This chapter presents experimental work on the flow behavior of a partially hydrolyzed polyacrylamide, HiVis 350, in a sandpack. HiVis 350 is the principal product used for colloidal dispersion gels. The polymer is crosslinked with aluminum(III) that is introduced as aluminum citrate in the gel system. This gel system been used to modify in-depth permeability variation in oil reservoirs to improve oil recovery [Mack and Smith, 1994].

The aim of the study was to examine the flow of HiVis 350 solutions that do not contain the aluminum cross-linker. The effects of flow rate on flow resistance and polymer retention were examined. Laboratory polymer displacement experiments in sandpacks were conducted to accomplish the objectives. This work provides a basis for a study of the HiVis 350-aluminum citrate gel system.

A portion of this study was reported previously in an annual report [Green et al., 1998] and the details can be found there. In those experiments, the HiVis 300 polymer solutions were not filtered before they were injected through the sandpack. The polymer solutions exhibited shear-thickening behavior over the range of flow rates studied. Hydrodynamic retention and degradation of the polymer were indicated. It was decided to repeat the experiments to confirm the unusual behavior that was observed in those runs. The new experiments used polymer solutions that were filtered. The new results and a summary of the previous runs are reported.

Experimental

A schematic diagram of the experimental apparatus is presented in Figure 6.1. The sandpack holder was made of acrylic tubing that was 1 ft long and 1.5 inch in diameter. Pressure ports were attached along the length of the sandpack at intervals of 2 inches dividing the sandpack into 6 sections. Pressure drops were measured across the sections that were labeled A through F. The pressure drop across the entire length was also measured and labeled as T. Two sets of transducers were installed to measure at high and low pressure ranges.

An automatic packer was used to pack the tube with Wedron Silica sand. Ottawa sand (20-30 mesh) was placed at the inlet and outlet of the sandpack holder. The sandpack was saturated with 0.5% potassium chloride (KCl) brine. Brine was flowed through the pack resulting in some settling of sand. Sand was added to the pack until no more settling was observed. The porosity of the SP3 was 35.1% and the pore volume was 122 mL. Permeabilities to brine for the individual sections and the overall sandpack length are given in Table 6.1.

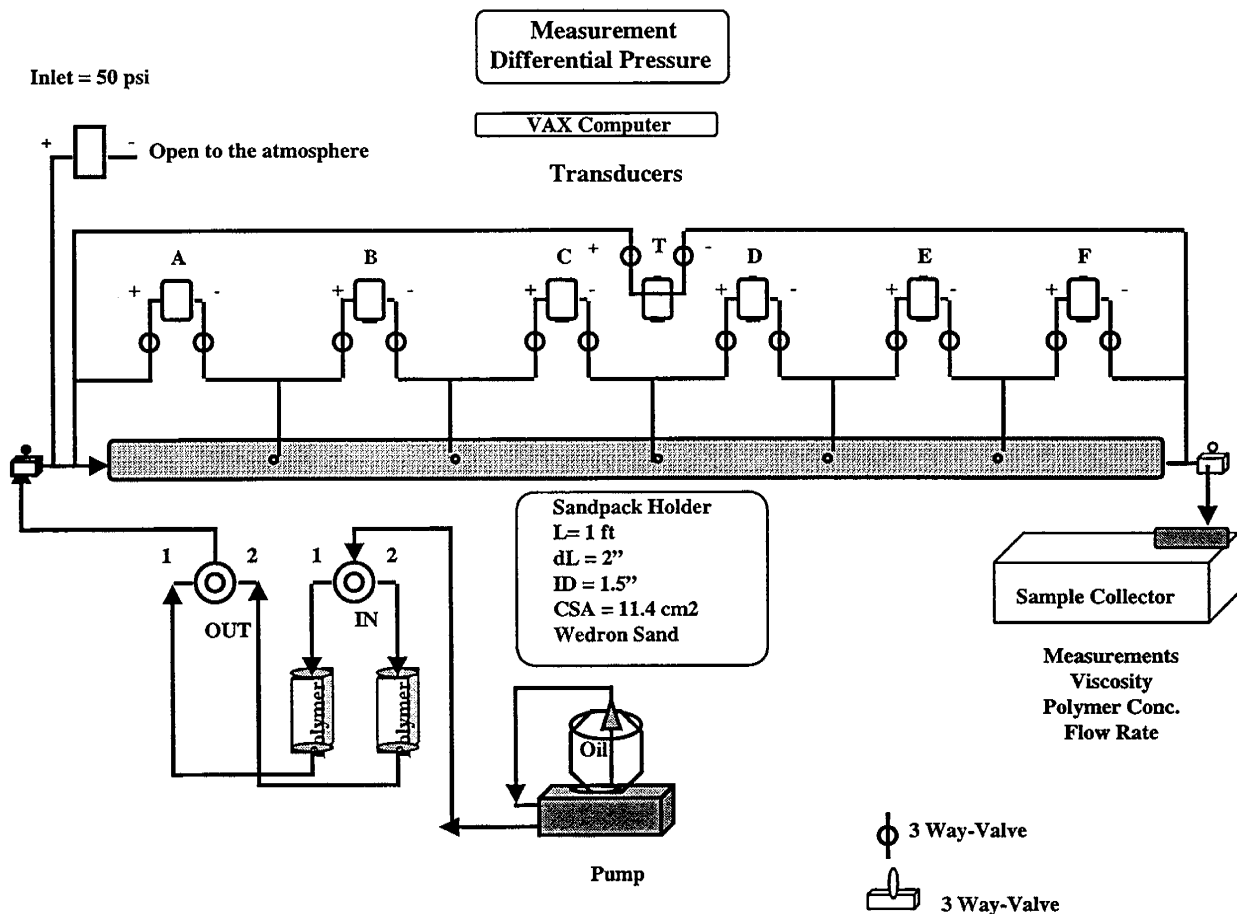


Figure 6.1 - Polymer Displacement Apparatus.

Table 6.1 – Initial permeability of sections for sandpack SP3.

Section	T	A	B	C	D	E	F
Permeability (md)	4620	4910	3980	4930	3850	4510	6800

The polymer used in this study was HiVis 350 (TIORCO, Inc., Denver, CO). HiVis 350 has a viscosity-average molecular weight of 28 million and an average hydrolysis of 23%. The polymer stock solution consisted of 3000 ppm HiVis 350 and 5000 ppm potassium chloride. The polymer stock solution was stirred for 24 hours and then stored for a minimum of two days before use. The 3000 ppm polymer stock solution was diluted with a 5000 ppm KCl solution to a final polymer concentration of 300 ppm. The polymer solution was then filtered through a 1.0 μm glass-fiber filter under a head of 10 psi.

The filtered 300 ppm HiVis 350 was injected into the sandpack column and the pressure drop data in each section and across the sandpack column were monitored by pressure transducers. The sandpack was maintained at a constant temperature of 25°C in a water bath. Effluent samples were collected in approximately 15 mL fractions for the first 1.5 pore volumes and 30

mL fractions thereafter by an automated collector. Polymer concentrations of the injected solution and effluent fractions were determined using a turbidity method [Allison et al., 1987]. The viscosity of each sample was measured at shear rates of 225 and 450 sec⁻¹. All viscosity measurements were taken at the temperature of 25°C.

Results and Discussion

Experiments were conducted to determine the effect of velocity on the flow of a HiVis 350 polyacrylamide solution through a sandpack. The solution was filtered and contained 300 ppm polymer. Three series of runs (SP3.A, SP3.B, and SP3.C) were conducted in the same sandpack. The principal parameter varied was the frontal advance velocity (FAV). The flow conditions used for each run are given in Table 6.2. In series SP3.A and SP3.B, the flow rate was changed without stopping the pump. In series SP3.C, the flow was stopped for a period of time between the different flow rates.

Table 6.2 - Conditions for the Displacement Experiments.

RUN	Frontal Advance Velocity (ft/day)	Flow Rate (mL/min)	Residence Time (hr)	Shut-In Time After Run (hr)	Pore Volumes Injected
SP3.A Series					
SP3.A1	2.37	0.20	10.1	-	4.04
SP3.A2	5.45	0.46	4.40	-	9.18
SP3.A3	10.7	0.90	2.25	-	6.73
SP3.A4	2.37	0.20	10.1	7.3	4.51
SP3.B Series					
SP3.B1	10.7	0.90	2.25		4.64
SP3.B2	21.4	1.81	1.12	-	4.91
SP3.B3	32.4	2.74	0.74	-	4.71
SP3.B4	53.3	4.50	0.45	-	4.98
SP3.B5	11.0	0.93	2.18	30.3	3.98
SP3.C Series					
SP3.C1	10.7	0.90	2.25	12.4	6.54
SP3.C2	21.4	1.81	1.12	12.47	8.04
SP3.C3	53.6	4.53	0.45	19.2	4.79
SP3.C4	10.5	0.89	2.26		2.16

The flow resistance in the sandpack during the polymer displacement experiment was monitored by the measurement of pressure differentials along the sandpack length and across sections labeled A through F (see Figure 6.1). Pressure differentials were converted to apparent viscosities using the following form of Darcy's equation.

$$\mu_{app} = \frac{K A \Delta P}{245 Q \Delta L}$$

where

- μ_{app} = apparent viscosity (cp)
- K = initial brine permeability (md)
- ΔP = pressure differential across a section (psi)
- Q = flow rate (mL/min)
- ΔL = section length (cm)
- A = cross-sectional area (cm²)

Series SP3.A. The effluent polymer concentration, effluent viscosity, and apparent viscosity as functions of pore volumes injected are presented in Figure 6.2. The apparent viscosity profile was calculated from the differential pressure across the total length of the pack.

The flow rate for run SP3.A1 was 0.20 mL/min that corresponded to a frontal advance velocity (FAV) of 2.37 ft/day. Four pore volumes were injected at this flow rate. The normalized polymer concentration curve presented in Figure 6.2 shows the breakthrough of polymer occurred at 1.20 pore volumes injected (PVI). The effluent polymer concentration reached the injection concentration after 1.40 PVI. After 2 PVI, the apparent viscosity decreased slightly with time, indicating degradation of the polymer. The normalized effluent viscosity approached 85% of the injected polymer viscosity.

Run SP3.A2 was initiated by increasing the injection flow rate to 0.46 mL/min (FAV = 5.45 ft/day). Figure 6.2 shows that the overall apparent viscosity increased linearly as a function of pore volumes injected and it never reached steady state, even after the injection of 9.2 PV. The cause for the change in the slope in the apparent viscosity profile during run SP3.A2 is unknown except it corresponded to a change in the transfer cylinder (see Figure 6.2). This change was not detected in the viscosity or polymer concentration of the effluent. The overall apparent viscosity at the end of this run was 22 cp. The normalized polymer concentration fluctuated between 0.94 to 1.05. The effluent viscosity was about 84% of the injected polymer viscosity.

The flow rate was increased to 0.90 mL/min (FAV = 10.68 ft/day) for run SP3.A3. The apparent viscosity increased during this run without leveling off during the injection of 6.8 PV. The increase in flow rate from 0.46 to 0.90 mL/min resulted in a decrease in the normalized polymer concentration during the first PVI. Thereafter, the effluent polymer concentration slowly increased but did not reach the value of the injected polymer concentration. The normalized viscosities also approached the injected level, which did not occur during the previous runs at lower flow rates.

The flow rate was decreased to 0.2 mL/min (FAV = 2.37 ft/day) for Run SP3.A4. This rate was the same as for Run SP3.A1. The decrease in the flow rate resulted in an increase in the effluent normalized polymer concentration and normalized viscosity during the first PVI. The polymer concentration and viscosity in the effluent was greater than the injected value, indicating a release of polymer that was retained during the previous run at a higher flow rate. After the first

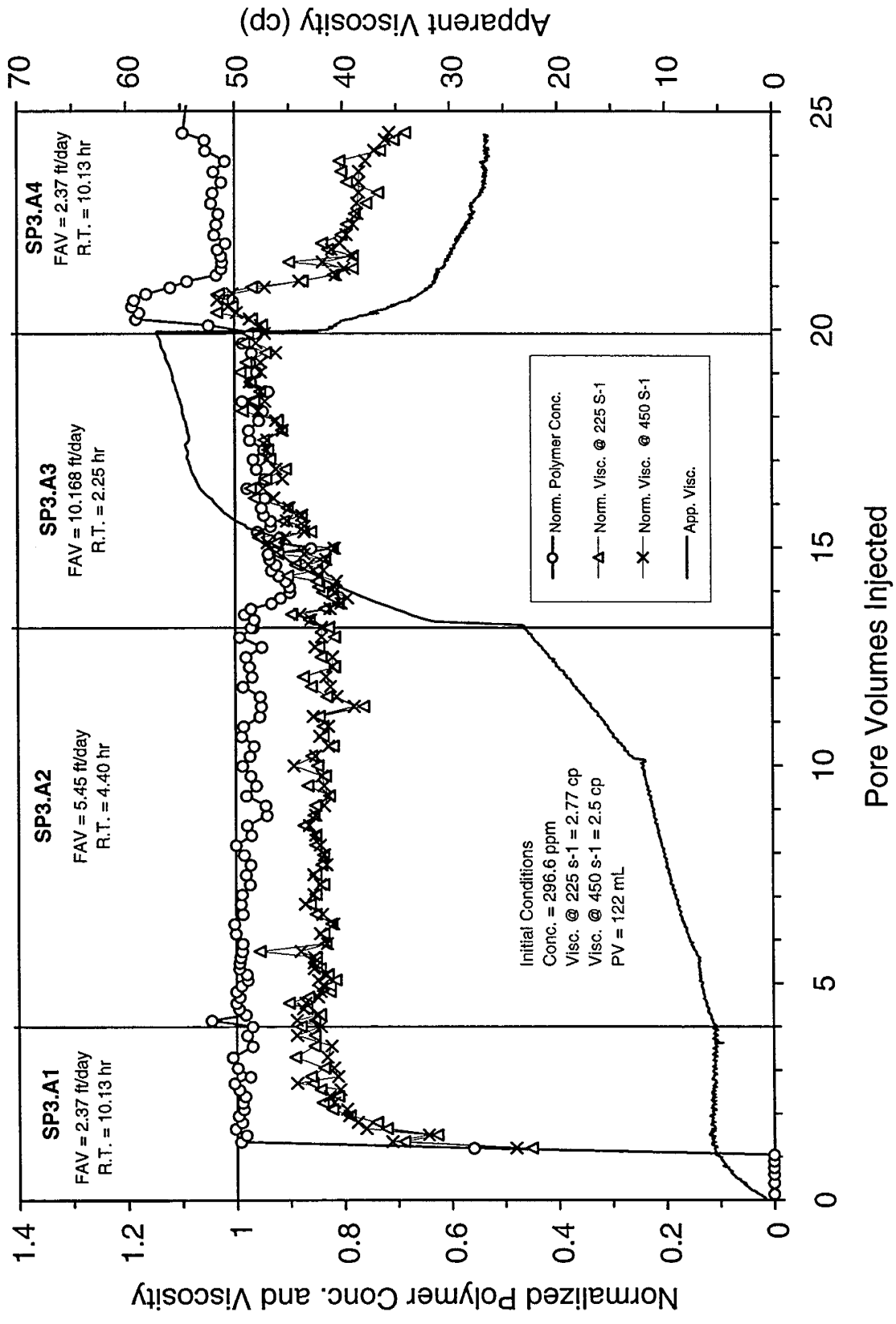


Figure 6.2 - Normalized polymer concentration, normalized viscosity, and apparent viscosity as a function of pore volumes injected during SP3.A Series

PVI in Run SP3.A4, the effluent polymer concentration continued to be greater than the injected value, but the viscosity of the effluent was much less than the injected value.

The apparent viscosity during Run SP3.A4 decreased and stabilized at a value approximately five times the value observed during Run SP3.A1 that was conducted at the same rate. The effluent measurements were also quite different between Runs SP3.A1 and SP3.A4 as shown in Figure 6.2.

The amount of polymer retained in the sandpack during the SP3.A series was calculated using the following equation:

$$M = C_{INJ} V_{INJ} - \sum_{I=1}^N C_{EFF} V_{EFF}$$

- where
- M = amount of polymer retained (mg)
 - C_{INJ} = injected polymer concentration (mg/mL)
 - V_{INJ} = volume of polymer solution injected (mL)
 - C_{EFF} = polymer concentration in effluent fraction (mg/mL)
 - V_{EFF} = volume of effluent fraction (mL)
 - N = number of effluent fractions collected during each run

Polymer retention values for the SP3.A series are given in Table 6.3. Polymer was retained in each run as the flow rate was increased. A significant portion of the retained polymer was expelled when the flow rate was decreased during Run SP3.A4.

Table 6.3 - Polymer retention during SP3.A series.

RUN	Frontal Advance Velocity (ft/day)	Volume Injected (mL)	Polymer in Effluent (mg)	Polymer Injected (mg)	Polymer Retained (mg)	Polymer Retained ($\mu\text{g/g}$ sand)	Polymer Retained (% of amount injected)
SP3A1	2.37	371*	103	111*	8	14	7.2
SP3A2	5.45	1120	326	333	7	12	2.1
SP3A3	10.7	821	232	244	12	21	4.9
SP3A4	2.37	550	174	164	-10	-18	-6.1
Total		2862	835	852	17	29	2.0

* Excludes the first pore volume injected during the displacement of brine by the polymer solution.

SP3.B Series. The flow rate in the SP3.B series was increased from 0.90 mL/min (FAV = 10.68 ft/day) to 4.5 mL/min (FAV = 53.28 ft/day) and then cut back to 0.93 mL/min (FAV = 11.01 ft/day) as given in Table 6.2. The effluent polymer concentration, effluent viscosity and apparent

viscosity as a function of pore volumes injected during SP3.B series are shown in Figure 6.3. The apparent viscosity profile in Figure 6.3 was calculated from the differential pressure drop across the total length.

The normalized polymer concentration generally behaved as in the previous Series SP3.A. The polymer concentration in the effluent was less than the injected concentration during the first PVI after the flow rate was increased in Runs SP3.B1 and SP3.B2. Little change in polymer concentration was observed during early times in Runs SP3.B3 and SP3.B4, possibly due to the relatively smaller increase in flow rate. The increase in polymer concentration during the first PVI after the flow rate was reduced in Run SP3.B5 was consistent with earlier observations.

The normalized effluent viscosity generally tracked the normalized effluent polymer concentration, except for Run SP3.B1. The low viscosity observed in Run SP3.B1 occurred during the injection of more than four PV. It appears this low viscosity was a concentration of behavior of Run SP3.A4 where the viscosity decreased during the injection of five PV. This behavior was unusual, particularly the length of duration which was more than two PVI.

The effluent viscosity generally tracked the effluent polymer concentration at the higher flow rates and was lower than expected based on the effluent polymer concentration at the lower flow rates. This indicated that the polymer was degraded more by the flow at the lower rates, which seems unlikely. Rather, this phenomenon is more likely the result of complex mechanisms of polymer retention and the effect of retained polymer on the flow.

Flow resistance in the sandpack during Series SP3.B runs was also unusual as shown by the apparent viscosity data in Figure 6.3. Steady apparent viscosities were not achieved for any of the runs except SP3.B5, even though about five PV of fluid were injected at each flow rate. Quite different values of apparent viscosity were observed for Runs SP3.B1 and SP3.B5, which were conducted at approximately the same flow rate. These results show that the flow resistance in the pack was dependent on the flow rate and strongly dependent on the previous flow through the pack. Generally, the flow resistance increased with flow rate.

The amounts of polymer retained in the sandpack during Series SP3.B runs are presented in Table 6.4. Polymer was retained during Runs SP3.B1, SP3.B2, SP3.B3 and SP3.B4 where the flow rate was increased for each run. Polymer was expelled during SP3.B4 when the flow rate was reduced.

Series SP3.C. Series SP3.C runs were conducted over the same flow rate range used in the SP3.B runs. In the SP3.C series the sandpack was shut-in for a time period between runs as shown in Table 6.2. The effluent polymer concentration and apparent viscosity as a function of pore volumes injected during the SP3.C series are shown in Figures 6.4.

A small amount of polymer was expelled from the sandpack during the first PV injected in Run SP3.C1. This might have been caused by the shut-in time before the run and/or the slight decrease in flow rate compared to Run SP3.B5. Increases in flow rate (Runs SP3.C2 and SP3.C3)

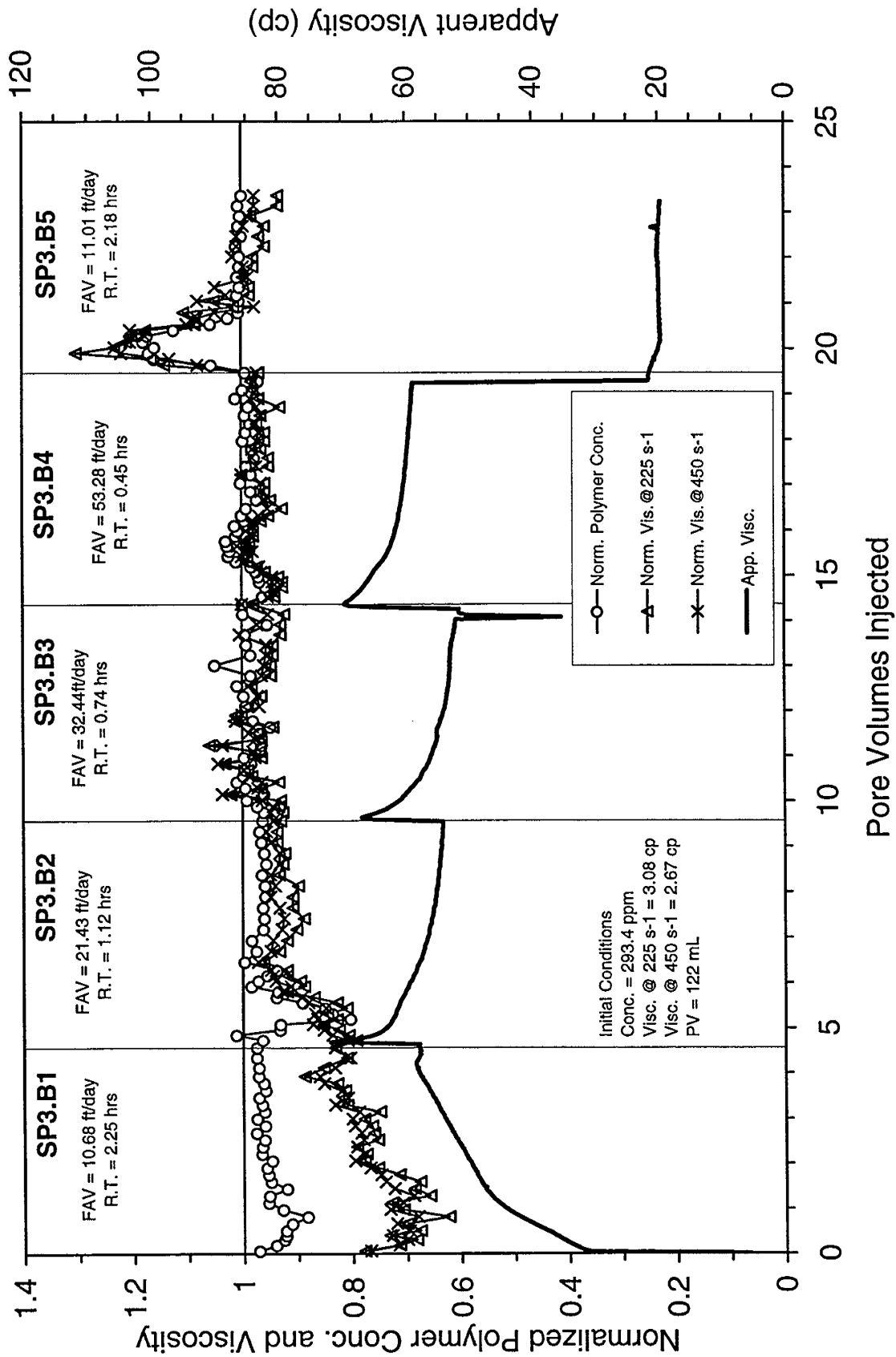


Figure 6.3 - Normalized polymer concentration, normalized viscosity, and apparent viscosity as a function of pore volumes injected during SP3.B Series

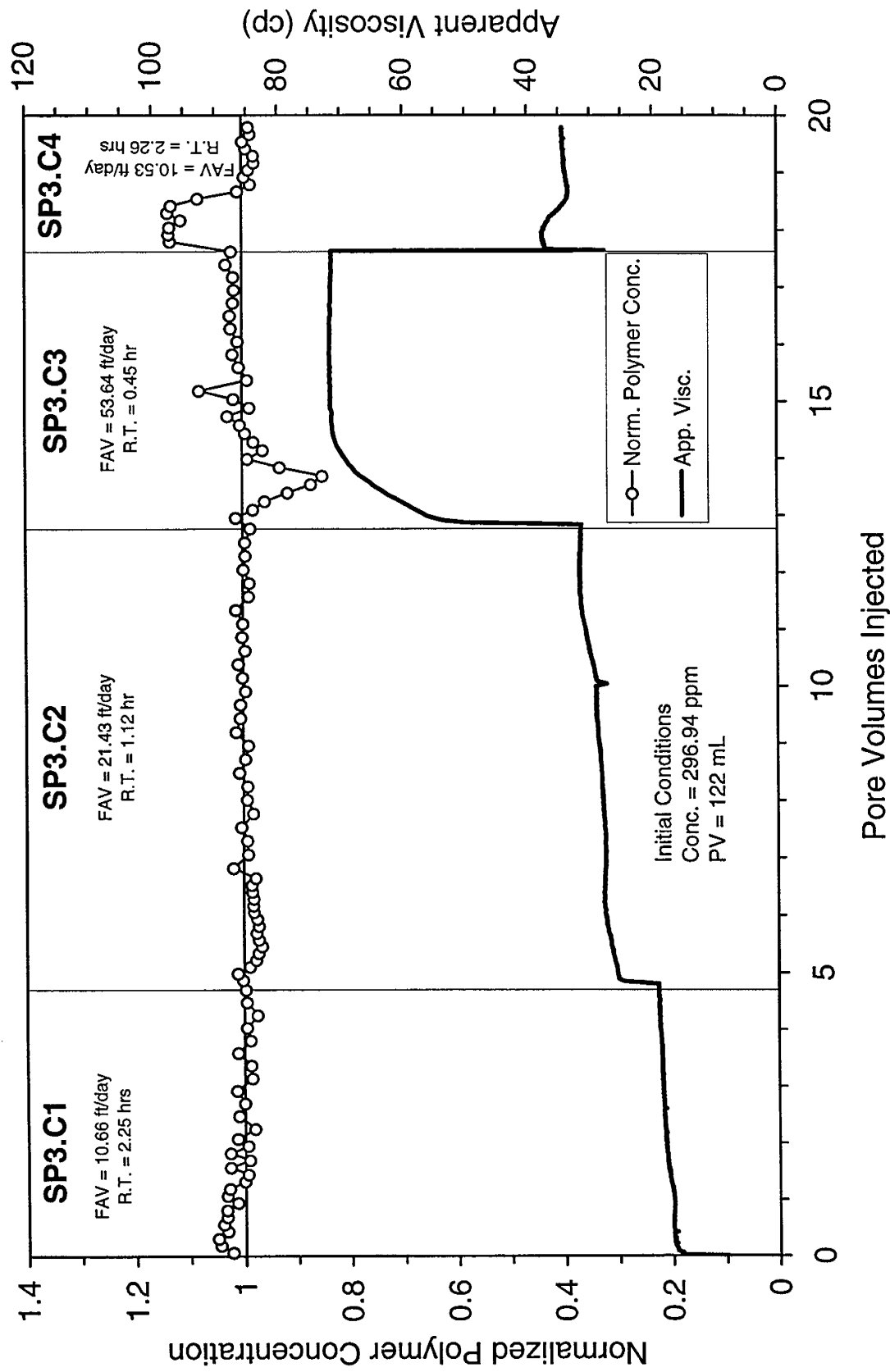


Figure 6.4 - Normalized polymer concentration and apparent viscosity as a function of pore volumes injected during SP3.C Series

Table 6.4 - Polymer retention during SP3.B series.

RUN	Frontal Advance Velocity (ft/day)	Volume Injected (mL)	Polymer in Effluent (mg)	Polymer Injected (mg)	Polymer Retained (mg)	Polymer Retained ($\mu\text{g/g}$ sand)	Polymer Retained (% of amount injected)
SP3.B1	10.7	566	160	167	7	13	4.2
SP3.B2	21.4	562	171	180	9	15	5.0
SP3.B3	32.4	574	169	171	2	3.6	1.2
SP3.B4	53.3	607	178	182	4	7.1	2.2
SP3.B5	11.0	485	143	140	-3	-5.3	-2.1
Total		2794	821	840	19	33	4.0

resulted in the initial decrease in the effluent polymer concentration. Reduction in flow rate resulted in the release of polymer during the initial PV of Run SP3.C4. Amounts of polymer retained during the SP3.C runs are given in Table 6.5.

Flow resistance in the sandpack increased with increased velocity as shown by the apparent viscosity data in Figure 6.4. The apparent viscosity of the effluent during Run SP3.C4 was higher than during Run SP3.C1 that was conducted at a similar velocity.

Table 6.5 - Polymer retention during SP3.C series.

RUN	Frontal Advance Velocity (ft/day)	Volume Injected (mL)	Polymer in Effluent (mg)	Polymer Injected (mg)	Polymer Retained (mg)	Polymer Retained (μg sand)	Polymer Retained (% of amount injected)
SP3.C1	10.7	798	173	172	-1	-1.8	-0.6
SP3.C2	21.4	981	287	289	2	3.5	0.7
SP3.C3	53.6	584	174	173	-1	-1.8	-0.6
SP3.C4	10.5	264	80	76	-4	-7.0	-5.3
Total		2627	714	710	-4	-7.1	-1.0

Previous Work. Two series of runs were conducted with unfiltered HiVis 350 solutions and previously reported [Green et al., 1998]. The principal parameter varied was the frontal advance velocity. The flow conditions used are given in Table 6.6. Flow was stopped for a period of time and then resumed at a different flow rate in the Series SP1.A. In SP1.B, the flow rates were changed without stopping the pump. The injected solutions contained 300 ppm HiVis 350 and 5000 ppm KCl. The solutions were not filtered.

Table 6.6 - Flow Conditions for Displacement Experiments SP1.A and SP1.B.

RUN	Frontal Advance Velocity (ft/day)	Flow Rate (mL/min)	Residence Time (hr)	Shut-In Time After Run (hr)	Pore Volumes Injected		
SP1.A Series							
SP1.A1	2.33	0.2	10.5	50	10.8		
SP1.A2	19.4	1.67	1.24	1.2	3.67		
SP1.A3A	46.9	4.03	0.51	0.5	3.91		
SP1.A3B	49.9	4.29	0.48	0.82	2.43		
SP1.A4	58.3	5.01	0.41	1.67	1.66		
SP1.A5	10.2	0.88	2.34	140	6.24		
SP1.B Series							
SP1.B1	10.4	0.89	2.32	-	2.31		
SP1.B2	19.9	1.71	1.21	-	2.33		
SP1.B3	36.1	3.10	0.67	-	2.83		
SP1.B4	47.5	4.08	0.51	-	3.23		
SP1.B5	12.1	1.04	1.98	-	5.24		
Permeability to brine for SP1							
Section	T	A	B	C	D	E	F
Permeability (md)	4796	4503	4802	4713	4576	5414	5726

The effluent apparent viscosity, normalized polymer concentration and normalized viscosity as a functions of pore volumes injected during Series SP1.A and SP1.B are presented in Figures 6.5 and 6.6, respectively. Material balances on the injected and eluted polymer are given in Tables 6.7 and 6.8 for the SP1 runs. The results presented in these figures and tables were qualitatively similar to the results described above for the SP3.A, SP3.B, and SP3.C series. No significant differences between the data could be attributed to the filtering of the injected polymer solution.

The apparent viscosities at the end of each run as a function of frontal advance rate are presented in a log-log graph in Figure 6.7 for all of the series of runs. The apparent viscosity generally increased with an increase in the frontal advance rate as indicated by the regressed line. Both the filtered and unfiltered 300 ppm HiVis 350 solutions exhibiting shear-thickening type behavior over the range of the flow rates studied. The shear thickening behavior, as well as the scatter in the data presented in Figure 6.7, is the result of retention of polymer. The retention process occurs over many PVI and is affected by previous runs.

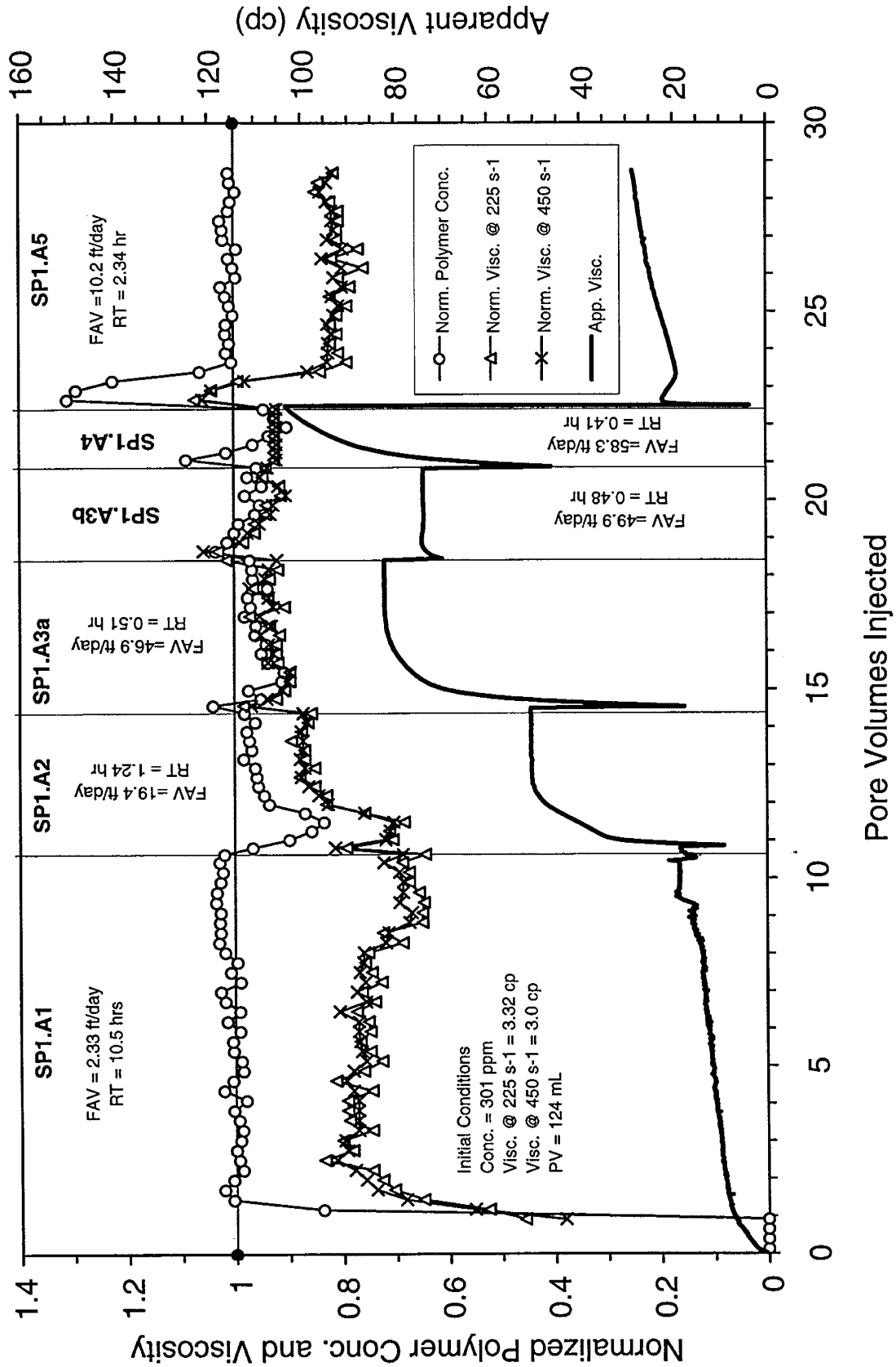


Figure 6.5 - Normalized polymer concentration, normalized viscosity, and apparent viscosity as a function of pore volumes injected during SP1.A Series

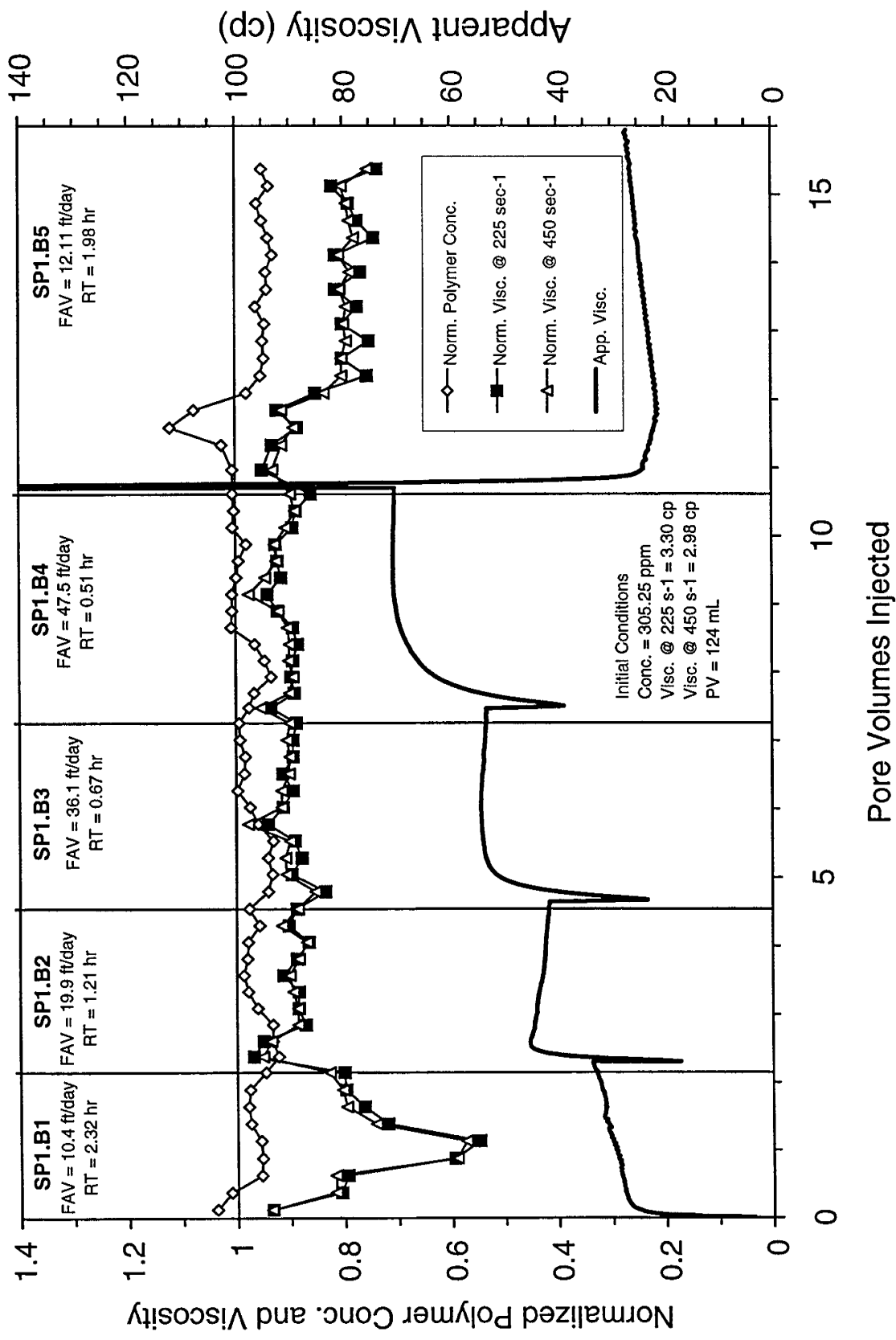


Figure 6.6 - Normalized polymer concentration, normalized viscosity, and apparent viscosity as a function of pore volumes injected during SP1.B Series

Table 6.7 - Polymer retention during SP1.A series.

RUN	Frontal Advance Velocity (ft/day)	Volume Injected (mL)	Polymer in Effluent (mg)	Polymer Injected (mg)	Polymer Retained (mg)	Polymer Retained (μg sand)	Polymer Retained (% of amount injected)
SP1.A1	2.33	1337*	362	399*	37	64	9.4
SP1.A2	19.4	454	132	139	7	13	5.5
SP1.A3a	46.9	484	144	150	6	11	4.3
SP1.A3b	49.9	301	90	92	1.8	3.0	1.9
SP1.A4	58.3	205	55	57	2	3.4	3.5
SP1.A5	10.2	772	244	236	-8	-14	-3.3
Total		3553	1027	1073	46	80	4.3

* Excludes the first pore volume injected during the displacement of brine by the polymer solution.

Table 6.8. - Polymer retention during SP1.B series.

RUN	Frontal Advance Velocity (ft/day)	Volume Injected (mL)	Polymer in Effluent (mg)	Polymer Injected (mg)	Polymer Retained (mg)	Polymer Retained (μg sand)	Polymer Retained (% of amount injected)
SP1.B1	10.4	286	83.8	86.0	2.2	3.8	2.6
SP1.B2	19.9	288	86.7	90.4	3.7	6.3	4.1
SP1.B3	36.1	350	99.4	104.0	4.6	7.8	4.4
SP1.B4	47.5	400	125	128	3	5.4	2.4
SP1.B5	12.1	649	175	177	2	2.8	1.0
Total		1973	570	585	15	26.1	2.6

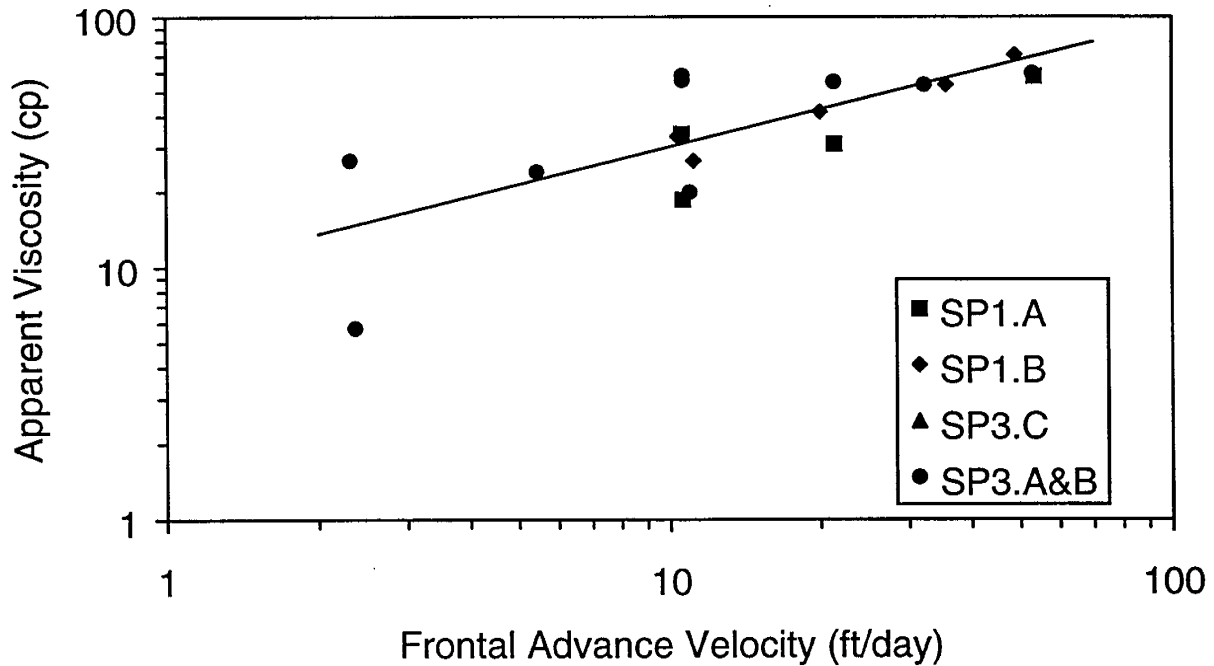


Figure 6.7 - The apparent Viscosity for 300 ppm unfiltered and filtered HiVis 350 solutions as a function of frontal advance velocity during SP1.A, SP1.B, SP3.A, SP3.B and SP3.C series.

Conclusions

The following conclusions were drawn from and are applied to the flow of a HiVis 350 polymer solution under the conditions studied.

1. A 300-ppm HiVis 350 solution in a sandpack exhibited shear-thickening behavior over the range of frontal advance rates between 2.3 and 58 ft/day.
2. The retention of polymer played a significant role in the development of flow resistance of HiVis 350 solutions in a sandpack. Retention of polymer occurred over many pore volumes of injection and was affected by flow that had occurred previously.

Chapter 7

A Study of Gelation and Injection Characteristics of a Polyacrylamide–Chromium Acetate System in the Presence of Added Acetate Ions

Principal Investigators: G. P. Willhite, D. W. Green and C. S. McCool
Graduate Research Assistant: Dilip Natarajan

Introduction

Chromium acetate-polyacrylamide gel systems have been used primarily to treat fracture systems, casing leaks and near wellbore regions in matrix rock [Sydansk, 1993] where short gel times are acceptable. The application of this technology to in-depth treatment of matrix rock is limited because the chromium acetate-polyacrylamide reaction is rapid. The objective of this study was to increase the gelation time of chromium-polyacrylamide systems by adding acetate ion to reduce the rate of crosslinking between chromium and the polymer. Measurements were conducted on bulk gel samples to study the effect of sodium acetate concentration on the gel time of partially hydrolyzed polyacrylamide (PHPA)–chromium acetate ($\text{Cr}(\text{OAc})_3$) gel systems. The effect of sodium chloride concentration on the gel times of PHPA– $\text{Cr}(\text{OAc})_3$ – NaOAc gel systems was also studied. Displacement experiments were conducted to investigate the injection characteristics of this gel system.

Background

Sydansk [1990], Sydansk, Argabright [1987], Sydansk [1997] developed that a family of chromium(III)–polyacrylamide gels ranging from highly flowing to rigid rubbery gels, with a wide range of gel times. Burrafato and Lockhart [1989] and Burrafato et al. [1990] proposed that the chromium uptake from chromium-carboxylate complexes is a ligand exchange reaction in which a carboxyl group on the polyacrylamide displaces ligands (i.e. acetate). Crosslinking occurs when a second polyacrylamide molecule reacts with the attached chromium. Addition of acetate to a gel solution should limit the amount of chromium uptake and reduce the amount of crosslinking.

Several researchers have explored the use of competing ligands for delaying gelation. Albonica et al. [1993] demonstrated that organic chromium salts and added organic ligands like salicylate and malonate prevented gelation of chromium-polyacrylamide systems at low temperatures and delayed gelation at elevated temperatures. They also demonstrated that chromium-polyacrylamide gels can be “degelled” by adding a solution containing a ligand that is stronger than the carboxyl group on the partially hydrolyzed polyacrylamide such as glycolate or malonate.

Bottle tests conducted as a part of this research and their results were presented in a previous report [Green et al., 1997] along with a few preliminary displacement experiments. Gel solutions were prepared from different polymer and chromium acetate sources and the effect of added acetate (provided as sodium acetate), sodium chloride and chromium stock age on the gel times, were studied. Increasing concentrations of sodium acetate were shown to delay gelation. Delays in gel times were significant beyond a certain threshold acetate concentration. Figure 7.1 shows

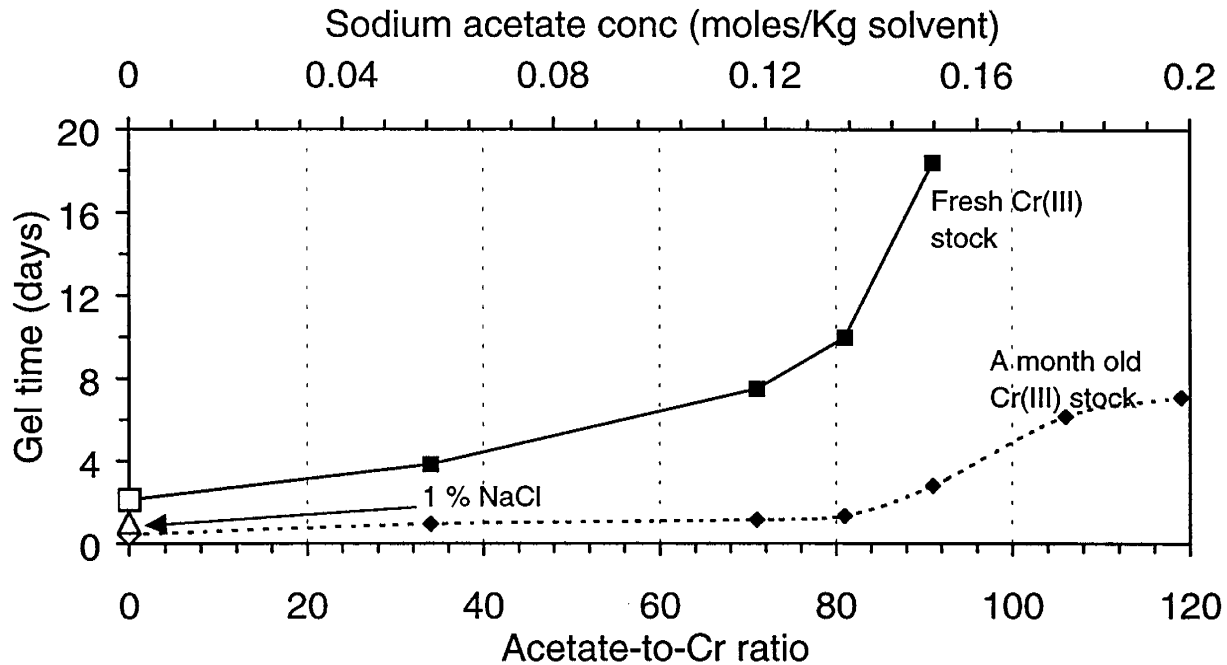


Figure 7.1 - Effect of NaOAc and Cr(III) stock age on gel times of PHPA-Cr(OAc)₃ system. [polymer (Alcoflood 935) - 5000 ppm, Cr(III) (Mcgeane & Rohco)-109 ppm and initial pH - 5.0 at 25°C]. Sample with no NaOAc measured at shear rate of 4.5 s⁻¹ while the rest were measured at 11.25 s⁻¹.

the effect of sodium acetate and chromium stock age on the gel times of PHPA-Cr(OAc)₃ systems. Aging the chromium stock significantly reduced the gel times of this system. The effect of sodium chloride on PHPA-Cr(OAc)₃-NaOAc systems is shown in Figure 7.2. Sodium chloride at high concentrations relative to the acetate salt reduced gel times of PHPA-(CrOAc)₃-NaOAc gel systems. Preliminary displacement experiments showed that increasing acetate concentrations delayed the development of flow resistance during gelant injection in the porous media. However, the flow resistance development was significantly faster than the gelation rates observed in bottle tests.

The objective of this research was to demonstrate in packs of different dimensions that increasing acetate ion concentrations would delay in-situ gelation of chromium acetate-polyacrylamide systems. Delayed in-situ gelation would improve the injection characteristics of the system by allowing deeper penetration of gelant before the development of significant flow resistance.

Experimental

Displacement experiments were designed to study the injection characteristics of the gel system in porous media. The composition of the gel solution used in the displacement experiments was 5000 ppm PHPA (Alcoflood 935, 10% hydrolyzed), 109 ppm Cr(III) (McGean Rohco) and an initial pH of 5.0. Parameters like concentration of sodium acetate, sodium chloride and age of the

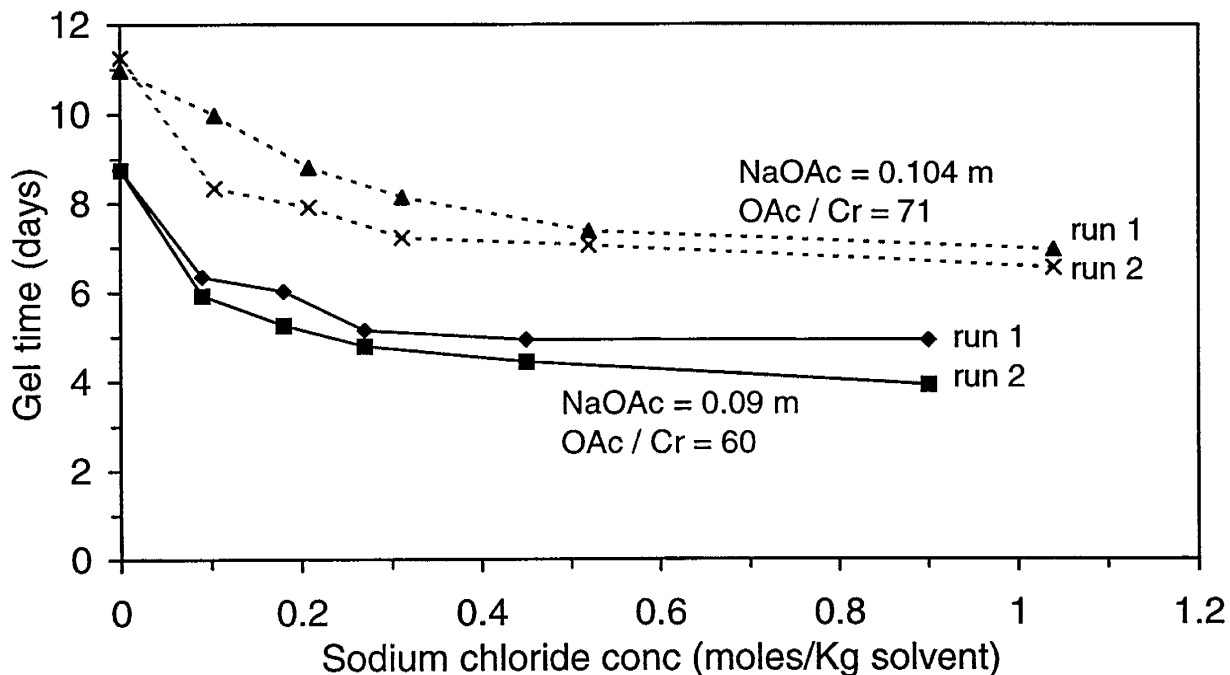


Figure 7.2 - Effect of NaCl on the gel times of PHPA-Cr(OAc)₃ - NaOAc system. [polymer (Alcoflood 935) - 5000 ppm, Cr(III) (McGean & Rohco) - 109 ppm and initial pH - 5.0 at 25°C]. Gel times estimated at shear rate of 11.25 s⁻¹.

chromium stock were studied along with the reproducibility of the injection characteristics. The experiments were conducted in unconsolidated sandpacks with lengths of 1, 4 and 6 feet. Experimental details are described by Green et al. [1998].

Stock solutions of polymer and crosslinker were pumped and mixed in-line at a 3:1 ratio, respectively. Chromium stock solutions were used fresh or aged for a month depending on the experiment. The pH of the polymer stock solutions was adjusted so that the gel solution pH was 5.0 (± 0.1) at the entrance of the sandpack. The injection rate was maintained around a darcy velocity of 2.49 ft/day, which correspond to a frontal advance velocity of 7.5 ft/day. Pressure was measured during gel injection using the transducer setup. Gel injection was terminated when a specified volume of gelant was injected or when the overall injection pressure increased to 80 psi. For runs where bulk gel time was less than 21 days, the sandpack was shut-in at 25°C for a period equal to or greater than its bulk gel time. Brine injection at constant pressure was used to determine the post-treatment permeabilities.

Results and Discussion

A listing of the displacement experiments is given in Table 7.1. Runs B2 and SP11 were conducted in 4-ft long packs with 1.5" ID and Runs SP14 and SP15 were conducted in 6-ft long packs with an ID of 1". All the other runs were conducted in 1-ft long packs with 1.5" ID. The porosity of the sandpacks was in the range of 30-35%. The pore volume of 1-ft packs were in the range of 100-120 mL while the 4-ft packs had a pore volume of 460 mL. The 6-ft packs had a

Table 7.1 - Summary of displacement experiments.

Run #	NaOAc conc. (m)	OAc/Cr ratio	Bulk gel times	Pore volumes injected
B 1	No NaOAc	3.05	48 hrs	5
B 2	No NaOAc (1% NaCl)	3.00	24 hrs	0.65
SP2	0.12	81	20 hrs	1.2
SP3	1.0	600	> 1 year	3.75
SP5	0.088	60	148 hrs	7
SP6	0.104	71	200 hrs	7.3
SP8	0.14	91	17-18 days	7.5
SP9	0.14	91	17-18 days	8
SP10	0.14 (0.7 m NaCl)	91	13-14 days	7.5
SP11	0.14	91	17-18 days	2
SP14	0.104	71	200 hrs	1.2
SP15	0.14	91	17-18 days	1.8

pore volume of 400–410 mL. Fresh chromium stock was used in most of the experiments except SP2 and SP3 where the crosslinker solution was aged for one month before gel injection.

The acetate/Cr ratios provided in Table 7.1 are about 30% higher than the values corresponding to the added sodium acetate, due to the addition of acetic acid for pH adjustment. At least 1 PV of gelant was injected into each sandpack with the exception of Run B2 where the pressure limitation was reached after 0.65 PV of gelant was injected. All sandpacks were shut-in at 25°C for a time corresponding to the gel times of the gelant injected and post-treatment permeabilities were estimated by injecting brine. The post-treatment permeabilities of the packs were in the range of 30 - 40 micro-darcies, except in SP3. No permeability reduction was observed in SP3 when brine was injected after 4 months of shut-in time.

Pressure drop data collected during injection of gelant are presented as apparent viscosities as a function of pore volumes injected. Apparent viscosities were calculated from the pressure differentials and the initial permeabilities using Darcy's law (Eq.7.1). Apparent viscosity is a

measure of the average flow resistance in the sandpack over which the pressure differential was measured.

$$\mu_{app} = \frac{k \cdot A \cdot \Delta p}{q \cdot L} \quad \text{Eq. 7.1}$$

where,

- μ_{app} = apparent viscosity
- k = permeability
- A = cross-sectional area
- Δp = pressure differential across a section
- q = volumetric flow rate
- L = section length

Base Case(s). Runs B1 and B2 were conducted as baseline runs in that the injected gelant contained no added acetate. The gel solution used in Run B1 contained no added salts except for a small amount of acetic acid that was used to adjust pH. Run B2 was a more appropriate baseline run to judge the effect of added acetate has on the injectivity of the polyacrylamide-chromium acetate system. The gelant for Run B2 was the same as in Run B1 except KCl (1.0% concentration) was added to give a similar initial solution viscosity as in the runs that contained added acetate. The overall pressure drop exceeded 80 psi by 0.65 PV and injection was terminated. The gelant penetrated about 2.8 ft. of the pack.

Effect of added acetate ions. The effect of added acetate ions on the injection characteristics in the first foot of the porous media is demonstrated by a comparison of Runs B2, SP3, SP5, SP6, and SP8 (OAc/Cr ratios were 3,60, 71, 91 and 600).The overall apparent viscosities in the foot long packs i.e. SP3, SP5, SP6 & SP8 and the first one-foot of the four-foot long pack B2 are shown in Figure 7.3. The data show that increasing concentrations of added acetate ions delayed the development of flow resistance during gel injection in the porous medium. In B2 (OAc/Cr = 3), the flow resistance development was significant and the apparent viscosity across the first foot of the pack increased rapidly to about 200 cp with the injection of about 300 mL. At an OAc/Cr ratio of 60 (Run SP5), about 500 mL (4.5 PV for the foot long pack) was injected before the apparent viscosity increased to 200 cp. An acetate/Cr(III) ratio of 71 was used in SP6 and 700 mL of gel solution was injected before the apparent viscosity increased to 200 cp.

Only small increases in apparent viscosities were observed when the OAc/Cr ratios were 91 and 600. In these runs, the OAc/Cr ratios were sufficiently high to inhibit development of high apparent viscosities in the sandpack during gel placement. Brine was injected in SP8 (OAc/CR = 91) after 20 days of shut-in. The permeability was approximately a few microdarcies, indicating gelation. Brine was injected into SP3 (acetate/Cr = 600) after about 4 months of shut-in. The brine fingered through the pack at very low pressure differentials, indicating that the high acetate concentration inhibited gelation. Permeability reduction did not occur.

In all cases where flow resistance development was observed during injection (i.e. SP2, SP5, SP6, and SP11), the flow resistance developed much sooner than the respective gel times observed in the bottle tests. For example, the gel solution used in SP5 had a gel time of about

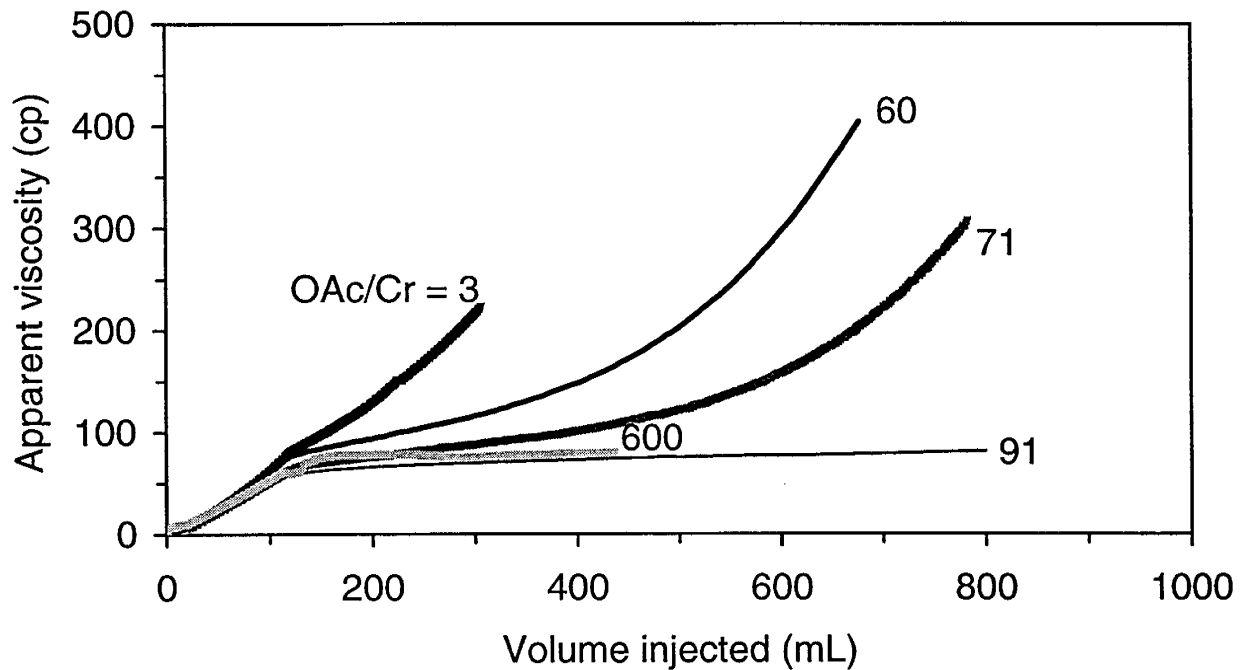


Figure 7.3 - Effect of added acetate on injection characteristics. Comparison of apparent viscosities across the first foot of sandpack in runs SP3, SP5, SP6, SP8 and B2.

150 hours but showed significant flow resistance within an injection time of 24 hours. The probable reason for this behavior is the formation of aggregates and the filtration of pre-gel aggregates as the gel progressed through the pack. This combination of progressive crosslinking and filtration probably had a compounding effect that resulted in a near exponential increase in the resistance development. Hence the injection time before the development of substantial flow resistance is a function of the residence time (or flow rate), gelation kinetics (influenced by the added acetate) and properties of the porous media.

The effect of acetate ions in delaying the development of flow resistance within the first foot of the porous medium was clearly demonstrated in SP2, SP3, SP5, SP6, and SP8. The injection characteristics of this gel system in four-foot packs, at different OAc/Cr ratios are presented in Figure 7.4. The plot shows that increasing the ratio from 3 to 91 increased the time to reach an apparent viscosity of 150 cp by a factor of about four. The effect of added acetate on the injection into 6-foot long packs is shown in Figure 7.5. OAc/Cr ratios of 71 and 91 were used in these runs. This comparison shows that increasing the OAc/Cr ratio from 71 to 91 facilitated the injection of about 70% more gelant for the same flow resistance development.

Gelant propagation. Apparent viscosity profiles along the length of the sandpacks are included in Reference Green et al. [1998] as Figures 7.9-11. These plots show that by increasing the OAc/Cr ratios, one can delay the development of flow resistance and improve gelant propagation for a given injection pressure limitation.

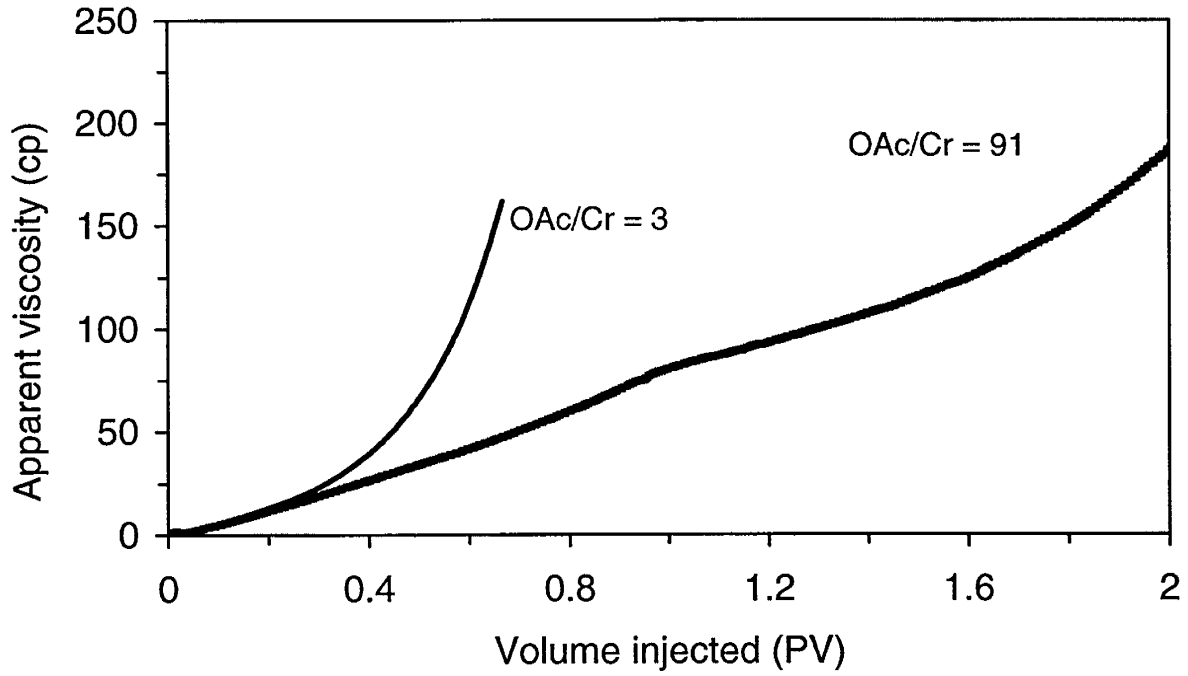


Figure 7.4 - Effect of added acetate on injection characteristics. Comparison of overall apparent viscosities across 4 ft in runs SP11 and B2.

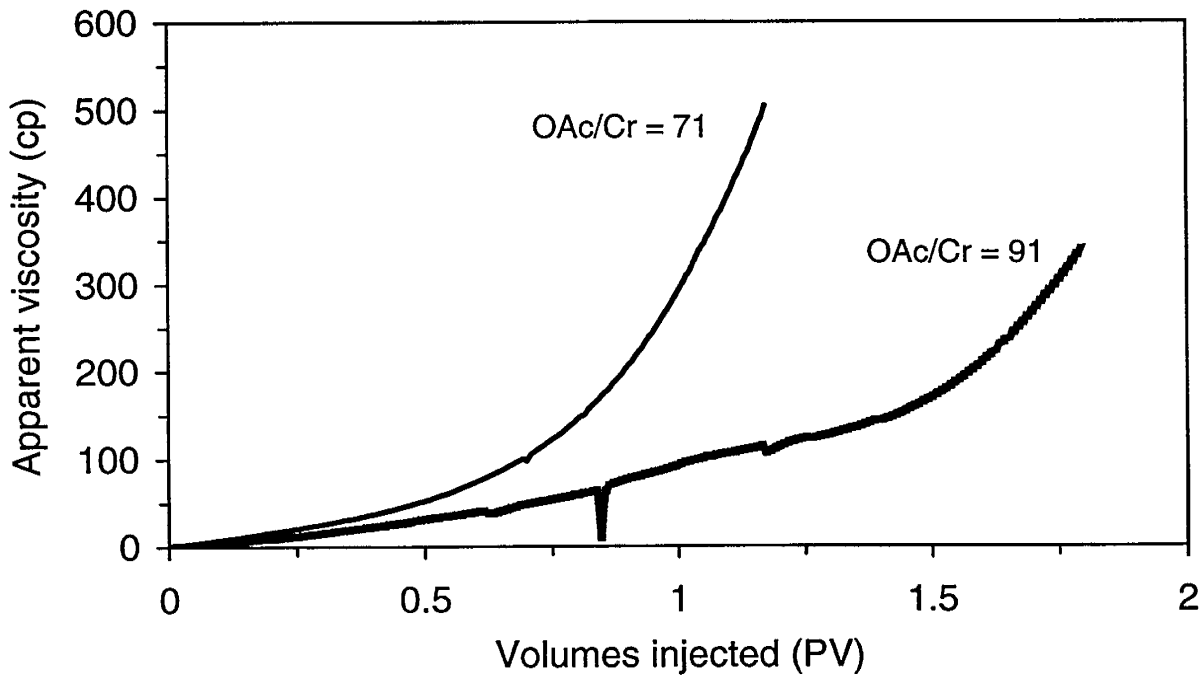


Figure 7.5 - Effect of added acetate on injection characteristics. Comparison of overall apparent viscosities across 6 ft in SP14 and SP15.

Effect of sodium chloride. A displacement experiment using a gel solution with an acetate/Cr ratio of 91 and a sodium chloride concentration of 0.7 m was conducted to verify bottle test results which showed a 20% reduction in gel times of this system in the presence of high sodium chloride concentrations. Sodium chloride did not affect the injection characteristics of this system within 1 ft of the porous medium in spite of the reduction in bulk gel time.

Effect of chromium stock age. The effect of chromium stock age that was observed in bottle tests was also studied in the porous media (SP2). The delaying effect of the added acetate ions was completely offset by the use of aged chromium stock. Fresh chromium solution is likely to be used in field applications so gel times would not be affected by solution age.

Reproducibility. Gel times in bottle tests were reproducible to within 10%. Gel times and viscosity behavior with time for bulk samples and in-line samples prepared during the displacement runs were also consistent with the bottle samples [Green et al., 1998].

Conclusions

The conclusions are limited to the chromium acetate-polyacrylamide system studied at 25°C under conditions where the pH was controlled at $\text{pH } 5 \pm 0.1$ with displacement experiments conducted in unconsolidated sandpacks.

1. The gel times of PHPA–chromium acetate gel systems can be increased by adding acetate ions. Gel times in the range of a few hours to several days were achieved by varying the OAc/Cr ratios from 3 to 91 in gel solutions containing 5000 ppm polymer and 109 ppm chromium. OAc/Cr ratios greater than 260 inhibited gelation for more than a year.
2. Gelation delays were significant beyond a threshold acetate ion concentration. The threshold OAc/Cr(III) ratio for the gel composition studied was about 80.
3. Gel solutions prepared from aged chromium stock had significantly shorter gel times than fresh stock samples. High concentrations of acetate ions in solution were offset by the effect of chromium stock age.
4. Increasing concentrations of sodium chloride were found to reduce the gel times of the PHPA–CrOAc–NaOAc system.
5. Increasing OAc/Cr ratios were found to delay the development of flow resistance during gel injection in unconsolidated sandpacks.
6. The use of aged stock significantly reduced the time available for gel injection at reasonable pressures.
7. The time available for gel injection using reasonable injection pressures was significantly shorter than the gel times in most of the displacement experiments which was probably due to filtration of pre-gel aggregates.
8. High acetate ion concentrations (OAc/Cr(III) = 600) completely inhibited *in situ* gelation and hence any permeability modification.
9. Gel times and injection characteristics for this system were reproducible within acceptable limits.

Chapter 8

Gel Behavior in Fractured Media

Principal Investigators: D.W.Green, G.P.Willhite, C.S.McCool
Graduate Research Assistant: S. Ganguly

Introduction

Many reservoirs are fractured to some extent. In addition to naturally occurring fractures, reservoir rocks are hydraulically fractured at production wells to increase production rates. Thermal stresses and over-pressuring at injection wells also create fractures. Injected water channels through the fractures and leads to inefficient displacement of oil. One method to control water channeling is to block the fractures with a gelled polymer treatment.

During placement of a gelant into a fracture within a porous matrix, some of the gelant leaks off to the adjoining matrix. "Leakoff" of gelant into the matrix adjoining the fracture contributes to flow dynamics during placement. It affects fracture gel strength, and is responsible for additional resistance in matrix after placement. The objectives of this research are to study the behavior of gelant/gel in fracture and in adjacent matrix during placement (with leakoff), and during brine injection after placement.

This chapter summarizes the displacement of Cr(III)-PHPA gelant in physical model of a fracture, and the behavior of the gel after treatment. A theoretical model, accounting for simultaneous flows in fracture and matrix was developed to describe the flow of a viscous solution displacing resident brine. The extrusion of gel from a fracture after placement with and without leakoff was studied. Leakoff was investigated through displacement experiments where gelant was injected under constant pressure into unfractured linear cores. A model was developed to describe the flow and pressure profile for gelant leakoff based on the displacement experiments in unfractured cores.

Background

The application of gelled polymer treatments to fractured systems was investigated by Seright [1994, 1996]. Seright studied the performance of several immature, preformed, and mechanically degraded gels by displacing them through fractured cores without any significant leak off into the adjacent matrix.

Injection of bulk mixed Cr(III) acetate PHPA gelant / gel under constant pressure is reported by Seright [1994] and Sydansk [1988]. Build up of resistance was observed with continuous injection. The build up was rapid for matured gel. However, the effect of gelant leakoff on gel placement and gel displacement was not studied.

Experimental

Gel system. Cr(III)-PHPA gelant was studied for fracture application. The polymer, used, was hydrolyzed polyacrylamide (Alcoflood 935, molecular weight 5×10^6 daltons, degree of hydrolysis 5-10%). Chromium tri acetate (McGean Rhoco) was the crosslinker. The composition

of the gelant was 5000 ppm polymer, 417 ppm chromium triacetate, and 1% NaCl. pH of the mixture was 4.78 (unadjusted). The gel time for this composition at 25° C was 12-16 hours. The viscosity of the polymer solution (5000 ppm PHPA, with 1% NaCl), at different shear rates, was measured by Bohlin rheometer. Flow experiments in Berea core were conducted with polymer solution without crosslinker to determine the apparent viscosity in porous media (using Darcy's law). Viscosity of the polymer solution and the apparent viscosity from the flow study are presented in Figure 8.1. The polymer solution exhibited shear-thinning behavior, with a power law exponent of 0.23-0.25 for frontal advance rates less than 15 ft/day. Shear thickening behavior was observed at frontal advance rates greater than 15 ft/day.

Fracture Model. A physical model of a fracture was developed to study the behavior of gel in controlled experiments. Leakoff from the fracture into the matrix was accomplished by opening the sides of the fractured slab to atmospheric pressure. Leakoff was controlled by a back pressure regulator at the fracture exit. It was found that there was an upper bound on back pressure, beyond which all the influent to the fracture exits through the matrix. The upper bound on back pressure was critical for controlling the back pressure during displacement. A mathematical model was developed that describes the influence of the flow rate and slab properties on the upper bound of the back pressure. The mathematical model was used to select the dimensions and permeability (primarily a thin and wide slab with low permeability) of the flow cell.

Berea slabs were fractured into two symmetric halves by a hydraulically operated fracturing blade. The two halves were held together and the entire assembly was coated with epoxy. Flow into the fracture enters through a small compartment and exits the fracture through a similar compartment. The rest of the inlet and outlet faces were sealed with epoxy. Leak off from the fracture into the matrix exited the model from the two sides. Pressure ports were drilled at different positions on the top of the assembly to sense pressure differentials across the various sections of the slab. The assembly was saturated with 1% NaCl solution. The fracture permeability, fracture aperture width, matrix permeability and matrix porosity were determined from a series of flow tests prior to displacement.

Permeability of the fracture was determined by closing the matrix outlets and flowing brine through the fracture. Flow rate and pressure differentials across fracture sections were measured. The 'cubic law' [Iwai, 1976] was used to compute the aperture width of the fracture.

Matrix permeability was determined by injecting brine into the fracture and measuring flow rate at the matrix outlets. Pressure differentials were measured between the ports, which divide the matrix into sections.

Tracer tests were conducted in each half of the cell assembly to determine the pore volume of the matrix. A step change in influent concentration was introduced and effluent concentrations of the matrix segments were monitored with time. Typical data is presented in Figure 8.2. Typical permeability of the matrix was between 50 and 150 md. Permeability of the fracture was on the order of 5000 darcy (aperture =0.03 cm).

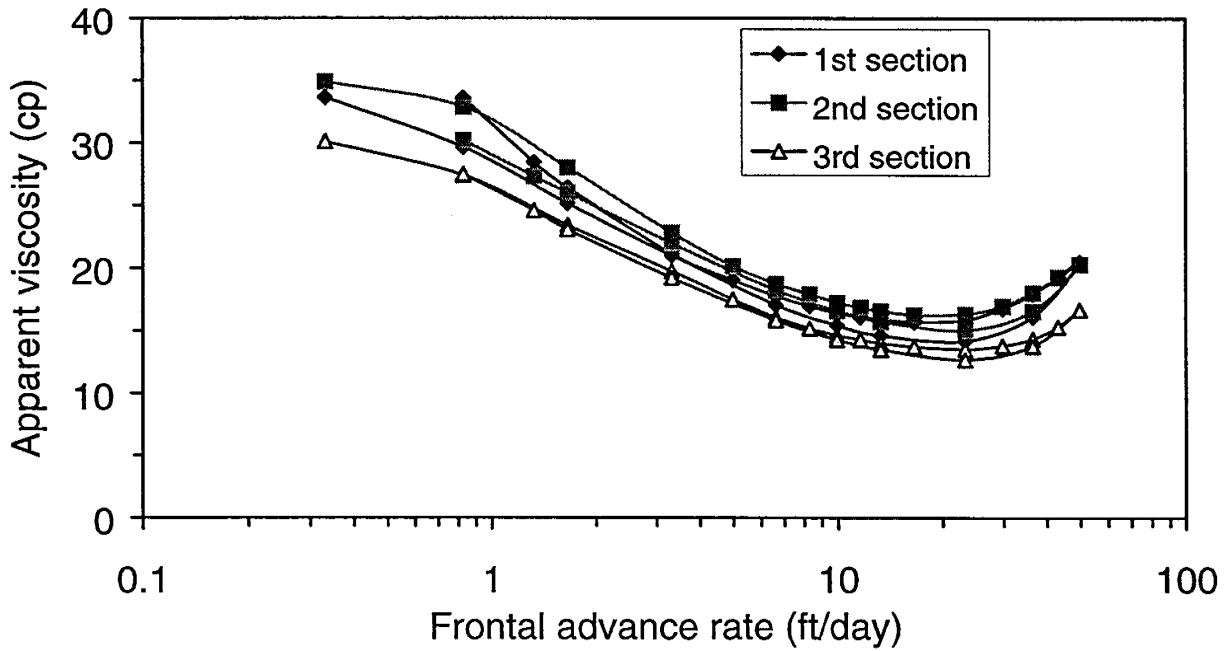
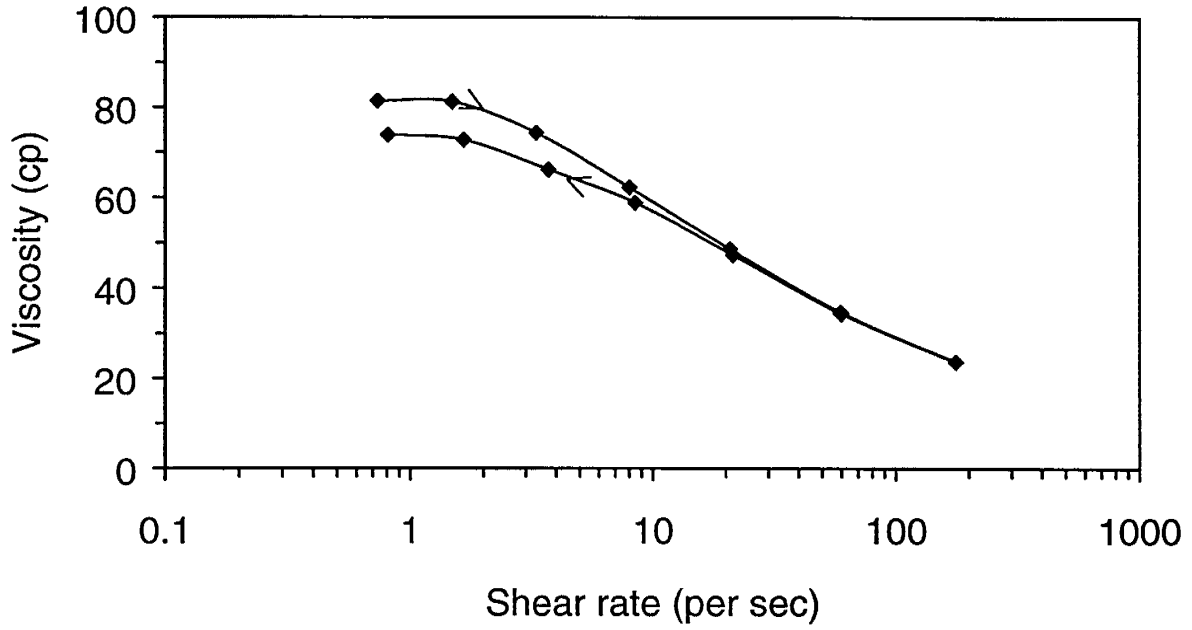


Figure 8.1 - Viscosity of uncrosslinked PHPA (5000 ppm Alcoflood 935 with 1% NaCl) obtained using Bohlin rheometer (upper plot), and from displacement studies (lower plot).

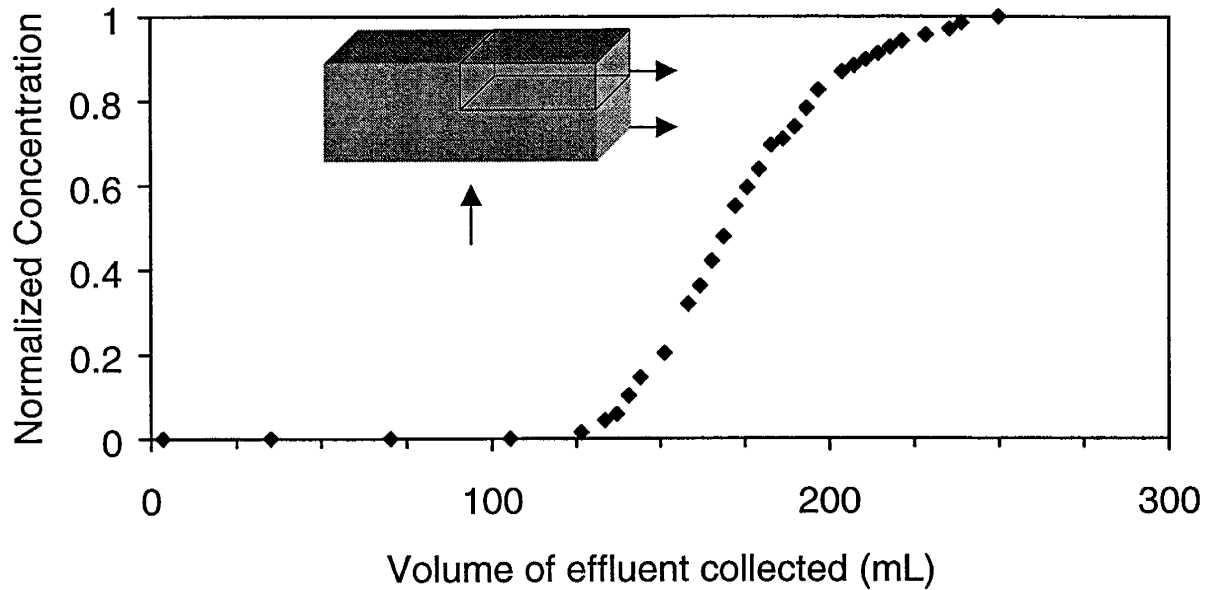


Figure 8.2 - Tracer response from a matrix outlet of the fracture model.

A schematic diagram of the equipment and set up used for the gelant displacement experiment is shown in Figure 8.3. Oil displaced polymer from the transfer cylinder. The polymer solution was mixed with the crosslinker solution in the ratio of 2:1 in an in-line mixer, prior to entering into the fracture. Matrix outlets were open to atmospheric pressure. The back pressure at the fracture outlet was set at a specified value by the back pressure regulator. The effluents from the fracture and matrix outlets were collected in graduated cylinders. Volume in the cylinders was recorded with time. Samples of the fracture and matrix effluents were collected at specified intervals for analyses. Pressure transducers, attached to various sections of the core, continuously recorded the pressure differential, through a demodulator assembly.

Displacement of glycerol (simulating viscous gelant without added complication of gelation) was accomplished using a similar setup as described in Figure 8.3. Oil displaced glycerol (instead of polymer) from the transfer cylinder. The crosslinker stream was not connected.

Leak off experiments (unfractured core). During injection of a Cr(III)-PHPA gelant into a long fracture, the pressure drop in the fracture is small at injection rates observed in field applications. Thus, the injection pressure in the fracture remains constant with time and the fracture acts as a line source extended from the well. As the gelant travels down the fracture, the age of the gelant increases. Leakoff experiments that simulate these effects were performed in unfractured Berea cores as a part of this research. In the experiments, the injection pressure was held constant and the inline mixed gelants were allowed to age by displacing them through a tubing section prior to injection.

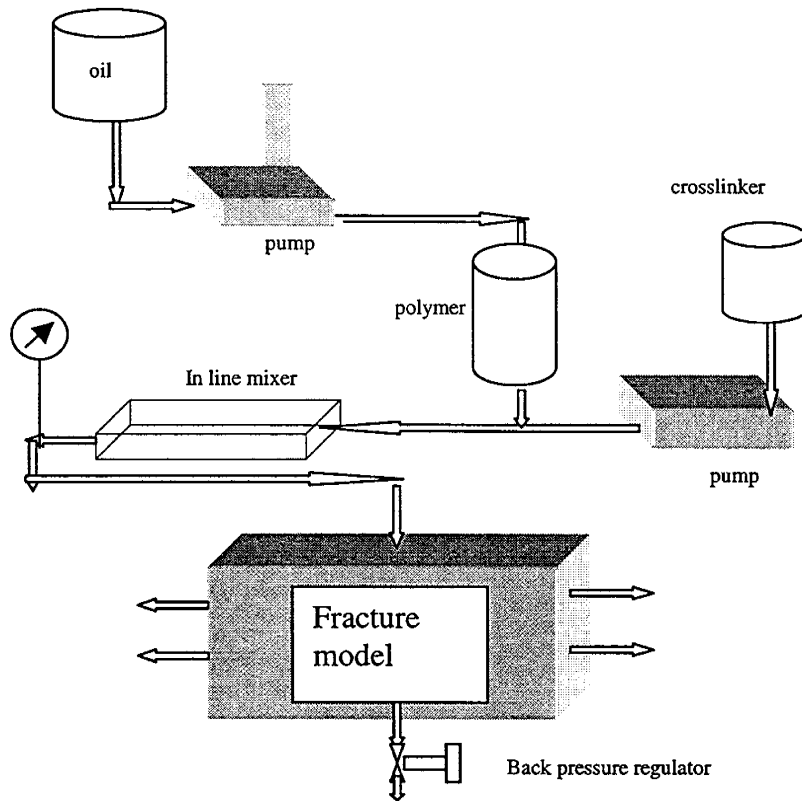


Figure 8.3 - Flow schematics for gelant displacement.

Foot long Berea sandstone cores were used to study leakoff of gelant under constant pressure. Each core was fitted with end caps and was coated with epoxy. Equidistant pressure ports along the length were installed to divide the cores into six sections. The core was saturated with 1% NaCl. Permeability of each section was determined to be 60-65 md from measurement of pressure differentials at five different flow rates. Tracer tests indicated porosities of the cores to be between 0.17 to 0.18.

Four displacement experiments were performed with Cr(III)-PHPA gelling solutions at a constant injection pressure of 70 psi (limited by the epoxy coating). For the first displacement experiment, polymer and crosslinker were mixed in bulk and an air source displaced the gelling solution from transfer cylinder into the core. In the other three runs, gel was mixed inline in the ratio of 2:1. After inline mixing, the gelant flowed through tubes of pre designed length for controlled aging to following extents.

1. zero age (no delay between inline mixing and injection)
2. three hours of flow between inline mixing and injection
3. six hours of flow between inline mixing and injection

Flow schematics were similar as described in Figure 8.3 with following exceptions.

1. The Berea core replaced the fracture model.
2. The back pressure regulator was installed immediately before the inlet to the core. The flow through the regulator went parallel to the main flow down the core, to maintain a constant pressure at the inlet face of the core.
3. A transfer cylinder, on the inlet line after the delay loop, provided the extra flow for the initial period. The transfer cylinder was filled with gelant of required age, immediately before the displacement, and the cylinder was pressurized externally by a nitrogen source.

Pressure transducers, attached to various sections of the core, continuously recorded the pressure differential, through a demodulator assembly. Cumulative volume, collected at the effluent end was measured with time. Samples were drawn from the effluent for subsidiary measurements (viscosity, pH, Cr content).

About one pore volume of bulk mixed gelant was injected before the flow rate dropped to zero. A similar situation happened with inline mixed gelants. More than two pore volumes of gelant could be injected with no prior aging, one and half pore volumes of gelant could be injected with three hours of prior aging, and three quarters of a pore volume of gelant could be injected for six hours of prior aging.

Results and Discussions

Displacement in fracture model. Cr(III) PHPA gelant was injected into the fracture at a constant flow rate of 4.6 mL/min. The back pressure, set at the fracture end, was 50 psi. The fraction of injected fluid that leaked off into the matrix during this period is plotted as a function of time in Figure 8.4. For first 1.25 hours, there was no flow at the fracture outlet. All the influent went out of the matrix at constant flow rate. Beyond this period, fracture flow increased for a short period, with matrix flow dropping significantly. Then both fracture and matrix flow gradually approached a steady value.

Pressure gradients (psi/inch) for the three fracture sections are plotted in Figure 8.5. There was a short initial plateau when there was no gelant leaving the fracture outlet. As the flow started at the fracture outlet, there was a discrete change in the pressure differential for three fracture sections. Subsequently a slow increase in pressure differentials (which gradually flattened out) was due to increase in fracture flow rate with time. The maximum pressure gradient was observed in the first section, followed by second and third sections. This is in agreement with the fracture pressure profile (convex downward), deduced theoretically.

Pressure profiles for the matrix sections were nearly the same for all quadrants of the flow cell. Figure 8.6 represents pressure profile for one of the quadrants. All sections registered an immediate rise in pressure differential as the flow started. The maximum in the pressure differential for each section corresponds to the arrival of the viscous front. No second build up of

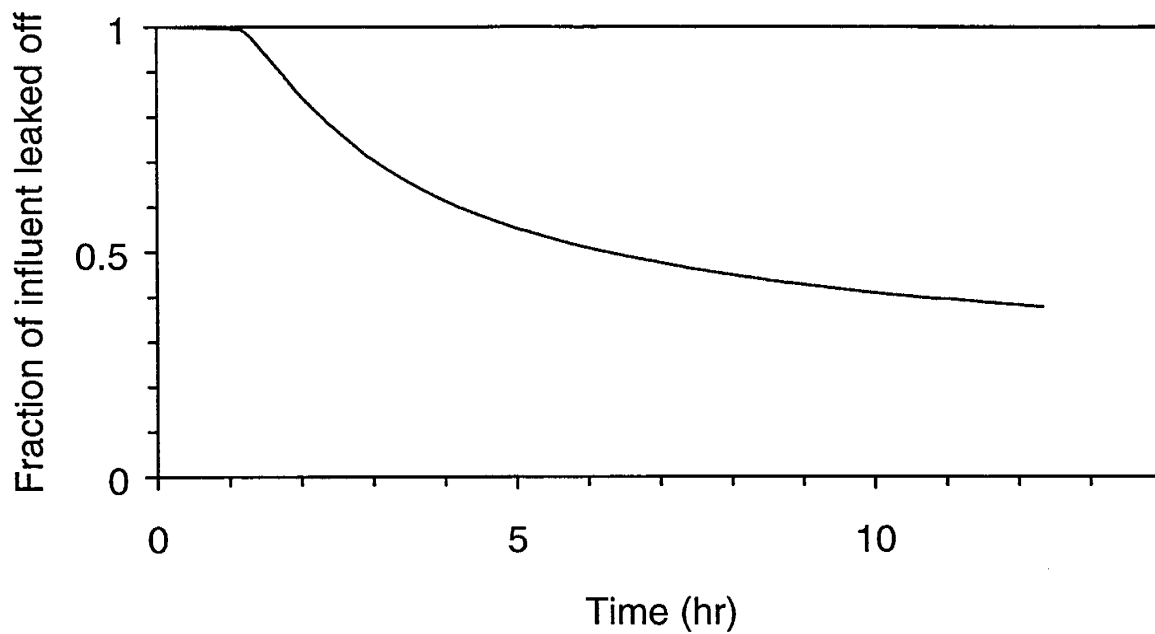


Figure 8.4 - Fractional leakoff in the fracture model during gelant displacement.

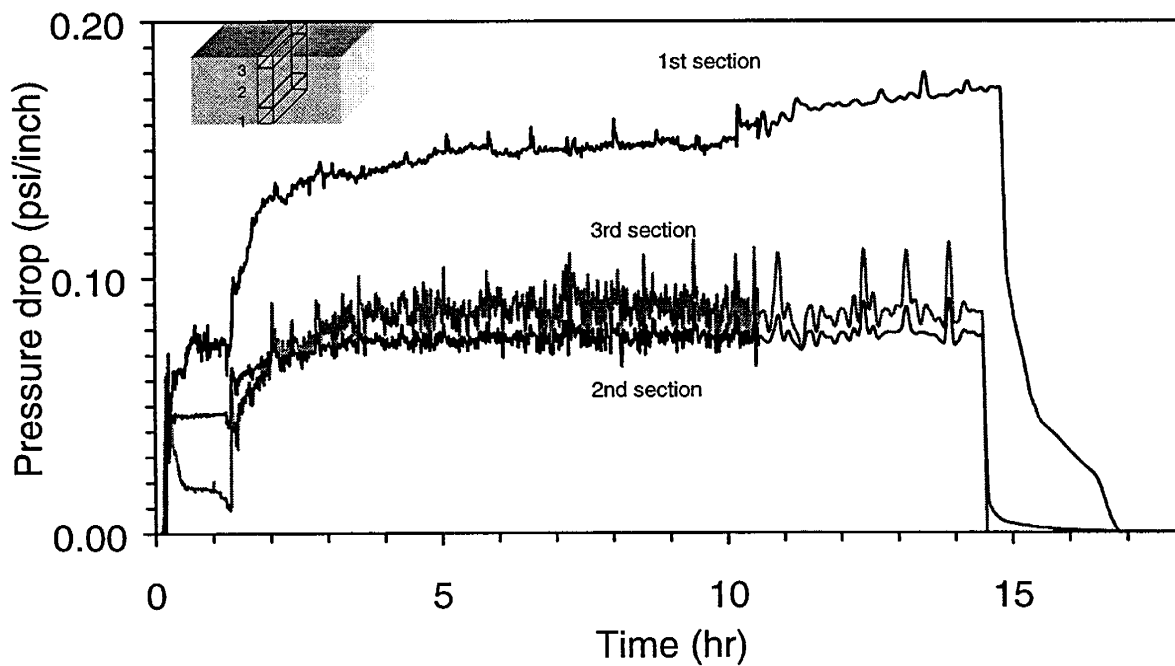


Figure 8.5 - Pressure profile for the fracture sections during gelant displacement.

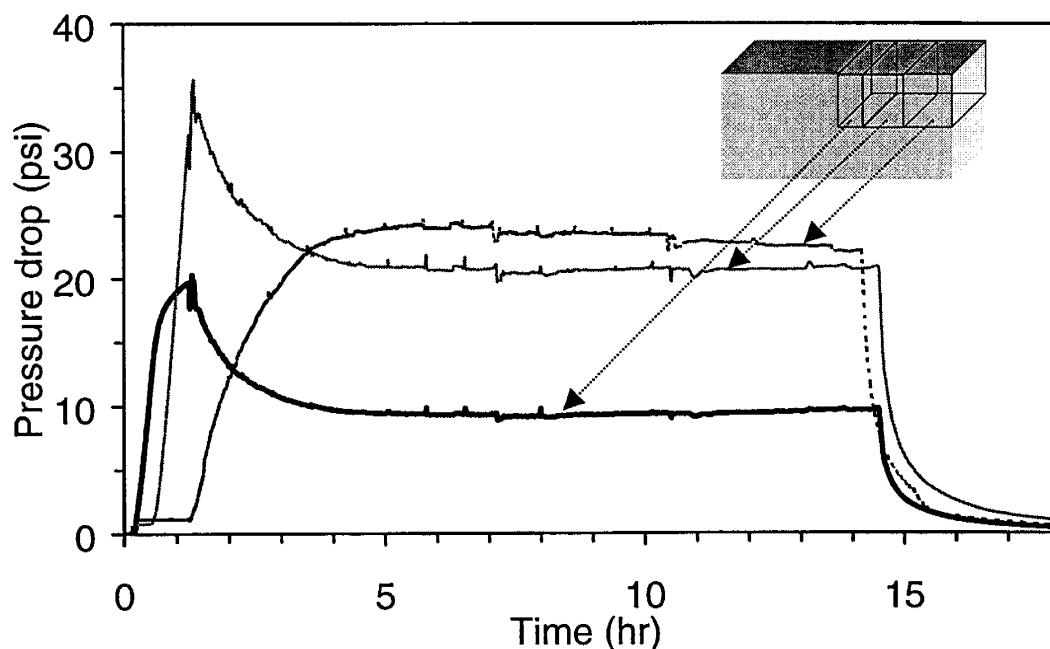


Figure 8.6 - Pressure profile for the matrix sections in the fracture model during gelant displacement.

pressure (expected for significant filtration) was observed during the course of the displacement experiment. Similar trends for cumulative flow and pressure profiles were observed in a similar displacement that used a viscous glycerol-water solution in place of gelant.

Effluent from the fracture gelled at the same time as the injected gelant. Effluent from the matrix was colorless, had a pH of 8.0, and had the same viscosity as the injected gelant. Atomic absorption spectrophotometry was performed on degelled effluents to determine chromium concentrations. The matrix effluent contained 3 ppm of chromium compared to more than 100 ppm, in the injected gelant. That is, chromium was retained extensively in the matrix.

Gel was allowed to mature in the flow cell for seven days. Brine was then injected into the fracture at constant pressure with the matrix outlets closed and the fracture outlet open to atmosphere. Pressure at the injection port was raised in steps of 5 psi. At each step, the pressure was held for 15 minutes. At a pressure of 10 psi, a sudden surge of brine flow began at fracture outlet. Within a couple of minutes a gelatinous mass exuded from the fracture and uninhibited fracture flow continued. Fracture permeability was found to be close to as it was before gel displacement.

Subsequently, the fracture end was closed, and matrix outlets were opened to atmosphere. Brine was injected into the fracture at constant pressure. Pressure profile for the matrix sections went through a transient phase, and a polymer solution was displaced from the matrix. When the

pressure profile reached a steady state, flow rates from the matrix outlets were measured to estimate the permeability of the matrix sections. Pre and post gelation permeability values are presented in Figure 8.7. The permeability values suggest that there was a moderate reduction in permeability all over the matrix, and a significant reduction of permeability near the fracture face.

Displacement and subsequent extrusion of gelant were conducted in several fractured cores, and similar behavior was observed. During extrusion in next set of experiments, pressure at the inlet face of the fracture was increased continuously, instead of steps. This was accomplished by injecting the displacing fluid at constant flow rate, and introducing a compressibility (tube filled with air) at the inlet line. A typical plot for such continuous build up of pressure at the fracture inlet is presented in Figure 8.8. The extrusion is represented in Figure 8.8 by the drop of pressure near the end of the experiment. The fracture in this experiment was 1.5 ft long, 2 inches high, 0.32 cm wide. There was three centimeter of leakoff into the matrix during placement, and the gel was allowed to mature for seven days before extrusion.

Gelling solution (few fracture pore volumes) was displaced in fractured core with no leakoff and the subsequent extrusion occurred with less than 2 psi of pressure drop across the fracture. Atomic absorption spectrophotometry, performed on the displaced fluid (after degelation with sodium hypochlorite) indicated that chromium was almost absent from the displaced fluid (<3 ppm as against more than 100 ppm in the injected gelant). The pH of the displaced fluid was 7.7, and the viscosity was significantly lower than the injected gelant (indicating three to four fold loss of polymer).

Two sets of gelant displacement and subsequent extrusion were conducted on the same fracture model to understand the effect of the extent of leakoff on the pressure at which the fracture resident extrudes. For increase in the extent of leakoff from 1 cm to 10 cm, the extrusion pressure (after five days of stay of the gel in fracture) was found to increase by less than 20%. That is beyond a minimum leakoff, the extent of leakoff does not affect the extrusion pressure significantly.

Leak off studies in unfractured core. The first leakoff experiment was conducted with bulk mixed gelant. This created uncertainty in the experiment because the gel was injected over a period of several hours and gelation was occurring in the bulk solution during injection. Inline mixed gelant was used to provide gelant with a constant age.

Figure 8.9 compares the cumulative flow of gelant for the four displacements at constant injection pressure of 70 psi. Decline in flow rates with time is evident for all the four cases. Maximum cumulative flow was observed for the displacement with no prior crosslinking, followed by displacements with three and six hours of prior crosslinking respectively.

Cumulative flow for bulk mixed gelant was between the three cases at different extents of prior crosslinking because the age of the injected (bulk-mixed) gelant increased with time during placement. The lines represent the simulated cumulative flow, obtained from theoretical model.

Section No.	Pre displacement Permeability (md)	Post displacement permeability (md)	RRF
1	108	12.0	9.0
2	105	12.0	8.8
3	126	0.7	180
4	140	0.7	200
5	105	13.0	8.1
6	110	15.0	7.4
7	121	11.0	11
8	115	6.0	19
9	147	1.1	130
10	138	2.0	69
11	117	3.0	39
12	127	14.0	9.1

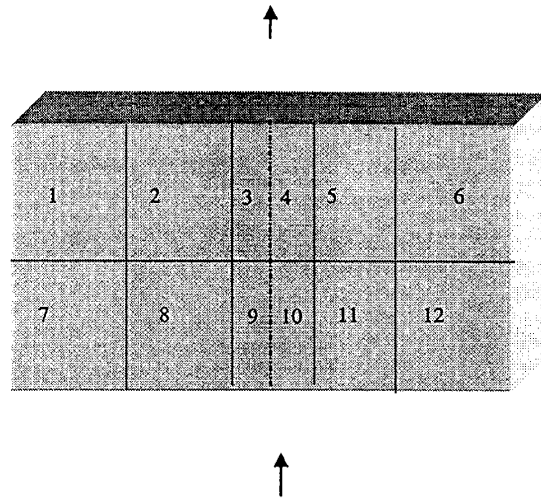


Figure 8.7 - Pre and post displacement permeability of the sections of the fracture model.

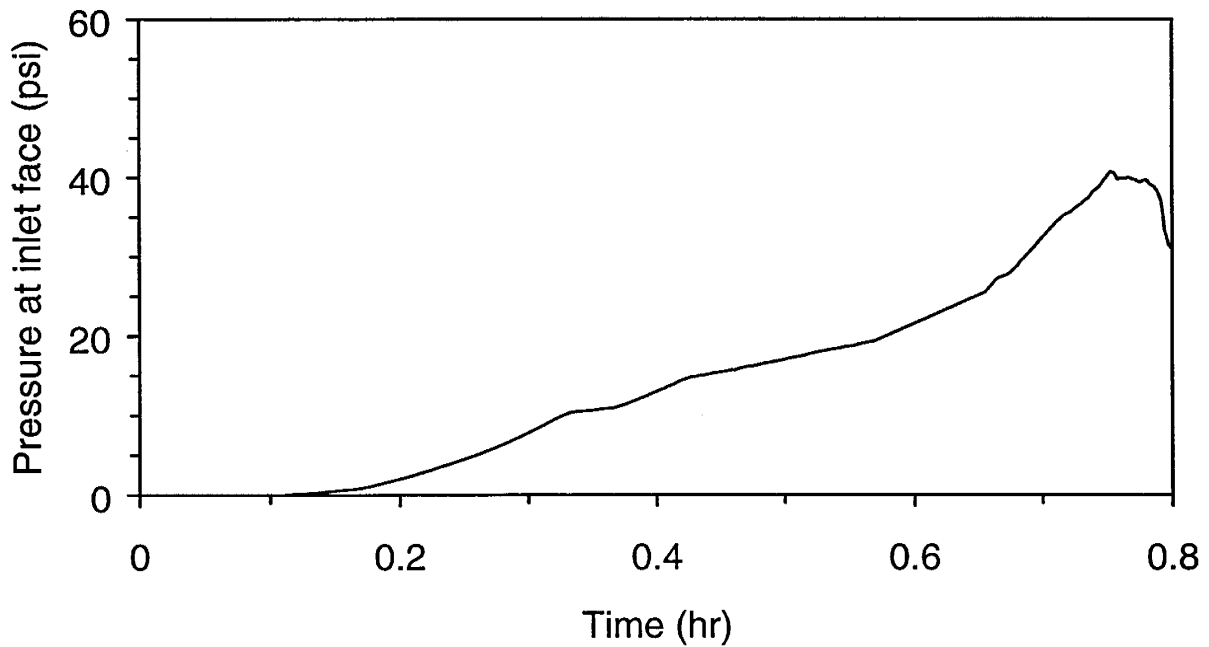


Figure 8.8 - Typical extrusion of gel from fracture after matured *in situ*.

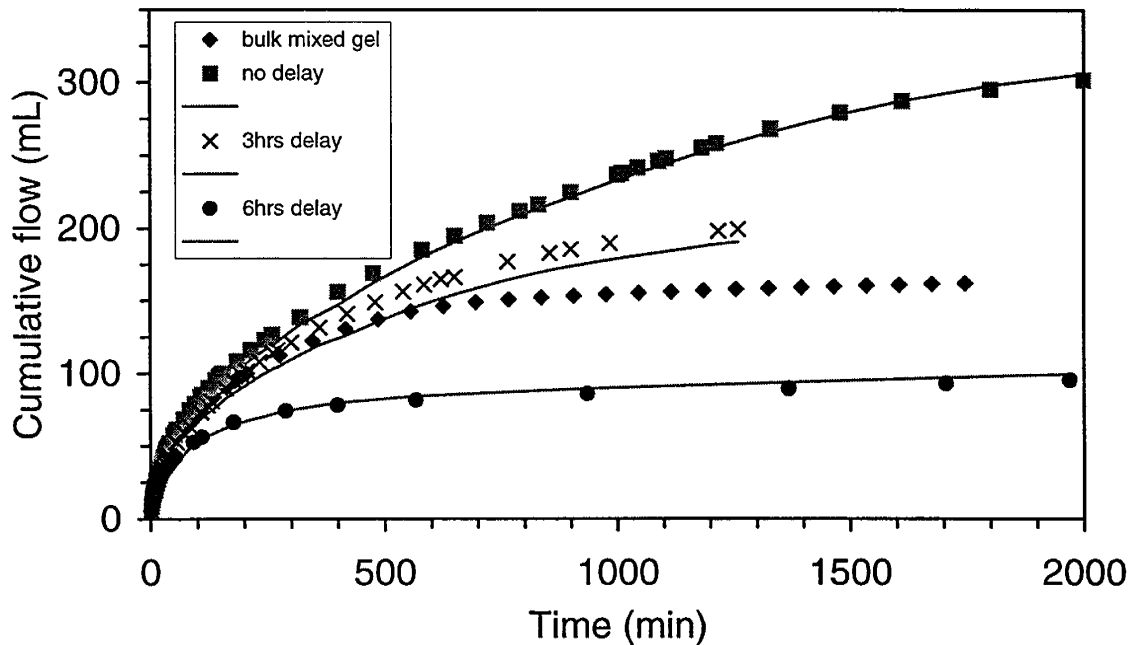


Figure 8.9 - Cumulative flow of gelant for the four displacements in unfractured cores.

Figure 8.10 presents the evolution of pressure differential across different sections of the core. Initial build up of pressure in each section represents the arrival of gel front in that section. Later, there was a sharp rise in pressure differential across the first section. The rise in pressure differential for the first section was hastened as the age of the injected gelant increased.

The injected gelant had a pH of 4.8, and the pH of displaced brine was 8.7. After the break through of the gelant, the effluent had same viscosity as that of the gelant, though the pH dropped gradually to a minimum of 8.0 for the case with no prior aging. The effluent was colorless, and never gelled. Atomic absorption spectrophotometry was performed on the degelled effluent to determine the chromium concentration. Chromium concentration in the effluent was 2 ppm while the injected concentration was more than 100 ppm. Thus, most of the chromium was stripped from the displacing gelant. Prior aging did not influence the chromium content in the effluent.

Gel was allowed to mature for seven days. Then, brine was injected at constant pressure (90 psi) to establish a brine flow through the core and to measure its permeability. Flow rate was transient as polymeric solution was displaced from the core (a quarter of a pore volume). Once a steady flow was reached, a reduction of over all permeability by three orders of magnitude was observed, with most of the flow resistance, contributed by the first two sections. In contrast, when polymer (without the crosslinker) was displaced through Berea core, the post-flush permeability to brine was reduced by half in all the sections of the core.

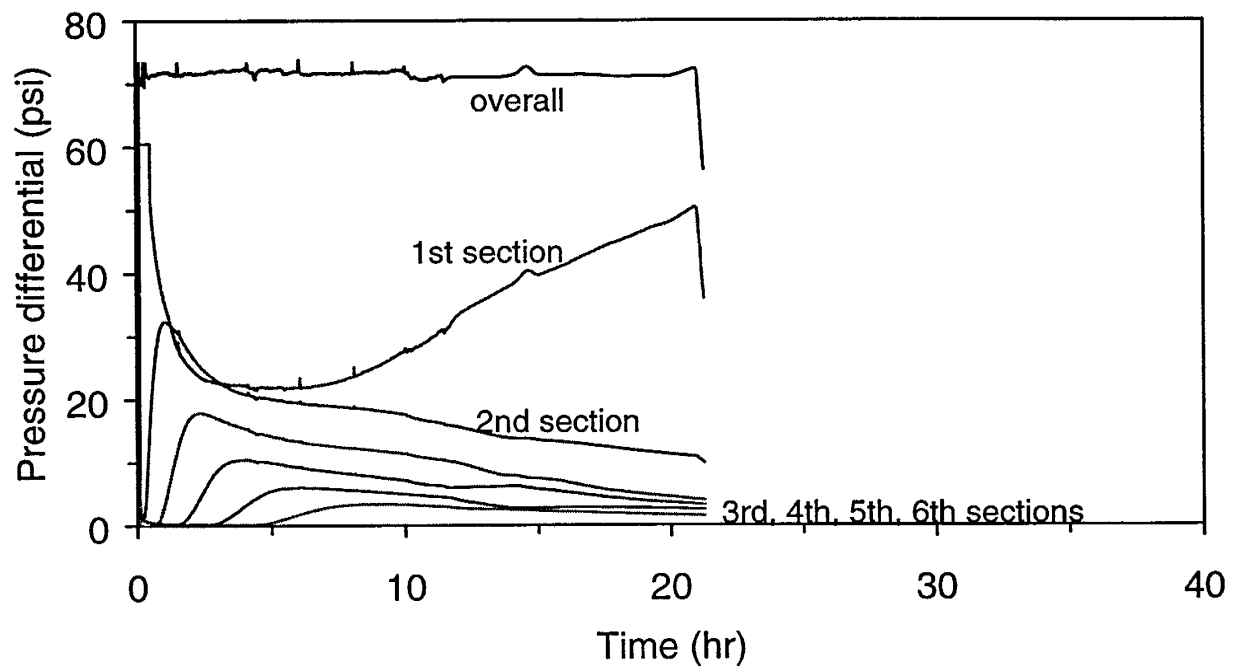
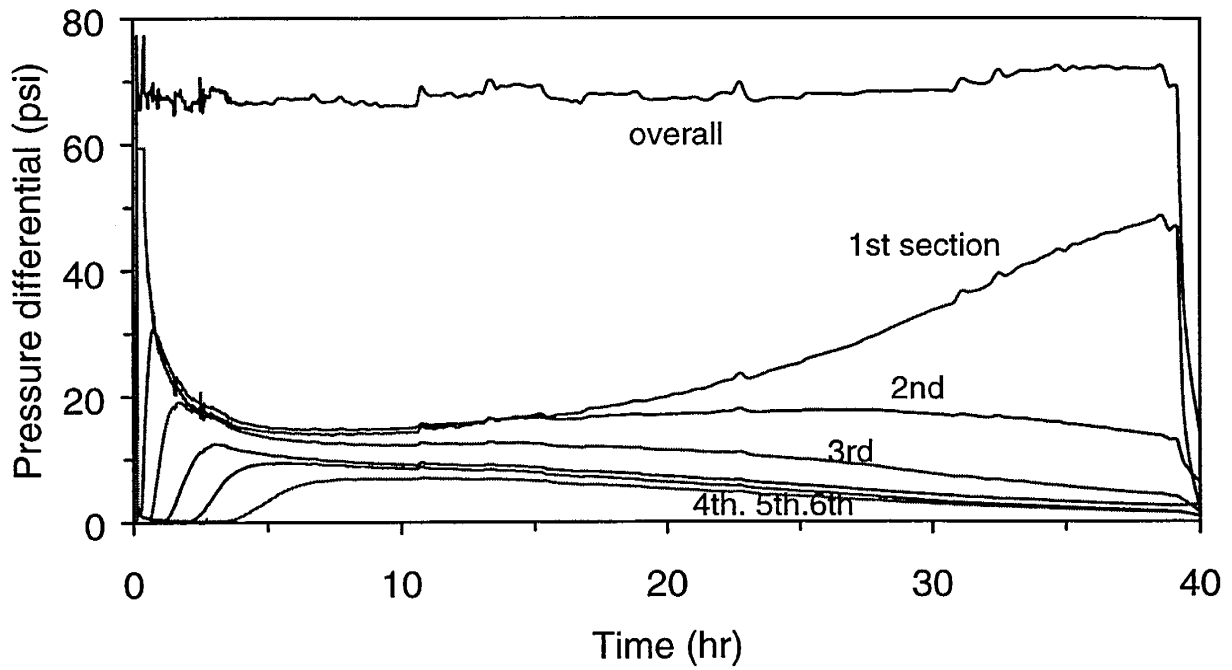


Figure 8.10 - Evolution of pressure differential across the sections of the unfractured core during displacement of zero hour old gelant (upper), and three hour old gelant (lower).

The apparent viscosity as function of time and distance from inlet face are shown in Figure 8.11 for the displacements using zero and three hour old gelant. There was a sharp gradient in apparent viscosity along the length of the core. The steep gradient in apparent viscosity is believed to be due to deep filtration of gel aggregates. Filtration was more extensive and filtration resistance was contained more near the inlet face when the gelant was aged prior to injection. For six hours of prior crosslinking, the gel front could travel only half way down the core.

A leakoff model from the hydraulic fracturing literature [Penny et al.,1989] was used to analyze the displacement data. In these models, the cumulative volume that leaks off during hydraulic fracturing increases linearly with the square root of time over certain regions of the leakoff. Two linear segments were expected for leakoff experiments in Berea cores; one for viscous flow and the other for filtration. Figure 8.12 describes the cumulative flow for three displacements as a function of square root of time. The linearity for the initial period of displacement was attributed to viscous displacement. The length of the linear region decreases as the age of the injected gelant increases, indicating the shift of regime from viscous displacement to another mechanism. Leakoff coefficient, computed on the basis of first linearity, is presented in Figure 8.12. However a second linearity could not be established clearly.

The apparent viscosity plots showed an increased in flow resistance developed with time behind the injected gelant front. Deep filtration of gel aggregates could explain these observations. A comprehensive model of gelant leakoff with deep filtration was developed and used to match the experimental flow and apparent viscosity data. The model is described in the following section.

Theoretical Modeling

Displacement of viscous solution in fracture model. A theoretical model was developed to predict cumulative flow and pressure profile for displacement of a viscous solution through a fractured slab. First an analytical solution was obtained for simultaneous linear flows along fracture and matrix with same viscosity for displacing and displaced fluids. Next the injection of a viscous fluid was modeled by assuming piston-like displacement with no dispersion. Movement of the viscous front in the matrix was accounted by considering a hypothetical width of the flow cell that is completely filled with viscous solution. The hypothetical width was taken to be changing with time from zero to the actual width of the flow cell.

Experimental data, available for glycerol displacement, was compared with the profile obtained from theoretical model. Cumulative flow from the fracture outlet is compared with the flow from the simulation in Figure 8.13 as a function of time. The profiles approached to linearity with time indicating stabilization of leakoff rate as the viscous front traveled down the matrix. Figure 8.14 compares the pressure drop for matrix sections of one of the quadrants with the simulated pressure drop.

A numerical experiment was performed with the theoretical model to ascertain the capability of the fracture cell in establishing a constant leakoff rate instead of leakoff at constant pressure in the fracture. This was accomplished by continuously increasing the back pressure at the fracture

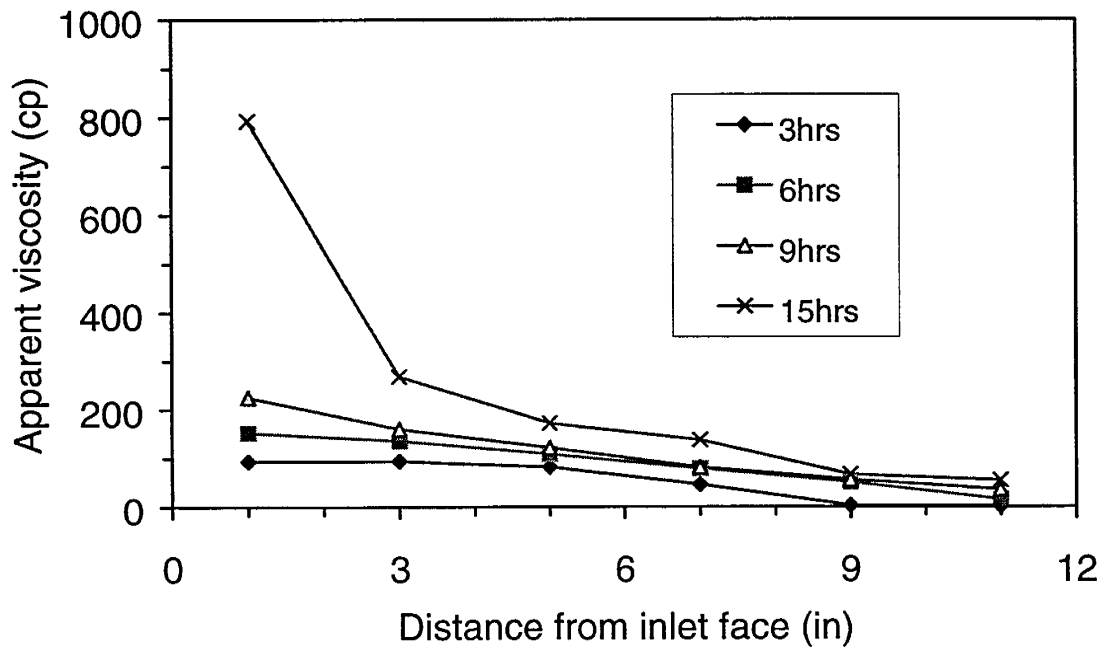
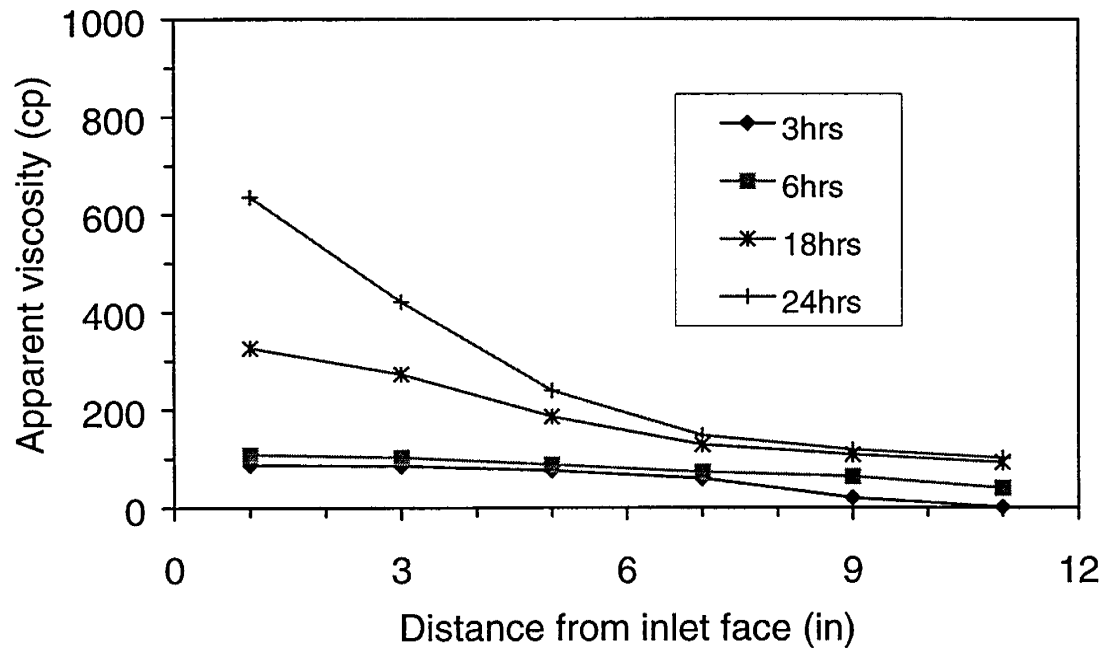


Figure 8.11 - Evolution of apparent viscosity at the sections of the unfractured core during displacement of zero hour old gelant (upper), and three hour old gelant (lower).

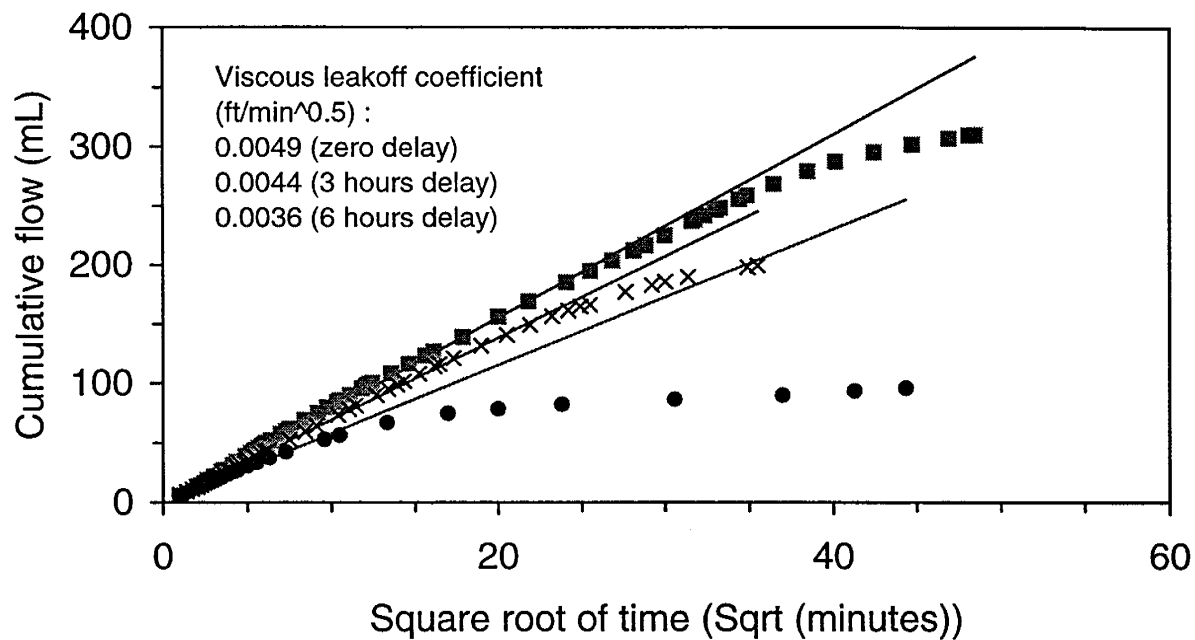


Figure 8.12 - Cumulative flow of gelant as function of square root of time.

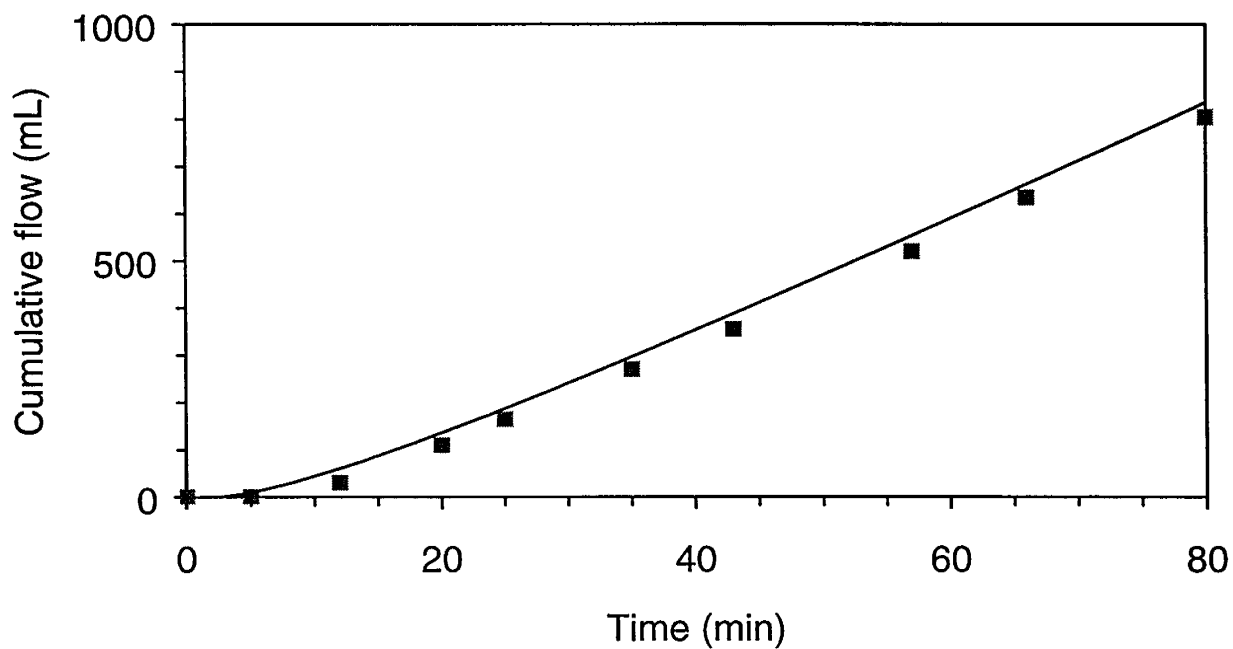


Figure 8.13 - A comparison of experimental and simulated flow at the fracture outlet for displacement of glycerol.

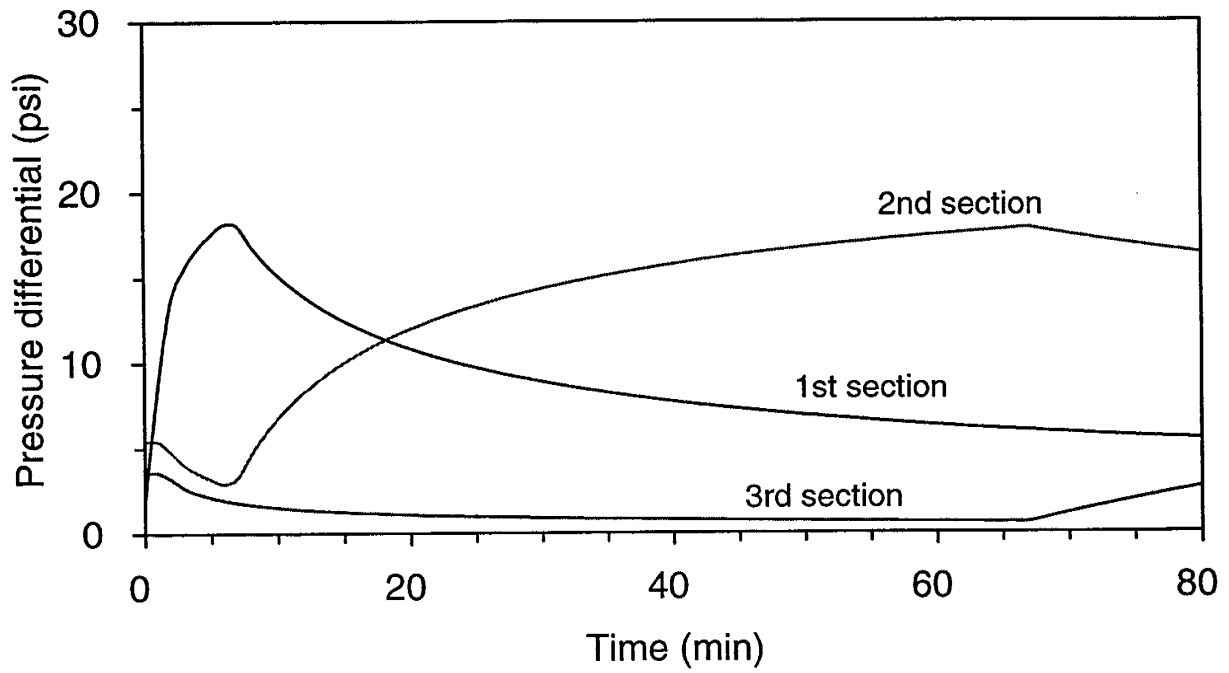
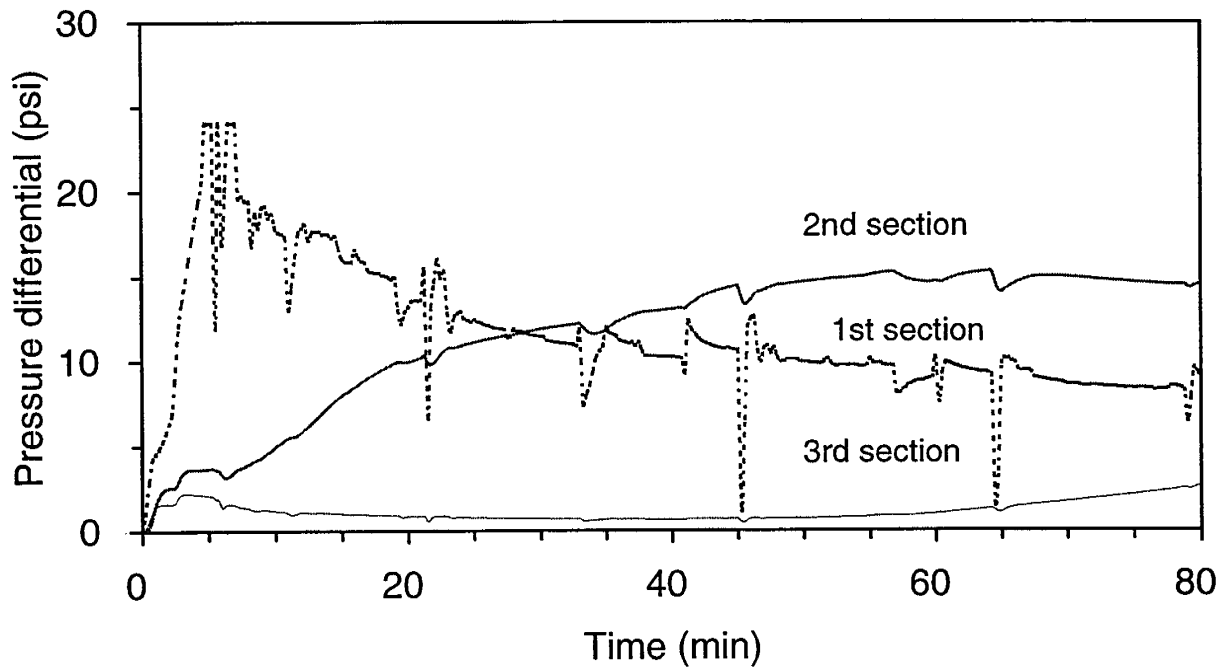


Figure 8.14 - A comparison of experimental (upper plot) and simulated (lower plot) pressure drop across the matrix sections in the fracture model during glycerol displacement.

outlet such that the differential pressure across the fracture remains constant with time. Figure 8.15 compares the two leakoff rates with time. For fracture pressure held constant, the leakoff rate drops rapidly to a stable value, with time. For differential pressure across the fracture held constant, the leakoff rate increases with time to a stable value though for practical purposes the increase is negligible.

Leakoff Model with Deep Filtration of Gel Aggregates. A model was developed to simulate the cumulative flow and apparent viscosity profile that were obtained from leakoff experiments in unfractured linear cores. A review of apparent viscosity plots suggests movement of a viscous front along with deep filtration of gel aggregates. Displacement of gelant through the core is represented by the following mechanisms:

1. Movement of viscous front through the core at constant pressure
2. Change in viscosity of the displacing fluid with flow rate due to shear thinning nature of the gelant.
3. Permeability modification behind the gelant front due to deep filtration.

Velocity of the viscous front, moving under constant pressure was expressed explicitly in terms of properties and dimensions of the core, injection pressure and viscosity of displaced and displacing fluids. The input parameters are available from direct measurements.

Next the viscosity term, in the expression for velocity of the viscous front, was made shear dependent. The power law constants were obtained from flow experiments with uncrosslinked polymer.

Deep filtration modified the term for upstream permeability in the expression for velocity of the viscous front. However deep filtration model required estimates of filtration related properties of the gelant that was not available directly. Cumulative flow data at a given time was used to obtain

- The length of the gelant slug
- The flow rate
- Pressure drop across the gelant slug

The above set of data was used to estimate the average permeability across the gelant slug. The average permeability as a function of cumulative flow was regressed to obtain the necessary filtration related parameters of the gelant. A comparison of experimental and regressed permeabilities is presented in Figure 8.16.

Cumulative flow with time was predicted by integrating the expression for velocity of the viscous front, with the modifications in viscosity and permeability. Apparent viscosity profile along the length of the core was estimated as the product of power law viscosity and the ratio of initial to updated permeability.

A comparison of predicted and experimental cumulative flow as function of time is presented in Figure 8.8. Simulated apparent viscosity profiles for the displacements of 0 and 3 hour old gelant are presented in Figure 8.17.

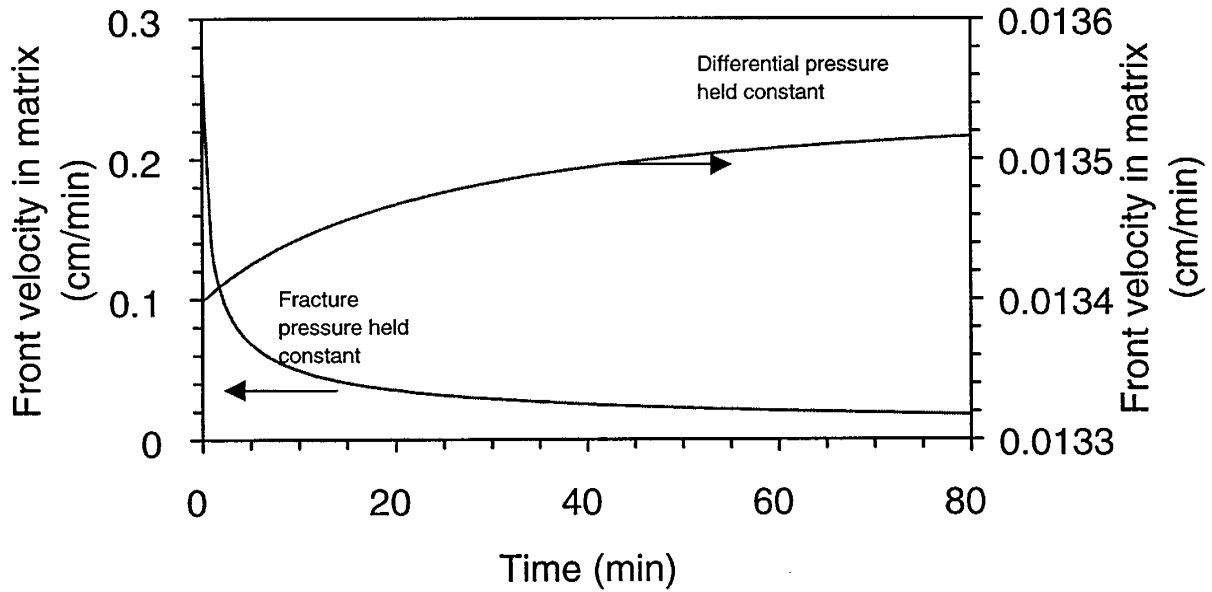


Figure 8.15 - A comparison of leakoff rate at constant pressure at the fracture, with the same at constant differential pressure along the fracture.

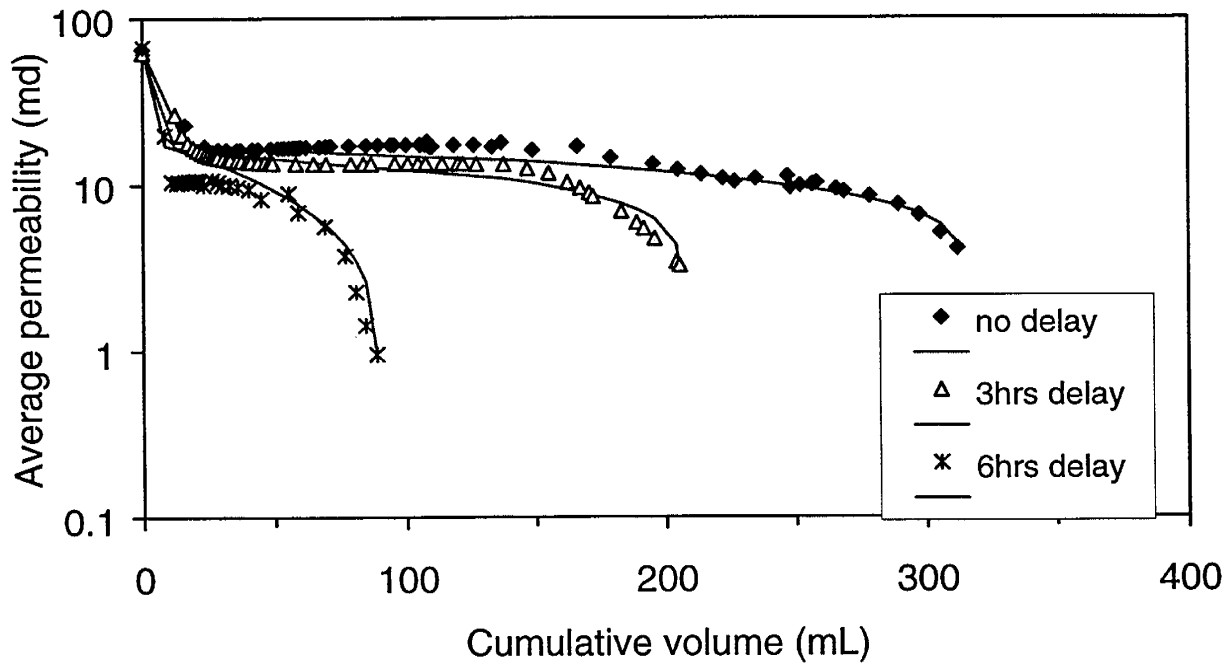


Figure 8.16 - A comparison of experimental and regressed permeability averaged over the gelant slug.

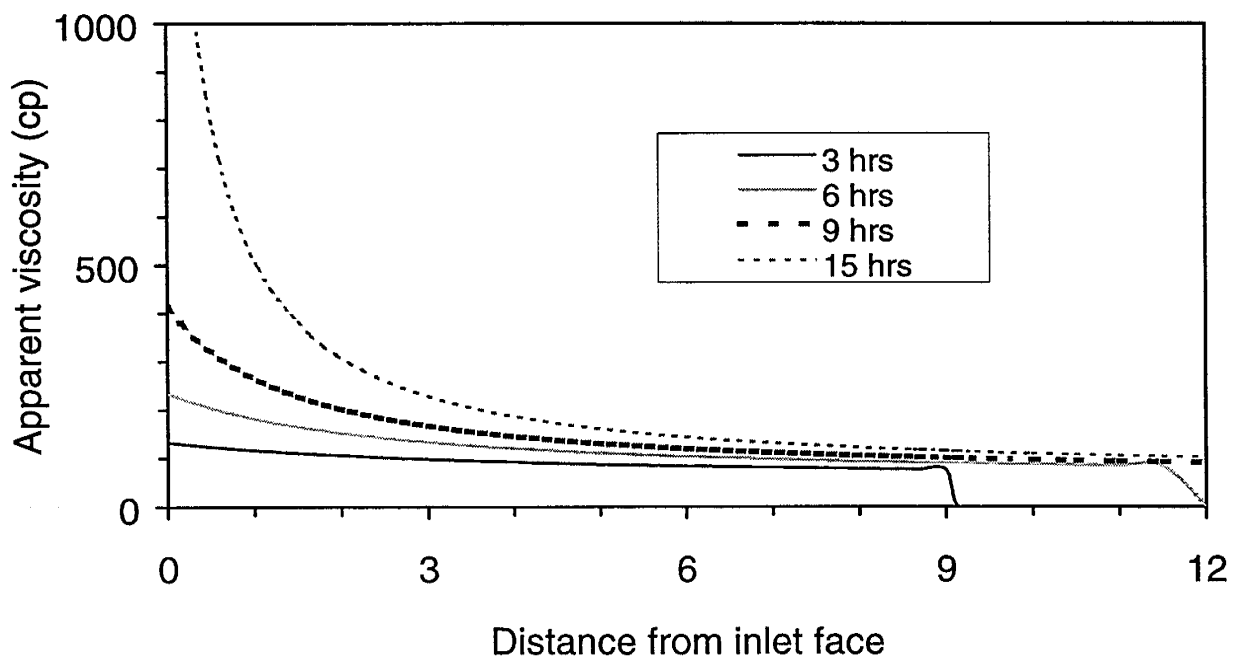
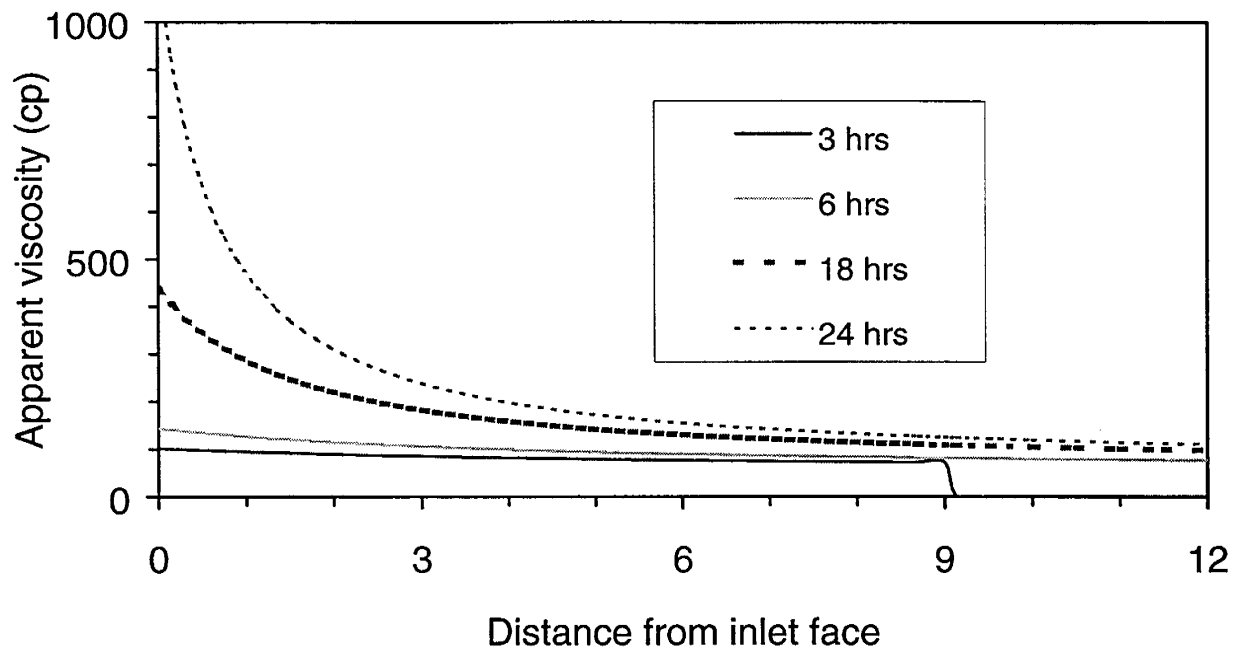


Figure 8.17 - Simulated profile for apparent viscosity in the unfractured core during displacement of zero and three hour old gelant.

The agreement between theoretical prediction and experimental data indicates that leakoff of Cr(III)-PHPA gelant in Berea sandstone can be described by displacement model of a viscous front of power law fluid, with deep filtration of large particles behind the gelant front.

Conclusions

1. During displacement with leakoff, velocity along the fracture decreases with distance from the inlet end.
2. Due to sharp contrast in permeability, the pressure drop along the fracture is small compared to the same along the matrix. Accordingly the leakoff front is linear, as it proceeds through the matrix.
3. The difference between the pressure imposed at the matrix outlet and the maximum pressure at the fracture outlet (beyond which all the flow goes into the matrix, before reaching the fracture outlet) is function of permeability, dimensions of the flow cell, viscosity of the fluid and the injection flow rate. A minimum difference is critical to control two simultaneous flows along and away from the fracture during displacement experiment. A thin and wide fractured slab provides this difference.
4. During displacement of a viscous fluid through the fracture model at constant pressure, leakoff rate drops and stabilizes rapidly.
5. A practically constant leakoff rate with a viscous solution can be established in this fracture model, by controlling the back pressure such that the differential pressure along the fracture remains constant with time.
6. Cr(III)-PHPA gelant behaves like a viscous fluid in the fracture model.
7. After maturity, the gel in the fracture extrudes on application of a pressure gradient.
8. When Cr(III)-PHPA gelant is placed with no leakoff, the extrusion takes place on application of much smaller pressure gradient.
9. Beyond a minimum leakoff, the extent of leakoff does not affect the extrusion pressure.
10. After displacement, permeability of the matrix, adjoining the fracture is reduced moderately all over the matrix, and significantly near the fracture face.
11. During leakoff in Berea sandstone, chromium is retained significantly in the matrix, rendering the leaked off fluid incapable of forming gel. Fracture effluent does not exhibit any loss of chromium during placement with leakoff.
12. Displacement of Cr(III)-PHPA gelant in Berea core leads to build up of flow resistance, that has a downward gradient along the length of the core. Aging of gelant, prior to displacement, hastens the build up near the inlet face of the core.
13. Partially hydrolyzed polyacrylamide (5000 ppm Alcoflood 935 in 1% NaCl) in Berea core was found to exhibit lower and upper newtonian behavior with a power law exponent of 0.23 – 0.25 in shear thinning region.
14. A theoretical model accounting for two simultaneous flows along and away from the fracture can simulate the displacement of viscous solution in the fracture model.
15. A theoretical model accounting for displacement of power law fluid under constant pressure, with deep filtration upstream, can simulate the leakoff in linear core.

Chapter 9

Gel Treatments in Production Wells

Principal Investigators: G. P. Willhite, D. W. Green and C. S. McCool
Graduate Research Assistant: Zhongchun Yan

Introduction

Some porous rocks, when treated with polymer solutions or gelants, show reduction of the permeability to water (at S_{or}) to a larger extent than the permeability to oil (at S_{iw}). This property is termed disproportionate permeability modification, and suggests that the water-oil ratio can be reduced by treating a production well with a gelant [Seright and Liang, 1994; Liang et al., 1995; Zaitoun and Kohler, 1989; 1991; 1988; Parsons, 1975; Dawe and Zhang, 1994; Liang et al., 1994; Matre et al., 1995; Seright, 1993; 1996; White et al., 1973; Liang and Seright, 1997; Thompson and Fogler, 1997].

The mechanism of disproportionate permeability modification is not understood. The objective of this research is to simulate gel treatments in production wells and to investigate the effect of gel treatments on the effective permeabilities to water and oil over the range of saturations where two-phase flow exists. The results of this study will be used to examine the mechanisms of disproportionate permeability modification.

The relative permeability experiments were conducted in a Berea sandstone slab. Water saturations in the slab were determined using a microwave apparatus. The gelant used was a polyacrylamide-chromium(VI)-thiourea system. Relative permeabilities to water and oil were measured in the slab before it was treated with gel. A quarter of the length of the slab was then treated with the gel system and relative permeability measurements were repeated. Microwave saturation measurements could not differentiate between water and gel for these latter measurements. The effect of flow rate on relative permeability after gel treatment was also investigated. This study is summarized here. Green et al. [1998] and Yan [1998] present details of the work.

Experimental

The principal apparatus for this study was a microwave scanning system shown in Figure 9.1. Microwave energy is absorbed by water to a significant degree, but relatively small amounts of the energy are absorbed by oil and rock. Thus the apparatus can be used to measure local water saturations in a rock-fluid system. Since a gel of the type used here is greater than 99% water, the microwave measurements cannot differentiate between water and gel. The microwave beam was focused on a one-inch diameter circle that was centered in the middle of the slab width. The microwave equipment is mounted on a trolley so that the device can scan along the length of a slab.

Pressure drops during flow tests were measured across the entire slab and four subsections using five differential pressure transducers as shown in Figure 9.2. Pressure drop was limited to 80 psi across the slab. A small-volume oil/water separator [Bretz et al., 1984] was used to separate the oil and water in the effluent. Oil and water were collected in graduated cylinders.

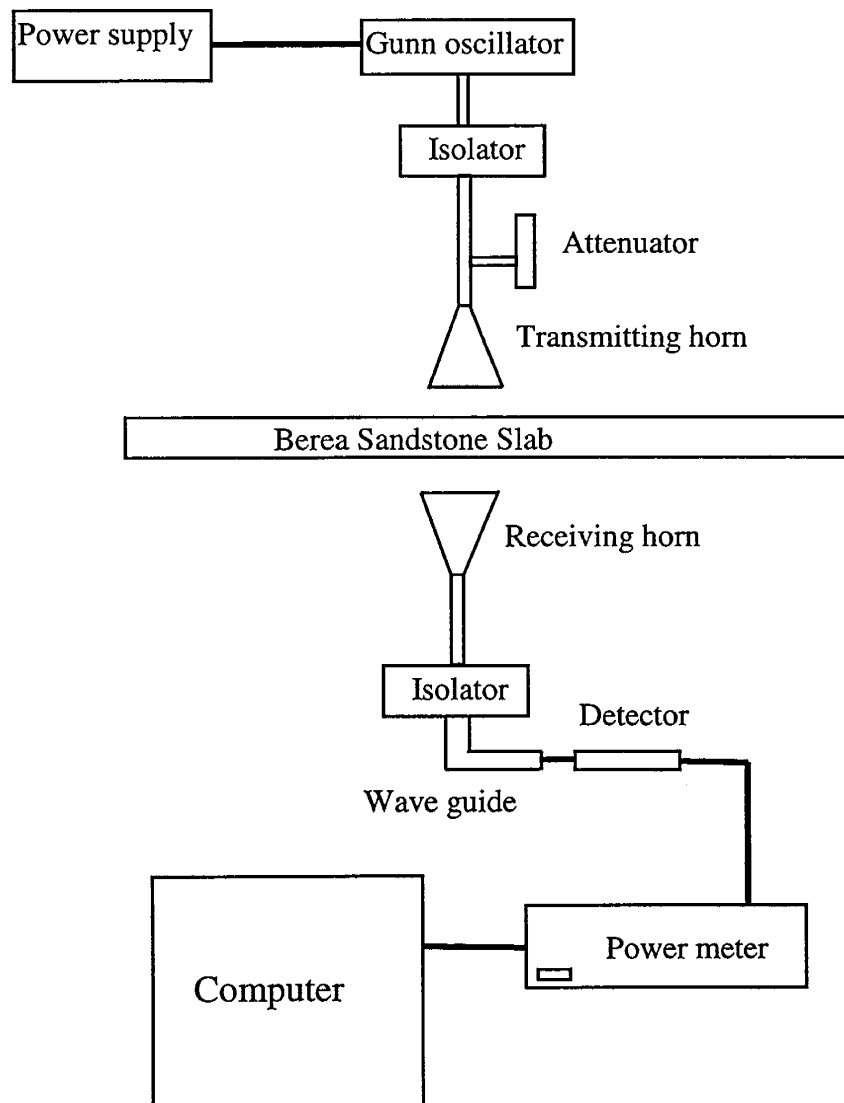
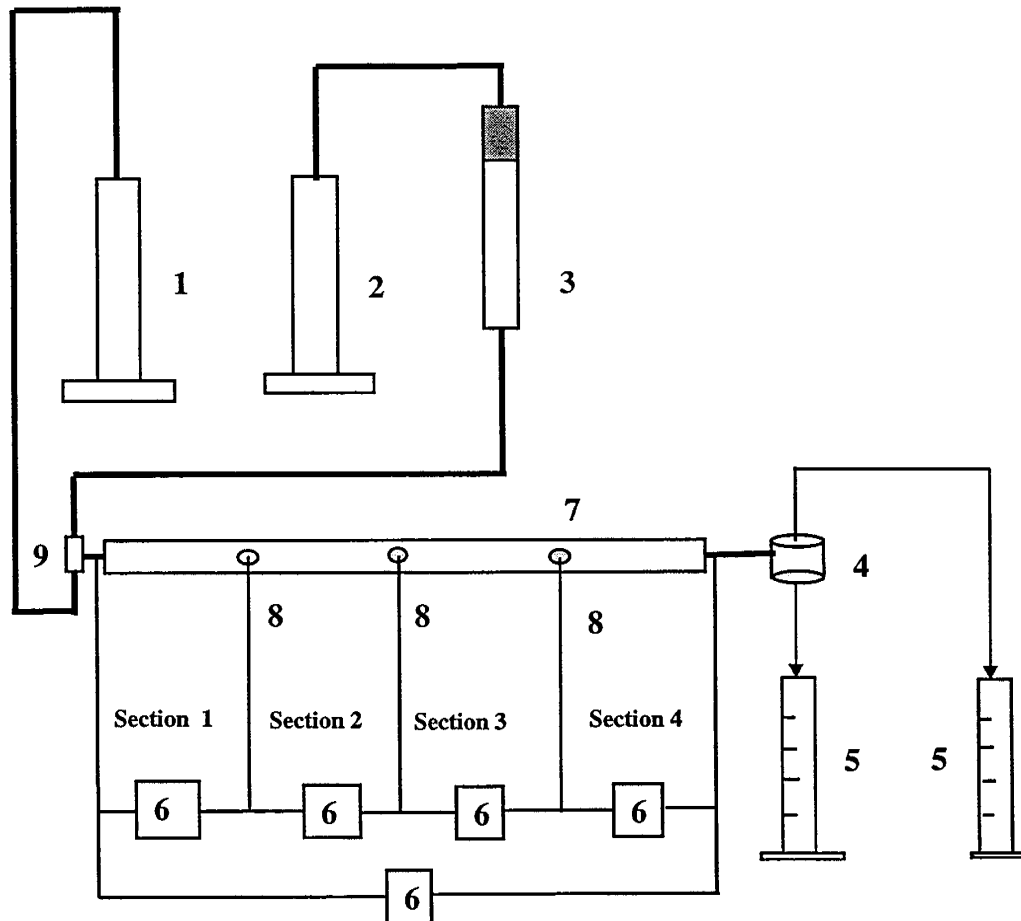


Figure 9.1 - Schematic of microwave apparatus.

A Berea sandstone slab (61.1 cm long, 10.5 cm wide, and 1.74 cm thick) was used for all flow tests. Porosity of the slab was 0.15 and the permeability was 190 md. Normal-dodecane and 2.0 wt% NaCl brine were used for all oil-water flow tests.

The gelant solution contained 5000 ppm AlcoFlood 935 polyacrylamide, 1500 ppm thiourea, 600 ppm sodium dichromate, and 2.0 wt% NaCl. The gelant had a gel time of 40 hours, which was judged to be sufficient to place the gel in the slab before gelation occurred.

Relative permeabilities were measured before and after the gel treatment using the steady-state method. Water and/or oil were injected at fixed ratios and in flow direction #1 (from section 1 to section 4) until steady state was achieved. Pressure drops and water saturations (using the



- | | |
|------------------------|-------------------------|
| 1. Oil pump | 6. Pressure transducers |
| 2. Water pump | 7. Berea sandstone slab |
| 3. Transfer cylinder | 8. Pressure taps |
| 4. Water/oil separator | 9. T-joint |
| 5. Graduated cylinders | |

Figure 9.2 - Apparatus for flow experiments.

microwave apparatus) were then measured. Relative permeability curves were determined for both decreasing (drainage) and increasing (imbibition) water saturations. Prior to the relative permeability measurements, an oilflood and then a waterflood were run until steady state was reached. The endpoint permeabilities of water and oil were used to estimate flow rate limitations for relative permeability experiments.

The direction of flows in the Berea slab was designed to simulate a treatment that would be applied to a production well. Two-phase flow at 60% water and 40% oil fractional flow was run from direction #1 (Section 1→ 4) until a steady state was reached. Gelant (0.13 PV) was then

injected in direction #2 (Section 4→ 1) over a time period of 27.5 hours. The gelant volume corresponded to 90% of the volume of water in Section 4 when this section was at residual oil saturation.

A 0.20 PV oil over-flush was injected immediately following the injection of gelant solution in direction #2 (Section 4→ 1). The oil overflush was injected to create oil flow channels within the treated section. The slab was shut in for eight days to allow for gelation before relative permeability measurements were taken. The flow for the relative permeability measurements were conducted in direction #1 (Section 1→ 4). Saturation measurements after the treatment reflect both the free brine saturation and the gel saturation.

The effect of flow rate on relative permeability to oil and water after the gel treatment was investigated. The procedure was to maintain the fractional flow of water and oil constant while the total flow rate was changed. Pressure data were recorded continuously.

Results and Discussion

Saturation profiles in the Berea slab during gelant injection and during the oil overflush are shown in Figures 9.3 and 9.4, respectively. The gelant and the oil overflush were injected in direction #2, from the right side of these figures. Gelant, or gel, was detected by the microwave as water in these profiles. Small saturation changes were observed during gelant injection as shown in Figure 9.3. The gelant was contained mostly in Section 4. During the oil overflush, an oil bank was observed to progress through the core slab (Figure 9.4). Some of the gelant might have been displaced into Section 3 during the oil overflush.

Water saturation profiles that were measured before and after the treatment for the drainage cycle are shown in Figures 9.5 and 9.6. The saturation profiles were measured after a run had reached steady state. Pre and post-treatment oil and/or water injections were in direction #1, from left to right in the figures. Most of the saturation change occurred at high oil cuts. The water saturation in Section 4 during these runs changed over a narrower range after the gel treatment. Similar results were obtained for the water saturation profiles during the imbibition cycle (increasing water saturation).

The effect of the gel treatment on oil and/or water flow is shown by the relative permeability curves for Section 4, the treated section, in Figure 9.7. The relative permeabilities to water and oil were both reduced significantly at all saturations. The relative permeability curves of Section 4 after gel treatment were obtained at specific flow rates. Latter experiments showed that the relative permeabilities of the gel-treated section were not independent of flow rate.

The performance of a gelled polymer treatment is commonly assessed using the factor by which the permeability was reduced. This factor is normally defined as a residual resistance factor (RRF) that is equal to the permeability measured before the treatment divided by the permeability after the treatment. For experiments where the permeability to oil and water are desired, the permeabilities need to be measured at comparable conditions. Residual resistance factors for this study were determined at two conditions. For water flow, the conditions were:

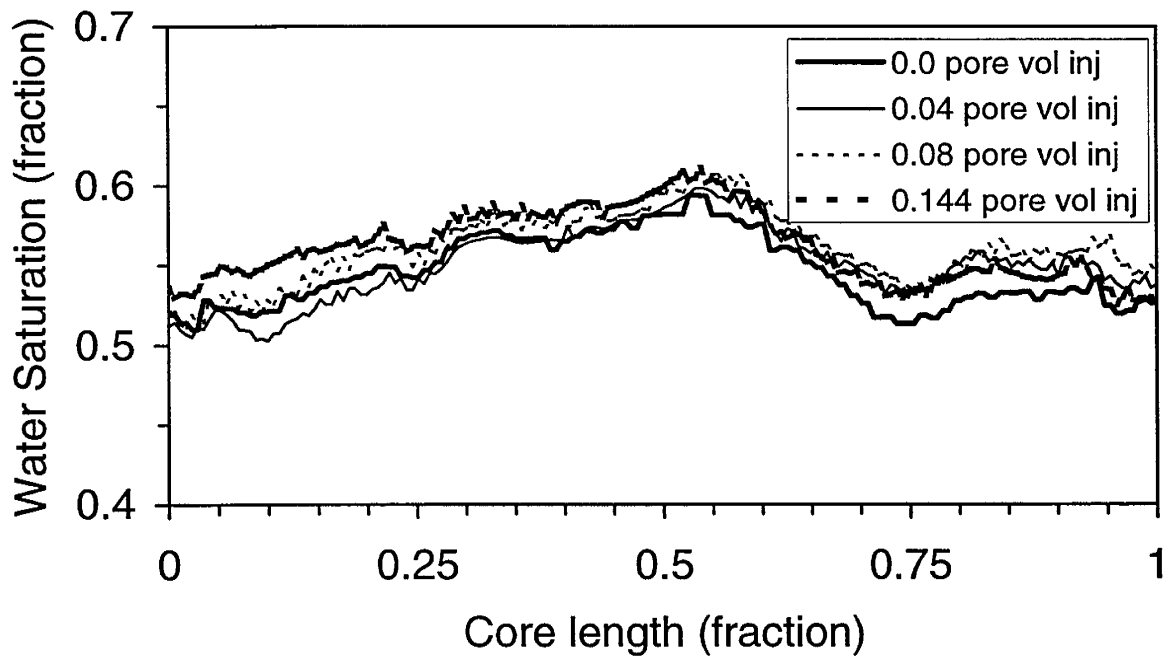


Figure 9.3 - Water saturation profiles during gelant injection; Injection from right side (Direction #2).

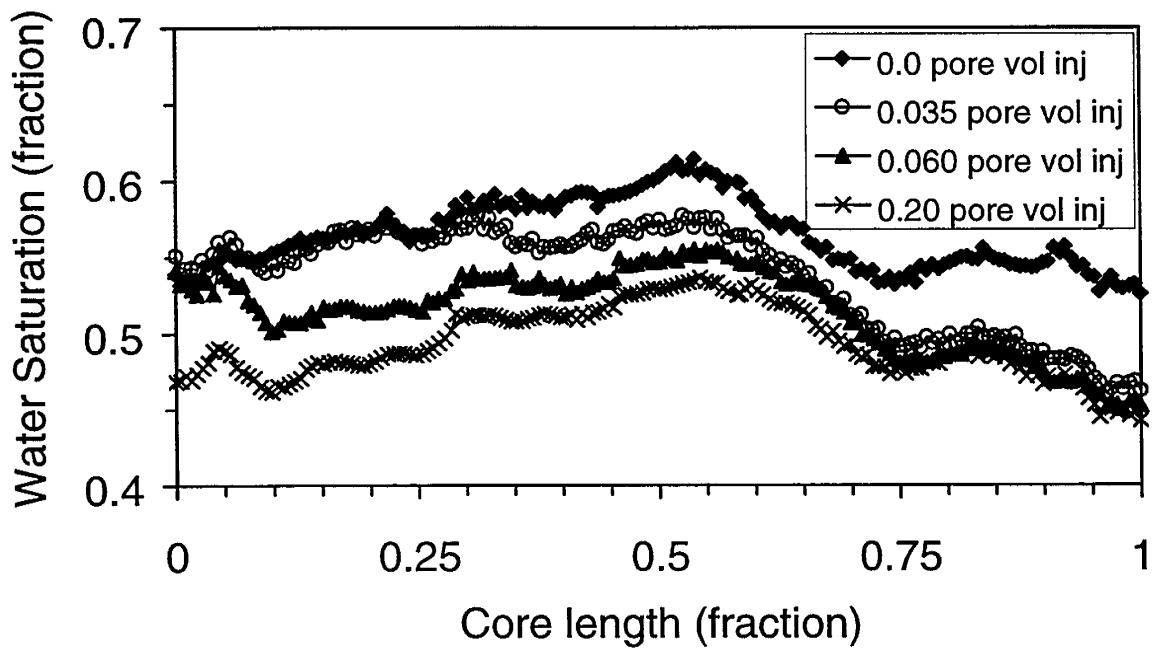


Figure 9.4 - Water saturation profiles during injection of oil overflush; Injection from right side (Direction #2).

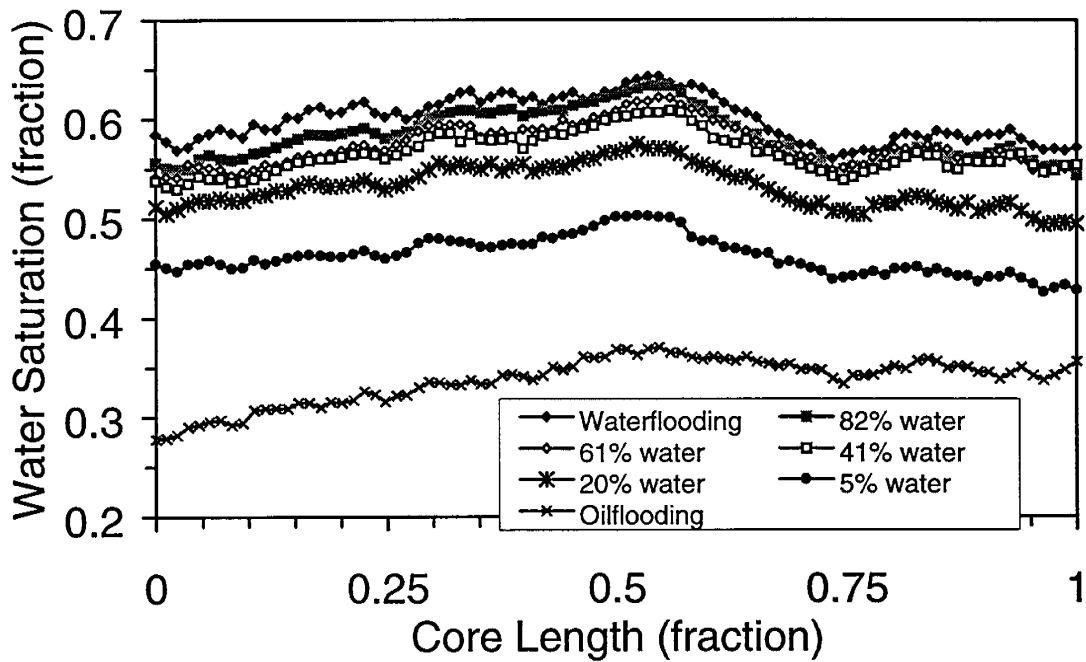


Figure 9.5 - Water saturation profiles during different fractional flows before gel treatment; Drainage path and steady state.

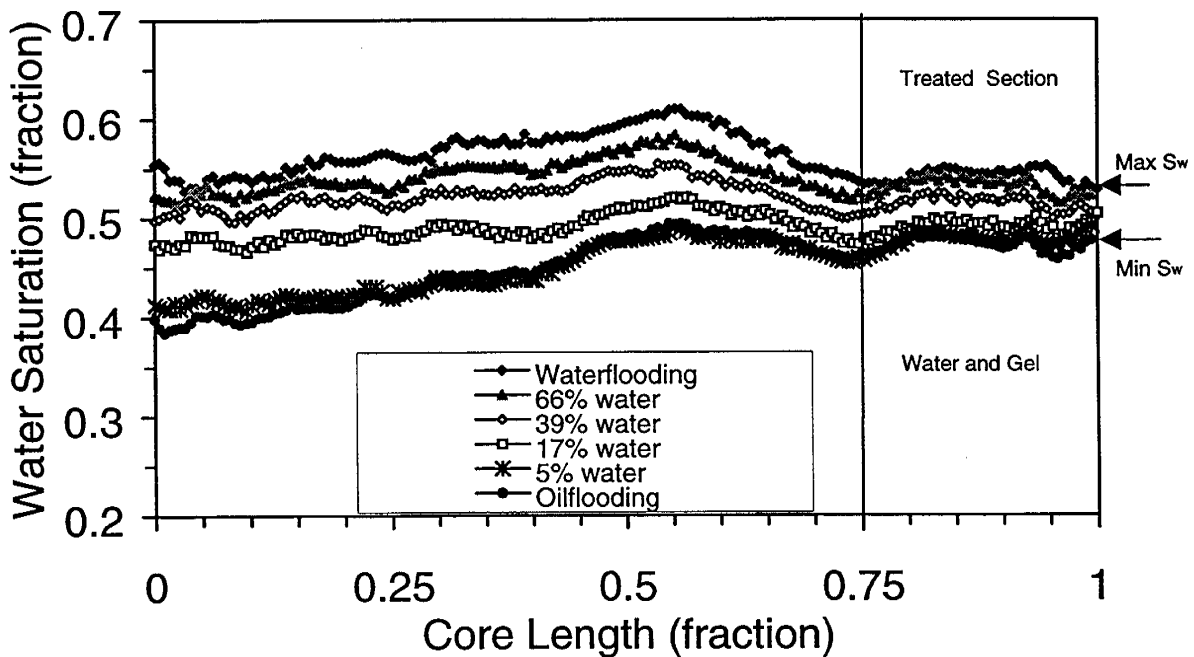


Figure 9.6 - Water saturation profiles during different fractional flows after gel treatment; Drainage path and steady state.

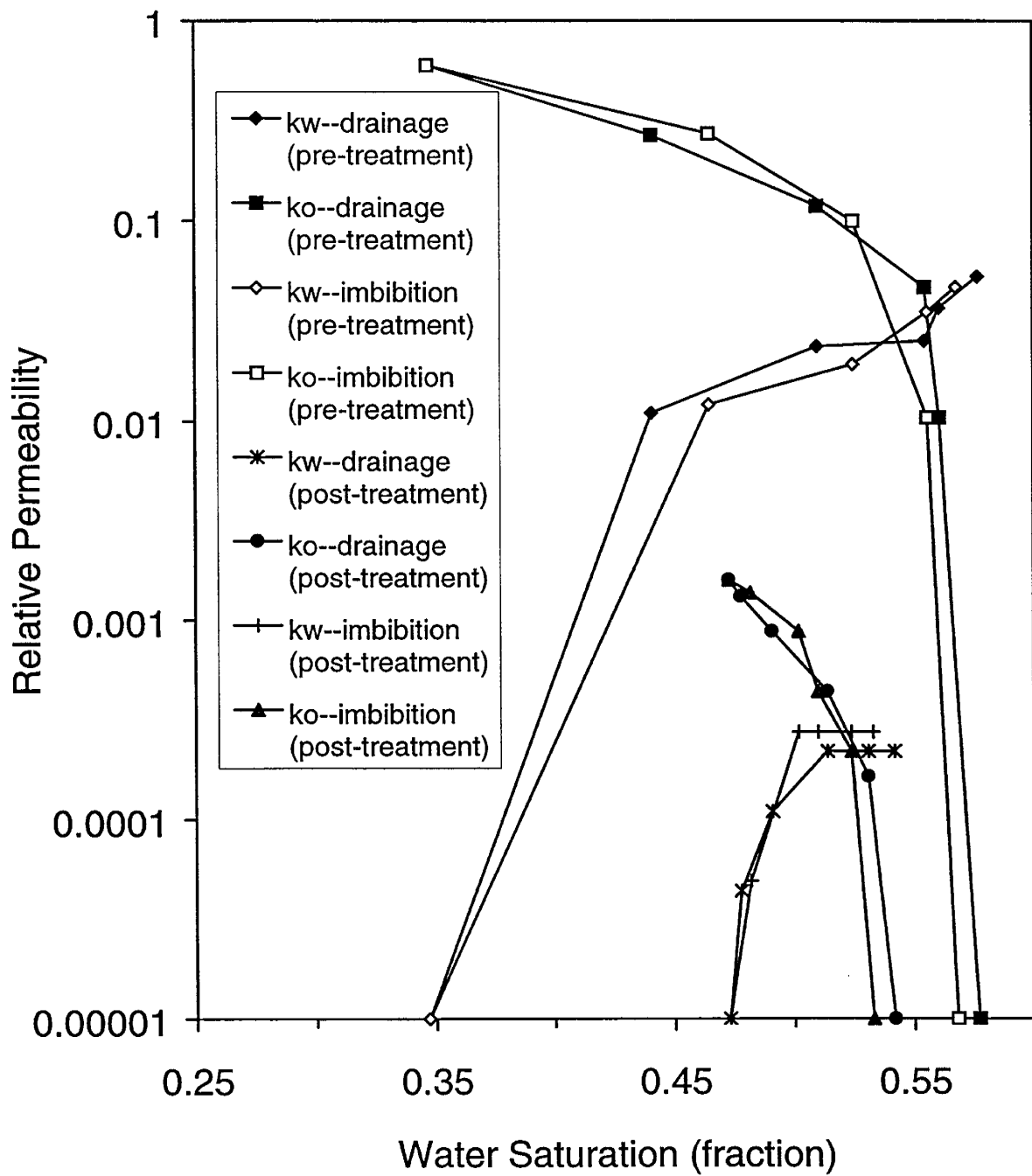


Figure 9.7 – Relative permeability curves of Section 4 before and after gel treatment;

Condition (A) the fractional flow of the water was the same at 100%, the endpoint permeability values; Water saturations were different at the endpoints.

Condition (B) the water saturations were the same and at the value during the 100% brine flow during the post treatment measurement; The fractional flow of water for the pre-treatment permeability value was less than 100%.

Similar conditions were used for oil flow. The RRFs calculated at these conditions are given for water and oil in Tables 9.1 and 9.2, respectively. The RRFs for the non-treated sections, Sections 1, 2, and 3, were closer to unity when the RRFs were calculated from permeability values measured at the same saturation (Condition B). This indicates that the treatment in Section 4 did not significantly affect the relative permeabilities of Sections 1, 2, and 3. The residual saturations of both oil and water in Sections 1, 2, and 3 were greater after treatment. This might be caused by the gel treatment in the downstream section and/or, in part, by the lower pressure drops and flow rates in those sections for the runs conducted after the treatment.

The RRFs for Section 4 show that both the both oil and water permeabilities were reduced significantly by the gel treatment. This occurred even with an oil postflush. This magnitude of reduction in the oil permeability would not be desired in a production well treatment. The RRFs for Section 4 that were calculated with the endpoint permeabilities (Condition A) show that the permeability of the oil was reduced by a larger factor than the water permeability. The opposite was true for the RRFs calculated using Condition B. The degree of disproportionate permeability reduction was low.

Permeabilities to oil and water at four fractional flows ($f_w = 100\%$, 25% , 50% , 0%) were determined as a function of the total flow rate. An example of these data for $f_w = 25\%$ are shown in Figure 9.8. Both the oil and water permeabilities increased with increased flow rate in Section 4. Permeabilities were not a function of flow rate in Sections 1, 2, and 3. No significant variation in the water saturation was observed under the four test conditions. Oil and water permeabilities in Section 4 were correlated with Darcy velocity using a power-law relationship. The equations are given in Table 9.3.

The variation of the relative permeability to water at S_{or} (or actually $S_{or} + S_{gel}$) with superficial velocity in the gel treated section is consistent with data reported by Liang et al. [1995].

However, our data show that relative permeabilities of both oil and water vary with flowrate and saturation between the region of 100% water flow and 100% oil flow. In contrast, Liang et al. report that values of residual resistance factors to oil (F_{ro}) were Newtonian and thus did not vary with flow rate for the systems they studied. Values of relative permeability at intermediate saturations were not measured by Liang et al.

We did not observe disproportionate permeability reduction for the system studied in this research. Residual resistance factors for oil and water were approximately the same after gel treatment. These experiments require much time to conduct and results from one system are

Table 9.1 – Residual resistance factors for water.

	Pre-treatment			Post-treatment		Condition A	Condition B
	Water saturation at residual oil	Permeability at residual oil saturation (md)	Permeability at the residual oil saturation during post-treatment (md)	Water saturation at residual oil	Permeability at residual oil saturation (md)	Residual resistance factor [Same fractional flow (100%)]	Residual resistance factor [Same saturations]
Overall	0.600	9.5	6.9	0.561	0.16	59	43
Section 1	0.595	8.7	6.0	0.549	4.13	2.1	1.5
Section 2	0.620	10.9	6.8	0.576	6.26	1.7	1.1
Section 3	0.609	9.2	6.1	0.579	4.76	1.9	1.3
Section 4	0.577	9.6	6.8	0.542	0.040	240	170

Table 9.2 – Residual resistance factors for oil.

	Pre-treatment			Post-treatment		Condition A	Condition B
	Residual water saturation	Permeability at residual saturation (md)	Permeability at the residual saturation during post-treatment (md)	Residual water saturation	Permeability at residual saturation (md)	Residual resistance factor [Same fractional flow (100%)]	Residual resistance factor [Same saturations]
Overall	0.337	145	62	0.451	1.1	130	56
Section 1	0.304	150	87	0.404	54	2.8	1.6
Section 2	0.341	175	87	0.447	72	2.4	1.2
Section 3	0.357	155	51	0.479	42	3.7	1.2
Section 4	0.347	109	36	0.473	0.29	380	120

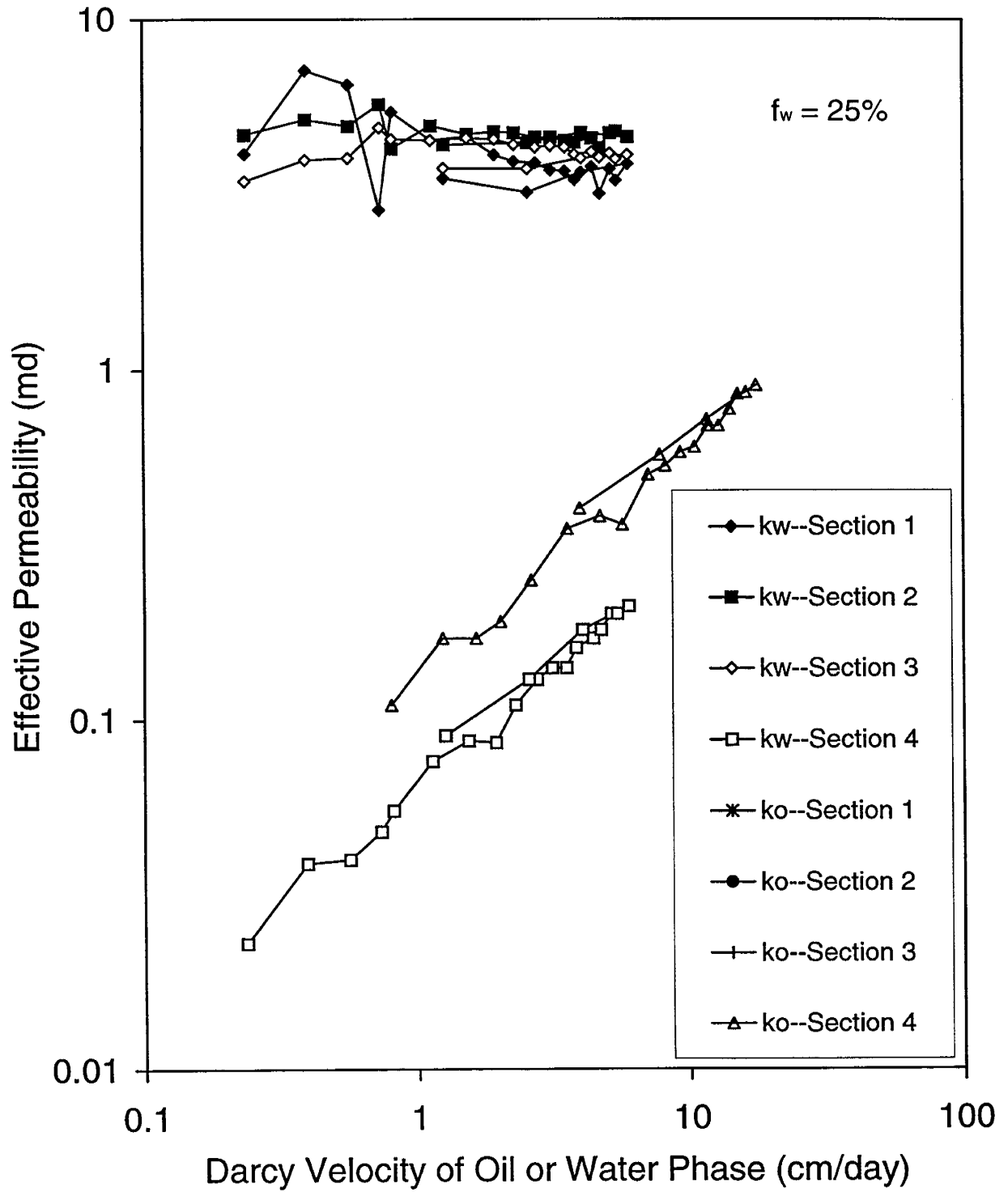


Figure 9.8 - The effect of flow rate on effective permeability to water and oil after gel treatment; Water fractional flow of 25%.

Table 9.3 - Permeability of Section 4 as a function of Darcy velocity.

Water fractional flow	Water effective permeability (md)	Oil effective permeability (md)
$f_w = 1.0$	$k_w = 0.081 u_w^{0.67}$	0
$f_w = 0.25$	$k_w = 0.064 u_w^{0.67}$	$k_o = 0.13 u_o^{0.67}$
$f_w = 0.50$	$k_w = 0.096 u_w^{0.48}$	$k_o = 0.18 u_o^{0.49}$
$f_w = 0.0$	0	$k_o = 0.66 u_o^{0.47}$

reported. We do not know if the absence of disproportionate permeability modification for this system is due to the composition of the gelant or the placement procedure. Both oil and water phases were mobile when the gelant was placed and a small post placement oil flush was used to insure oil connectivity in the treated region following gelation.

Conclusions

The following conclusions can be drawn for the particular gel system and porous medium used in this study:

1. The relative permeabilities to water and oil were decreased significantly by the gel treatment.
2. The residual resistance factors for oil and water are approximately the same.
3. The range of mobile saturation decreased significantly after gel treatment.
4. The permeabilities to both phases were functions of flow rates in the section of the slab treated by gel.
5. In the treated section, the effective permeability of each phase increased with increasing flow rate of that phase. The relationship between effective permeability and flow rate of each phase is logarithmically linear.
6. Hysteresis of relative permeability occurred both before and after gel treatment.
7. No hysteresis was observed in the gel-treated section due to flow rate changes.

Nomenclature

- f = fractional flow
- k = permeability
- S = saturation
- u = darcy velocity

Subscripts

- o = oil
- w = water or water and gel
- r = relative

Chapter 10

Gel Systems for Carbon Dioxide Flooding

Principal Investigators: G.P. Willhite, D.W. Green, S. Vossoughi, M.J. Michnick
Graduate Research Assistant: Koorosh Asghari

Introduction

Carbon dioxide flooding process is a multi-contact miscible process through which carbon dioxide, when injected into reservoir, forms a miscible bank that improves the overall oil recovery from the reservoir. For many reservoirs, the miscibility pressure for carbon dioxide is lower or around the reservoir pressure which makes this process very efficient and practical.

Because of the unfavorable mobility ratio between the injected carbon dioxide and the oil in place, carbon dioxide tends to finger through the high permeability zones of the reservoir and bypasses the oil in lower permeability, unswept zones of reservoir.

One way to improve the overall efficiency of carbon dioxide flooding is to block the already-swept high permeable zones and divert carbon dioxide toward unswept low permeability zones of the reservoir. This could be achieved by in-depth placement of polymer gels in the reservoir. In this technique, a gelling solution is injected into the reservoir, where the gelation takes place and the liquid solution change form to a gel which blocks that part of reservoir.

The objective of this research is to evaluate several gel systems for carbon dioxide flooding application.

Gel Systems Studied

Four different gel systems were tested for carbon dioxide flooding application.

KUSP1-Ester Gel System. KUSP1 (Kansas University Super Polymer One) is a biopolymer developed at the University of Kansas. The polymer is a β -1,3-polyglucan and is produced by fermentation of a bacterium known as *Alcaligenes faecalis* and certain species of *Agrobacterium* [Buller, 1990].

Vossoughi et al. [1991] showed that this biopolymer could be used for reducing permeability in sandpicks and Berea sandstones by reducing the pH of polymer solution via adding acid. Since KUSP1 forms gel at pH less than 10.8, any chemical reaction which reduces pH of the solution could be used for forming gel. One of these such methods is neutralization of the alkaline polymer solution using an ester. The chemistry of reducing the pH of solution was studied by Fichadia [1995].

KUSP1-Boric Acid Gel System. KUSP1 forms gel by adding orthoboric acid. The mechanism by which orthoboric acid gels KUSP1 is different than by pH reduction [Khana et al., 1996]. The gelation behavior of KUSP1-boric acid system was characterized elsewhere [Willhite et al.,

1995]. By selection of boric acid concentration, and the solution pH, it is possible to obtain gelation times from several minutes to several days.

Sulfomethylated Resorcinol Formaldehyde (SMRF). Sulfomethylated resorcinol formaldehyde gels [Zhuang et al., 1997] are a modified version of phenol formaldehyde gel system. Sulfomethylated resorcinol formaldehyde system forms a stable gel at pH=7.0, salinity of 5000 ppm, and temperature range of 25°C to 41°C.

AlcoFlood 254S-Chromium Gel System. AlcoFlood 254S [Lot 7079V] is a synthetic polyacrylamide polymer manufactured by Allied Colloids. It is a relatively low molecular weight polymer which is used at high concentrations. Chromium ions provide the cross linking in the gel. Chromic acetate solution with the ratio of 12:1 (polymer:active chromic acetate) is the source for chromium ions.

Experimental Setup and Procedure

Equipment and Materials. Figure 10.1 is a schematic presentation of the experimental apparatus used in this work. An ISCO syringe pump was used to inject carbon dioxide, brine, and gelants into the core. A TEMCO high-pressure core holder equipped with three pressure ports was used. Berea cores, one foot long and two inches in diameter, were used for these experiments. Pressure ports were located such that the core was divided into four sections. The first and fourth sections were 5 cm in length and sections 2 and 3 were 10 cm long. Details of the experimental set up are presented elsewhere [Raje, 1995].

Solution Preparation: KUSPI-Ester System. Concentrations of KUSP1 and sodium chloride in polymer solution were 1% by weight. The solution was prepared by dissolving KUSP1 and sodium chloride in 1.0 N sodium hydroxide solution and adding monoethylphthalate ester. Details of preparing KUSP1-ester solution are given elsewhere [Shaw, 1995].

Solution Preparation: KUSPI-Boric Acid System. Gelant samples were prepared by weight. Sufficient stock polymer and sodium chloride were weighed and dissolved in 1.0 N sodium hydroxide. Solid orthoboric acid was weighed to give 0.5 moles boric acid per one kilo gram of final gelant solution, and was dropped into the stirred polymer solution and allowed to dissolve. The pH of the solution was monitored and adjusted to the desired value of 10.5 by adding concentrated hydrochloric acid.

Solution Preparation: SMRF System. A fresh solution of SMRF was prepared in the laboratory. Sulfomethylation was carried out by initially reacting sodium sulfite with formaldehyde and subsequently reacting it with resorcinol [Green et al., 1996] at 60°C. The pH of the final solution was adjusted to 9.8 by adding 50% sodium hydroxide solution at the initiation of reaction.

SMRF gelant solution was prepared by adding brine (1% NaCl + 0.072% CaCl₂) and formaldehyde solution to the sulfomethylated resorcinol (SMR) solution. Solution pH was adjusted to approximately 7 by adding 20% acetic acid solution.

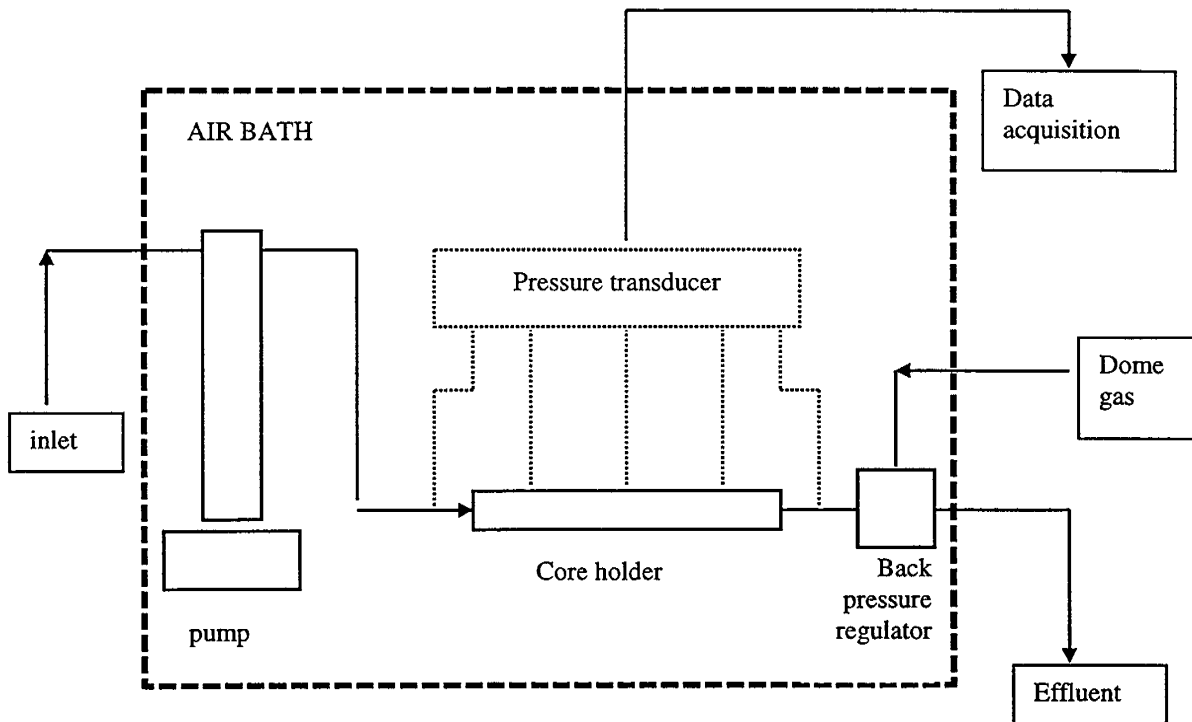


Figure 10.1 – Schematic diagram for the apparatus used for flow experiments.

Solution Preparation: *AlcoFlood 254S-Chromium System* . AlcoFlood 254S, was provided by Allied Colloid and was used as received. A 5% polymer solution was prepared by dissolving polymer in 1% brine solution. Polymer was added slowly to the stirred brine solution and the solution was stirred for 24 hours to ensure complete dissolution of polymer. The solution was filtered through a 0.5 micron filter before injection to prevent the plugging of core. Crosslinker source for this experiment was chromic acetate solution from McGean-Rohco. The ratio of active chromic acetate to the polymer was 1:12. Chromic acetate solution was added to the filtered polymer solution just before injecting the solution into the core.

Flow Experiment Procedure in Berea Core. The objective of these experiments was to investigate the performance of four gel systems in a Berea core at conditions similar to reservoirs that are candidates for carbon dioxide flooding. Experiments were conducted at 41°C unless otherwise indicated. Each flow experiments was conducted in the following sequences:

1. Measure the initial brine permeability in the core.
2. Displace brine with carbon dioxide at 1200 psi to a residual saturation and measure the initial permeability of carbon dioxide in the core in presence of the residual brine saturation.
3. Displace carbon dioxide with brine at 1200 psi and measure the brine permeability in presence of residual carbon dioxide in the core.
4. Inject several pore volumes of gelant into the core at atmospheric pressure.
5. Wash the inlet and outlet tubes and shut-in the core for sufficient time for gelation.

6. Inject brine into the core and determine the brine permeability and the residual resistance of the gelled core.
7. Increase the core pressure to 1200 psi.
8. Inject carbon dioxide in the gelled core and determine carbon dioxide permeability and the residual resistance factor for carbon dioxide.
9. Inject brine into the gelled core and determine brine permeability and the residual resistance factor for brine.
10. Repeat steps 8 and 9.

Results and Discussion

KUSP1-Ester Gel System. After gel formed in the core, brine was injected into the gelled core at 0.1 mL/min and atmospheric pressure to determine brine permeability in the gelled core. Table 10.1 presents the permeability data before and after gelation for this experiment.

Table 10.1 - Core permeability before and after gelation with KUSP1-ester gel (atmospheric pressure).

	Initial brine permeability (md)	After gelation brine permeability (md)
Overall	144	2.64
Section 1	167	0.40
Section 2	186	----
Section 3	164	----
Section 4	76	----

The missing values in Table 10.1 are due to the plugging of the corresponding pressure ports by gel. The overall permeability of the core shows a reduction of the order of 99% of the initial permeability in this experiment.

The pressure in the core was increased to 1200 psi and brine permeability was measured. Results are shown in Table 10.2. The higher permeability measured at high pressure might be due to the dehydration of the gel under high pressure.

Table 10.2 - Brine permeability in the core gelled with KUSP1-ester gel (1200 psi pressure).

Core section	Brine permeability (md)
Overall	7.64
Section 1	1.05
Section 2	----
Section 3	----
Section 4	----

Carbon dioxide at 1200 psi and 34°C was injected into the gelled core. The overall carbon dioxide permeability was 4.15 md. Carbon dioxide permeability after gelation was 3% of the initial brine permeability.

KUSP1-Boric Acid Gel System. Effect of temperature, pH, and environment on the syneresis of KUSP1-boric acid gel was studied. A detailed description of methods is given elsewhere [Green, 1997]. At 41°C, this gel loses more than 80% of its initial volume due to syneresis. Figure 10.2 shows the syneresis behavior of the gel at 41°C.

Effect of gel syneresis on permeability modification was studied by conducting flow experiments in a sandpack. The initial permeability and pore volume of the sandpack were about 4000 md and 85 mL, respectively. Tracer tests were used to estimate the fraction of the pore volume that was accessible to water. Figure 10.3 presents the available pore volume for flow and sandpack

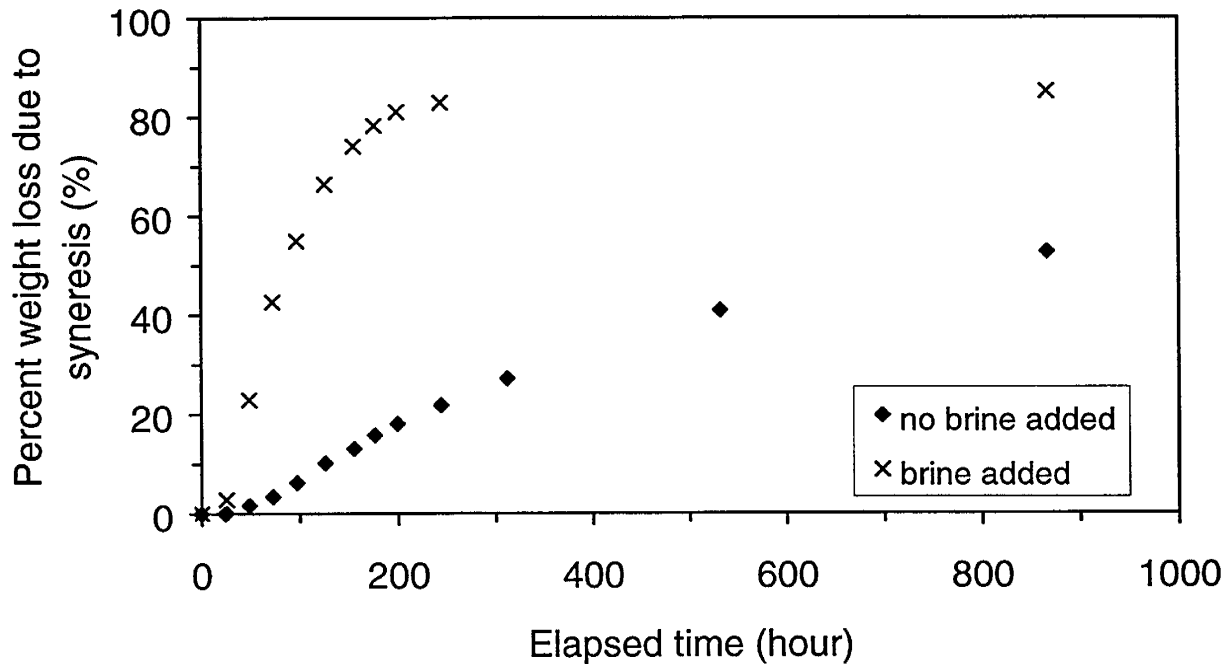


Figure 10.2 - KUSP1-boric acid syneresis at 41°C.

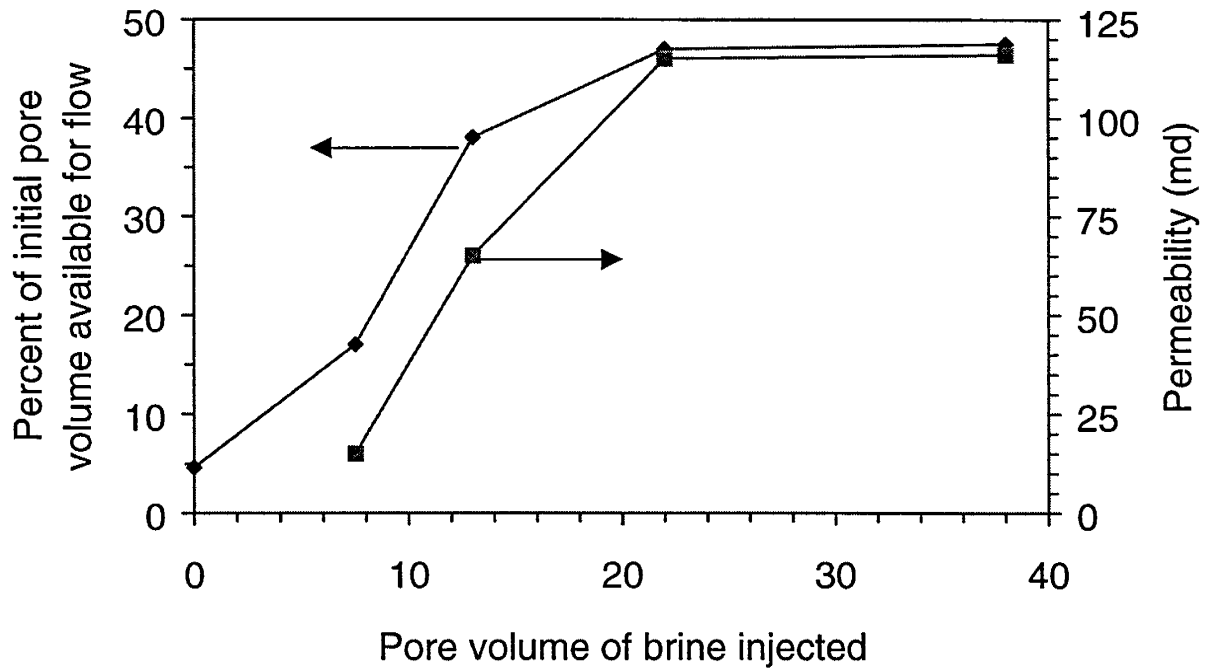


Figure 10.3 - Effect of syneresis of KUSP1-boric acid in a sandpack on permeability and available volume for flow.

permeability change as a function of pore volume brine injected. The volume available for flow in the gelled core increased from 5% at the beginning of the experiment to about 50% of the original pore volume of the sand pack after injecting about 35 pore volumes of brine through the gelled sandpack. The increase in the available volume for flow with time indicated the syneresis of the gel inside the sandpack. Although permeability of the gelled sandpack increased with increasing available pore volume for flow, the highest permeability was about 120 md which is much lower than the 4000 md the original permeability of the sandpack.

Evaluating KUSP1-Boric Acid Gel for Carbon Dioxide Applications. The initial pore volume and porosity of the core were 133.8 mL and 22%, respectively. About 600 mL of gelant (pH adjusted at 11) was prepared and filtered through a 5-micron filter before injecting the gelant into the core. Samples of effluent and injected gelant formed gel after about 48 hours. The core holder was shut-in for 4 days before brine injection into the gelled core started.

A 1% sodium chloride solution was injected into the gelled core, at a rate of 0.07 mL/min. The pressure drop between different sections of the core as well as the overall core pressure difference behavior was recorded and is shown in Figure 10.4. For all sections of the core, pressure difference reaches a maximum and decreases afterward. The maximum pressure drop observed for the first section was much lower than for other sections. Pressure drop maxima occur first in section one, followed by section two, then section three, and finally section four. Based on this behavior, we hypothesize that flow channels are formed during injecting brine into the gelled core and the onset of the pressure decrease is caused by the formation of these

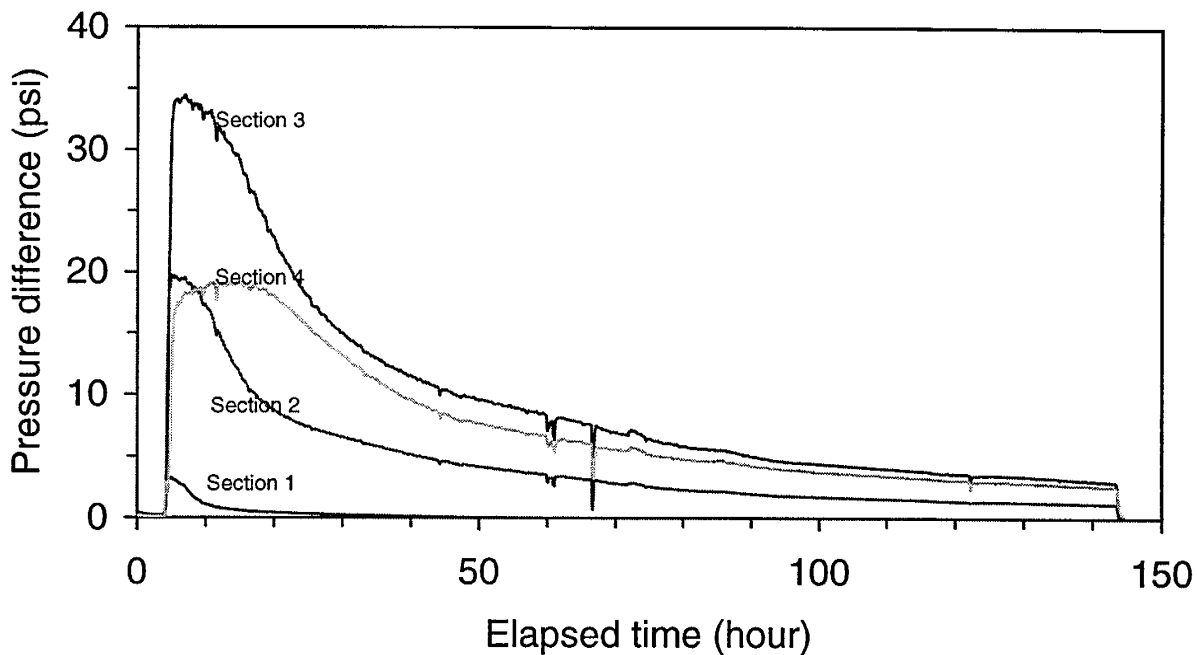


Figure 10.4 - Brine injection into the core gelled with KUSP1-boric acid gel.

channels. These channels are formed in section one, where brine enters the core, then by continued brine injection channels are formed in section two, three, and so on.

In order to study the performance of the KUSP1-boric acid gel for carbon dioxide flooding, carbon dioxide and water, at 41°C and 1200 psi, were injected alternately into the gelled core. About 20 pore volumes of carbon dioxide were injected into the core followed by the injection of about 20 pore volumes of brine. This cycle was repeated four times. A significant increase in the permeability was observed when carbon dioxide was injected for the first time into the gelled core. The overall permeability to brine which was stable and about 15 md before injecting carbon dioxide increased to 70 md after injecting carbon dioxide. Table 10.3 summarizes the permeability measurement data for the four cycles of water and carbon dioxide injection into the gelled core.

Table 10.3 - Permeability and residual resistance factors of the gelled core to carbon dioxide and brine for different cycles. 1200 psi and 41°C.

Initial Perm. (md)		OVERALL CORE PERMEABILITY (md)							
		CYCLE ONE		CYCLE TWO		CYCLE THREE		CYCLE FOUR	
CO ₂	brine	CO ₂	Brine	CO ₂	Brine	CO ₂	brine	CO ₂	brine
164	420	19	68	18	71	17	85	26	90
		OVERALL CORE RESIDUAL RESISTANCE FACTOR							
		8.6	6	9	6	9.5	5	6.3	4.7

Sulfomethylated Resorcinol Formaldehyde (SMRF) Gel System. Experimental procedure for SMRF gel system is described in detail elsewhere [Willhite, 1996]. Table 10.4 shows the permeability data before and after gelation.

Table 10.4 - Permeability modification for SMRF gel system (Atmospheric pressure and 41°C).

	Initial brine permeability (md)	Post gelation brine permeability (md)	RRF
Section 1	567	0.060	9450
Section 2	744	0.085	8453
Section 3	622	0.034	18294
Section 4	707	0.042	16833
Overall	695	0.049	14183

The SMRF gel effectively shuts off the flow of brine and reduces the effective permeability of the core to almost zero. Permeability of carbon dioxide in the gelled core is presented in Table 10.5.

Table 10.5 - Permeability of different sections of the SMRF gelled core to carbon dioxide at 1200 psi and 41°C.

Core section	Carbon dioxide permeability (md)
Section 1	----
Section 2	0.642
Section 3	0.406
Section 4	0.309
Overall	0.557

The above data shows an overall permeability of 0.557 md for the carbon dioxide in the gelled core.

AlcoFlood 254S-Chromium System

Experimental Procedure: AlcoFlood 254S System. Initial brine permeability in the core was determined by injecting brine at 10 mL/min into the core. Table 10.6 presents the permeability at different sections of the core.

Table 10.6 - Initial brine permeability in core.

Core section	Section 1	Section 2	Section 3	Section 4	overall
K (md)	636	672	636	432	595

Preparation of Gelant. 1000 mL of 5% ALCOFLOOD 254S solution was prepared. The polymer solution was filtered first through a one micron and then a 0.5 micron filter. Viscosity of the 5% polymer solution at 25°C showed shear thinning behavior, as shown in Table 10.7.

Table 10.7 - Viscosity of 5% polymer solution as measured by Brookfield viscometer at 25°C.

Shear rate (s^{-1})	2.25	4.5	11.25
Viscosity (cp)	104	95.1	87.8

A total of 535 mL of gelant was injected into the core at room temperature (~25°C) as shown in Figure 10.5. Then, the inlet and outlet lines were washed with brine. Temperature of air bath was increased to 41°C, and core was shut-in for the gel to form.

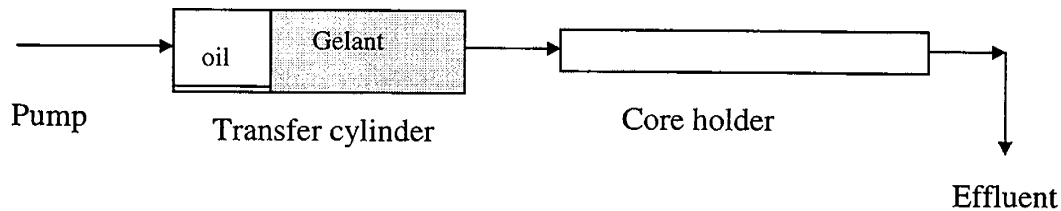


Figure 10.5 - AlcoFlood 254S gelant injection into the core.

When gelation was complete, brine was injected into the gelled core at 0.007 mL/min for about six hours. The pressure data from sections of the core are shown in Figure 10.6. Figure 10.7 also presents the overall pressure profile for this experiment. The pressure in section one went out of range (>100 psi). Meanwhile, the pressure difference in sections three and four remained very low, and pressure difference in section two showed an increase after about six hours of injection. Brine injection was stopped after about six hours, because the overall pressure drop exceeded 500 psi. This experiment clearly showed that this gel blocks the core so tight that even under a pressure gradient of 500 psi/ft, it is not possible to inject brine into the core at rates as low as 0.007 mL/min.

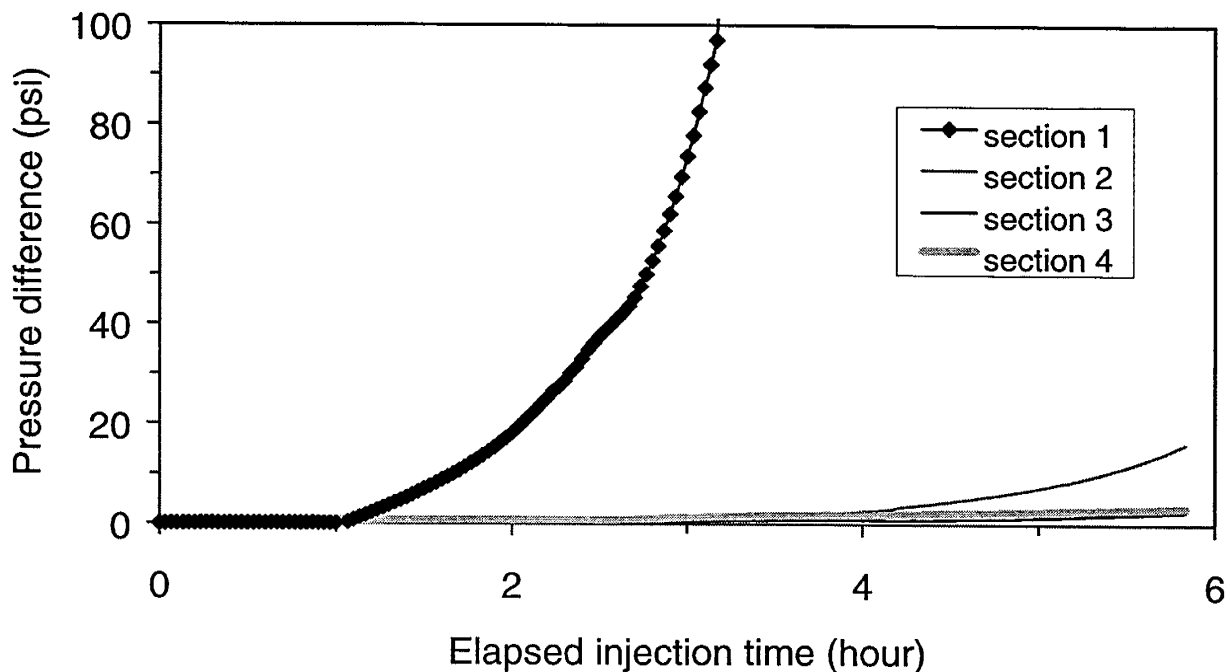


Figure 10.6 - Pressure response in different sections of the core gelled with AlcoFlood 254S. Brine injection at 0.007 mL/min.

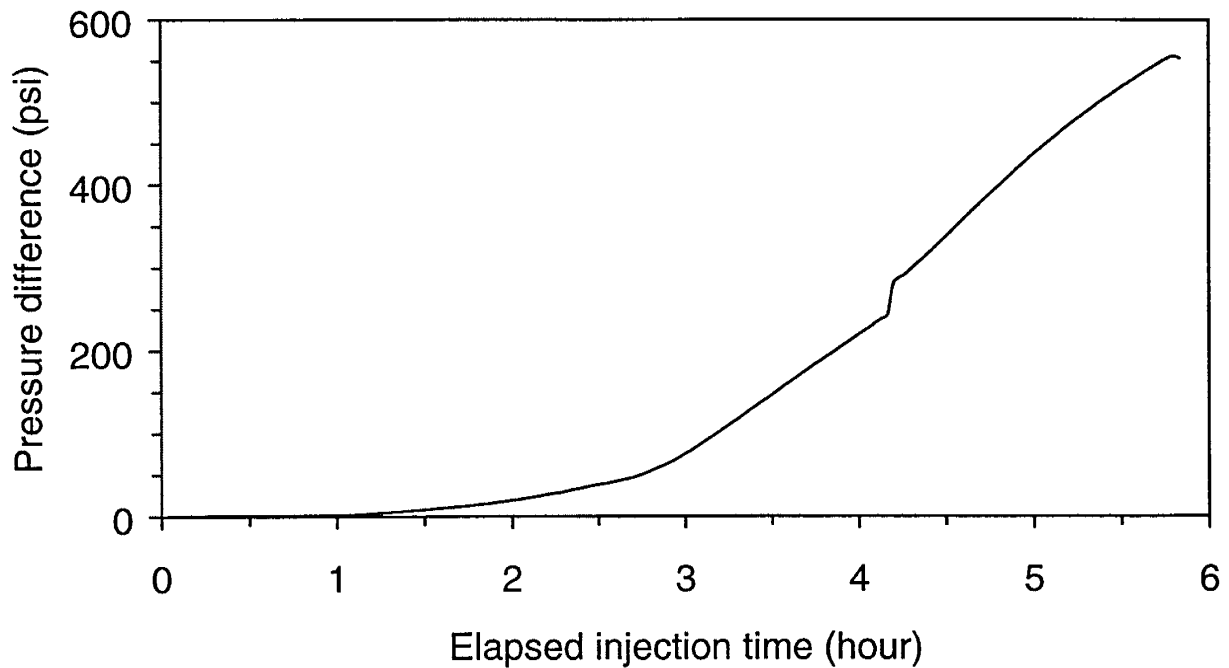


Figure 10.7 - Overall pressure response in the core gelled with AlcoFlood 254S. Brine injection at 0.007 mL/min.

Because of the very high pressure gradients obtained during constant flow experiment, it was decided to conduct experiments at constant pressure conditions. First, brine at constant pressure of 100 psi was injected into the gelled core, and effluent was collected with time. The effluent collection and flow rate data are presented in Table 10.8.

Table 10.8 - Effluent and flow rate data for brine injection at constant pressure of 100 psi.

time interval (min)	208	320	1443	1368	1401
effluent (g)	1.32	1.39	0.11	0.1	0.29
flow rate (mL/min)	0.00577	0.00434	0.00007	0.00007	0.00021
permeability (md)	0.02	0.016	0.00025	0.00025	0.00076

Above data show that at 100 psi, the permeability of the gelled core is almost zero. In the next step of experiment, the pressure was increased to 150 psi. Again effluent was collected and flow rate was calculated (Table 10.9).

Table 10.9 - Effluent and flow rate and data for brine injection at constant pressure of 150 psi.

time interval (min)	715	2425
Effluent collected (g)	0.05	0.03
flow rate (mL/min)	0.00007	0.00001
Permeability (md)	0.00017	0.000024

Even at 150 psi/one foot of the gelled core, there was an almost complete water shut off in the gelled core.

The same experiment was repeated at constant pressure of 300 psi. Figure 10.8 shows the pressure behavior in different sections of the core during more than 250 hours brine injection at 300 psi. Pressure difference in sections 1, 2, and 3 went over range. First section 1, then section 2, and finally section 3 went over range. Sections 1 and 2 got back in the measurement range, but section 3 remained out of range. Section 4 did not go over range. Pressure variation for sections 1 to 3 suggests the formation of channels during water injection through the gelled core. For this part of experiment, the effluent collection showed a flow rate of 0.000625 mL/min through the gelled core. Brine permeability in the core was 0.00076 md, which again indicates the almost total shut off for water injection application.

In order to investigate the strength of the gel and perseverance of water shut off characteristics of AF254S gel system, above gel system was remained under 300 psi constant pressure for about 2 months. Figure 10.9 presents the pressure behavior in different section of the core after applying constant pressure of 300 psi at the core inlet for 2 months. Sections 1 and 4 show the same pressure difference, and sections 2 and 3 show equal pressure differences, as well. The brine flow rate for this part of experiment was 0.000188 mL/min, which gives a permeability of 0.0002 md. This result showed that even after the core was subjected to a pressure gradient of about 300 psi/ft for 2 months, the gelled core still showed nearly total shut off behavior.

Pressure data presented in Figures 10.8 and 10.9 fluctuate with a cycle period of about 24 hours. The apparatus and lines are completely filled with liquid. This experiment was conducted at ambient temperature without temperature control. The fluctuation in pressure is probably due to the diurnal change of temperature of laboratory with time due to thermal expansion and contraction of the confined fluids.

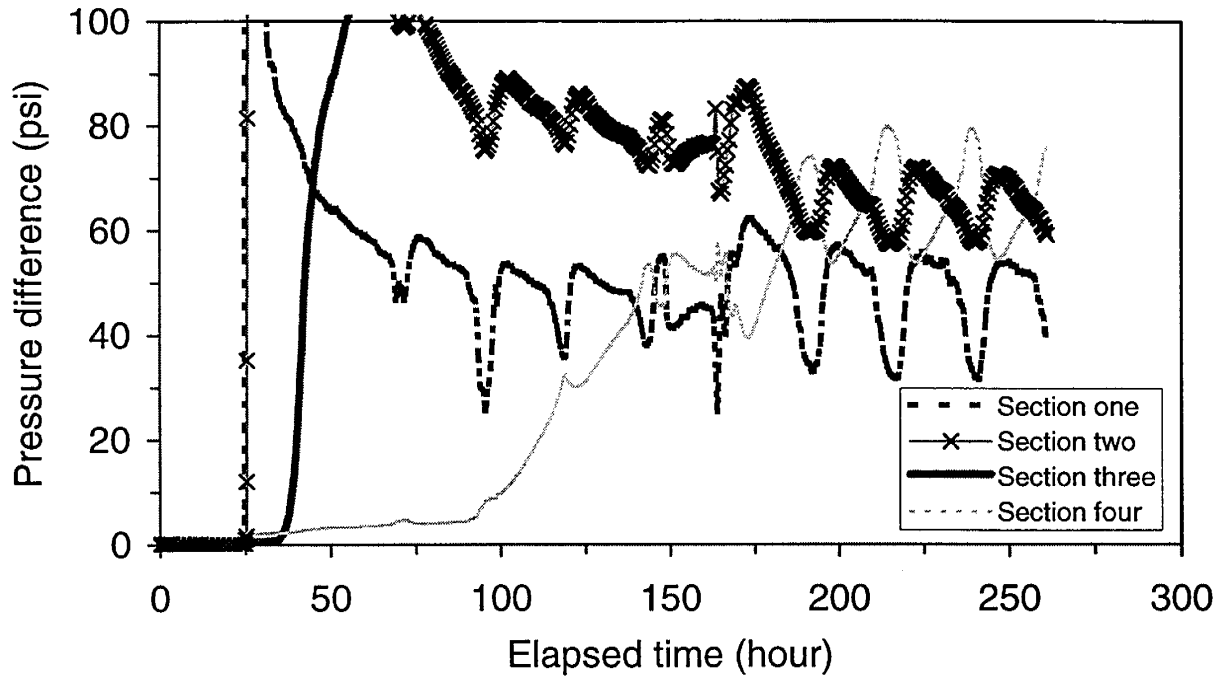


Figure 10.8 - Brine injection into the core gelled with AlcoFlood 254S at constant pressure of 300 psi.

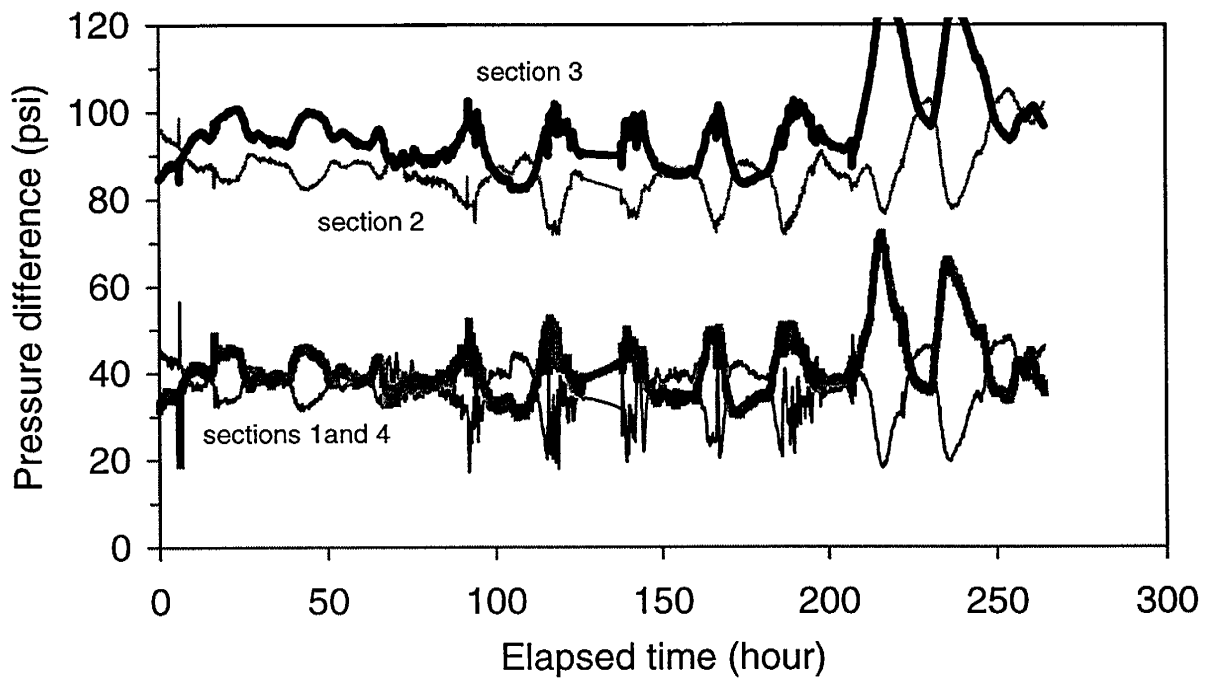


Figure 10.9 - Pressure response for brine injection into the core gelled with AlcoFlood 2543S at constant pressure of 300 psi after two months.

Pressurizing the Core

The core pressure was increased to 1200 psi for the carbon dioxide injection experiment. An additional pressure transducer was placed between the outlet of the core and the back pressure regulator to monitor the pressure increase at the outlet side of the core-holder. Pressurizing the core was done in several consecutive steps as follows:

1. Step one: While applying constant injection pressure of 300 psi, the back pressure regulator was set at 300 psi, as well. Figure 10.10 shows that it takes more than 120 hours for the outlet pressure to increase and stabilize. This long time required for pressure increase in the outlet is contributed to two major reasons of (1) very small flow rate in the core as shown earlier, and (2) compressing the rubber sleeve as the internal core pressure increases.
2. Step two: Injection pressure increased to 600 psi, back pressure regulator was increased to 600 psi .
3. Step three: Injection pressure increased to 900 psi, back pressure regulator was increased to 900 psi .
4. Step four: Injection pressure was increased to 1200 psi and back pressure regulator was increased to 1200 psi.

At steps 2, 3, and 4, the outlet pressure rose to the back pressure setting quickly. The delayed pressure increase observed for step one did not occur.

At the end of step four, the core pressure was increased to 1200 psi, and it was ready for carbon dioxide injection experiment.

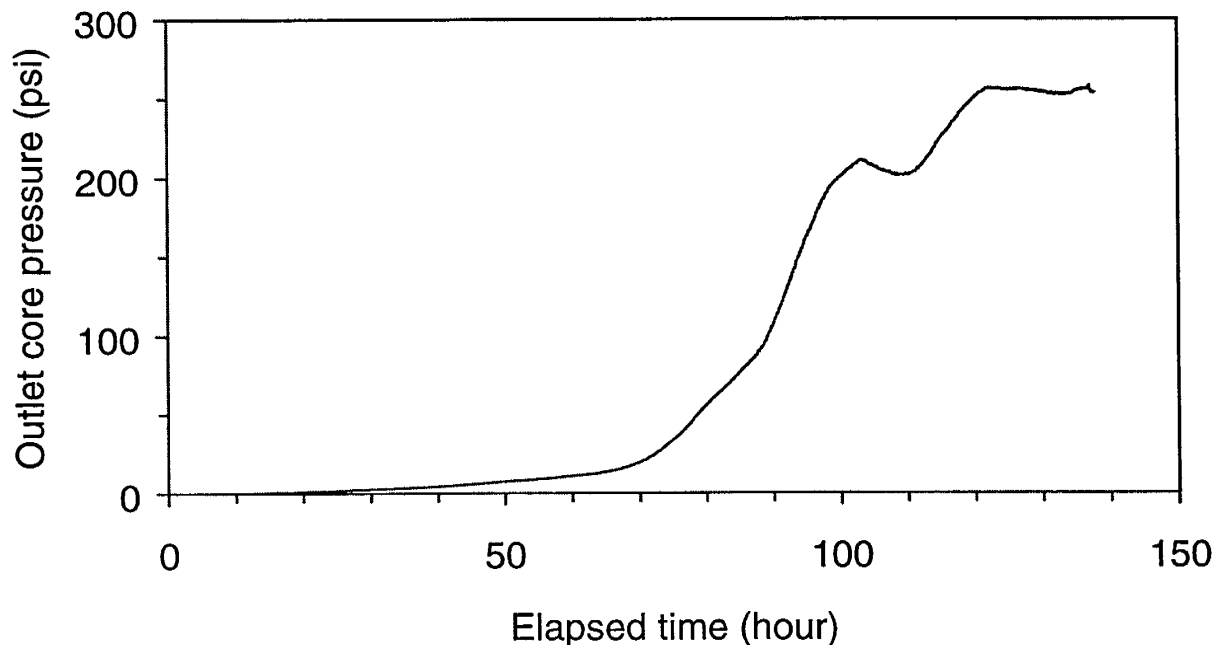


Figure 10.10 - Pressure response between the core exit and back pressure regulator (AlcoFlood 254S experiment).

Carbon Dioxide Injection into the Gelled Core

Constant Flow Rate Experiment

After pressurizing the core, the pump was filled with carbon dioxide. Pump pressure was increased to 1200 psi, and carbon dioxide injection into the core was started at constant injection rate of 2 mL/min. It was observed that the pump injection pressure (e.g. carbon dioxide pressure at injection point) increased from 1200 psi to 1300 psi and no carbon dioxide entered the core. It was concluded that for this gel system, it is not possible to inject carbon dioxide at 1200 psi and constant injection rate of 2 mL/min. Hence, it was decided to switch the experiment to a constant injection pressure experiment.

Constant Injection Pressure Experiment

The injection pressure of carbon dioxide was increased to 1300 psi and was kept constant while keeping the back pressure constant at 1200 psi. Carbon dioxide was injected into the gelled core for about 20 days at a constant pressure difference of 100 psi. The effluent was collected under oil to monitor the flow of carbon dioxide. No flow was observed during the period of the experiment. Based on the above experiments, it was concluded that this gel system shuts off the flow of carbon dioxide completely as well as brine flow in the gelled core.

Conclusions

1. KUSP1 was gelled in Berea sandstone by hydrolysis of monoethylphthalate ester with a gelation time of over 100 hours at 34°C and 1200 psi. Permeabilities of brine and carbon dioxide were reduced to 95% to 97% of the initial brine permeability.
2. The permeability reduction by KUSP1-ester gel system was stable after injecting several pore volumes of carbon dioxide under super critical conditions.
3. The SMRF system effectively shuts off the flow of brine in Berea sandstone and is equally effective in reducing the mobility of carbon dioxide under super critical conditions. Effective permeability was less than 1 md for a Berea core with initial brine permeability of 700 md.
4. Effect of permeability reduction by SMRF did deteriorate with the flow of super critical carbon dioxide through the treated core.
5. KUSP1-boric acid gel system shows a strong syneresis behavior in bottle tests.
6. Syneresis of KUSP1-boric acid gel in porous media leads to an increase in the available volume for flow. However, despite increase in available volume for flow, KUSP1-boric acid gel maintains a low permeability for brine flow.
7. Injecting carbon dioxide in a KUSP1-boric acid gelled core leads to a sharp increase in the brine permeability.
8. After injecting carbon dioxide into the gelled core for four WAG cycles, the residual resistance factor was 4.7 for the flow of brine and 6.3 for super critical carbon dioxide.
9. AlcoFlood 254S gel completely shuts off the flow of brine and carbon dioxide in a Berea sandstone at pressures as high as 300 psi/ft.

Chapter 11

References

1. Alaburda, J., De Groote, R. A.M.C., Curvelo, A.A.S.: "Synthesis of sodium 2-hydroxy-arylmethanesulfonates," *Bull. Soc. Chim. Fr.* (1987) **1**, 89-92.
2. Albonico, P., Burrafato, G., Di Lullo A. and Lockhart, T.P.: "Effective Gelation-Delaying Additives for Cr+3/Polymer Gels," paper SPE 25221 presented at the 1993 SPE International Symposium on Oilfield Chemistry, New Orleans, March 2-5.
3. Allison, J.D., Wimberley, J.W. and Ely, T.L.: "Automated and Manual Method for the Determination of Polyacrylamide and Other Anionic Polymers," *SPE Reservoir Engineering* (May 1978) pp. 527-539.
4. Benincasa, M.A., Giddings, J.C.: "Separation and Characterization of Cationic, Anionic, and Nonionic Water-Soluble Polymers by Flow FFF: Sample Recovery, Overloading, and Ionic Strength Effects," *John Wiley & Sons, Inc. J. Micro. Sep.* (1997) **9**, 479-495.
5. Benincasa, Maria Anna and Giddings, J. Calvin, "Separation and Molecular Weight Distribution of Anionic and Cationic water soluble polymers by Flow Field Fractionation," *Anal. Chem.* (1992) **64**, 790-798.
6. Blazevic, N., Kolbah, D.: "Hexamethylenetetramine, A Versatile Reagent in Organic Synthesis," *Synthesis* (March 1979) 161-176.
7. Bordwell, F. G., Suter, C. M., Bair, R. K.: "The Sulfomethylation Reaction," *J. Org. Chem.* (1945) **10**, 470-478.
8. Bretz, R.E., Pelletier, M.T. and Orr, F.M. Jr.: "A Small-Volume Continuous Oil/Water Separator for Laboratory Displacement Experiments," *JPT* (March 1984) 487-488.
9. Bryant, S.L., Bartosek, M., Lockhart, T.P.: "Propagation of Cr(III) in Porous Media and Its Effect on Polymer Gelant Performance," *J. Pet. Sci. Engr.* (1996).**16**, 1-13.
10. Buller, C. S.: "Water Insoluble Polysaccharide Polymer and Methods Thereof," U.S. Patent No. 4,908,310 (1990).
11. Burrafato, G. and Lockhart, T.P.: "A New, Mild Chemical Method for the Degelation of Cr+3-Polyacrylamide Gels," paper SPE 19354 (May 1989).
12. Burrafato, G. Albonico, P., Bucci, S. and Lockhart, T.P.: "Ligand-Exchange Chemistry of Cr+3-Polyacrylamide Gels," *Makromolec. Chem., Macromol. Symp.* (1990) **39**,137-141.

13. Dawe, R. A., and Zhang, Y.: "Mechanistic Study of the Selective Action of Oil and Water Penetrating into a Gel Emplaced in a Porous Medium," *Journal of Petroleum Science and Engineering* (1994) **12**,113-125.
14. Eggert, R.W., G.P. Willhite, and D.W. Green: "Experimental Measurement of the Persistence of Permeability Reduction in Porous Media Treated with Xanthan/Cr(III) Gel Systems," *SPE* (Feb. 1992) **7**, 29-35.
15. Fichadia, A.: "Survey of Gelation Systems and A Study of the Gelation of KUSP1 by Hydrolysis of Monoethylphthalate," M.S. Thesis, University of Kansas, Lawrence, KS (1995).
16. Gales, J.R., Willhite, G.P. and Green, D.W.: "Equilibrium Swelling and Syneresis Properties of Xanthan Gum-Cr(III) Gels," paper SPE 17328 presented at the SPE/DOE Enhanced Oil Recovery Symposium, Tulsa, OK (17-20 April 1988).
17. Giddings, J.C., Yang, F.J., Myers, M.N., "Theoretical and Experimental Characterization of Flow Field-Flow Fractionation," *Analytical Chemistry* (1976) **48**, 1126-1132.
18. Giddings, J.C., "Hydrodynamic Relaxation and Sample Concentration in Field-Flow Fractionation Using Permeable Wall Elements," *Anal. Chem.* (1990) **62**, 2306-2312.
19. Giddings, J.C., "Field-Flow Fractionation," *Separation Science and Technology*, (1984) **19**, 831-847.
20. Green, D.W., and Willhite, G.P.: "Improving Reservoir Conformance Using Gelled Polymer Systems," Annual Report for the period September 25, 1994 to September 24, 1995, DOE Contract No. DE-AC22-92BC14881, Report no. DOE/BC/14881-18, The University of Kansas (1996).
21. Green, D. W., Willhite, G. P., McCool, C. S., Heppert, J.A., and Vossoughi, S.: "In Situ Permeability Modification Using Gelled Polymer Systems," Topical Report June 10, 1996 to April 10, 1997, DOE/PC/91008-3, DOE Contract No. DE-AC22-94PC91008, Subcontract No. G4S60331, The University of Kansas (1997).
22. Green, D.W., Willhite, C.S. McCool, J.A. Heppert, S. Vossoughi, and Michnick, M.J.: "In Situ Permeability Modification Using Gelled Polymer Systems," Annual Report, April 11, 1997 to April 10, 1998, US Department of Energy Contract No. DE-AC22-94PC91008, Subcontract No. G4S60331 (1998).
23. Grundl T. and Delwiche J.: "Kinetics of Ferric Oxyhydroxide Precipitation," *Journal of Contaminant Hydrology* (1993).**14**, 71-97.
24. Ilievski D. And White E.T.: "Methods for Estimating the Kinetics of Precipitation Systems," *Emerging Separation Technologies for Metals II*, Ed. By Bautista, R.G., The Minerals, Metals & Materials Society (1996).

25. Iwai, K.: *Fundamental Studies of Fluid Flow Through a Single Fracture*, PhD dissertation, University of California - Berkeley (1976).
26. Khana, P., and Singh, A.: "Gelation Behavior and Permeability Reduction for the KUSP1 Biopolymer-Boric Acid System," Chapter 6 in *Improving Reservoir Conformance Using Gelled Polymer Systems*, Green, D.W., and Willhite, G.P., Eds., DOE/BC/14881-18.
27. Konishi Y., Murai T., and Asai S.: "Preparation and Characterization of Fine Ceria Powders by Hydrolysis of Cerium(III) carboxylate Dissolved in Organic Solvent," *Ind. Eng. Chem. Res.* (1997) **36**, 2641-2645.
28. Landgrebe, J. A.: *Theory and Practice in the Organic Laboratory with Microscale and Standard Scale Experiments*, Brooks/Cole Publishing Company. (1993).
29. Liang, J. and Seright, R. S.: "Further Investigations of Why Gels Reduce Kw More Than Ko," paper SPE 37249, 1997 SPE International Symposium on Oilfield Chemistry, Houston, TX (18-21 Feb. 1997).
30. Liang, J., Sun H., and Seright, R. S.: "Why do Gels Reduce Water Permeability More Than Oil Permeability," *SPE* (Nov. 1995) 282-286.
31. Mack, J.C. and Smith, J.E.: "In-Depth Colloidal Dispersion Gels Improve Oil Recovery Efficiency," SPE/DOE 27780 presented at the SPE/DOE Ninth Symposium on Improved Oil Recovery, Tulsa, OK, April 17-20, 1994.
32. Matre, B., Tengberg-Hansen, H. and Tyvold, T.: "Gel Systems for High Temperature Reservoirs," paper SPE 29013, 1995 SPE International Symposium on Oilfield Chemistry San Antonio, TX (15-17 Feb. 1995).
33. McCool, C.S., Green D.W., and Willhite, G.P.: "Permeability Reduction Mechanisms Involved in In Situ Gelation of a Polyacrylamide-Chromium(VI)-Thiourea System in Porous Media," *SPE Reservoir Engineering*, **6** (Feb. 1991) 77-83.
34. McCool, C.S., Green, D.W. and Willhite, G.P.: "Fluid-rock Interactions Between Xanthan-Cr³⁺ Gel Systems and Dolomite Core Material," paper SPE 28987, presented at SPE International Symposium on Oilfield Chemistry, San Antonio, Feb. 14-17, 1995.
35. McCool, C.S., Shaw. A.K., Singh, A., Bhattacharya, B., Green, D.W. and Willhite, G.P.: "Permeability Reduction by Treatment with KUSP1 Biopolymer Systems," paper SPE 40065, 1988 SPE/DOE Improved Oil Recovery Symposium, Tulsa, OK (19-22 April 1998).
36. Myers, M.N., "Overview of Field-Flow Fractionation," *John Wiley & Sons, Inc. J. Micro. Sep.* (1997) **9**, 151-162.

37. Nielsen, A. T., Moore, D. W., Ogan, M. D., and Atkins, R. L.: "Structure and Chemistry of the Aldehyde Ammonias. 3. Formaldehyde-Ammonia Reaction. 1,3,5-Hexahydrotriazine," *J. Org. Chem.* (1979) **44**, 1678-1684.
38. Parkhurst D.L., Thorstenson, and Plummer, L.N.: "PHREEQE-A Computer Program for Geochemical Calculations," U.S. Geological Survey Water Resource Investigations PB81-167801 (1980).
39. Parsons, R. W.: "Microwave Attenuation -- A New Tool for Monitoring Saturation in Laboratory Flooding Experiments," *SPEJ* (Aug. 1975) **15**, 302-310.
40. Penny, G.S. and Conwey, M.W.: "Fluid Leakoff", in *Recent advances in hydraulic fracturing, SPE Monograph*, Vol.12, Gidley, J.L. et al Eds (1989).
41. Rai, D., Sass B.M., and Moore, D.A.: "Chromium(III) Hydrolysis Constants and Solubility of Chromium(III) Hydroxide," *Inorganic Chemistry* (1987) **26**, 345-349.
42. Raje, M.: "Study of In Situ Gelation Initiated by CO₂ Injection in Porous Media Saturated with KUSP1 Solution," M.S. Thesis, University of Kansas, Lawrence, KS (1995).
43. Ravve, A.: *Organic Chemistry of Macromolecules*. Marcel Dekker. (1967).
44. Seright, R.S.: "Impact of Permeability and Lithology on Gel Performance," SPE/DOE 24190, presented at Eighth Symposium on Enhanced Oil Recovery, Tulsa, April 22-24, 1992.
45. Seright, R. S.: "Improved Techniques for Fluid Diversion in Oil Recovery," U. S. Department of Energy, Contract No. DE-AC22-92BC14880, Report No. DOE/BC/14880-5 (Dec. 1993).
46. Seright R.S.: "Gel Placement in Fractured Systems," paper SPE/DOE 27740 presented at the Ninth SPE/DOE Symposium on Improved Oil Recovery, Tulsa, April 1994.
47. Seright R.S.: "Use of Preformed Gel for Conformance Control in Fractured Systems," paper SPE/DOE 35351 presented at the Tenth SPE/DOE Symposium on Improved Oil Recovery, Tulsa, April 1996.
48. Seright R. S. and Liang, J.: "A Survey of Field Applications of Gel Treatments for Water Shutoff," paper SPE 26991 presented at the III Latin America/Caribbean Petroleum Engineering Conference, Buenos Aires, Argentina (27-29 April 1994).
49. Shaw, A.: "Study of Permeability Modification by In Situ Gelation of KUSP1-Monoethylphthalate Ester System in Porous Media," M.S. Thesis, University of Kansas, Lawrence, KS (1995).
50. Sorbie, K.S.: *Polymer-Improved Oil Recovery*, Blackie, London (1991) 62-102.

51. Stavland, A., Ersdal, T., Kvanik, B., Lohne, A., Lund, T. and Vikane, O.: "Evaluation of Xanthan-Cr Gels for Deep Emplacement: Retention of Cr(III) in North Sea Sandstone Reservoir," Seventh European Symposium on Improved Oil Recovery, Moscow, Russia, Oct. 27-29, 1993.
52. Sydansk, R.D.: "A New Conformance Improvement Treatment Chromium (III) Gel Technology", paper SPE/DOE 17329, presented at Enhanced Oil Recovery Symposium, Tulsa, April 17-20, 1988.
53. Sydansk, R.D.: "A Newly Developed Chromium(III) Gel Technology," *SPE*, (Aug. 1990) 346-352.
54. Sydansk, R.D.: "pH Dependent Process for Retarding the Gelation Rate of a Polymer Gel Utilized to Reduce Permeability in or Near a Subterranean Hydrocarbon-Bearing Formation," U.S. Patent 5,609,208 (11 March 1997).
55. Sydansk, R.D. and Argabright, P.A.: "Conformance Improvement in a Subterranean Hydrocarbon - Bearing Formation Using a Polymer Gel," U.S. Patent 4,683,949 (4 Aug. 1987).
56. Tackett, J.E.: "Characterization of Chromium(III) Acetate in Aqueous Solution," *Applied Spectroscopy*, (1989) **43**, 490-499.
57. Thompson, K. E. and Fogler H. S.: "Pore-Level Mechanisms for Altering Multiphase Permeability With Gel," *SPEJ* (1997) **2**, 350-362.
58. Vossoughi, S., and Putz, A.: "Reversible In Situ Gelation by the Change of pH within the Rock," paper SPE 20997 presented at the 1991 SPE International Symposium on Oilfield Chemistry, Anaheim, CA, Feb. 20-22.
59. Vossoughi, S., and Buller, C.S.: "Permeability Modification by In Situ Gelation with a Newly Discovered Biopolymer," *SPE* (November 1991) 485.
60. White, J.L., Goddard, J.E., and Phillips, H.M.: "Use of Polymers to Control Water Production in Oil Wells," *JPT* (Feb. 1973) 143-150.
61. Willhite, G.P., and Green, D.W.: "Improving Reservoir Conformance Using Gelled Polymer Systems," Annual Report for the Period September 25, 1994 to September 24, 1995, DOE contract no. DE-AC22-92BC14881, report no. DOE/BC/14881-18, The University of Kansas.
62. Yan, Z. "Effect of gel treatment with a polyacrylamide-chromium-thiourea system on the relative permeabilities of a Berea sandstone to water and oil," MS thesis, University of Kansas, Lawrence, KS (1998).

63. Zaitoun, A. and Kohler, N.: "Modification of Water/Oil and Water/Gas Relative Permeabilities After Polymer Treatment of Oil and Gas Wells," *In situ* (1989) **13**, 55-57.
64. Zhuang, Y., Pandey, S.N., McCool, C.S. and Willhite, G.P.: "Permeability Modification Using Sulfomethylated Resorcinol-Formaldehyde Gel System," paper SPE 37245 presented at the 1997 SPE International Symposium on Oilfield Chemistry, Houston, TX (18-21 Feb. 1997).
65. Zou, B., McCool, C.S., Green, D.W., and Willhite, G.P.: "A Study of the Chemical Interactions Between Brine Solutions and Dolomite," paper SPE 39695 presented at the Eleventh SPE/DOE Improved Oil Recovery Symposium, Tulsa, April 19-22, 1998.

